

Dynamins and myosin-II regulate the distinct modes of synaptic vesicle exocytosis in mature cerebrocortical nerve terminals and this involves calcium dependent phosphorylations.

by

Dilip Arvind Bhuvra

A thesis submitted in partial fulfilment for the requirements for the degree of
Doctorate of Philosophy at the University of Central Lancashire

January, 2015

Jay Shree Shakti Maa ॥

वक्रतुण्डमहाकायसुर्यकोटिसमप्रभा
निर्विघ्नं कुरु मे देव सर्वकार्येषु सर्वदा ॥

“The larger the island of knowledge, the longer the shoreline of mystery.”

- Mary B. Yates

© Copyright by Dilip Arvind Bhuva Jan, 2015

All Right Reserved

Dedication

This work is dedicated to my beloved father.

Declaration



Concurrent registration for two or more academic awards

I declare that while registered as a candidate for the research degree, I have not been a registered candidate or enrolled student for another award of the University or other academic or professional institution.

Material submitted for another award

I declare that no material contained in the thesis has been used in any other submission for an academic award and is solely my own work.

Signature of candidate

A handwritten signature in black ink, appearing to read "Dilip Arvind Bhuva".

Dilip Arvind Bhuva (B.Sc)

Type of award

Doctorate of Philosophy, Ph.D.

School

School of Pharmacy and Biomedical Sciences,
University of central Lancashire

Acknowledgements

This thesis would be incomplete without me thanking people who supported me through this journey. First, I would like to sincerely thank my supervisor, Dr. Anthony Ashton for mentoring me with his knowledge and expertise in the field. It is because of his untiring support, guidance and motivation that this seemed possible. One simply could not wish for a better supervisor! I would also like to thank my second supervisor, Prof. Jaipaul Singh for the encouragement and insight offered throughout these four years.

I am thankful to all the staff members at UCLan for impromptu discussions and helpful insights on various research works carried out at UCLan. This made my time at UCLan very enjoyable and expanded my sphere of knowledge. I am also grateful to all the technical staff for providing a helping hand whenever I needed one.

A special mention to my father, Arvind Bhuva; my mother, Kanta Bhuva; and my lovely sister, Vaishali Mangukiya, thank you for everything! I am thankful to my father for having confidence in me and supporting me in all my pursuits, for encouraging me to achieve my dreams and providing finance needed to pursue them. I am grateful for all the love and care showered on me by my family. I am forever indebted by all the sacrifices my family has made on my behalf. I also appreciate my fiancée Ms. Reshmi Siroya for providing support during final phases of this project.

I am also thankful to my friends, especially Deeba, Shraddha, Vivianna and Minhaaj for being there whenever I needed a friend.

I would like to acknowledge the funding provided under Overseas Research Student Associate Scheme, UK and by School of Pharmacy and Biomedical Sciences, UCLan. Without their funding, It would not have been possible to complete this PhD project.

Abstract

Synaptic vesicle (SV) exocytosis is vital to maintaining neuronal transmission at chemical synapses and defects in this processes has been linked to various psychiatric and neuronal disorders. Further, distinct modes of exocytosis have been implicated in post-synaptic plasticity and these latter processes maybe compromised in many neurodegenerative disorders. Therefore, it is vitally important to elucidate the machinery involved in SV exocytosis and decode the regulatory pathways for distinct modes of SV exocytosis. Herein, synaptosomes, pinched off nerve terminals, prepared from cerebral cortex of adult male Wistar rats were used as a model system to investigate these processes. Especially, A. Ashton had previously demonstrated the existence of KR mode of exocytosis in these synaptosomes and determined that the distinct modes can be regulated by adjusting the activity of various kinases and phosphatases.

Synaptosomes were maximally labelled with 100 μM FM2-10 dye such that all the releasable vesicles, from readily releasable pool (RRP) and reserve pool (RP), were loaded with the dye. The exocytosis of the dye was then studied by employing various secretagogues (high K^+ {HK}, 4-aminopyridine {4AP} or ionomycin {ION}) in the presence of 5 mM $[\text{Ca}^{2+}]_e$; these stimuli only induced a single round of release. This dye release was then directly compared to Glu release from terminals treated identically (more than 80% of these synaptosomes are glutamatergic), and differences between dye and Glu release were studied following various drug treatments.

The results show that the inhibition of dynamins can increase the FM2-10 dye release during certain stimulation conditions (4AP5C and ION5C; where 5C represents 5 mM $[\text{Ca}^{2+}]_e$) without changing the Glu released indicating that

dynamins) are required for the closure of the fusion pore (and therefore KR) during the employment of these stimuli. However experiments involving blockade of the ATPase activity of non-muscle myosin-II suggest that myosin-II may also be able to regulate the fusion pore, independent of dynamin-I, when a different stimulus (HK5C) is employed. The three stimuli employed here produced distinct kinetics for changes in $[Ca^{2+}]_i$ and suggest that dynamin-I may only be able to regulate KR mode of exocytosis when the $\Delta[Ca^{2+}]_i$ is relatively lower (overall $\Delta[Ca^{2+}]_i < 140$ nM) and that myosin-II replaces dynamin-I in this function when these Ca^{2+} changes are relatively higher (overall $\Delta[Ca^{2+}]_i > 140$ nM).

In order to investigate the phosphoregulatory pathways of these two phosphoproteins (dynamins and myosin-II) the activity of various enzymes including protein phosphatase (PP) 2A, PP1, calcineurin and PKC protein kinase C (PKC) was modulated externally. The data indicate that the properties of dynamin-I and myosin-II can be regulated by phosphoregulation induced by PKC and this induces their function in the KR mode of exocytosis. When the $\Delta[Ca^{2+}]_i$ is lower (overall $\Delta[Ca^{2+}]_i < 140$ nM), the relevant PKC remains deactivated and dynamin-I can continue to close the fusion pore of exocytosing vesicles thereby causing KR. On the other hand if the overall $\Delta[Ca^{2+}]_i$ is greater than 140 nM then relevant PKCs are activated which will then phosphorylate dynamin-I and myosin-II rendering the former inactive and the latter active such that myosin-II can now replace dynamin-I in closing the fusion pore. Western blot analysis revealed that dynamin-I is dephosphorylated at Ser 795 residue by PP2A, and that this residue can be phosphorylated by Ca^{2+} activated PKC as increase in phosphorylation of Ser 795 (by blockade of PP2A) or by supramaximal stimulation of PKC by active phorbol esters leads to a switch in the RRP to a FF mode, it would appear that this site may be important for defining the mode of exocytosis. Activated PKC can also

phosphorylate myosin-II but the phosphorylation sites on the myosin-II oligomer that play such a role remain to be determined.

These significant new findings help establish that SVs can switch between modes of exocytosis and that there are specific proteins implicated in this process. Clearly, further work may reveal the importance of these processes for synaptic plasticity and whether certain psychiatric or neuronal diseases could be explained by perturbation of these distinct modes of exocytosis.

Table of Contents

Dedication.....	I
Declaration.....	II
Acknowledgements.....	III
Abstract.....	IV
List of Figures.....	XI
List of Tables.....	XV
List of abbreviations.....	XVI
Chapter 1 Introduction.....	1
1.1 Introduction.....	2
1.2 Synaptic vesicle pools.....	2
1.3 Synaptic Vesicle.....	4
1.4 Synaptic vesicle fusion/exocytosis.....	6
1.4.1 Role of SNAREs.....	6
1.4.2 Role of Sec1/Munc18-1 (SM).....	7
1.4.3 Munc 13s and RIMs.....	9
1.4.4 Synaptotagmin and complexins.....	9
1.5 Synaptic vesicle endocytosis.....	12
1.5.1 Clathrin-mediated endocytosis (CME).....	12
1.5.2 Bulk endocytosis.....	13
1.5.2 Kiss-and-run exo/endocytosis.....	13
1.6 Dynamins.....	16
1.7 Myosin II.....	21
1.8 Working hypothesis.....	23
1.9 Main Aim.....	24
1.9.1 Specific Aims.....	24
Chapter 2 Materials and Methods.....	25

2.1 Preparation of Synaptosomes	26
2.2 Glutamate Release Assay	28
2.3 FM2-10 Dye Release Assay.....	32
2.4 Measurement of Intracellular Free Calcium Concentration.....	35
2.5 Result for biochemical assays	39
2.6 Western Blotting	40
Chapter 3 Studies to Establish Optimal Conditions for Investigating Synaptic Vesicle Exocytosis.....	46
3.1 Introduction	47
3.2 Justification for the Interpretation of Results.....	47
3.3 Achieving Maximal Glu Release.....	50
3.4 SVs Undergo Only One Round of Exocytosis	54
3.5 Maximal labelling of Synaptic Vesicles by FM2-10 dye.....	57
3.6 Mode of SV Exocytosis Is Dependent on the Stimulus Employed	59
3.7 RRP undergoes spontaneous release at 37 °C	64
3.8 Conclusion	70
Chapter 4 Role of Dynamins and Myosin II	71
4.1 Introduction	72
4.2 Results.....	73
4.2.1 Inhibition of Dynamins	73
4.2.2 Inhibition of specific dynamin isoforms.....	79
4.2.3 Inhibition of Myosin-II	84
4.3 Discussion	91
4.3.1 Inhibition of dynamins.....	91
4.3.2 Inhibition of dynamin-I.....	93
4.3.3 Inhibition of dynamin-II	99
4.3.4 Inhibition of non-muscle myosin-II	101
4.3.5 Why two proteins for the same process?.....	102

4.4 Conclusions	104
Chapter 5 Role of Calcium	105
5.1 Introduction.....	106
5.2 Results.....	107
5.2.1 Inhibition of calcineurin.....	107
5.2.2 Inhibition of Protein Kinase C.....	117
5.2.3 Activation of Protein Kinase C.....	121
5.3 Discussions.....	127
5.3.1 Role of Calcineurin.....	127
5.3.2 Inhibition of Protein Kinase C (PKC).....	131
5.3.3 Activation of Protein Kinase C (PKC).....	133
5.4 Conclusions	136
Chapter 6 Dynamin-I Phosphorylation Studies	137
6.1 Introduction.....	138
6.2 Results.....	138
6.2.1 Phosphorylation of dynamin-I on Ser-774.....	139
6.2.2 Phosphorylation of dynamin-I on Ser-778.....	145
6.2.3 Phosphorylation of dynamin-I on Ser-795.....	149
6.3 Discussions.....	154
6.3.1 Phosphorylation of dynamin-I at Ser 774	155
6.3.2 Phosphorylation of dynamin-I at Ser 778.....	158
6.3.3 Phosphorylation of dynamin-I at Ser 795.....	159
6.4 Conclusions	164
Chapter 7 General Discussion and Conclusion.....	165
7.1 General conclusions	166
7.2 Future directions.....	172
References.....	174
Appendix.....	190

A.1 List of Materials.....	191
A.2 Calculations for Biochemical Assays.....	195
A.3 Sample size and p values	196
A.4 Okadaic acid (OA) experiments	203
A.5 FM2-10 dye content at the start of measurement.	204
A.6 Full-sized immuno blots	207
A.7 List of publications arising from this work	208

List of Figures

Figure 1.1: The diagrammatic representation of (a) Kiss-an-run and (b) full-fusion modes of exocytosis.	3
Figure 1.2: Molecular model of an average brain SV showing all the surface vesicular proteins.	5
Figure 1.3: Synaptic vesicle fusion mediated by SNARE and SM proteins.	8
Figure 1.4: A diagram illustrating the notion that all the discussed proteins interact at the fusion pore site.	11
Figure 1.5: A schematic representation of different pathways of SV endocytosis.	15
Figure 1.6: The diagrammatic representation of the Dynamin showing all the domains and the phosphorylation sites.	17
Figure 1.7: The regulatory cycle of dynamin in relation to vesicle endocytosis.	20
Figure 1.8: Schematic representation of structure of myosin-II.	22
Figure 2.1: Schematic representation of synaptosome preparation from rat cerebral cortex.	27
Figure 2.2: A schematic representation of the generalised microtitre plate setup used during glutamate measurement assay.	31
Figure 2.3: A schematic representation of the generalised microtitre plate setup used during FM2-10 dye release assay.	34
Figure 2.4: A schematic representation of the generalised microtitre plate setup used during Fura-2-AM assay.	38
Figure 3.1: A schematic representation of the rationale behind the interpretation of the results/data.	48

Figure 3.2: Measurement of evoked glutamate in the presence of various extracellular calcium concentrations show that 5 mM $[Ca^{2+}]_e$ induces maximum glutamate release.	52
Figure 3.3: Measurement of cytosolic free calcium show that all the three stimuli employed in this study produced a change in $[Ca^{2+}]_i$ with different kinetics.	53
Figure 3.4: The amount of Glu released by SV exocytosis is not affected by the acute treatment of 1 μ M BAF.	56
Figure 3.5: Use of 0.1 or 1 mM FM2-10 dye for labelling the SVs does not have any effect on its SV loading.	58
Figure 3.6: Inhibition of PP2A and PP1 induces all SVs to release by FF.	61
Figure 3.7: SVs undergo KR exocytosis during initial 2 sec of stimulation and FF thereafter.	62
Figure 3.8: Some SVs undergo spontaneous exocytosis at 37 °C.	67
Figure 3.9: SVs undergoing spontaneous release at 37 °C belong to RRP.	68
Figure 3.10: Loss of FM dye prior to stimulate confirm spontaneous release of RRP vesicles.	69
Figure 4.1: Inhibition of dynamins by 160 μ M dynasore does not affect the total SV turn over	74
Figure 4.2: Dynamin(s) is required for KR exocytosis of RRP when ION5C and 4AP5C stimuli are employed.	75
Figure 4.3: Pre-treatment with 160 μ M dynasore does not affect the changes in $[Ca^{2+}]_i$ achieved upon stimulation.	77
Figure 4.4: Role of dynamin(s) in KR exocytosis is independent of clathrin.	78
Figure 4.5: Dynamin-I isoform is required for KR of RRP vesicles when	81

ION5C is employed as a stimulus.

- Figure 4.6:** Dynamin-II isoforms may be required for FF of the RP. 83
- Figure 4.7:** When non-muscle myosin-II was inhibited by 50 μM blebbistatin, no differences in the Glu release was observed 86
- Figure 4.8:** Myosin-II is required for KR of RRP when HK5C is employed as a stimulus. 87
- Figure 4.9:** The activity of dynamin-I and myosin-II appears to be dependent on the $\Delta[\text{Ca}^{2+}]_i$ achieved upon stimulation. 88
- Figure 4.10:** Pre-treatment with 50 μM blebbistatin does not affect the $[\text{Ca}^{2+}]_i$ achieved upon stimulation. 89
- Figure 5.1:** Blockade of calcineurin by 1 μM Cyclosporin A does not affect the total amount of glutamate released 108
- Figure 5.2:** Inhibition of calcineurin causes some RP vesicles to undergo KR. 110
- Figure 5.3:** Cys A produces larger $\Delta[\text{Ca}^{2+}]_i$ for all three stimuli. 112
- Figure 5.4:** A combination treatment of CysA+Blebb or Cys A+DYN does not affect the Glu released. 114
- Figure 5.5:** Distinct effects of DYN+Cys A and Blebb+Cys A treatment on FM2-10 dye release. 115
- Figure 5.6:** Inhibition of PKC, dynamins or myosin-II does not affect the total Glu released. 118
- Figure 5.7:** Inhibition of PKCs by 1 μM Go6983 switched the protein dependence for KR during HK5C stimulation. 120
- Figure 5.8:** Various sub-maximal concentrations PMA failed to switch the protein dependency for KR mode of exocytosis. 123

Figure 5.9: 40 nM PMA was able to switch the protein dependency for KR during ION5C stimulation.	125
Figure 6.1: Western blot images showing dynamin-I phosphorylated at Ser 774 site.	142
Figure 6.2: Inhibition of calcineurin prevents stimulation dependent dephosphorylation of dynamin-I at Ser 774 site.	144
Figure 6.3: Western blot images showing dynamin-I phosphorylated at Ser 778 site following various treatments.	146
Figure 6.4: Densitometric analysis of blots presented in Figure 6.3 confirmed the stimulation time dependent decrease in the Ser 778 phosphorylation of dynamin-I.	148
Figure 6.5: Phosphorylation at Ser 795 of dynamin-I seems to be under regulation of PP2A and PMA.	151
Figure 6.6: Densitometric analysis of blots presented in Figure 6.5 confirmed the stimulation time dependent decrease in the Ser 795 phosphorylation of dynamin-I.	152
Figure 6.7: PMA exhibited a dose dependent phosphorylation of Ser 795 in intact synaptosomes.	153
Figure 7.1: A schematic representation of exocytosis of a RRP vesicle during a mild stimulation.	167
Figure 7.2: A schematic representation of exocytosis of a RRP vesicle during a strong stimulation.	169
Figure 7.3: A schematic representation of mechanism responsible for switching the protein dependency for KR.	171

List of Tables

Table 2.1: Table of information showing the concentrations of various antibodies used in this study.	43
Table A.3.1: A table of information showing sample size and p values for data presented in chapter 4 of this thesis.	196
Table A.3.2: A table of information showing sample size and p values for data presented in chapter 5 of this thesis.	199

List of abbreviations

$[Ca^{2+}]_e$	Extracellular Calcium concentration
$[Ca^{2+}]_i$	Cytosolic free Calcium concentration
$\Delta[Ca^{2+}]_i$	Change in intracellular free Calcium concentration
4AP	4-Aminopyridine; 1 mM in this study
4AP5C	4AP with 5 mM $[Ca^{2+}]_e$
AAGA	Assembly-assisted GTPase activity
BAF	Bafilomycin A1, 1 μ M in this study
BGA	Basal GTPase activity
Blebb	Blebbistatin; 50 μ M in this study
BPB	Bromophenol blue, 0.08 mM in this study
Ca^{2+}	Calcium
Cdk5	Cyclin-dependent kinase 5
CME	Clathrin mediated endocytosis
Cys A	Cyclosporin A; 1 μ M in this study
DB	Diabetic
DYN	Dynasore; 160 μ M in this study
Fura-2-AM	Fura-2-acetoxymethyl ester
GLDH2	Glutamate dehydrogenase type-II
Glu	Glutamate/Glutamic acid
GSK3	Glycogen synthase kinase 3
HK	High K^+ ion concentration, external; 30 mM in this study
HKxC	HK with x mM $[Ca^{2+}]_e$
ION	Ionomycin, 5 μ M in this study
IONxC	ION with x mM $[Ca^{2+}]_e$

NDB	Non-diabetic
NSF	N-ethylmaleimide sensitive factor
OA	Okadaic Acid; 0.8 μ M in this study
PIT 2	Pitstop 2; 15 μ M in this study
PKC	Protein Kinase C
PP1	Protein phosphatase 1
PP2A	Protein phosphatase 2A
PRD	Proline rich domain
RP	Reserve pool
RRP	Ready releasable pool
RT	Room temperature
sec	Second(s)
Ser	Serine
SNARE	Soluble NSF-attachment Protein Receptor
SV	Synaptic vesicle
β -NADP ⁺	β -Nicotinamide adenine dinucleotide 2'-phosphate, Oxidised form
β -NADPH	β -Nicotinamide adenine dinucleotide 2'-phosphate, reduced form

Chapter 1

Introduction

1.1 Introduction

The nervous system of a vertebrate performs a variety of diverse and complex functions that require the exchange of information between neurons and/or between a neuron and a target cell (Rizo and Rosenmund, 2008). In chemical synapses, this information is mainly exchanged through synaptic vesicles (SVs) that release the neurotransmitter in all-or-none manner — the quantal vesicular model of neurotransmitter release (Shupliakov and Brodin, 2010). The neurotransmitter release is a highly regulated event and is very fast in its action, typically taking only 0.1 milliseconds from the arrival of an action potential to the Ca^{2+} -evoked SV exocytosis. Apart from transmitting a signal, neurotransmitter release also contribute to the acute, dynamic and long term efficiency of pre-synaptic plasticity and it helps in shaping the properties of neural networks and information processing in the brain. Due to this, the SV exocytosis is tightly regulated so that it occurs at the right time and with the correct probability (Rizo and Rosenmund, 2008).

1.2 Synaptic vesicle pools

The SVs are broadly divided into three vesicle pools depending upon their location in the pre-synaptic nerve terminal. The Ready Releasable Pool (RRP) is situated closest to the membrane and possibly even docked to the pre-synaptic membrane making them the first set of vesicles to be released upon stimulation. The reserve/recycling pool (RP) is situated proximate to the pre-synaptic membrane and is released once the RRP has exhausted. The third pool, called Resting/silent pool, is located relatively far from the pre-synaptic membrane and it is believed that it is not released under normal physiological conditions (Harata, *et al.*, 2006). It is widely believed that after the fusion, the SV fully collapses into the plasma

membrane and loses its integrity and identity, a process called full-fusion (FF; Figure 1.1b). On the other hand, a SV, after its fusion, may be retrieved back into the nerve terminal without the loss of its identity and can be recycled quickly, a process called kiss-and-run (KR; Figure 1.1a). Although, the KR mode of vesicular exocytosis is not widely accepted, the data obtained by Ashton and group strongly supports the KR mode of exocytosis (Ashton *et al.*, unpublished work). The data also suggests that the stimulation of synaptosomes with strong stimuli (in the presence of 5 mM Ca^{2+} ; see later for definition) causes the RRP to undergo KR mode of exocytosis and the RP fuses via the FF mode of exocytosis (Ashton *et al.*, unpublished work).

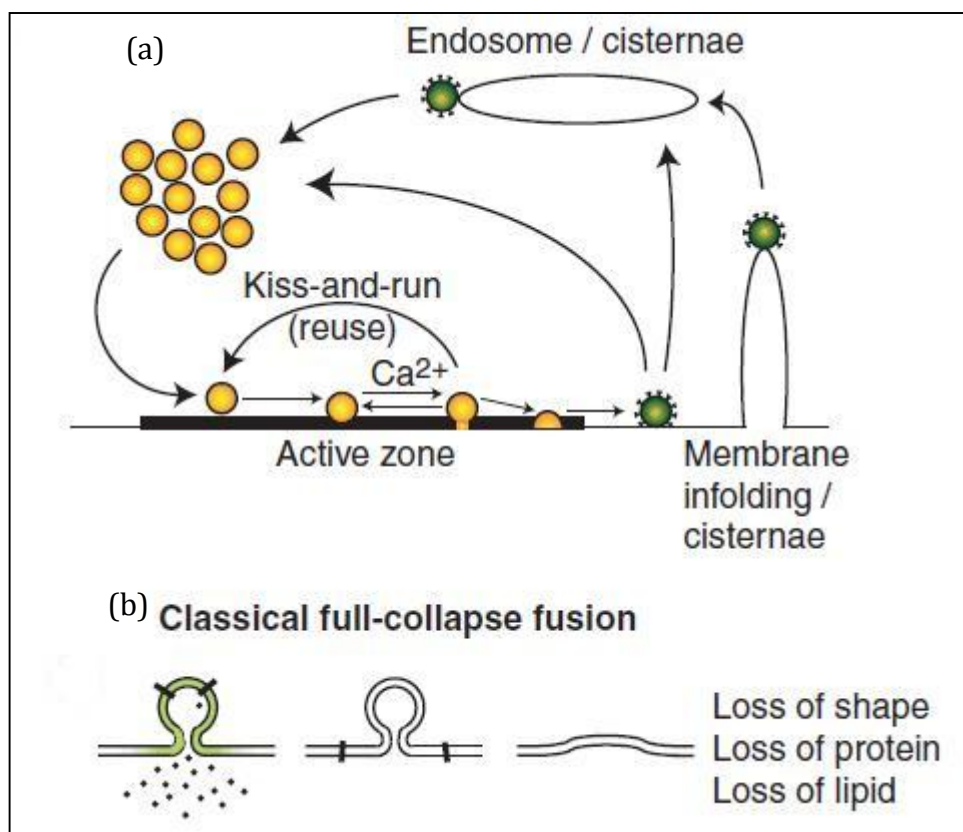


Figure 1.1: The diagrammatic representation of (a) Kiss-an-run and (b) full-fusion modes of exocytosis. Partially adapted from (Harata, *et al.*, 2006)

1.3 Synaptic Vesicle

A synaptic vesicle is an important organelle of a pre-synaptic neuron as it acts as storage for the neurotransmitter and facilitates its release into the post synaptic cleft via stimulation dependent exocytosis. The SVs are roughly 40 nm in diameter (Figure 1.2) and undergo fusion when terminals are depolarised and the $[Ca^{2+}]_i$ increases due to Ca^{2+} entry through various VGCCs. This fusion of SVs occurs in specific regions, called the active zone, of the presynaptic membrane and involves release of the neurotransmitter that they contain. Following exocytosis, the SVs are retrieved through various endocytic pathways and are reloaded with the neurotransmitter, ready for next round of release (Figure 1.5). Although the SVs were first identified in early 1950s, the complete regulatory mechanism involved in their exo and endocytosis is not yet fully understood. Various mechanisms of exo and endocytosis are discussed further in the chapter.

A SV is shown to have more than 400 different types of proteins including a wide variety of transport and trafficking proteins that help in SV loading and trafficking respectively (Shupliakov and Brodin, 2010). Some of the important proteins of a SV include vacuolar H^+ ATPase (acidification of SV), neurotransmitter specific transporter proteins (like VGLUT), synaptotagmin, synaptobrevin, synapsin, and synaptophysin, among others (Takamori *et al.*, 2006; Lang & Jahn, 2008). Typically, proteins account for almost 60% of the dry weight of a synaptic vesicle (Figure. 1.2) demonstrating the complex regulatory mechanisms through which the SV exo and endocytosis may be controlled by these proteins (Shupliakov and Brodin, 2010). The functions of many of these proteins still remain to be identified but it is believed that the functions of SV proteins are divided into four major categories: (i) those involved in neurotransmitter uptake and storage, (ii) those involved in

facilitating or regulating exocytosis/fusion, (iii) those that participate in endocytosis/recycling of SV, and finally (iv) those that are involved in SV biogenesis and maintenance (Sudhof & Rizo, 2011).

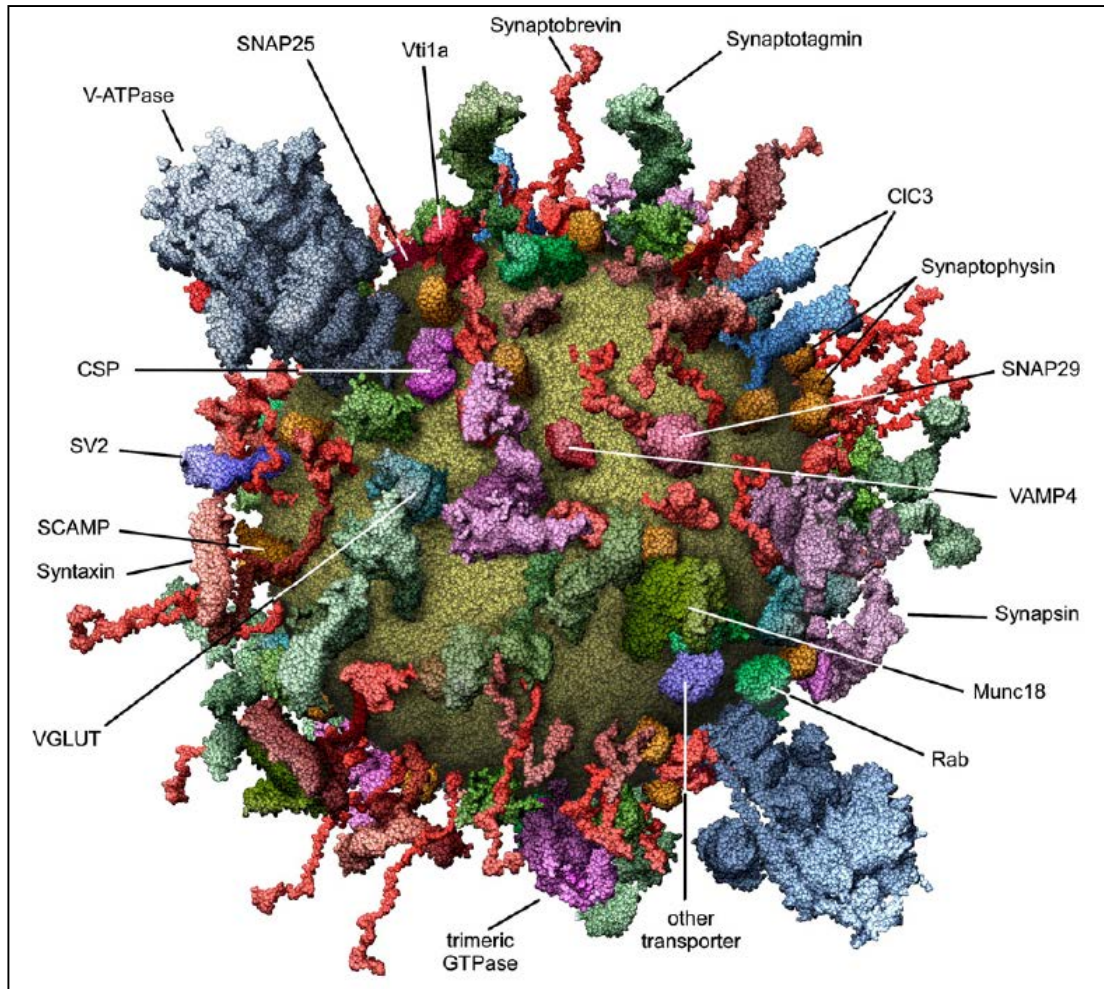


Figure 1.2: Molecular model of an average brain SV showing all the surface vesicular proteins. (Shupliakov and Brodin, 2010)

1.4 Synaptic vesicle fusion/exocytosis

Synaptic vesicle fusion/exocytosis is essential for the transmission of neuronal signal across a synapse. The synaptic vesicle fusion is mediated by a number of proteins and only a few of the important proteins are discussed below.

1.4.1 Role of SNAREs

Soluble NSF Attachment Protein Receptor (SNARE) proteins regulate most types of intracellular membrane traffic and contain characteristic sequences called SNARE motifs that have a high tendency to form coiled coils. The three SNARE proteins — synaptic vesicle SNARE synaptobrevin and the plasma membrane SNAREs syntaxin-1 and Synaptosomal-associated protein-25 (SNAP) — form a highly stable 'SNARE complex' that is disassembled upon binding to SNAPs and N-ethylmaleimide sensitive fusion protein (NSF) through the ATPase activity of NSF (hence the name SNARE). The SNARE complexes play a major role in the formation of the fusion pore (Figure 1.3) although Alabi & Tsien (2013) suggest that one SNARE complex is sufficient for fusion pore formation whilst three SNARE complexes can drive expansion of the fusion pore.

Due to its involvement in the formation of fusion pore, the modulation of the binding activities of all the three SNARE proteins can play a crucial role in the mechanism of neurotransmitter release. There have been few studies to determine the phosphorylation sites of SNARE proteins. For e.g.: Dubois et al., 2002 identified Thr 21 and Ser 14 as the phosphorylation sites on syntaxin-1A by casein kinase (CK) I and II respectively. Syntaxin-I can also be phosphorylated at Ser¹⁸⁸ by death-associated protein in a Ca²⁺ dependent manner. The phosphorylation at this site decreases Syntaxin-I binding to mammalian uncoordinated 18-1 (Munc 18-1), a syntaxin-binding protein that regulates SNARE complex formation and is required

for synaptic vesicle docking, there by affecting the vesicle exocytosis (Tian, et al., 2003). Note, in more recent times Munc 18-1 has also been implicated in a late step in fusion (Jahn & Fasshauer, 2012). Similarly, SNAP-25 can be phosphorylated at Ser 187 and Thr 138 (Nagy, et al., 2004; Kataoka, et al., 2008; Takahashi, et al., 2003)

1.4.2 Role of Sec1/Munc18-1 (SM)

Similar to SANRE proteins, SM proteins are essential for most types of intracellular membrane traffic and this theory is strongly supported by the fact that the Munc 18-1 knockout mice show totally impaired neurotransmitter release. There are several models proposed in order to explain the precise mechanism by which the interaction of Munc 18-1, SNARE complex and other factors leads to the vesicular exocytosis. However, it is clear from these proposed models that Munc 18-1 interaction with SNARE complex, especially syntaxin-1, leads to the conformational changes of the SNARE complex that favours fusion (Figure 1.3; Südhof & Rizo, 2011). However it still remains unclear whether Munc 18-1 stimulates fusion indirectly (that is, by promoting SNARE complex assembly) or directly.

Munc 18-1 is a substrate for protein kinase C and Cyclin-dependent kinase 5 and it has been successfully shown that Munc 18-1 can be phosphorylated by these two kinases (Lilja, et al., 2003). The two major sites of phosphorylation of Munc 18-1 are Ser306 and Ser313 and phosphorylation of these sites leads to inhibition of its interaction with syntaxin 1A (as determined by binding assays *in vitro* using glutathione S-transferase-syntaxin-1A fusion proteins). However, it is not confirmed yet as to whether these sites can be phosphorylated by protein kinase C *in vivo* but it can be phosphorylated *in vitro* including in synaptosomes (Vries, et al., 2000).

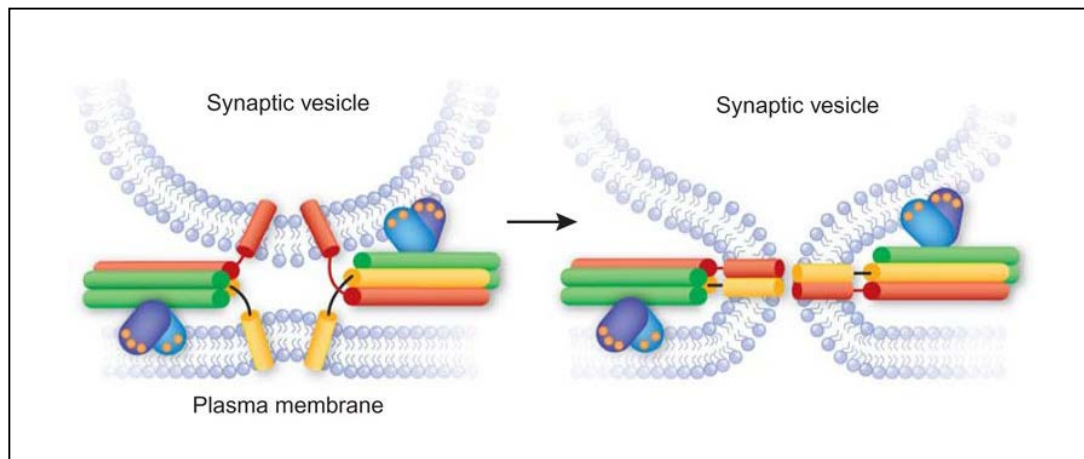


Figure 1.3: Synaptic vesicle fusion mediated by SNARE and SM proteins. Syntaxin is shown in yellow (without its N-terminal region), synaptobrevin is shown in red, SNAP-25 in green and Syntaxin in yellow (without its N-terminal region). The synaptotagmin C2A and C2B domains are shown in purple and blue respectively, orange circles representing bound Ca²⁺ ions. The left panel represents the two membranes before fusion, with some bending in the middle that is induced by the mechanical action of the assembled SNARE complex. This effect, together with perturbations caused by binding of synaptotagmin to one or both of the membranes, would lead to membrane fusion, represented in the right panel (Rizo, 2010).

1.4.3 Munc 13s and RIMs

Munc 13s and RIMs play important roles in vesicle priming and diverse forms of presynaptic plasticity. The two major isoforms of these families include Munc 13-1 and RIM1a. The Munc 13s are primarily involved in the vesicle priming and in the Munc 13 knockout mice there is a complete removal of spontaneous and evoked vesicular release. Munc 13-1 is also shown to participate in pre-synaptic plasticity which was demonstrated by distinct changes in synaptic amplitudes upon high-frequency stimulation following manipulation of Munc 13-1 or Munc 13-2 (Rosenmund, et al., 2002).

RIMs were initially thought to act as a Rab3 effector but now it is believed that it has many more functions because only a subset of the family has Rab-binding region and upon the deletion of RIM1a, a much stronger inhibition of neurotransmitter release is observed as compared to the absence of Rab3A itself (Südhof & Rizo, 2011). Similar to Munc 13s, RIMs also play a role in vesicle priming. Moreover, RIMs also shows the ability to interact with several other proteins at the active zone indicating that RIMs might be also involved in organising the active zone.

Lonart, et al., 2003 demonstrated that RIM1 α can be phosphorylated at Ser⁴¹³ and Ser¹⁵⁴⁸ by protein kinase A suggesting that PKA-mediated phosphorylation of the active zone protein, RIM1 α induces pre-synaptic Long-term potentiation.

1.4.4 Synaptotagmin and complexins

Synaptotagmin and complexins are considered to be the Ca²⁺ sensors and are responsible for the Ca²⁺ triggered vesicle release. Synaptotagmin-1 is a vesicle protein with two C2 domains that assume the β -sandwich structures. The two C2

domains are C2A and C2B domains that bind to three and two Ca^{2+} ions respectively. It has been found that mutations that modulates the Ca^{2+} affinity of the synaptotagmin-1 leads to the parallel changes in the Ca^{2+} sensitivity of release (Figure 1.3; Xu, et al., 2009). Apart from acting as Ca^{2+} sensors, Synaptotagmin-1 also interacts with the plasma membrane and with the SNARE complex there and regulates vesicular release.

The function of complexins (Jahn & Fasshauer, 2012) is also closely coupled to that of synaptotagmin-1 and SNARE complex (Figure 1.4). It is believed that complexins acts as clamps for the fusion machinery at the active zone and interaction of complexins with SNARE complex helps creating a metastable state that serves as a substrate for synaptotagmin-1 to trigger fast release. However, it has also been implicated in facilitation of fusion via its N-terminal end which, like its central helix which binds to a groove on the surface of the SNARE complex, may have other interactions (Jahn & Fasshauer, 2012).

Davletov, et al., 1993 showed that that synaptotagmin-1 can be phosphorylated at Thr 128 by casein Kinase II. Later it was also found that synaptotagmin-1 is a substrate for various kinases like Ca^{2+} /calmodulin-dependent protein kinase II (CaMKII), protein kinase C (PKC), and casein kinase II (caskII). It was shown, *in vitro*, that the CaMKII and PKC phosphorylates Thr 112 and CASKII phosphorylates an additional Thr 125 residue (Hilfiker, et al., 2001).

1.5 Synaptic vesicle endocytosis

A typical nerve terminal in the brain contains about 200 releasable SVs and yet the individual exocytic events can occur with high frequency in the range of 5–50 Hz and for prolonged lengths of time (greater than 30s) which may cause synaptic fatigue. However, the synaptic fatigue does not occur under normal physiological conditions as the SVs are rapidly recycled to prevent the depletion of the releasable vesicles (Heymann and Hinshaw, 2009). SV endocytosis can occur via three pathways, Clathrin-mediated endocytosis, bulk endocytosis and Kiss-and-run endocytosis.

1.5.1 Clathrin-mediated endocytosis (CME)

Clathrin-mediated endocytosis involves retrieval of exocytosed SV with the help of clathrin and this occurs away from the active zone (peri-active zone). The SVs that undergo full-fusion mode of exocytosis – where the SV membrane completely collapses into pre-synaptic membrane – are usually retrieved by this mechanism of endocytosis (Figure 1.5). Clathrin-mediated endocytosis extensively involves curvature generation and sensing by various proteins as the fused SV membrane needs to be recovered by an invagination of the pre-synaptic plasma membrane (Kleist *et al.*, 2011). The initial stage of CME involves formation of clathrin coat on the SV to be retrieved. The clathrin coat is composed of two layers: (i) an inner layer of adaptor proteins that include AP-2, AP180/CALM, Epsin and Stonin, and (ii) an outer layer of clathrin. During the formation of the coat, proteins like endophilin, amphiphysin, and syndapin contribute to the membrane curvature generation and sensing (Milosevic *et al.*, 2011; Südhof & Rizo, 2011; Guan *et al.*, 2010). Once a substantial invagination of the membrane is achieved, the SV is retrieved by membrane fission by proteins like dynamin (Ferguson & De Camilli,

2012; discussed later). After this fission stage, the clathrin-coat disassembles from the vesicle membrane and the vesicle thus generated is made available for use in subsequent round of exocytosis. Since the protein composition of a SV membrane is vital to proper functioning of a SV, there must be check points to ensure that all the essential proteins are included during recycling via this pathway. However, such mechanisms are not fully understood yet.

1.5.2 Bulk endocytosis

This type of endocytosis involves retrieval of a large portion of the plasma membrane from which the SVs are later generated by distinct pathways. Bulk endocytosis is mainly thought to be involved only during strong stimulations where multiple SVs may fully fuse into the plasma membrane in a very short duration. This excess plasma membrane can be rapidly retrieved using formation of large invaginations that later contribute to the formation of several SVs (Figure 1.5; Clayton et al., 2008; Hayashi et al. 2008). The exact mechanism of SV retrieval from this bulk endocytosed membrane is not yet clear and it is thought that the increase in surface to volume ration during bulk exocytosis may lead to buckling of the plasma membrane resulting into large invaginations (Saheki & De Camilli, 2012). Once a large endosomal membrane is retrieved by this process, a coat (similar to clathrin) dependent process may be involved in retrieving individual SVs from the large endocytosed membrane with the help of actin and F-BAR (Andersson *et al.*, 2008; Wu *et al.*, 2010).

1.5.2 Kiss-and-run exo/endocytosis

A SV may release its neurotransmitter via a transiently open fusion pore such that this pore closes within a short duration of exocytosis (<0.5 sec; Figure 1.5). This allows the SV to be recycled without fully collapsing into the plasma membrane. If

this occurs, the SV bypasses the entire process of CME and the need for molecular sorting of essential SV proteins/cargo can be avoided. Thus, this type of exo/endocytosis provides rapid means for replenishing the releasable pool of SVs. Many studies have suggested the existence of Kiss-and-run (KR) in various model systems (Aravanis *et al.*, 2003; He *et al.*, 2006; Zhang *et al.*, 2009) but its existence still remains debatable for SV exocytosis in nerve terminals of the CNS. Most of the evidence provided for the existence of KR remains indirect and are based on observations that are usually incompatible with CME or bulk endocytosis (He *et al.*, 2006; Zhang *et al.*, 2009).

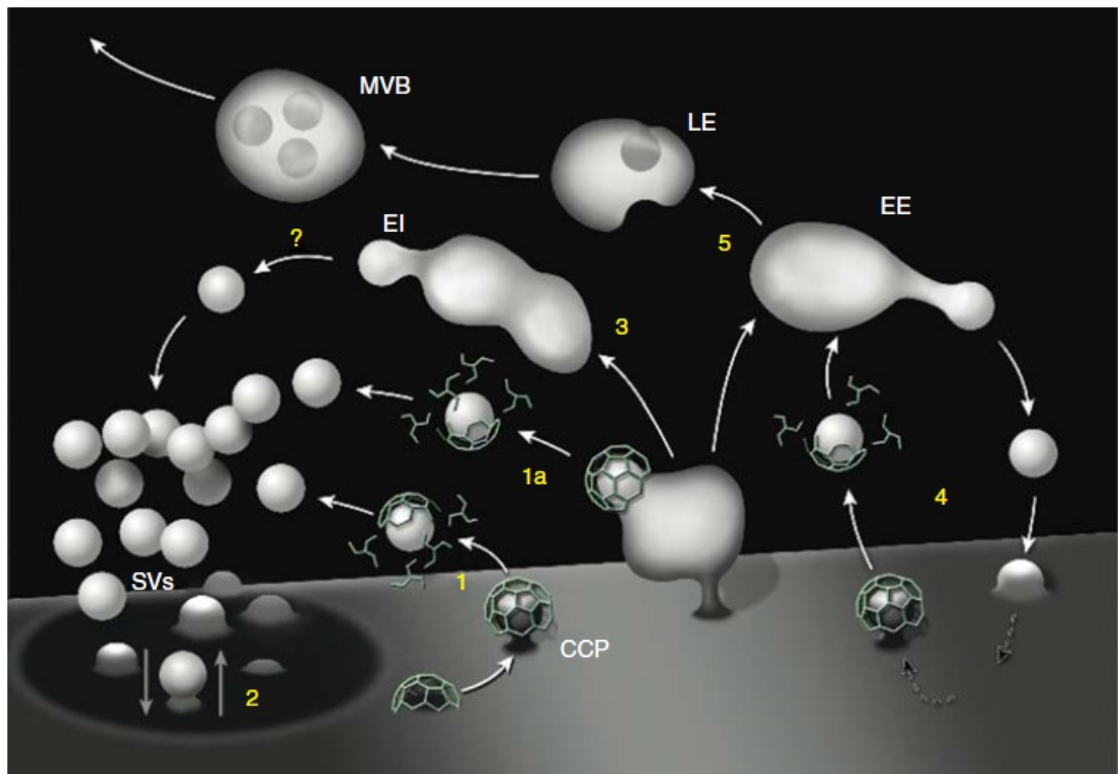


Figure 1.5: A schematic representation of different pathways of SV endocytosis. Following exocytosis, the SVs can be retrieved via (1) CME, (2) KR, or (3) Bulk endocytosis. Stages (4) and (5) represent the alternative pathways that a bulk endocytosed membrane could follow for the retrieval of SVs. Abbreviations: EI – Endocytic intermediates; LE – late endosome; EE – early endosome; CCP – clathrin coated pit; MVB – multivesicular body. (taken from Saheki and De Camilli, 2012)

1.6 Dynamins

Dynamin is a 100 kDa GTPase enzyme belonging to a family of large GTP-binding proteins that is known to play a crucial role in vesicle endocytosis. There are three isoforms of dynamin: dynamin-I, dynamin-II and dynamin-III. The dynamins have a role in the multiple forms of membrane fission and fusion events such as vesicle fission from the plasma membrane and membrane budding events within intracellular organelles. All forms of dynamins have unique properties of self-assembly and the ability to bind and tubulate lipids which make them “fit” for the membrane fission and fusion functionality. All the three isoforms of Dynamin have an N-terminal GTPase domain, a middle pleckstrin-homology domain (mediates lipid membrane binding via interaction with a family of phosphoinositide phospholipids), a GTPase effector domain and a proline-rich domain (protein-protein interaction domain for various signalling and cytoskeleton proteins) at the C-terminus (Figure. 1.6). During rapid SV recycling, all the three dynamins play a role in vesicle scission. In particular, dynamin-I can mediate the bulk of SV endocytosis during a depolarization stimulus and is essential for vesicle recycling during high or prolonged synaptic activity. Dynamin-II is mainly involved in the conventional clathrin-mediated uptake of surface receptors or membrane and in the slow vesicle endocytosis that occurs after the removal of the stimulus. Lastly, dynamin-III has been shown to perform similar functions as that of dynamin-I but is much lower in abundance. Dynamins appear to be involved twice in the endocytic mechanism: early in the constriction of the invaginating vesicle and late in its scission (Lu, *et al.*, 2009; Heymann and Hinshaw, 2009).

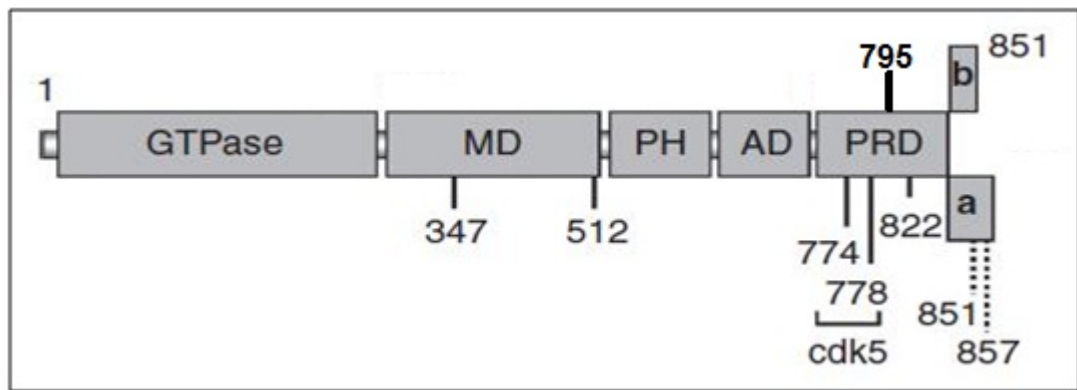


Figure 1.6: The diagrammatic representation of the Dynamin showing all the domains and the phosphorylation sites. GTPase: N-terminal GTPase domain, involved in hydrolysing the GTP; MD: Middle Domain; PH: Pleckstrin-Homology domain, together with MD mediates lipid membrane binding; AD: Arginine rich domain; PRD: Proline rich domain, together with RD involved in interaction with other BAR domain proteins (adapted from Heymann and Hinshaw, 2009).

The role of dynamin, in nerve terminals, is regulated by various kinases and phosphatases. Although, the importance of phospho-regulation of dynamin is not elucidated in exocytosis, it is known, to some extent, as to how the phospho-regulation of dynamin can affect the vesicle endocytosis. In non-stimulated neurons, the dynamin-I is constitutively phosphorylated and is inactive. Upon stimulation, an influx of Ca^{2+} stimulates vesicle exocytosis and dephosphorylation of dynamin-I by calcineurin. The dephosphorylated dynamin-I can in some model of dynamin-I action form a complex with the bin-amphiphysin-rvs (BAR) domain of syndapin-I which may help in localization of dynamin-I to the site of endocytosis. This localisation of dynamin—syndapin-I complex is necessary for the membrane retrieval, in which other BAR domain containing proteins may also be involved. After the endocytosis is complete, the cyclin-dependent kinase 5 (cdk5) and GSK3 rephosphorylates dynamin-I and this may promote the disassembly of the dynamin—syndapin-I complex (see Figure 1.7).

Graham, *et al.*, 2007 undertook a systematic identification of all phosphorylation sites of dynamin-I in rat brain nerve terminals and confirmed that the synaptosomal (pinched off nerve terminal) dynamin-I has seven phosphorylation sites *in vivo*: Ser 774, Ser 778, Ser 822, Ser 851, Ser 857, Ser 512, and Ser 347 (Figure 1.6). Their findings also revealed that the initially believed Thr 780 phosphorylation site does not undergo phosphorylation *in vivo* and that it is restricted to *in vitro* conditions only (Tomizawa *et al.*, 2003). Moreover, their quantification analysis led to the conclusions that Ser 774 and Ser 778 were the major sites of phosphorylation (up to 69% of the total), followed by Ser 851 and Ser 857 (12%), and Ser 853 (2%) (Graham *et al.*, 2007). The functional role for the two major phosphorylation sites of dynamin-I has been identified. Upon the influx of Ca^{2+} - in response to a depolarisation - calcineurin (PP2B) is activated which then dephosphorylates dynamin-I at Ser 774 and Ser 778 (Xue *et al.*, 2011). This promotes mobilisation of dynamin-I for SV endocytosis, especially CME, and brings about the scission of the “budding” vesicle membrane and therefore complete the recycling of the SV (Figure 1.5). After the scission is completed, dynamin-I gets re-phosphorylated at Ser 778 by Cdk5 (Graham, *et al.*, 2007) and at Ser 774 by GSK3 (Clayton *et al.*, 2010). The phosphorylation at these sites causes dissociation of dynamin-I from the endocytic machinery and is localised back to the cytosol until next round of endocytosis (Graham, *et al.*, 2007; Saheki & De Camilli, 2012) (see Figure 1.7).

Similar to dynamin-I, dynamin-III is also phosphorylated at homologous sites strongly supporting the hypothesis that dynamins I and III share common functions and control mechanisms. On the other hand, there is not much data available on the phosphorylation of dynamin-II except for the fact that dynamin-II can undergo *src*-induced phosphorylation at Tyr 416 which then facilitates scission

of caveolae in endothelial cells (Shajahan, *et al.*, 2004). Moreover, it is also known to be phosphorylated and dephosphorylated at Ser 764 by cyclin-dependent kinase 1 and calcineurin respectively (Chircop *et al.*, 2011). This site appears to be a major phosphorylation site (~80%) and is linked to the regulation of cytokinesis. Mutation at this site, to produce a phospho-mimetic or phospho-deficient dynamin, did not affect CME or bulk endocytosis (Chircop *et al.*, 2011).

Dynasore (DYN) is a rapid, selective and potent inhibitor of the GTPase activity of dynamin 1, 2, Drp1 and mitochondrial dynamin (at $\geq 80 \mu\text{M}$). After its discovery in 2006, it has been extensively used in various model systems to study SV endocytosis (Macia *et al.*, 2006; Lu *et al.*, 2009; Chung *et al.*, 2010). It has also been established that the inhibition of dynamins by DYN has no immediate effect on the SV exocytosis. The majority of the previous research involving pre-synaptic neurons as a model system have used between $80 \mu\text{M}$ to $160 \mu\text{M}$ DYN to completely block endocytosis (Newton *et al.*, 2006; Chung *et al.*, 2010). In this study, $160 \mu\text{M}$ DYN was used to ensure complete inhibition of all the dynamins that are normally blocked by DYN.

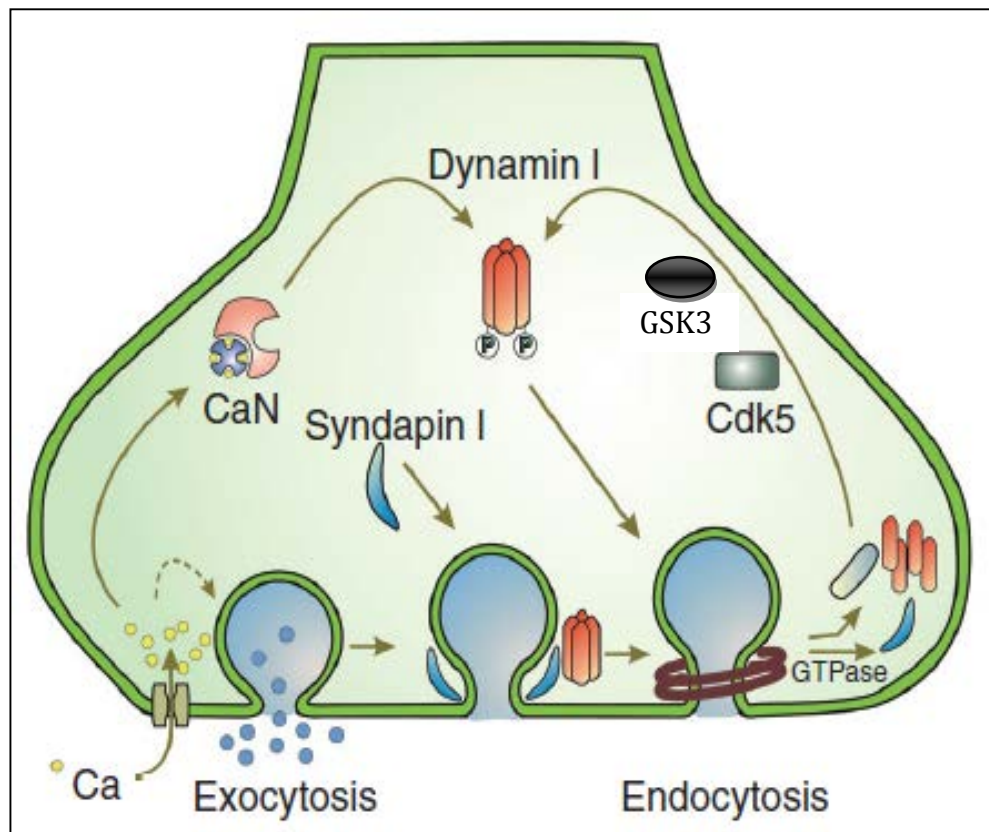


Figure 1.7: The regulatory cycle of dynamin in relation to vesicle endocytosis.

The influx of Ca^{2+} during a stimulus induces synaptic vesicle exocytosis with the help of syndapin-I (please note that many other proteins are involved as discussed earlier). The influxed Ca^{2+} also activates calcineurin (CaN) which will then dephosphorylate dynamin-I making it active. The activated dynamin-I can then form the rings around the neck of the fused vesicle membrane and its GTPase activity will lead to the recycling of the vesicle and dissociation of dynamin-I, syndapin-I and other associated proteins. Following the passage of the stimulus, Cdk5 and GSK3 will rephosphorylate dynamin thereby replenishing the cytosolic pool of phosphorylated dynamin-I. (Adapted from results obtained by Robinson and colleagues, eg. Clayton et al. (2009).

1.7 Myosin II

The non-muscle myosin-II has a diverse cellular function and is composed of a pair of heavy chains (HCs), a pair of essential light chains and a pair of regulatory light chains (RLCs) (Figure 1.8). The myosin-II has been proved to be involved in the mobilization of RP to near the synaptic membrane (Ryan, 1999). Recently, it has been suggested that dephosphorylated myosin-II can act as a molecular motor by hindering the dilation of fusion pores thereby possibly regulating the size of the pore (Neco, *et al.*, 2008). Moreover, it can also regulate the amount of vesicular release by manipulating the duration of the fusion pore opening (Aoki, *et al.*, 2010).

It has been widely accepted that phosphorylation of myosin-II regulates the motor activity and filament assembly. During many cellular events, the myosin-II HCs and RLC are phosphorylated thereby regulating its function. The phosphorylation on Ser 19 of the RLC stimulates the actin-activated ATPase of myosin-II and promotes the assembly of myosin-II into filaments. This phosphorylation can be carried out *in vitro* by Ca²⁺/calmodulin- dependent myosin light chain kinase (MLCK), Rho kinase or p21-activated kinase. Myosin-II is also a good substrate for protein kinase C (PKC). When activated by phorbol esters (PMA), PKC can phosphorylate Ser 1/2 residues of RLC *in vivo* and it can also phosphorylate Thr 9 *in vitro*. This PKC phosphorylation, not only inhibits the rate of MLCK phosphorylation, but also inhibits the ATPase activity of myosin-II once it is phosphorylated by MLCK (Bresnick, 1999). In case of heavy chains of myosin-IIa, Ser 1917 and Ser 1944 are phosphorylated by PKC and casein kinase II; whereas, on the other hand, Ser 1939 and Ser 1941 of myosin-IIb are phosphorylated by PKC (Bresnick, 1999).

Myosin-II can be selectively but reversibly inhibited by using a cell permeable inhibitor called blebbistatin (Blebb). Blebb has a high affinity and selectivity for the

non-muscle class-II myosin and inhibits them by inhibiting the actin-activated ATPase activity (Kovacs *et al.*, 2004; Shuet *al.*, 2005). In this study, 50 μ M Blebb was used to selectively inhibit the myosin-II.

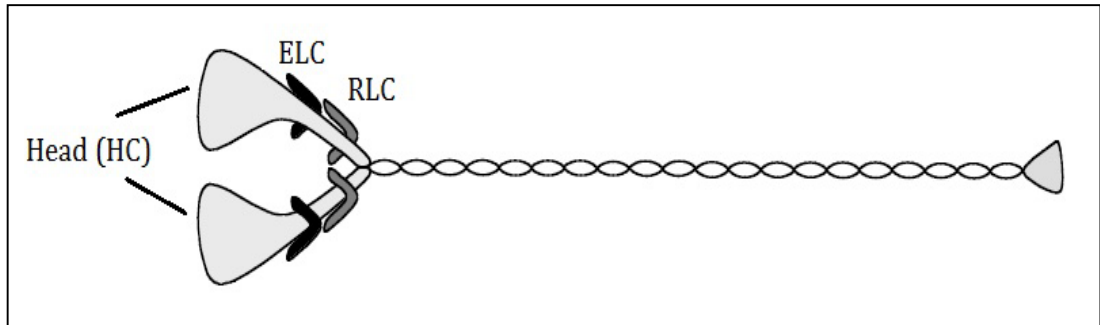


Figure 1.8: Schematic representation of structure of myosin-II. The long coiled structure represents the two heavy chains (HC) and the globular amino-terminal head contains ATP and actin binding sites. Two essential light chains (ELC; black) and two regulatory light chains (RLC; gray) which regulate the function of myosin-II are also shown. The regulatory light chains contain many of the phosphorylation sites identified so far. (Bresnick, 1999)

1.8 Working hypothesis

Previous research by A. Ashton and colleagues provided evidence for the existence of KR in synaptosomes and also demonstrated that the two modes of exocytosis, KR and FF, can be regulated by regulating various phosphatases and kinases (Unpublished observations). Since dynamins and myosin-II are phosphor-proteins that have been previously shown to regulate the fusion pore in various non-neuronal systems, it was hypothesised that these proteins may also be involved in the regulation of the fusion of small synaptic vesicles in the central nervous system. Furthermore, their contribution to the closure of fusion pores to induce KR exocytosis should depend upon their phosphorylated state.

1.9 Main Aim

The main aim of this study was to determine the role of dynamins and myosin-II in the regulation of the mode of SV exocytosis and to establish the identity of phosphatases and kinases that would regulate the functions of these proteins in this process. Finally, an attempt was made to establish a link between specific phosphoregulation sites on dynamin-I and the role of this protein in regulating the mode of exocytosis by the use of phospho-serine specific antibodies and western blotting of synaptosomal samples that were known to be undergoing a specific mode of exocytosis.

1.9.1 Specific Aims

1. To determine if dynamins (I and II) played any role in regulating the mode of SV exocytosis.
2. To determine if myosin-II can regulate the fusion pore of exocytosing SVs.
3. To investigate if phosphatases like PP2A and calcineurin can affect the mode of exocytosis.
4. To determine if protein kinase C is involved in the regulation of the fusion mode.
5. To investigate the relation between various phosphatases, kinases and proteins (identified herein) for their role in regulating the SV exocytosis mode.
6. To identify specific phosphorylation sites of dynamin-I important for their regulation of the mode of exocytosis.

Chapter 2

Materials and Methods

2.1 Preparation of Synaptosomes

The synaptosomes – pinched off nerve terminals – prepared from the cerebral cortex of the adult male Wistar rats (Charles River, USA) were used as a model system in this study. The synaptosomes are well established model system that contained all the machinery required for the neurotransmitter storage and release via SVs. They exhibited the normal physiological properties of a pre-synaptic neuron and responded well to the pharmacological treatments (Fernandez-Busnadiego *et al.*, 2010).

In order to obtain the synaptosomes, the rats were killed humanely by cervical dislocation and the cerebral cortex was swiftly removed and placed into 320 mM sucrose plus 10 mM Hepes (pH 7.4; 4 °C) buffer (homogenisation buffer; Figure 2.1). This tissue was then homogenised using a motor driven Teflon (pestle)-based homogeniser (Potter-Elvehjem tissue homogenizers) that was especially made for preparing synaptosomes. The shear force is provided by the rotating pestle (900 rpm) and the clearance of 150 µm ensures the production of intact and functional synaptosomes (Sihra, 1997). This was then centrifuged at $1941 \times g$ for 10 min to separate the cell bodies from the synaptosomes. The supernatant was then centrifuged at $21,075 \times g$ for 20 min followed by the suspension of the resulting pellet, containing the synaptosomes, in basal physiological buffer (L_0). The suspension was again centrifuged at $21,075 \times g$ for 20 min and the pellet, thus obtained, was re-suspended in 16ml of oxygenated L_0 buffer (4 °C). Once prepared, the synaptosome suspension was constantly gassed with Oxygen. These synaptosomes represent the P2 fraction and were not purified further.

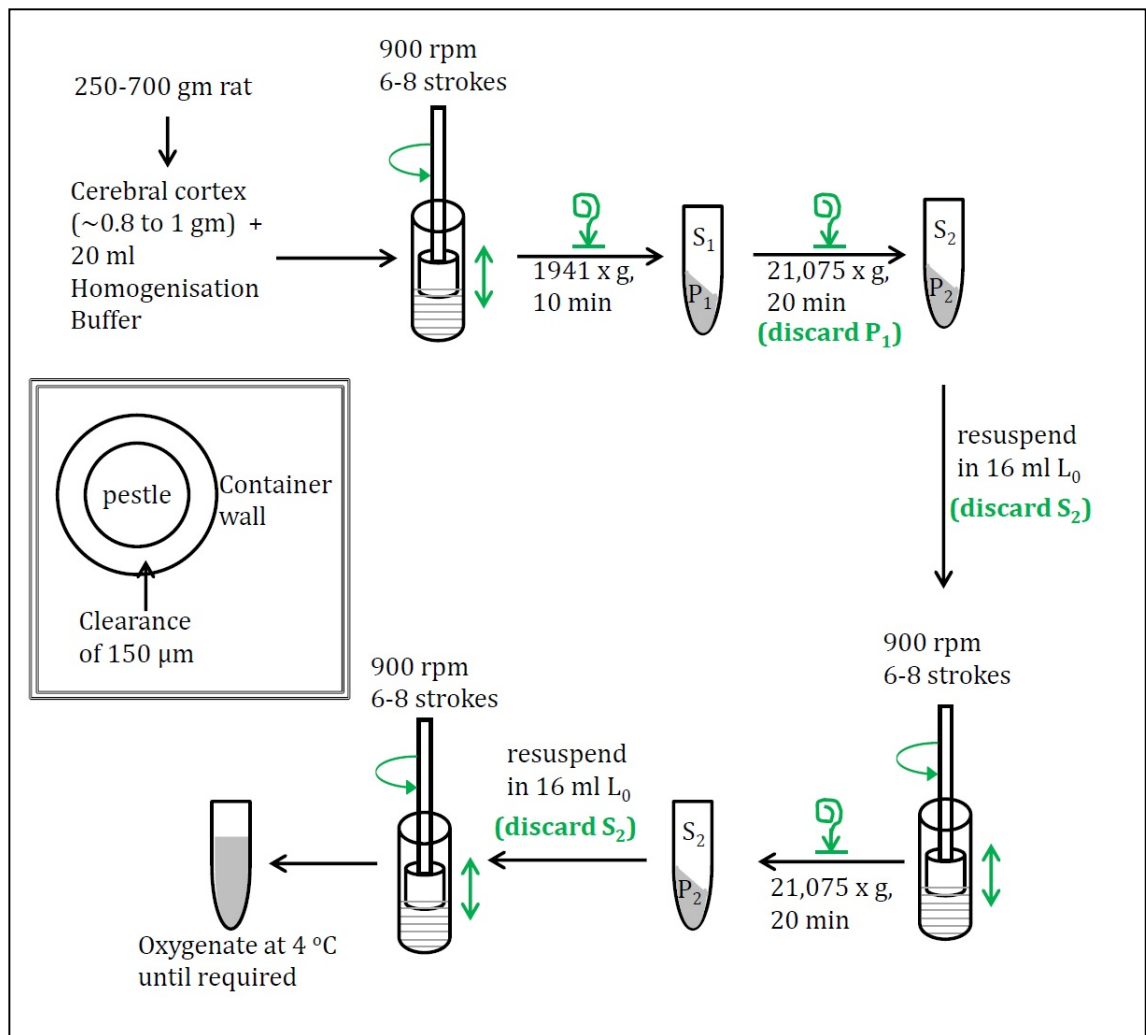


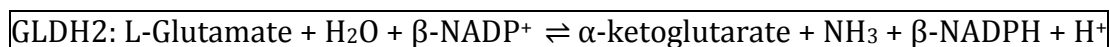
Figure 2.1: Schematic representation of synaptosome preparation from rat cerebral cortex.

2.2 Glutamate Release Assay

2 ml of the synaptosomes, prepared by using method described in 2.1, was washed (with L_0 buffer) and re-suspended in 1 ml of L_0 buffer at RT (between 20-22 °C). The suspension was then stimulated with 30 mM K^+ and 5 mM $[Ca^{2+}]_e$ (HK5C) – that caused all the releasable vesicles to exocytose – for 90 sec. The synaptosomes were then incubated at RT for 10 min. It should be noted that although these previous two steps are not related to the actual assay itself, they were performed in order to treat the synaptosomes identically to those synaptosomes used for the FM2-10 dye release assay – where a pre-stimulation with HK5C is required to load terminals with the dye. Thus, these two extra steps make it possible to directly compare the results from the two studies due to identical sample treatments. After this, the synaptosomes were incubated with the relevant drug or the equivalent amount of solvent (dimethyl sulfoxide (DMSO); for control samples) at 37 °C for 5 min unless stated otherwise. The samples were then washed and finally re-suspended in 1.6 ml of L_0 buffer plus the corresponding amount of drug or DMSO (to compensate for the reversibility of certain drugs) unless stated otherwise. 121 μ l aliquots of these were then added to the 12 wells of a row of Greiner 96 well microtitre plate (black with transparent bottom) that already contained 20 μ l of L_0 buffer (see Figure 2.2).

After this, 10 μ l of 20 mM β -NADP⁺ (1 mM final) and 9 μ l of glutamate dehydrogenase type-II (GLDH2; 36 mUnits final) were added to each well and the resulting mixture was incubated at RT for 10min. At this stage, all the glutamate present outside the synaptosomes – if any – would be converted to α -ketoglutarate by GLDH2 in the presence of a cofactor β -NADP⁺ which itself was converted to β -NADPH. Although the oxidative deamination of glutamate by GLDH2 is a reversible

reaction, in these experiments the reaction always favours forward direction due to loss of ammonia from the open well plate.



The production of β -NADPH produced “background” fluorescence at this step (since it is a fluorophore unlike its oxidised state) and helped in an indirect quantification of the glutamate released from synaptosomes upon stimulation with the relevant stimulus. This step ensured that there was no glutamate left in the extracellular buffer prior to the stimulation of the synaptosomes and that after the stimulation, only the glutamate released by SVs contributes to the increase in fluorescence.

After the incubation, wells 6-12 were treated with the desired stimulus, but without $[\text{Ca}^{2+}]_e$ (for e.g., K^+ concentration was raised to 30 mM if the stimulus to be used was HK5C) and the corresponding Ca^{2+} containing stimulus to the wells 1-5 (e.g., 30 mM K^+ plus 5 mM Ca^{2+} in case of HK5C). The effect of these stimuli was then measured in wells 1-9 using Tecan GENios Pro™ plate reader (at excitation wavelength: 340 nm; emission wavelength: 465 nm; gain: 70; read mode: bottom; and for 21 cycles/308 sec). The measurement was performed for approximately 5 minutes in order to ensure that all the glutamate exocytosed from synaptosomes is hydrolysed by GLDH2. Following the measurement, a volume of 10 μl of L_0 buffer was added to wells 7-9 and 10 μl of 1 mM glutamic acid (freshly prepared) was added to wells 10-12,. The effect of the addition of 10 nmol of Glu was then measured for 15 cycles/194 sec (in wells 7-12) using the same settings. This last step was crucial as it helped in, after complex calculations (see appendix A.1), converting the arbitrary fluorescence units into glutamate release (nmole/mg

protein) if required and also helped in normalising the sensitivity of the overall assay.

In initial assays we looked to see when all the glutamate that was released had been hydrolysed by GLDH2 so that the fluorescence signal plateaued at this point. At room temperature, this took over three minutes and to ensure that we did measure maximal release we set the time to be approximately five minutes which translates to 21 cycles for the measurement of 9 wells. Also, only 9 wells were used for the initial measurement because the use of 9 wells conveniently gave us just over five minutes of measurement for 21 cycles. Using more wells would have taken longer or we would have less individual time points. The use of wells 7-9 and 10-12 were adapted earlier by A. Ashton and was not changed during this research (continued excluding well 6 for final measurement) as addition of one more row would mean longer time required for the assay and would generate less data points per minute.

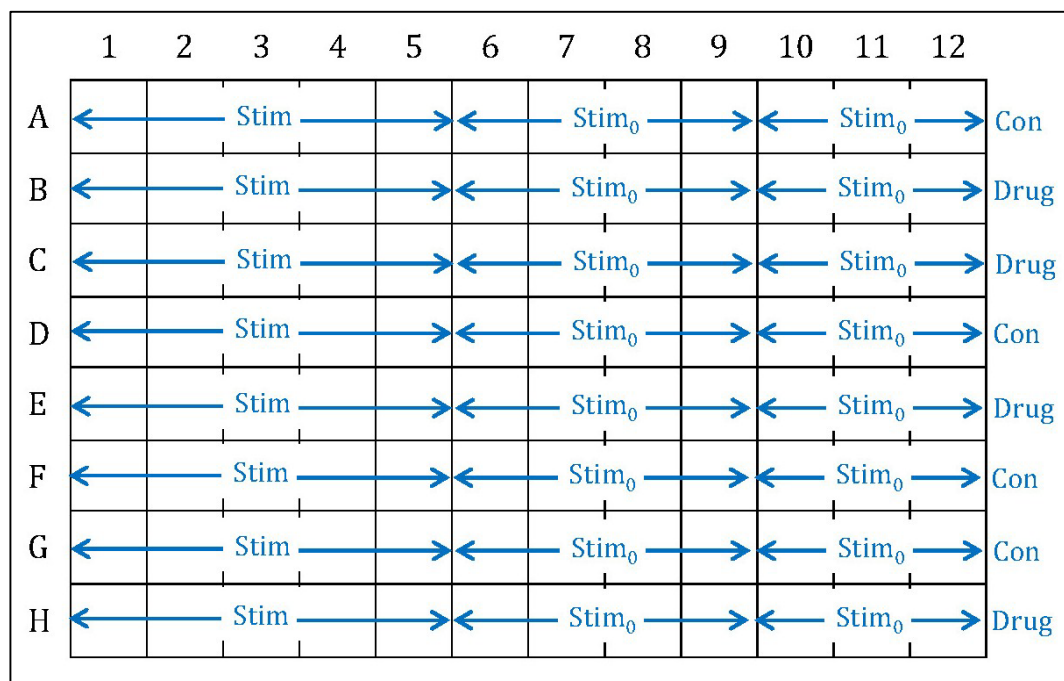


Figure 2.2: A schematic representation of the generalised microtitre plate setup used during glutamate measurement assay. For each row, wells 1-5 were used for stimulated samples while 6-12 were used for corresponding basal buffer. Following this measurement, wells 10-12 were used for glutamate quantification (by adding 10 nmol glutamic acid, final) while wells 7-9 were used for background subtraction. Among independent experiments, the sequence of drug and control samples was shuffled among different rows in order to compensate for the differences in time delay between synaptosome preparation and final fluorescence measurement.

2.3 FM2-10 Dye Release Assay

For each test (represents wells 1-8 of a row on microtitre plate), a volume of 2 ml synaptosomes, prepared by using method described in 2.1, was gassed with O₂ at RT for 15 min after which the synaptosomes were washed and re-suspended in 1 ml L₀ buffer. To this, 100 µM of FM2-10 dye was added and incubated for 60 sec followed by stimulation with HK5C for 90sec. During this stage, all the releasable SVs (RRP and RP) were released (see section 3.4) thereby facilitating the labelling of these vesicles by FM2-10 dye. After the incubation, the stimulus was removed (by centrifugation at 9589 x g for 45 sec) and the synaptosomes were re-suspended in 1ml L₀ with 100µM of FM2-10 dye and incubated for 5 min. This step ensured that even the vesicles that might take several minutes to internalise (for e.g. RP SVs) were labelled with the dye, thus all the releasable SVs contained dye. After this, the synaptosomes were treated with the desired amount of drug of interest or equivalent amount of DMSO (v/v; for control samples) and incubated at 37 °C for 5 min (unless stated otherwise) giving the drug enough time to act on its target. After this point, 1 mM advasep-7 (final concentration) was added to the mixture (at RT). This removed the FM2-10 dye from the synaptosomal plasma membrane reducing the background fluorescence, so that mainly the SVs were labelled with the dye (as advasep-7 is membrane impermeable). This step was followed by repetitive washings before finally re-suspending the synaptosomes in 1.5 ml of L₀ along with the corresponding concentration of the drug or DMSO (to ensure constant presence of the drug in the system thus preventing the reversibility of the drug) unless stated otherwise.

Aliquots of 160 µL were then added to wells 1-8 of a row of a Greiner 96 well microtitre plate (black with opaque bottom; Figure 2.3). Fluorescence

measurements were performed using Tecan GENios Pro™ plate reader (at excitation wavelength: 465 nm; emission wavelength: 555 nm; gain: 40; read mode: top; and for 461 cycles). Just prior to the measurement of each well, the synaptosomes in that well were either stimulated with the desired stimulus (HK5C, ION5C or 4AP5C) or were subjected to the equivalent volume of L₀ by using the injector function of the plate reader. Out of the eight wells from each row, four were stimulated (stimuli samples) and in the remaining four wells equal amount of L₀ (basal) was added to each. This procedure was repeated for all the eight rows of the plate. After the experiment, all the basal data were subtracted from the stimuli data of the corresponding treatment and the resulting data were thus a true representation of the Ca²⁺ dependent SV release, expressed in terms of decrease in fluorescence.

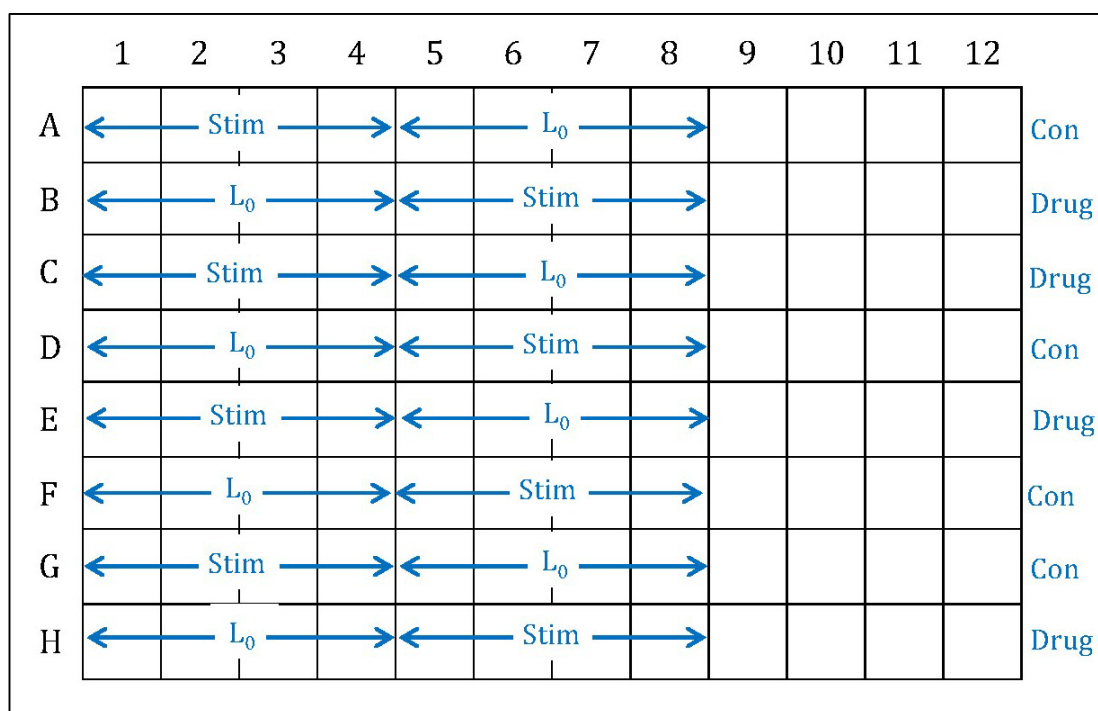


Figure 2.3: A schematic representation of the generalised microtitre plate setup used during FM2-10 dye release assay. For each row, wells 1-4 were used for stimulated samples while 5-8 were used for L₀ basal buffer, or vice a versa. Among independent experiments, the sequence of drug and control samples was shuffled among different rows in order to compensate for the differences in time delay between synaptosome preparation, stimulation and final fluorescence measurement.

2.4 Measurement of Intracellular Free Calcium Concentration

BACKGROUND

In order to estimate the $[Ca^{2+}]_i$ achieved after stimulation, Fura-2-acetoxymethyl ester (Fura-2-AM) assay was used in this study. Fura-2-AM is a cell permeable but Ca^{2+} insensitive ester form of the Fura-2 acid. When Fura-2-AM enters the cell, esterases cleave off the acetoxymethyl(AM) groups leaving the negatively charged Fura-2 fluorophore molecules trapped inside the cell as they are unable to cross the plasma membrane. This acid form of Fura-2 is sensitive to Ca^{2+} which produces maximum fluorescence when bound to Ca^{2+} and excited with 340 nm wavelength. It also produces maximum fluorescence in Ca^{2+} free environment when excited at 380 nm. For both the conditions, the emission wavelength remains at 512 nm. Thus, the concentration of $[Ca^{2+}]_i$ is proportional to the ratio of fluorescence at 340/380 and can be expressed by Grynkiewicz equation (Grynkiewicz *et al.*, 1985):

$$[Ca^{2+}]_i(nM) = K_d \times \beta \times \frac{(R - R_{min})}{(R_{max} - R)}$$

Where, K_d (for Ca^{2+} binding) = 224 nM, R = 340/380 ratio, R_{max} = 340/380 ratio under Ca^{2+} -saturating conditions, R_{min} = 340/380 ratio under Ca^{2+} -free conditions, and β = ratio of average fluorescence at 380 nm under Ca^{2+} -free and -bound conditions.

PROCEDURE

For this set of experiments, synaptosomes were prepared using the method described in section 2.2.1 of this chapter. Synaptosomes were then incubated with 5 μ M Fura-2-AM at 37°C for 30 min while being oxygenated constantly. At this

stage, Fura-2-AM would enter the synaptosomes where it would be hydrolysed by esterases there by trapping the dye inside the synaptosomes. Following the incubation, synaptosomes were washed twice - in small aliquots of 1 ml - with cold L₀ buffer using bench top centrifuge (9589 x g for 45 sec) to remove extracellular Fura-2-AM, if any, before oxygenating the final re-suspension at 4°C until required. From this pool of synaptosomes, a volume of 2 x 0.8 ml of aliquots was taken for each row of microtitre plate to be used for a single test condition. These aliquots of synaptosomes were stimulated with 2 x 0.2 ml of HK5C for 90 sec following which the stimulus was removed by centrifugation at 9589 x g for 45 sec. The resulting pellets were re-suspended in 2 x 0.5 ml of L₀ buffer before finally incubating them at RT for 10 min. Although, these last two steps involving stimulation and incubation of synaptosomes at RT was not required for this assay, they were nevertheless performed in order to make the sample treatments comparable across different assays used in this study (see earlier comments about comparing Glu and FM2-10 dye assay; section 2.2.2).

Following the 10 min incubation period, the synaptosomes were incubated for 5 min at 37 °C with the relevant concentration of drug of interest or an equivalent volume of DMSO for control conditions. The extracellular drug, if any, was then removed by centrifugation followed by washing with 1 ml of L₀ buffer and centrifugation at 9589 x g for 45 sec. The resulting pellet was re-suspended in 1.6 ml of oxygenated L₀ buffer containing the desired concentration or volume of the drug (unless stated otherwise) or DMSO, respectively. A volume of 120 µl aliquots of this re-suspension was then added to each of the 12 wells of a row of a black Greiner 96 well plate along with 40 µl of L₀ buffer in each of the wells making the total volume to 160 µl for each wells. The fluorescence of the Fura-2 was then

measured at excitation wavelength: 340 ± 35 or 390 ± 25 nm; emission wavelength: 535 nm; gain: 30; read mode: top; and for 40 or 160 cycles.

The ratiometric nature of this assay added to the complication of the fluorescence measurement and could be described, in summary, as follows. Each well was measured for its fluorescence one at a time with the first well being measured for 40 cycles at excitation wavelength of 340 nm and emission of 535 nm. Following the 40 cycles of measurement, the well was injected with 40 μ l of either a desired stimulus (see Figure 2.5) or L_0 buffer and measured for 160 cycles. The same method was repeated for well number 2 but in this case the measurement was taken at the excitation wavelength of 390 nm which would be later used to estimate the 340/390 ratio for this pair of wells. For each row, six wells were stimulated with 40 μ l of stimulus and the rest were subjected to 40 μ l of L_0 buffer just prior to the measurement using the injector function of the plate reader. The ratios of 340/390 estimated from wells subjected to L_0 buffer were subtracted from the ratios estimated from stimulated wells in order to estimate the $\Delta[Ca^{2+}]_i$ exclusively due to the external stimulus employed. Thus, each row of 12 wells produced three sets (triplicates) of 340/390 ratio for the given stimulus and drug (or control).

After measuring all the 12 wells of a row, aliquots of 2.25 mM Ca^{2+} and 0.3% Triton X-100 (final concentrations) were added to each of the wells that was previously stimulated with a Ca^{2+} containing stimulant (either 1-6 or 7-12) such that the final volume reached 240 μ l per well. Similarly, for the remaining wells that were subjected to L_0 buffer previously, were treated with a final concentration of 15 mM EGTA (a Ca^{2+} chelator) and 0.3% Triton X-100. Following this, all the twelve wells were measured simultaneously for 40 cycles, first at the excitation wavelength of

340 nm followed by that of 390 nm. These fluorescence values were then used to calculate R_{\max} from those added with extra Ca^{2+} and R_{\min} from those treated with EGTA (see appendix A.2).

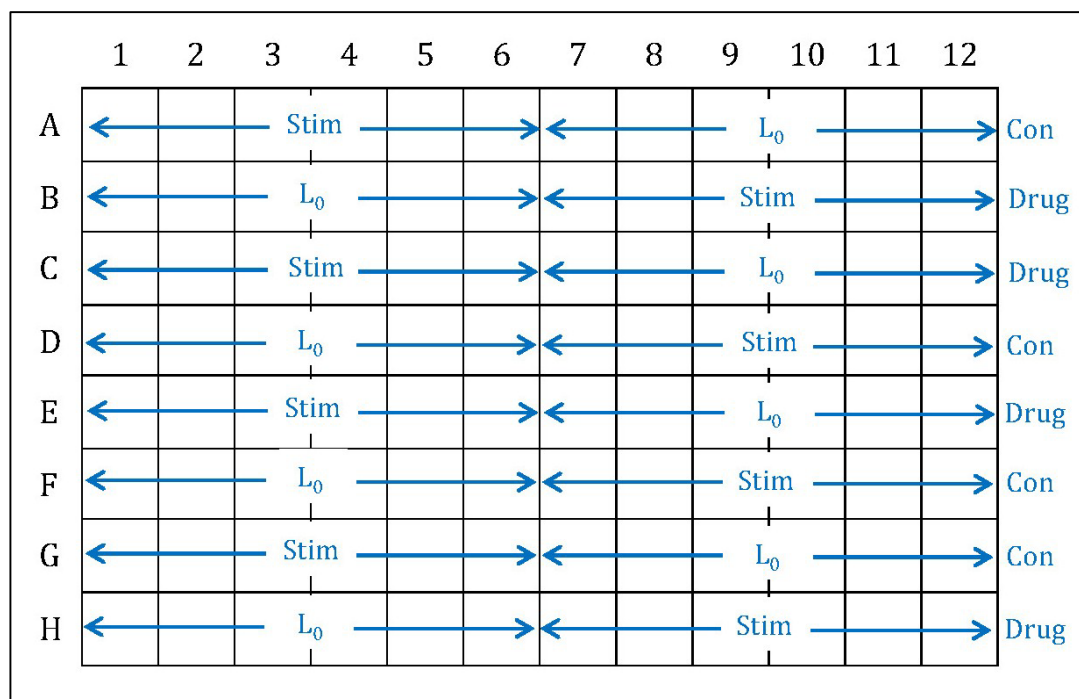


Figure 2.5: A schematic representation of the generalised microtitre plate setup used during Fura-2-AM assay. For each row, wells 1-6 were used for stimulating the samples while 7-12 were used for subjecting them to L_0 basal buffer, or vice a versa. After the first set of measurements were taken, each wells containing a stimulant was used for calculating R_{\max} (e.g. A1-A6 in this case) while the remaining were used to calculate R_{\min} (e.g. A7-A12 in this case). Among independent experiments, the sequence of drug and control samples was shuffled among different rows in order to compensate for the differences in time delay between synaptosome preparation and final fluorescence measurement.

2.5 Result for biochemical assays

All the graphs presented in chapters 3, 4 and 5 represent the average of 2-6 independent experiments with each individual experiment having 2-4 independent sample treatments. For ease of presentation, only selected data points – at an interval of 2-10 sec – are shown with the error bars representing standard error of the means. Two tailed unpaired student t-test was employed to determine the significance level between the two treatments of interest.

For a given sample, the time interval data obtained from individual experiments were averaged together to obtain mean fluorescence, glutamate concentration, or calcium concentration values at various time points with corresponding standard error of means. An unpaired student t-test was performed between two such data points of different samples, at a given time point, to obtain the significance level at that time point. The statistical test was similarly performed on all data points at time intervals of 10-15 sec and if the significance value was less than 0.05 for most of the time points, it was considered a significant difference between the two samples. In graphs, where more than two samples are shown, either the samples were analysed in pairs using student t-test or they were all compared together using two way ANOVA. The sample size (n value) used for performing the statistical tests was the summation of all the independent sample treatments used for producing the average. Please note that a table of information with “n” values and “p” values for all the data presented in chapter 4 and 5 is presented in Appendix A.3.

2.6 Western Blotting

SAMPLE PREPRATION

In order to study the phosphorylation of dynamin-I, Western blotting was employed in this study. For sample preparation, synaptosomes were first prepared from mature rat cerebral cortex using method described in 2.2.1. Following the synaptosomal preparation, the synaptosomes were treated with the desired drug or DMSO exactly as described during the glutamate sample preparation. However, during the final step of re-suspension, the synaptosomes were re-suspended in 225 μ l of L₀ buffer (along with the drug) instead of 1.6 ml of L₀ buffer. From this final re-suspension, 2 x 100 μ l aliquots were taken into new separate microfuge tubes and the remaining 25 μ l was saved for performing Bradford assay to determine the protein concentration in the given sample.

From the 2 x 100 μ l aliquots, one was stimulated with the desired stimulation and the other was subjected to L₀ buffer giving the basal conditions for the corresponding stimulated sample. After stimulating the samples for desired amount of time (typically for 2, 15, 30 and 120 sec in this study), NuPAGE® LDS sample buffer and NuPAGE® sample reducing agent (dithiothreitol) were added to the sample to instantly denature the synaptosomes and all proteins. The samples were then mixed well using a bench top vortex mixer and were heated at 70°C for 10 min before storing them at -20°C until further required. The protein concentration estimated using standard Bradford assay was used to dilute the prepared samples to achieve the final protein concentration of 1.5 mg of protein per ml of sample.

ELECTROPHORESIS

Once all the samples were diluted to the desired protein concentration, proteins in the samples were separated based on their molecular weight by Lithium dodecyl sulphate (LDS)-electrophoresis. The LDS was a constituent of NuPAGE® LDS sample buffer, a product obtained from Invitrogen, UK, and has same functions as that of Lithium dodecyl sulphate (LDS) in protein denaturation and electrophoresis. According to the company, LDS is as effective as SDS and was possibly used to enhance the shelf life of the product. The electrophoresis was performed using Novex® NuPAGE® SDS-PAGE gel system obtained from life technologies, UK. The process of electrophoresis was followed as described in the user manual from the company and can be described in summary as follows. NuPAGE®Novex®4-12% Bis-Tris Midi Protein Gel (12+2 wells) was assembled in the electrophoresis tank as described in the manual and 1 x's NuPAGE® MES SDS buffer was used as the running buffer. To each of the sample wells, 45 µl (67.5 µg protein) was loaded after they were incubated for 10 min at 70 °C. To the remaining two marker lanes, either 7 µl of diluted (1:7 dilution) MagicMark™ XP western protein standard or 7 µl of Novex® sharp unstained protein standard was loaded depending on the desired post-electrophoresis process of western blotting or coomassie protein stain respectively. The electrophoresis was then carried out for 90 min by applying a constant electric current of 120 mA (0.867 mA per cm² of gel) across the height of a gel such that the electron flow is from top of the gel (towards sample wells) to the bottom of the gel. After electrophoresis, the gel was removed from its plastic housing and was subjected to either standard coomassie protein staining method using SimplyBlue™ SafeStain or was subjected to western blotting as described in the following paragraph.

WESTERN BLOTTING AND DETECTION

Following electrophoresis, the separated proteins were transferred on to a Polyvinylidene fluoride (PVDF) membrane using an iBlot system from Invitrogen. After LDS-PAGE, the gel was set up on iBlot® PVDF transfer stack as described in the user manual and the western blotting was carried out by using P3 programme (20 V; 7 min) on iBlot® gel transfer device. Following the protein transfer, the PVDF membrane was blocked using 30 ml of blocking buffer (3% dried milk powder, 1% Tween-20 in TBS; pH 7.4) for 60 min. After this point, the blocking buffer was removed and the PVDF membrane was incubated with the desired concentration of desired primary antibody (see table 2.1) for 60 min at RT. Following the incubation, the antibody solution was removed from the system and the PVDF membrane was washed for 6 x 5 min using washing buffer (TBS) and bench top shaker/rocker. The PVDF membrane was then incubated with the relevant HRP conjugated secondary antibody for 60 min at RT followed by washing as described earlier. After the final wash, the PVDF membrane was incubated for 120 sec with a volume of SuperSignal™ west dura chemiluminescent substrate such that it covers the entire PVDF membrane (3 ml in this case). The PVDF membrane was then visualised using ChemiDoc™ XRS+ with image lab software (version 3.0.1 β) obtained from Bio-Rad.

RE-PROBING PVDF MEMBRANES

Each of the blots that were previously probed for any of the phosphoserine sites were stripped using a stripping buffer called Restore™ Plus Western Blot Stripping Buffer, obtained from Thermo scientific, USA. This proprietary buffer composition is not revealed by the company. However, like all the stripping buffers, this buffer is probably composed of a surfactant (like SDS) and a reducing agent to reduce

disulfide bonds (like β -mercaptoethanol) dissolved in an acidic buffer (like Tris-HCl).

Following the visualisation using ChemiDoc XRS+ system, the blots were washed in 25 ml of washing buffer for 3 x 5 min. Following the washing, the blots were incubated in 15 ml of the Restore™ Plus Western Blot Stripping Buffer at RT with gentle shaking throughout the incubation period. After the stripping step, the blots were washed for 4 x 5 min with 25 ml of washing buffer to remove excess stripping buffer. Following this the membranes were blocked using 25 ml of blocking buffer as described earlier and subsequently probed with desired primary antibody, anti-dynamin-I 4E67 in this case.

Table 2.1: Table of information showing the concentrations of various antibodies used in this study.

Name	Source	Dilution factor	Final concentration
Dynamin-I (4E67)	Mouse monoclonal	1:1000	0.2 μ g IgG/ml
p-Dynamin I (Ser 774)	Sheep polyclonal	1:1000	No information available for stock concentration
p-Dynamin I (Ser 778)	Sheep polyclonal	1:400	No information available for stock concentration
p-Dynamin I (Ser 795)	Goat polyclonal	1:150	1.33 μ g IgG/ml
Anti-mouse IgG-HRP	Goat	1:5000	0.08 μ g IgG/ml
Anti-sheep IgG-HRP	Donkey	1:5000	0.08 μ g IgG/ml
Anti-goat IgG-HRP	Donkey	1:5000	0.08 μ g IgG/ml

QUANTIFICATION OF BANDS FROM BLOT IMAGES

ChemiDoc XRS+ system detects the chemiluminescence of protein bands on the blots and the signal intensity of the bands is directly proportional to the amount of protein present in corresponding bands. The band intensity also has a direct relation between the exposure time period and thus if a blot is exposed for an excessive duration, the intensity of the bands will increase and thus this would contribute to the error in subsequent quantification of the bands. The semi-quantification carried out in this thesis should eliminate such discrepancies arising out of exposure time period, as all the bands are expressed as relative to one another. However, it is possible that if a blot has varying protein quantity per band – as with blots probed with phosphoserine antibodies – the darkest band(s) may become overexposed by the time other faint bands appear with acceptable intensity. For this reason, the blots were exposed for varying exposure time periods – by utilising auto exposure feature – to select a range of optimal exposure periods where the intensity of the band still maintains a linear relationship with the protein quantity. The same blot was then exposed manually for 3-4 different time periods (in the linear range determined by auto exposure) to get multiple images of the same blot.

Once multiple images – exposed for different time periods – of a blot was obtained, the bands of interest were quantified using volume calculation function of the software and were then averaged together. The volume analysis tool of the software allows the user to draw a rectangle around the band of interest and the software then provides the summation of intensities of each pixel in the rectangle (a given protein band) in arbitrary units. Before summation, the software also subtracts the average intensity of all pixels immediately surrounding the drawn

rectangle (local background) from each pixel inside the rectangle. This local background subtraction helps in reducing the error in quantification due to uneven background across the blot, if any. The arbitrary unit thus generated is directly proportional to the intensity of the band and therefore to the amount of protein or phosphorylated protein in a given band. Once all the bands present on a blot were quantified in this manner, they were expressed as a percentage of a particular selected band – generally, unstimulated control sample – in order to get the relative quantities of protein present in the given set of bands.

The semi-quantification process was repeated for 2-3 independent experiments and the resulting values were averaged together and are presented in histograms of chapter 6. The error bars in these histograms represent standard error of the means and their statistical significance was calculated using unpaired student t-test (α level at 0.05). Although the blots presented in chapter 6 gives clear visual evidence of the differences in protein quantities present per band, the semi-quantification (and resulting histograms) provides a means to perform a statistical significance test on these differences.

Chapter 3

Studies to Establish Optimal Conditions for Investigating Synaptic Vesicle Exocytosis

3.1 Introduction

This chapter aims at establishing optimal experimental conditions required in order to distinguish between the two modes of SV exocytosis, viz. KR and FF. These optimal conditions were previously established by Dr. A Ashton before inception of this project. The data presented in this particular chapter is a combination of results obtained by Dr. A. Ashton's previous work and the work carried out as part of this project. These are presented here purely to aid in better understanding of the study.

3.2 Justification for the Interpretation of Results

This study mainly aimed at investigating the effects of various drugs on the mode of SV exocytosis using the FM2-10 dye release assay and glutamate assay. The glutamate assay was used in this study as the cerebral cortex – used to prepare the synaptosomes – consisted of more than 80% glutamatergic neurons that release glutamate as their neurotransmitter via SVs (Omiatek *et al.*, 2010).

It has been established that in order for the FM2-10 dye to be maximally released from the loaded SVs, the SVs need to undergo the FF mode of exocytosis as this exposes the internal SV membrane to the extracellular milieu for a relatively longer duration giving the dye enough time to be released, thereby losing its fluorescence (Cheung & Cousin, 2011; Omiatek *et al.*, 2010). On the other hand, the glutamate can be fully and quickly released even if the exocytosis is via a transiently open fusion pore as observed during KR (Omiatek *et al.*, 2010; Zhang *et al.*, 2007). Thus, the release of glutamate occurs during both, KR and FF whereas the FM2-10 dye requires FF mode of exocytosis for its release. Thus, if a drug has no effect on the glutamate release but can affect the FM2-10 dye release, then one can say that the drug is affecting the mode of SV exocytosis (see Figure 3.1).

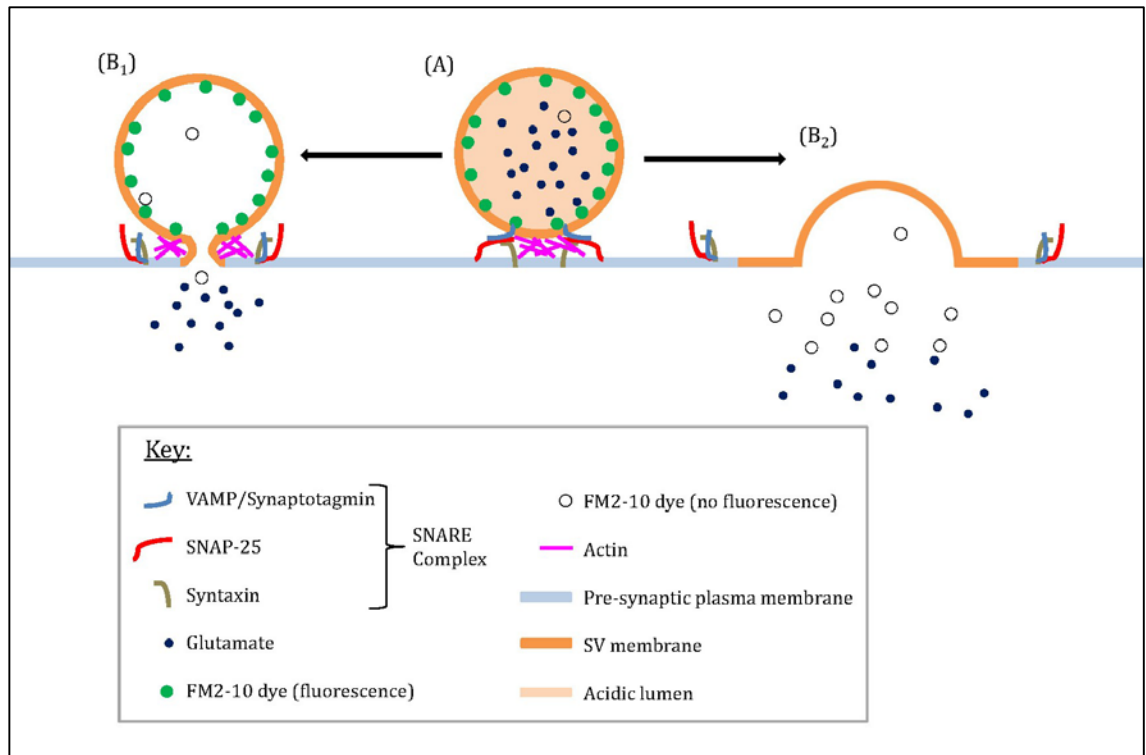


Figure 3.1: A schematic representation of the rationale behind the interpretation of the results/data. (A) A SV can undergo exocytosis either via (B₁) KR where Glu is maximally released but FM2-10 dye is not or via (B₂) classical FF mode of exocytosis where both, Glu and FM2-10 dye are maximally released. This efflux of FM2-10 dye from the SV membrane causes it to lose its fluorescence. Thus when the Glu release remains unaltered, differences in FM2-10 dye fluorescence can be used to identify the mode of SV exocytosis. Representation is over simplified, not true to scale and many other proteins involved in these processes are not shown/known.

It could be argued that the FM2-10 dye may be released by means other than SV exocytosis and in such situation one would be measuring fluorescence changes that cannot be fully attributed to SV exocytosis. In the absence of Ca^{2+} , A. Ashton has shown that HK and 4AP stimulations fail to release any FM2-10 dye from the synaptosomes. Therefore, FM dye release is Ca^{2+} dependent, a classic criterion for SV exocytosis. If we had the relevant safety approvals, this could perhaps be demonstrated by prior treatment of synaptosomes with clostridial neurotoxins e.g. botulinum type A toxin or tetanus toxin. However, this experiment is not as easy as one might expect, because one may have problems in loading SVs with dye during the intoxication. However, in work presented here and A. Ashton's unpublished work there is always a close correlation between the amount of Ca^{2+} dependent Glu exocytosis and FM2-10 dye exocytosis (under conditions where all release is by full fusion).

3.3 Achieving Maximal Glu Release

For the direct comparison of FM2-10 dye and Glu release data, it is also necessary that the stimuli employed in the study produces maximal Glu release and thereby induces the maximum number of SVs to release (RRP and RP). Submaximal Glu release would make it impossible to determine if a particular drug has an effect on the distinct pools of SVs and such drug treatment could even have excitatory or inhibitory effects on these different pools which may not be apparent. In order to establish this condition, various secretagogues employed in this study were used in the presence of different $[Ca^{2+}]_e$ and the data is presented in Figure 3.2. It is evident that 5 mM $[Ca^{2+}]_e$ produces the maximal Glu release and any further increase in $[Ca^{2+}]_e$ either has no effect on the Glu release (for e.g. HK) or decreases the Glu release, as seen with ION and 4AP. Thus, for all the study, a concentration of 5 mM $[Ca^{2+}]_e$ was used to stimulate the synaptosomes unless otherwise stated. The biphasic response to $[Ca^{2+}]_e$ as seen here has been described previously and was not further investigated herein.

Figure 3.2 also shows that 4AP5C produces much lower Glu release when compared to HK5C and ION5C. The changes in $[Ca^{2+}]_i$ upon stimulation are presented in Figure 3.3 which provides a possible explanation for this. 4AP5C produces much smaller change in $[Ca^{2+}]_i$ relative to the other two stimuli and thus it can only release a part of the releasable SVs (Ashton *et al.*, unpublished work). It has been previously established in Dr. A. Ashton's laboratory that these SVs belong to the RRP and the other two stimuli release both, RRP and RP (data not presented). It is also note worthy that even though HK5C and ION5C eventually achieves the same level of $[Ca^{2+}]_i$, the kinetics associated with $\Delta[Ca^{2+}]_i$ is different. HK5C produces much of its increase in the $[Ca^{2+}]_i$ during the initial stimulation period which

eventually plateaus (<10 sec) probably due to the densitisation of VGCCs (Bähring & Covarrubias, 2011). On the other hand, ION5C produces an increase in the $[Ca^{2+}]_i$ at a slower rate and continues to do so during the rest of the stimulation period eventually achieving the same magnitude of change in $[Ca^{2+}]_i$ as that observed during stimulation with HK5C.

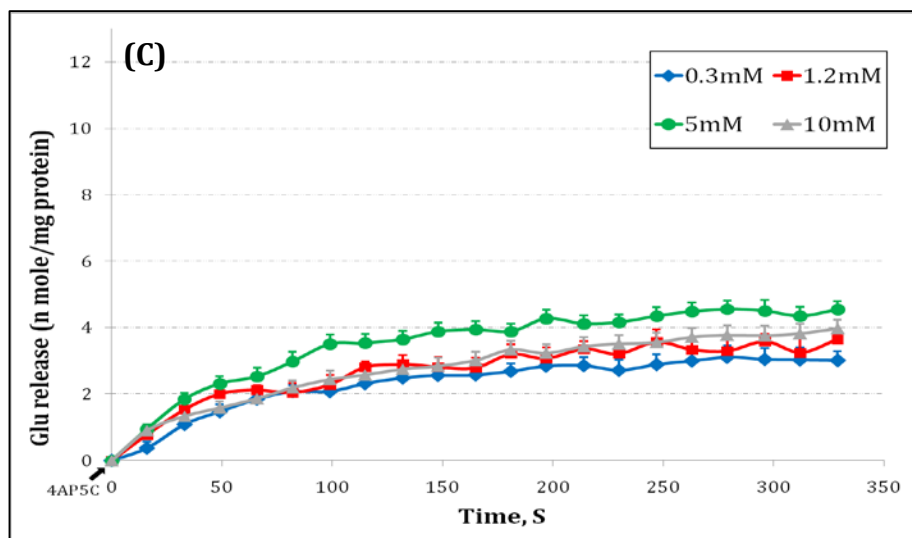
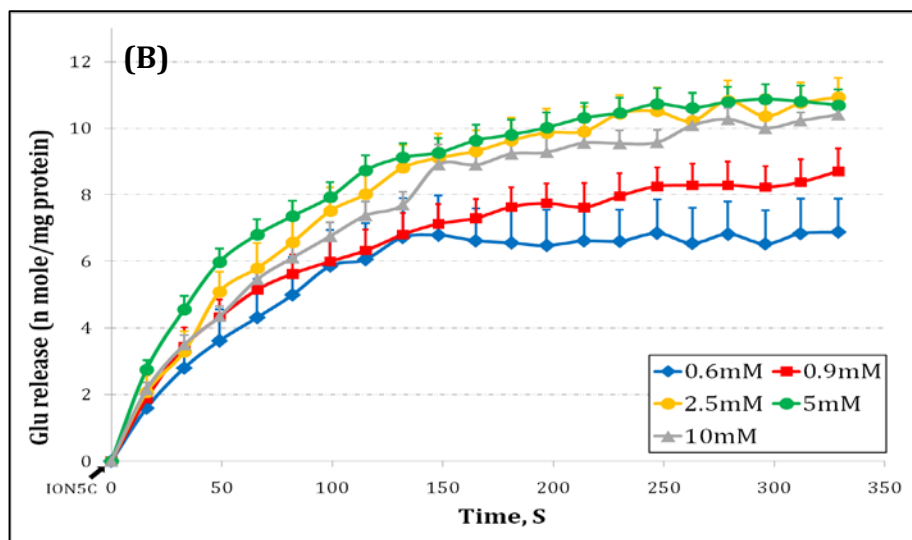
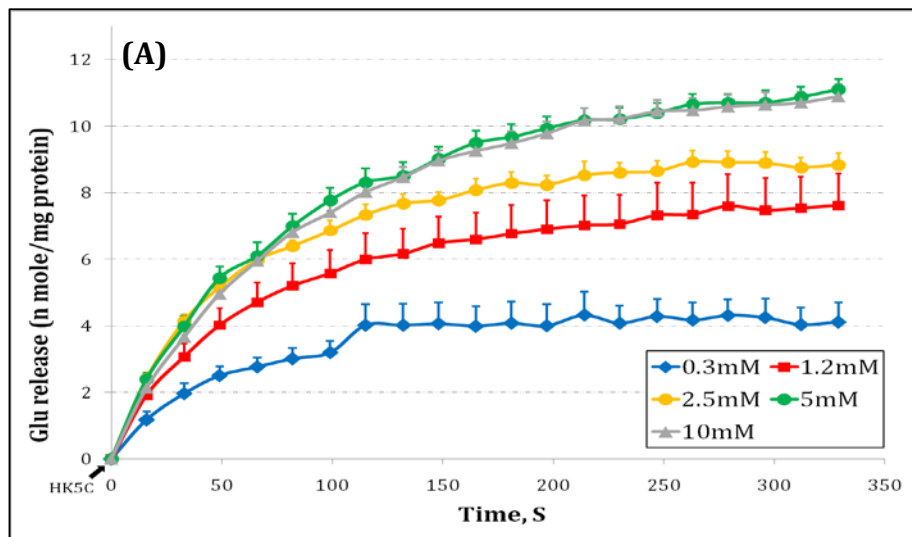


Figure 3.2: Measurement of evoked glutamate in the presence of various extracellular calcium concentrations show that 5 mM $[Ca^{2+}]_e$ induces maximum glutamate release for all the three secretagogues (A) HK (B) ION and (C) 4AP (independent experiments ≥ 3). The data in this Figure represents an average of author's and A. Ashton et al.'s experiments.

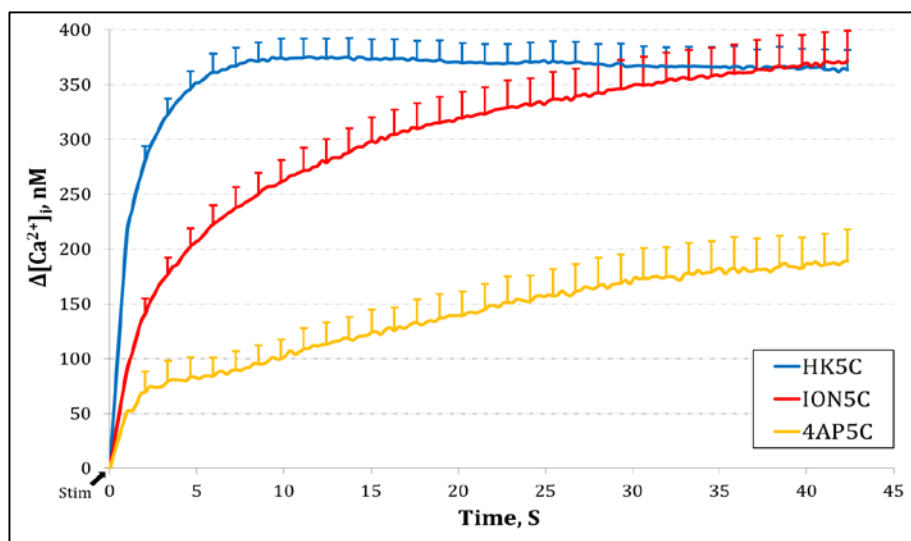


Figure 3.3: Measurement of cytosolic free calcium show that all the three stimuli employed in this study produced a change in $[Ca^{2+}]_i$ with different kinetics and the final $[Ca^{2+}]_i$ achieved was much lower for 4AP5C when compared to that of HK5C or ION5C stimulations (independent experiments ≥ 3). The data in this Figure represents an average of author's and A. Ashton et al.'s experiments.

3.4 SVs Undergo Only One Round of Exocytosis

The synaptosomes in this study are subjected to a long duration of stimulation and measurement (typically between 60 – 330 sec) due to the kinetics of the FM2-10 dye release and the GLDH2 assay. Thus, there is the possibility that the SVs can undergo multiple rounds of exocytosis during stimulation/measurement period. If this occurs, then the recycled vesicles could re-load with neurotransmitter – in this case Glu – and release it in the extracellular buffer there by contributing to the amount of Glu released. On the other hand, once a SV loses its FM2-10 dye, it cannot be re-labelled during the subsequent release cycles and thus no dye will be released. It is also possible that the SVs can undergo several rounds of Glu release (by KR) before ultimately releasing their FM2-10 dye content (by FF). Thus, in order to compare the Glu and FM2-10 dye release assay for mode determination, it is necessary to establish that the SVs undergo only one round of release throughout the stimulation/measurement period.

This hypothesis was tested by acutely treating the synaptosomes with 1 μ M bafilomycin A1 which irreversibly blocks the Glu reloading in all the SVs by blocking the vacuolar H⁺ATPase pump that is required for SV reacidification after endocytosis. It has been shown, however, that the BAF does not affect the Glu content of the non-exocytosed SVs and does not interfere with their release under these acute conditions (Ikeda & Bekkers, 2008). In the current study, a concentration of 1 μ M BAF was added to the synaptosomes at the same time as the stimulus and the Glu release was measured. If the SVs were undergoing multiple rounds of exocytosis, then the Glu release during control conditions would be higher than the acutely treated BAF synaptosomes. It is apparent from Figure 3.4 that this acute treatment produced the same Glu release as the control

synaptosomes for all the three stimuli employed indicating that there was only one round of SV fusions. Thus one can compare the Glu and FM2-10 dye release assays of this study in order to determine the mode of SV exocytosis.

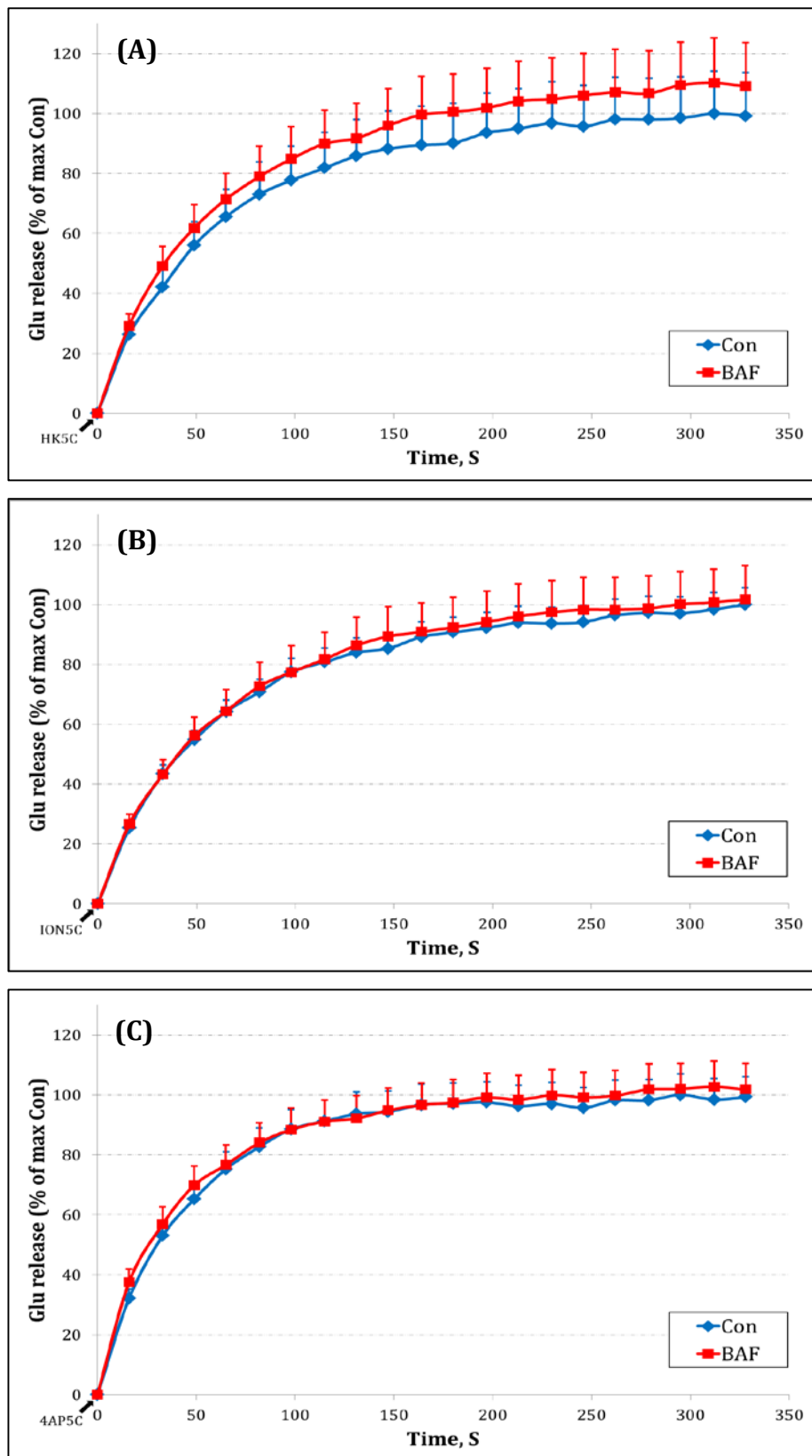


Figure 3.4: The amount of Glu released by SV exocytosis is not affected by the acute treatment of 1 μ M BAF during (A) HK5C, (B) ION5C and (C) 4AP5C stimulation (independent experiments \geq 3). Please note that the data in this Figure is a courtesy of A. Ashton et al. and author did not directly contribute towards these experiments.

3.5 Maximal labelling of Synaptic Vesicles by FM2-10 dye

In all experiments reported herein, 100 μ M FM2-10 dye was employed. This was the concentration employed by many researchers (Cheung *et al.*, 2010; Baldwin *et al.*, 2003). However, a study conducted by Clayton *et al.* (2008a) suggested that the labelling of SVs via bulk endocytosis using FM2-10 dye was actually dependent on the concentration of the dye used with FM2-10 dye being able to label the bulk endocytic membrane only at 1 mM concentration. They claimed that 100 μ M FM2-10 dye (as used in this study) failed to label all of the endocytic membrane retrieved through bulk endocytosis (Clayton *et al.* 2008a), and that a great majority of SVs would recycle via bulk endocytosis during strong stimulation paradigms (Clayton *et al.* 2008b). This paper is very confusing and convoluted since these authors had previously used 100 μ M FM2-10 dye and it has provided them with much of the evidence for their conclusions about bulk endocytosis (Clayton *et al.* 2008b). In fact, it is not clear that the interpretations are correct (Clayton *et al.* 2008a), but just to ensure that the results reported, herein, are valid (due to labelling of all releasable SVs), some experiments were performed using 1 mM FM2-10 dye.

The data presented in Figure 3.5 clearly demonstrates that in our model system, all the releasable vesicles are labelled with either 100 μ M or 1 mM FM2-10 dye and that the drug treatment does not preferentially affect the FM2-10 dye labelling or its release during subsequent exocytosis according to initial dye concentration employed. Similar results were obtained with HK5C stimulation and Blebb or OA treatment (data not shown). Thus it can be concluded that 100 μ M FM2-10 dye can be used – at least for the model system used in this study – to study SV exocytosis

and that the dye is able to label all the releasable vesicles at the given concentration.

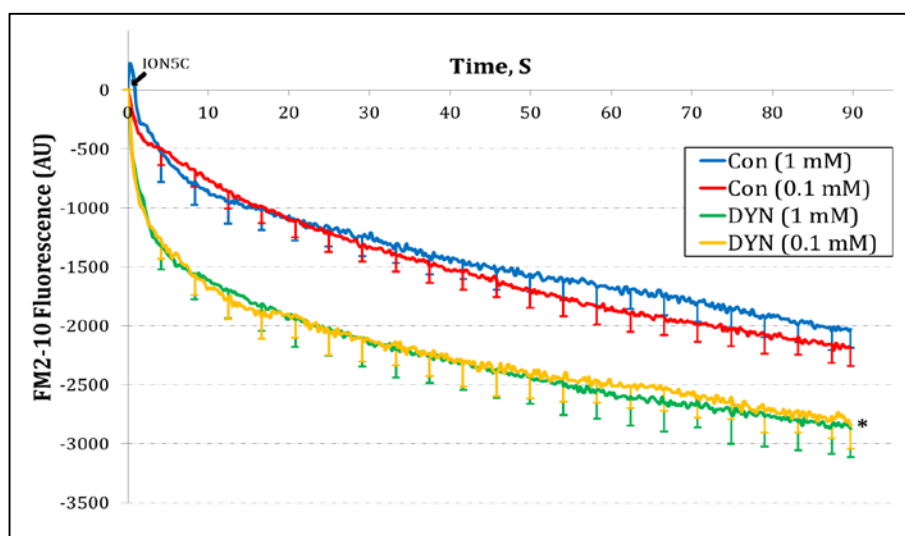


Figure 3.5: Use of 0.1 or 1 mM FM2-10 dye for labelling the SVs does not have any effect on its SV loading and subsequent release from them following the application of a suitable stimulus, in this case ION5C. The Figure also demonstrates that the drug treatment, in this case 160 μ M DYN, does not affect these properties of the FM2-10 dye.

3.6 Mode of SV Exocytosis Is Dependent on the Stimulus Employed

Figure 3.6A shows the FM2-10 dye release during the initial 2 sec of stimulation using all the three stimulation conditions, viz. HK5C, ION5C and 4AP5C. During this initial 2 sec of stimulation, RRP should have undergone exocytosis as suggested by many of the previous research (Rizzoli & Betz, 2005). Unlike 4AP5C, HK5C and ION5C do not cause any significant decrease in the Fluorescence of FM2-10 dye indicating that the SVs during the application of latter two stimuli must be undergoing KR mode of exocytosis. One might argue that it is possible that no SV exocytosis occurs during the initial 2 sec of stimulation by HK5C or ION5C. This argument could be dismissed based on the FM2-10 dye release data from the synaptosomes pre-treated with 0.8 μ M Okadaic acid (OA)– an inhibitor of protein phosphatase 1 and 2A – that is known to convert all the RRP SVs to FF (Ashton *et al.*, 2011; Figure 3.6 B). Comparison of the data in Figure 3.6 A and B also indicates that the amount of 4AP5C evoked FM2-10 dye increases when treated with OA suggesting that 4AP5C is able to release RRP by a combination of both, KR and FF under control conditions.

Figure 3.7 shows the contribution of both the exocytosis mode at various time points for HK5C and 4AP5C. These graphs were obtained by subtracting the control fluorescence value from the OA fluorescence value to obtain the contribution of vesicles that were undergoing KR under control conditions. It is evident that during HK5C stimulation, all the RRP undergoes KR mode of exocytosis (released in <2 sec; Figure 3.7A) and all the RP SVs undergo FF mode of exocytosis (released after 2 sec; Figure 3.7B). ION5C showed similar trend to HK5C and thus this data are not shown here. 4AP5C, on the other hand, releases RRP vesicles by a combination of KR and FF with both the mode contributing almost

equally (Figure 3.7C). RP vesicles fail to exocytose when 4AP5C is employed as a stimulus, probably because it is unable to achieve sufficiently large change in $[Ca^{2+}]_i$ to drive the fusion of the RP (see Figure 3.2 and 3.3).

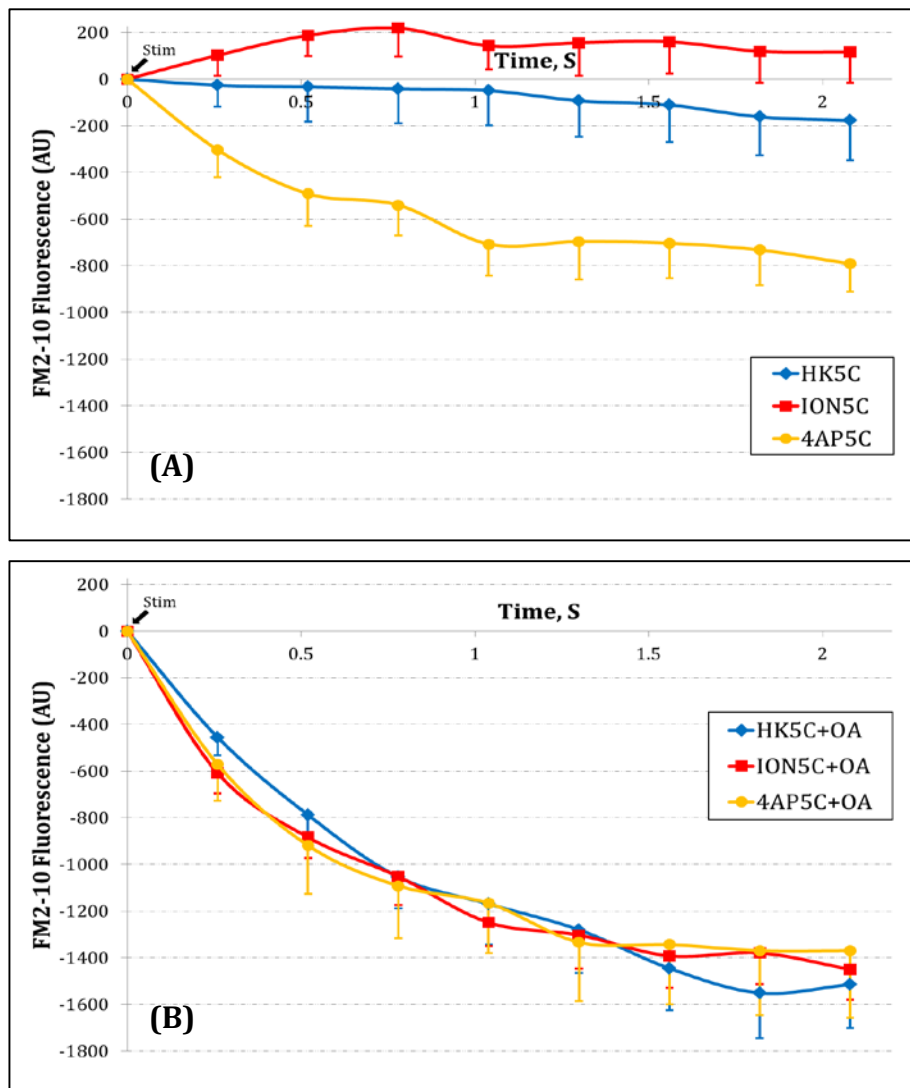


Figure 3.6: Inhibition of PP2A and PP1 induces all SVs to release by FF. Measurement of FM2-10 dye fluorescence following the application of various stimuli show (A) distinct levels of decrease in FM2-10 fluorescence and that (B) these levels of fluorescence decreases by same magnitude when synaptosomes are pre-treated with 0.8 μ M OA, an inhibitor of PP1 and PP2A (independent experiments ≥ 3). *The data in this Figure represents an average of author's and A. Ashton et al.'s experiments.*

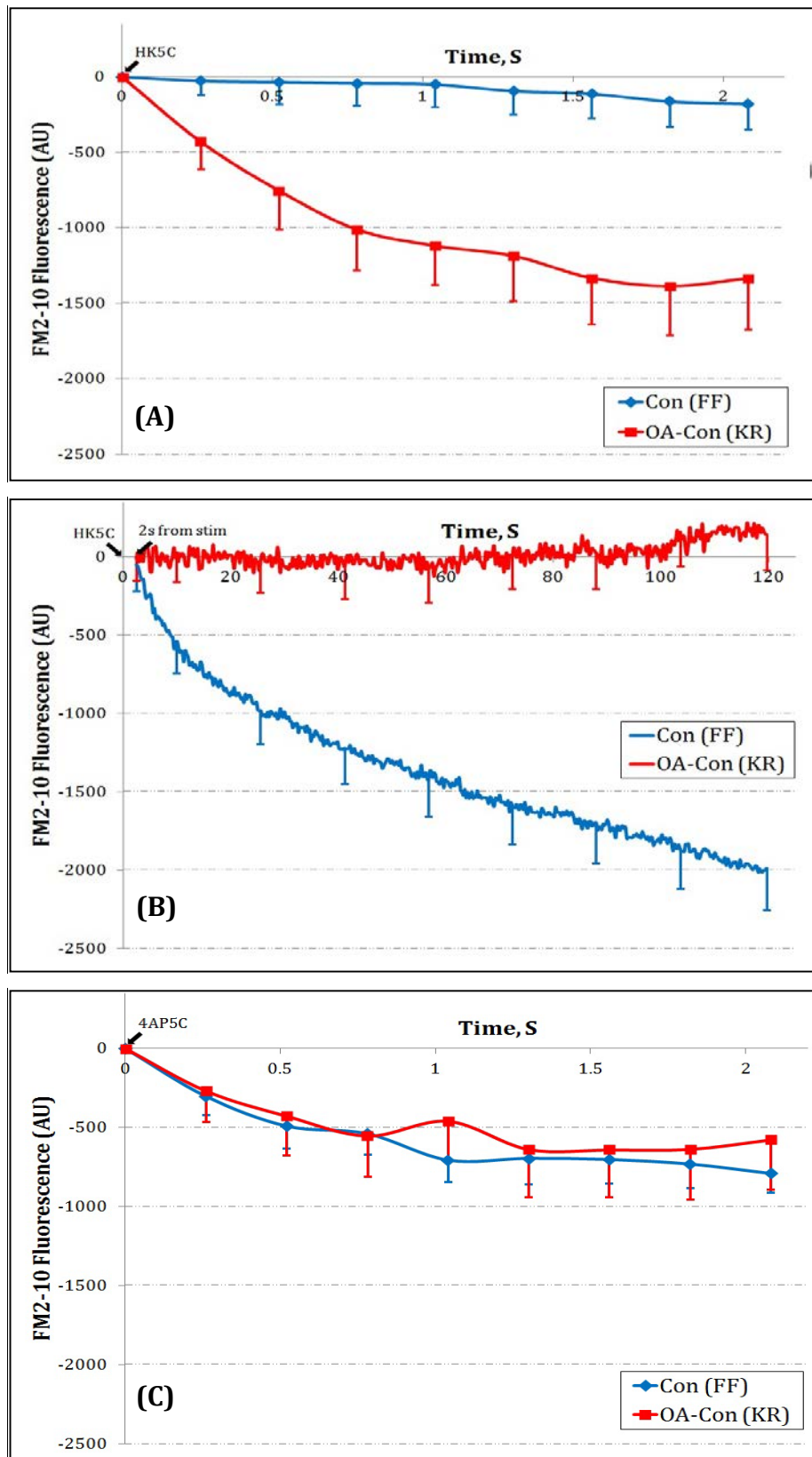


Figure 3.7: SVs undergo KR exocytosis during initial 2 sec of stimulation and FF thereafter. When the FM2-10 dye fluorescence of control was subtracted from OA treatment conditions, (A) it was found that all the SVs are released by KR during the initial 2 sec of HK5C stimulation and (B) the remaining are released by FF after 2 sec of stimulation. However, (C) during 4AP5C stimulation all the SVs are

released by a combination of KR and FF for the initial 2 sec (independent experiments ≥ 3). *The data in this Figure represents an average of author's and A. Ashton et al.'s experiments. Supplementary data is presented in Appendix A.4 that helps in better understanding of how these were produced.*

3.7 RRP undergoes spontaneous release at 37 °C

In order to be able to compare Glu release and FM2-10 dye release one must ensure that one only studies one round of release for both the RRP and RP of SVs. We established that this is the case for the stimuli employed in this study (see chapter 3.3). However, prior to stimulation, there is a possibility that some SVs could undergo spontaneous release and if this is via FF then some FM2-10 dye labelled SVs could be lost prior to the stimulation. This would clearly interfere with the comparison between Glu release and dye release as spontaneously released SVs should be able to re-load and release Glu during the stimulation/measurement but such vesicles will be devoid of any FM2-10 dye. Whilst there appeared to be a good correlation between Glu release and FM2-10 dye release at 22 °C, we investigated the release when terminals were stimulated at 37 °C. During the final resuspension of synaptosomes, instead of resuspending it in L₀ buffer at 22 °C (see chapter 2.3), they were resuspended in 1.5 ml of L₀ buffer at 37 °C and were subsequently stimulated at 37 °C.

As previously discussed, FM2-10 dye can only be released maximally if the SVs undergo FF mode of exocytosis and KR mode would prevent most of the dye from departing the SV membrane and thus the fluorescence will not decrease during KR mode of exocytosis. The aim of this particular study was to compare the total SV exocytosis at 22 and 37 °C and thus it was necessary that the fluorescence from all the vesicles undergoing exocytosis is quenched irrespective of its mode of exocytosis. Bromophenol blue (BPB) is a small hydrophilic dye quencher that can enter the SV lumen even through a transiently open fusion pore (as during KR) and can quench the fluorescence of FM2-10 dye even if it is bound to the vesicular membrane and hasn't departed (Harata *et al.*, 2006; Hoopman *et al.*, 2013).

Thus, when BPB is used during stimulation, a decrease in the fluorescence will be observed during SV exocytosis independent of their release mode. For this reason, 0.08 mM of BPB was added along with the Ca^{2+} stimulus just before the measurement of FM2-10 fluorescence.

When the FM2-10 dye was measured at 22 °C, a significant decrease in FM2-10 dye was observed whilst using BPB as compared to control conditions (Figure 3.8A; 3.9A). This extra decrease in fluorescence is similar to that seen while using OA (Appendix A.4) and is a result of RRP that normally undergoes KR, as previously shown (see Figure 3.6). Surprisingly, when this release was measured at 37 °C, no such differences in the fluorescence were observed indicating that the RRP is spontaneously lost under these conditions (Figure 3.8B; 3.9B). Thus, in order to study both pools of SVs, all the biochemical measurements in this study were performed at 22 °C unless otherwise stated. It is also important to note that the RRP vesicles are fully recovered back and are labelled with FM2-10 dye after the incubation at 37 °C with the relevant drugs during sample preparations as the dye is constantly present in the external buffer during this incubation period (see chapter 2; Figure 3.10B). The absence of extracellular FM2-10 dye during this 37 °C incubation would render the spontaneously released RRP SVs unlabelled.

Intriguingly, such results indicate that the RRP alone undergo spontaneous release (compliments their preferential location at the active zone) and it does so by FF mode of exocytosis. It is noteworthy that only one round of spontaneous release needs to occur for the RRP SVs to be unlabelled with the dye. Other results from A. Ashton and group would also indicate that the RRP would undergo FF, rather than KR, at the low $[\text{Ca}^{2+}]_i$ in resting terminals. This important result could mean that

many studies using FM2-10 dye at 37 °C may not actually be labelling up all the releasable SV pools (for e.g.: Baldwin *et al.*, 2003; Cousin & Robinson, 2000).

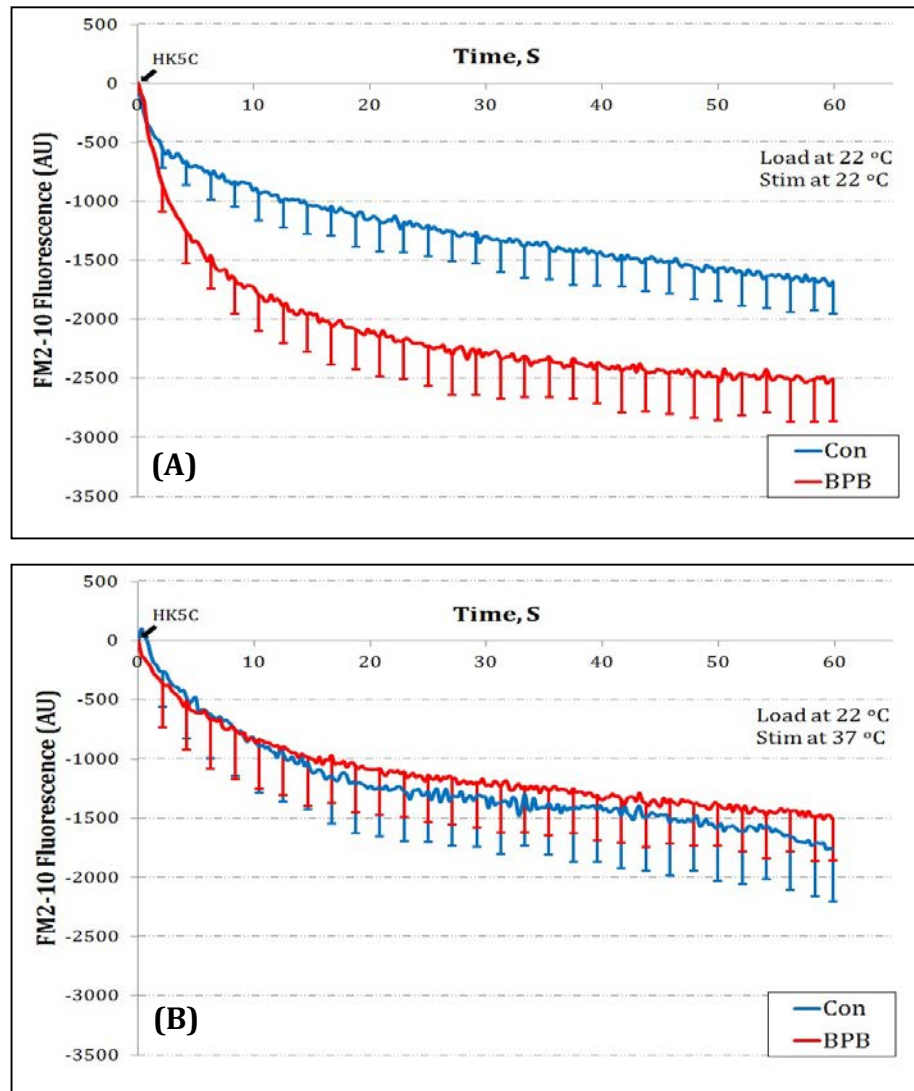


Figure 3.8: Some SVs undergo spontaneous exocytosis at 37 °C. Comparison of decrease in FM2-10 dye fluorescence, following acute treatment with BPB, at (A) 22 °C and (B) 37 °C revealed the loss of SVs undergoing KR at 22 °C indicating that the RRP is spontaneously released by FF mode at 37 °C but no such spontaneous release occurs prior to stimulation at 22 °C (independent experiments ≥ 3). *Please note that the data in this Figure is a courtesy of A. Ashton et al. and author did not directly contribute towards these experiments.*

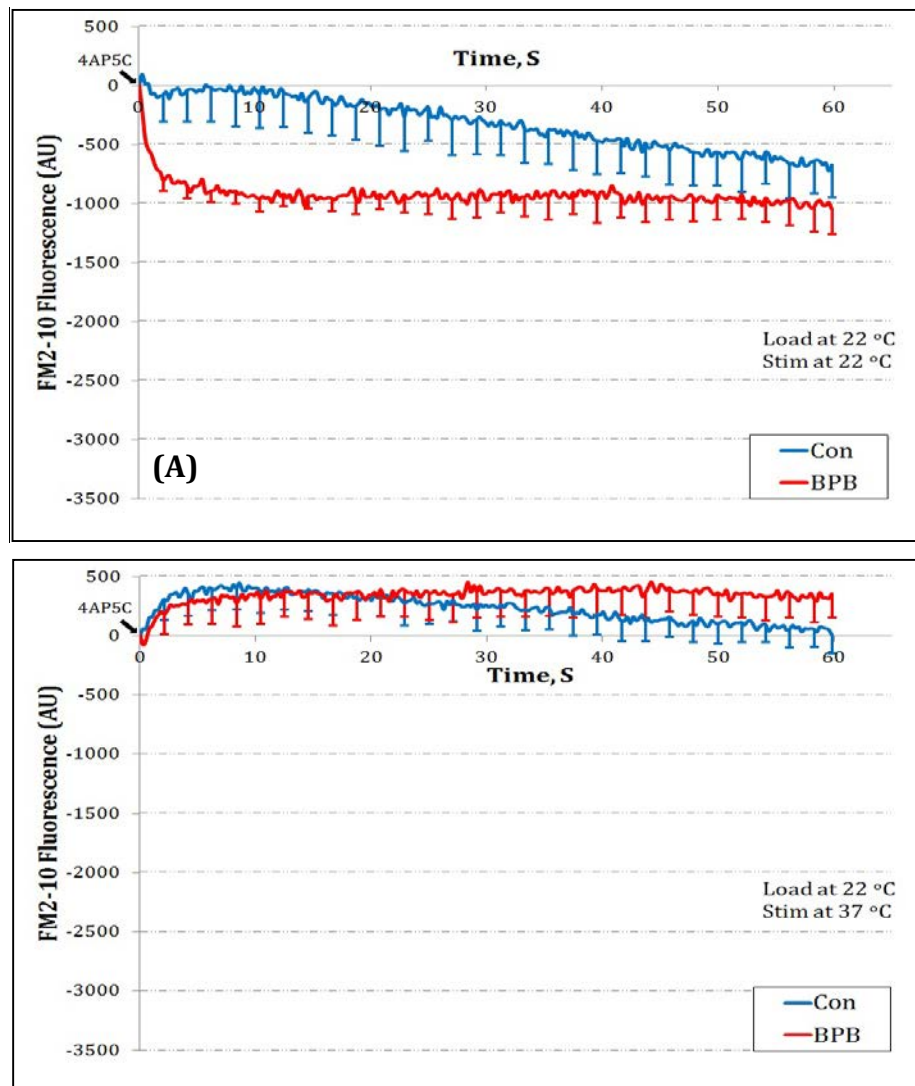


Figure 3.9: SVs undergoing spontaneous release at 37 °C belong to RRP. (A) Stimulation of synaptosomes by 4AP5C at 22 °C decreased FM2-10 dye fluorescence following the acute treatment of BPB. (B) However, No such decrease was observed when the synaptosomes were resuspended and stimulated at 37 °C thereby providing further evidence of spontaneous release of the RRP at 37 °C (independent experiments ≥ 3). Please note that the data in this Figure is a courtesy of A. Ashton et al. and author did not directly contribute towards these experiments.

The FM2-10 dye fluorescence value at time zero (just prior to stimulation) for sample at 37 °C was compared to that of sample at 22 °C. This helps us identify if there was an actual loss of dye labelled vesicles at 37 °C when compared to that of 22 °C. The data shown in Figure 3.10 and were produced by averaging (3-6 independent experiments) the fluorescence value at time zero before normalisation done during the subsequent calculations – and suggest that a pool of labelled SV was indeed lost at 37 °C (Figure 3.10A). Figure 3.10B signify that when the samples were loaded at 37 °C in the presence of FM2-10 dye and when were subsequently measured at 22 °C, no such loss of pool was observed thereby indicating that the intoxication of the sample at 37 °C during sample preparation does not lead to a loss of pool during subsequent measurement.

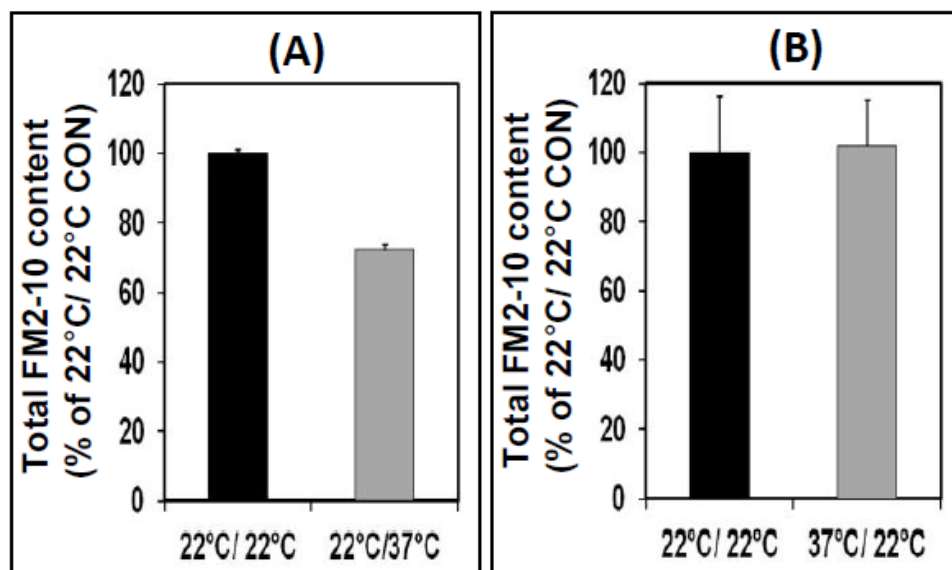


Figure 3.10: Loss of FM dye prior to stimulate confirm spontaneous release of RRP vesicles. (A) When the dye is loaded at 22 °C and subsequently measured at 37 °C, a significant loss of FM2-10 fluorescence is seen prior to stimulation. However, (B) when the dye is loaded at 37 °C and subsequently measure at 22 °C, no such loss in FM2-10 dye is observed.

3.8 Conclusion

Based on the arguments and data presented in this chapter, it can be concluded that the FM2-10 dye can be maximally released only during FF mode of exocytosis whereas Glu can be fully released independent of the mode of exocytosis. These differences in the release properties of two molecules can be exploited to study the two modes of exocytosis. Three stimuli used in this study produce different levels of $[Ca^{2+}]_i$ – with different kinetics – and thus HK5C and ION5C releases RRP by KR and RP by FF. 4AP5C on the other hand can only release RRP by a combination of KR and FF with both modes contributing equally. Finally, in order to study both pools of SVs, it is important to carry out all the washes, and stimulation measurements at 22 °C instead of 37 °C. This is an important finding as other studies using FM2-10 dye may not be studying all pools of SVs at 37 °C as they may not have labelled RRP of SVs.

Chapter 4

Role of Dynamins and Myosin II

4.1 Introduction

After having established all the necessary experimental conditions in chapter 3, chapter 4 of this study aims at identifying proteins which are involved in the regulation of KR and FF mode of exocytosis. Previously, Dr. A. Ashton and his group have established that the SVs of the synaptosomes, obtained from mature rat cerebral cortex, can exocytose either via KR or FF when a relevant stimulus is applied. They have also established that this mode of exocytosis can be regulated by activating and inhibiting various kinases and phosphatases (Ashton *et al.*, unpublished work). Thus, it is probable that at least one phospho-protein is involved in the regulation of these modes of exocytosis. A lot of work has been previously carried out on the FF mode of exocytosis but little is known with regards to the regulation of KR mode of exocytosis. This chapter discusses two proteins that were identified to be involved in the regulation of KR mode of SV exocytosis.

As discussed in chapter 1, dynamins and myosin-II are able to manipulate or regulate the fusion pore in non-neuronal systems and thus they seemed strong contenders that may be implicated in the two modes of SV exocytosis (KR and FF) in cerebral cortex. Here, the dynamin-I and dynamin-II (dynamin(s)) were blocked using 160 μ M dynasore (DYN) and myosin-II was blocked using 50 μ M blebbistatin (Blebb) and their effects on the glutamate and FM2-10 dye release was studied.

4.2 Results

4.2.1 Inhibition of Dynamins

Dynamins were inhibited by pre-treating synaptosomes with 160 μM DYN. The results show that DYN had no significant effect on the glutamate release induced by any of the three stimuli (HK5C, ION5C and 4AP5C; Figure 4.1) employed in this study, but that it increased the FM2-10 dye release during ION5C and 4AP5C evoked release (Figure 4.2). This observation indicates that the dynamins are involved in the closure of the fusion pore (thereby causing KR mode of exocytosis) during ION5C and 4AP5C stimulations and that the inhibition of dynamins during such conditions can cause all the vesicles to fuse by FF that would otherwise undergo KR mode of exocytosis. It can be concluded from Figure 4.3 that the use of 160 μM DYN has no effect on the $\Delta[\text{Ca}^{2+}]_i$ produced by the three distinct stimuli. To establish if this action of dynamins is independent of clathrin mediated endocytosis (CME), CME was blocked using 15 μM Pitstop 2 (PIT 2; von Kleist *et al.*, 2011). The inhibition of dynamins with or without PIT 2 resulted in the same observation for ION5C evoked Glu release or ION5C evoked FM2-10 dye release assays (Figure 4.4). This again indicates that this stimulus only induces one round of SV exocytosis, and that the perturbation of CME does not prevent the release of RRP or RP of SVs. The FM2-10 dye results also indicate that the inhibition of dynamins can still switch the KR to FF mode even when the clathrin dependent processes are inhibited. This establishes that the dynamin exerts its action of closing the fusion pore independently of clathrin.

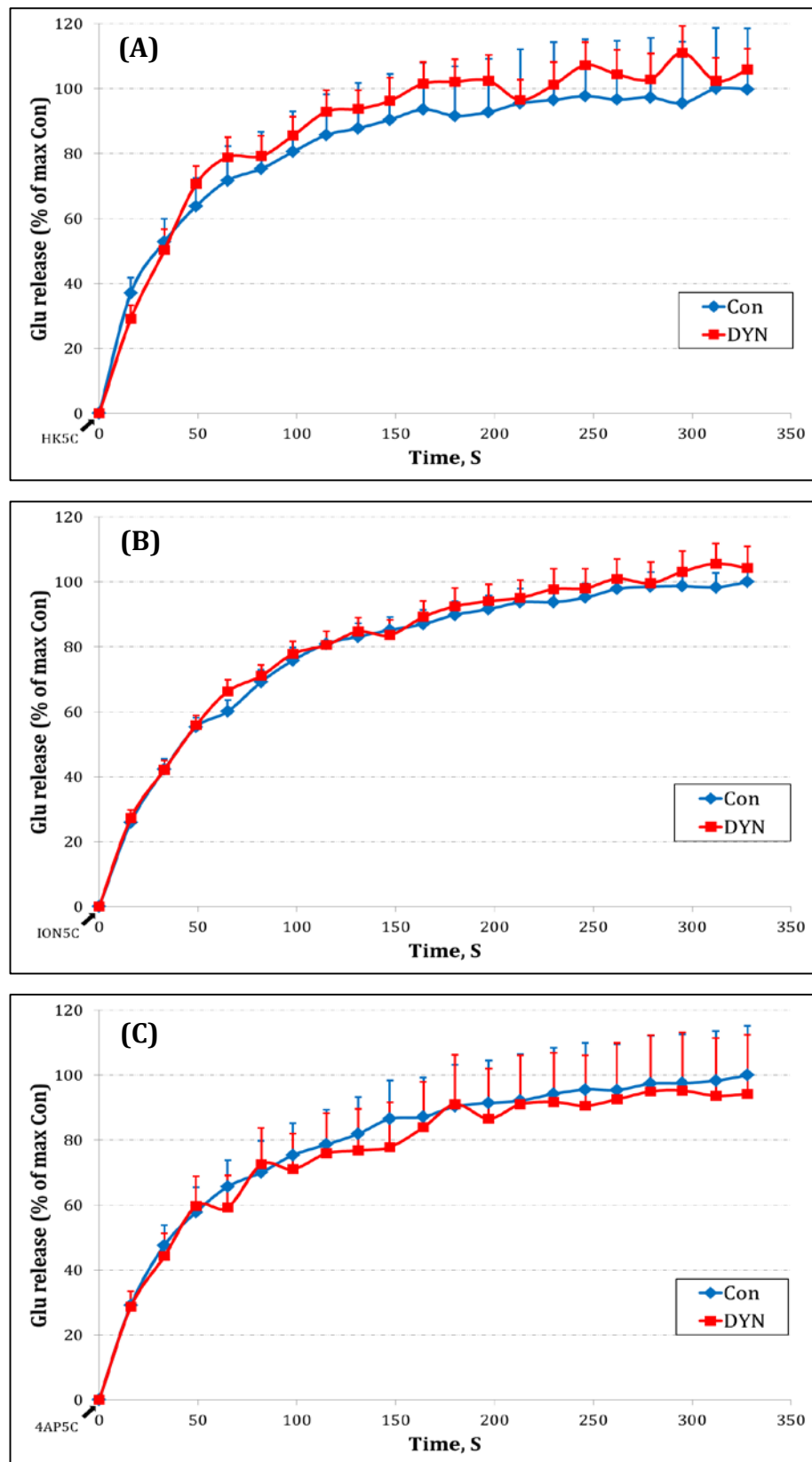


Figure 4.1: Inhibition of dynamins by 160 μM dynasore does not affect the total SV turn over for any of the three stimuli employed: (A) HK5C, (B) ION5C and (C) 4AP5C. The data points represent amount Glu released, expressed as percentage, with error bars representing SEM. Student t test resulted in $p > 0.05$ for all three experiments.

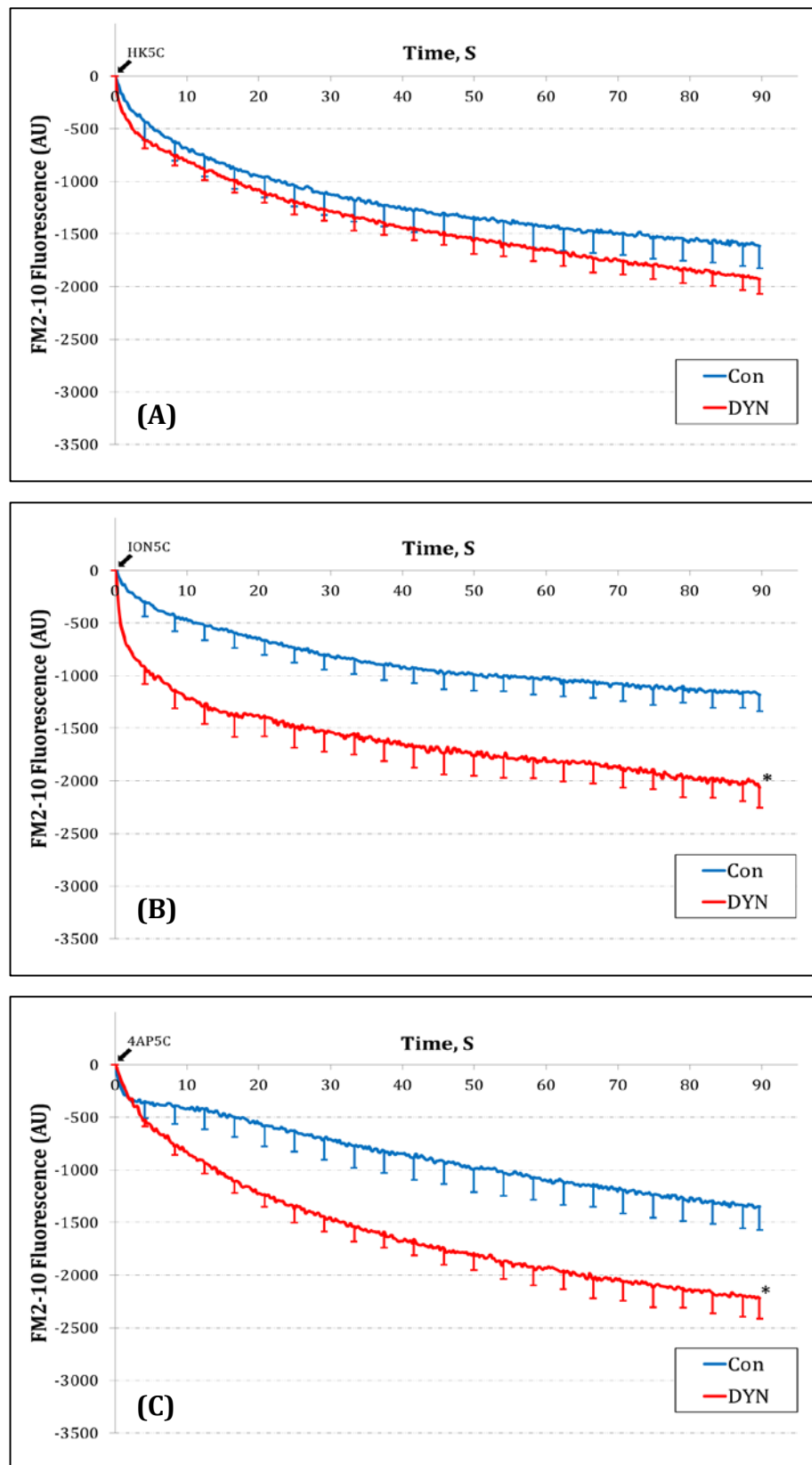


Figure 4.2: Dynamin(s) is required for KR exocytosis of RRP when ION5C and 4AP5C stimuli are employed. 160 μ M dynasore had no effect on the (A) HK5C evoked FM release ($p=0.508$) where as it increased the dye released during (B) ION5C ($p=0.014$) and (C) 4AP5C ($p=0.034$) stimulations indicating that the

inhibition of dynamins switched the KR mode of the RRP to FF mode for the latter two stimulation conditions. The error bars represent SEM.

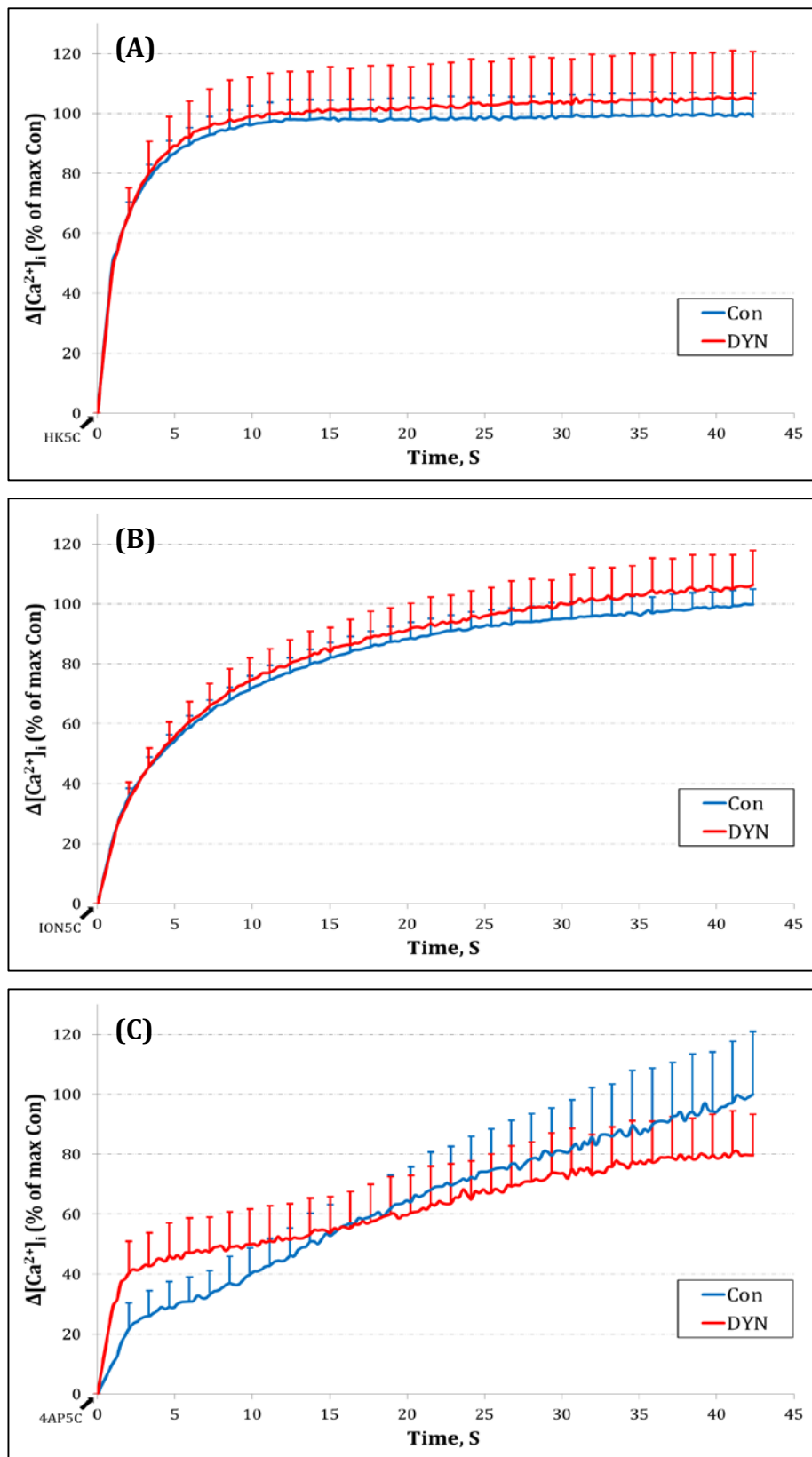


Figure 4.3: Pre-treatment with 160 μM dynasore does not affect the changes in $[\text{Ca}^{2+}]_i$ achieved upon stimulation with (A) HK5C, (B) ION5C and (C) 4AP5C when compared to that of control conditions. The data is representative of more than 3 experiments with error bars representing SEM and $p > 0.05$ for all experiments.

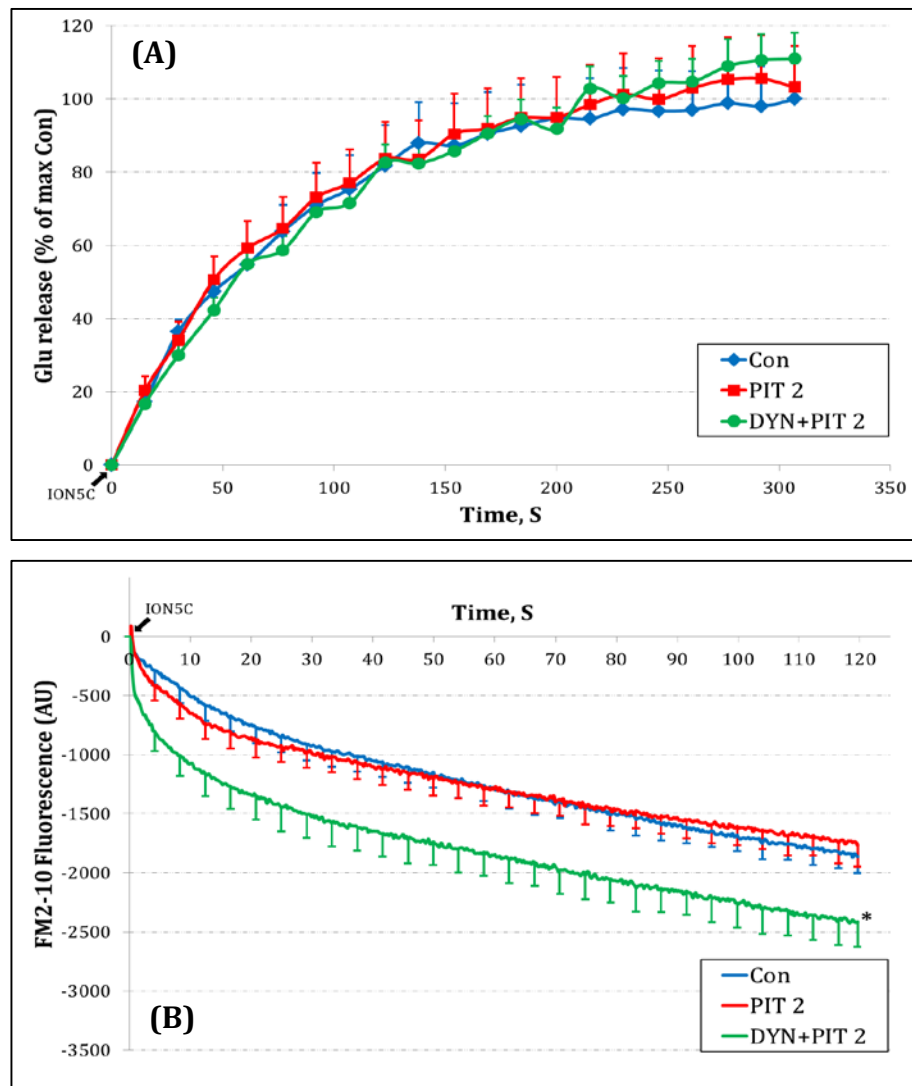


Figure 4.4: Role of dynamin(s) in KR exocytosis is independent of clathrin. When the synaptosomes were pre-treated with 15 μ M Pitstop 2, alone or in combination with 160 μ M dynasore, it did not affect the (A) overall glutamate release ($p > 0.05$), however (B) the combination treatment of DYN+PIT 2 significantly increases ($p = 0.0254$) the FM2-10 dye released during ION5C stimulation. These observations suggest that the action of dynamin(s) in closure of the fusion pore is distinct from its role in CME. The data is representative of more than 3 experiments with error bars representing SEM.

4.2.2 Inhibition of specific dynamin isoforms

In a quest to identify a specific isoform of dynamins involved in the regulation of KR mode of SV exocytosis, dynamin-I and II were specifically blocked using drugs that inhibit these isoforms in a dose dependent manner. In order to block dynamin-I, various concentrations of Dynole-34-2™ (here after referred to as dynole) were tested for its effect on the Glu and FM2-10 dye release assays. This novel dynamin inhibitor is a potent inhibitor of the GTPase activity of dynamins that has 15-fold more specificity for dynamin-I when compared to dynasore. The *in vitro* IC₅₀ value for the inhibition of dynamin-I is 1.3 μM whereas 14.2 μM has been reported to be the IC₅₀ for the inhibition of dynamin-II (together with dynamin-I) (Hill *et al.*, 2009).

As demonstrated in section 4.2.1 of this chapter, dynamin is involved in the regulation of the KR mode of exocytosis only when ION5C and 4AP5C stimuli are employed. However, for the study of the inhibition of specific isoforms of dynamins, only ION5C stimulus was employed and it was assumed that similar results would be obtained for 4AP5C stimulation. In this study, it was found that 20 μM dynole caused a decrease in the FM2-10 dye fluorescence as seen previously after the treatment with dynasore (Figure 4.5B; 4.2B). Thereafter the effects of 20μM dynole on the Glu release was assessed to ascertain if this increase in dye release was definitely due to the exocytosis mode switch and not due to any discrepancies in the Glu release (for. e.g. an increase in the Glu release). Figure 4.5A reveals that there was no apparent increase in the Glu release followed by the treatment with 20μM dynole and thus, it can be suggested that the increase in FM2-10 dye release is probably due to a switch in the mode of SV exocytosis (from KR to FF). Other concentrations of dynole (10 μM and 50 μM) did not have any

significant effect on the FM2-10 dye fluorescence (Figure 4.5B) and thus, these concentrations were not tested for their effect on the Glu release. At the concentration of 50 μ M, dynole may also start to inhibit dynamin-II which then could regulate some SVs such that this caused less FM2-10 dye release (see Figure 4.6; section 4.3.3) there by masking the effect of dynamin-I inhibition during the FM2-10 dye release.

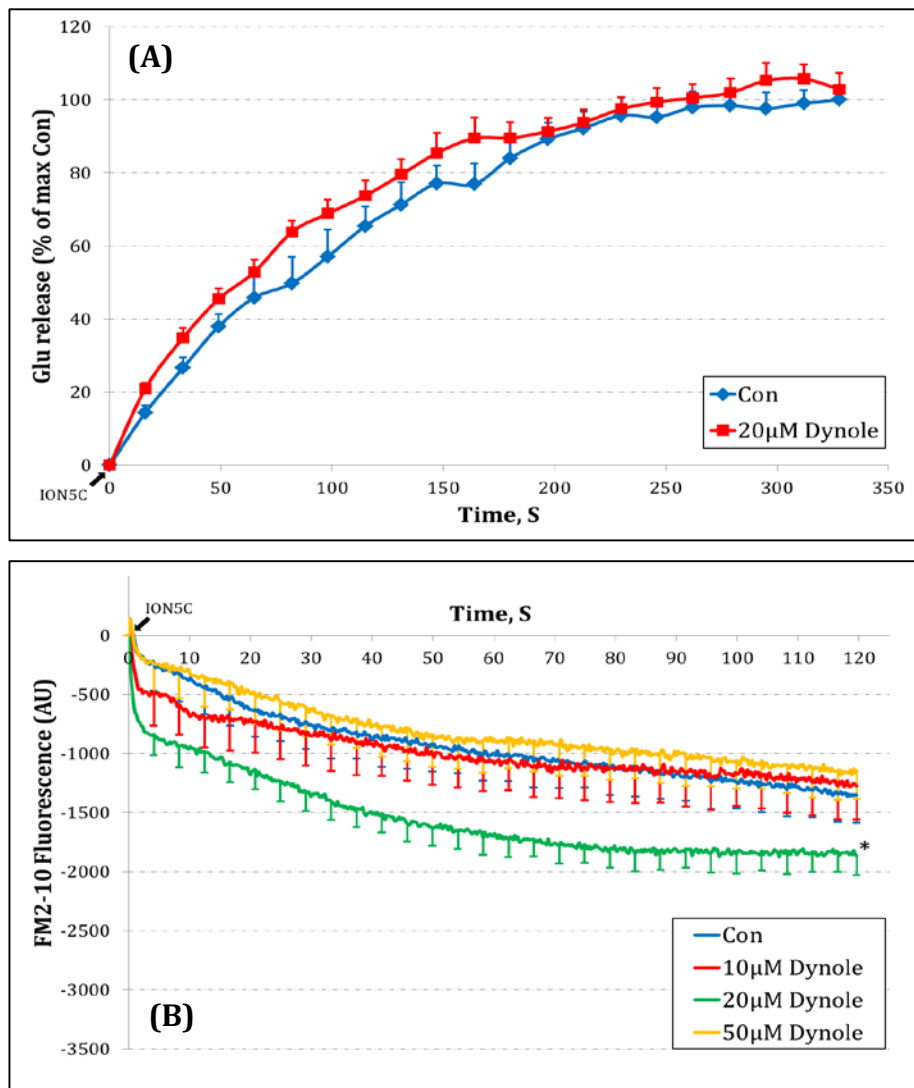


Figure 4.5: Dynamin-I isoform is required for KR of RRP vesicles when ION5C is employed as a stimulus. Inhibition of dynamin-I by pre-treatment with 20 µM dynole does not affect the (A) glutamate release ($p>0.05$) but (B) significantly increases the FM2-10 dye released ($p<0.0466$) from the synaptosomes upon ION5C stimulation. The data is representative of more than 3 experiments with error bars representing SEM.

In order to specifically block dynamin-II, another novel compound, Dyngo-4a™ (here after referred as dyngo) was used that preferentially blocks dynamin-II (*in vitro* IC₅₀ = 2.6 μM) than dynamin-I (*in vitro* IC₅₀ = 380μM). After testing various concentrations, it was found that whilst 20 μM dyngo had no effect, 50 and 100 μM dyngo reduced the FM2-10 dye release (Figure 4.6 B). The effect of 50 μM dyngo was then tested on the Glu release and it was found that the synaptosomes released the same amount of Glu as compared to the control conditions indicating the same number of SV were exocytosing with 50 μM dyngo treatment (Figure 4.6A). This result needs to be further investigated (currently studied by a different researcher under Dr. A. Ashton), but this would imply that dynamin-II is required for the FF of the RP vesicles but may not play any role during the exocytosis of the RRP (see 4.3.3 for further discussions). These results would also imply that 160 μM DYN only inhibits dynamin-I isoform in our model system otherwise one would see RP undergoing KR (instead of the usual FF) when dynamin-II is blocked by DYN.

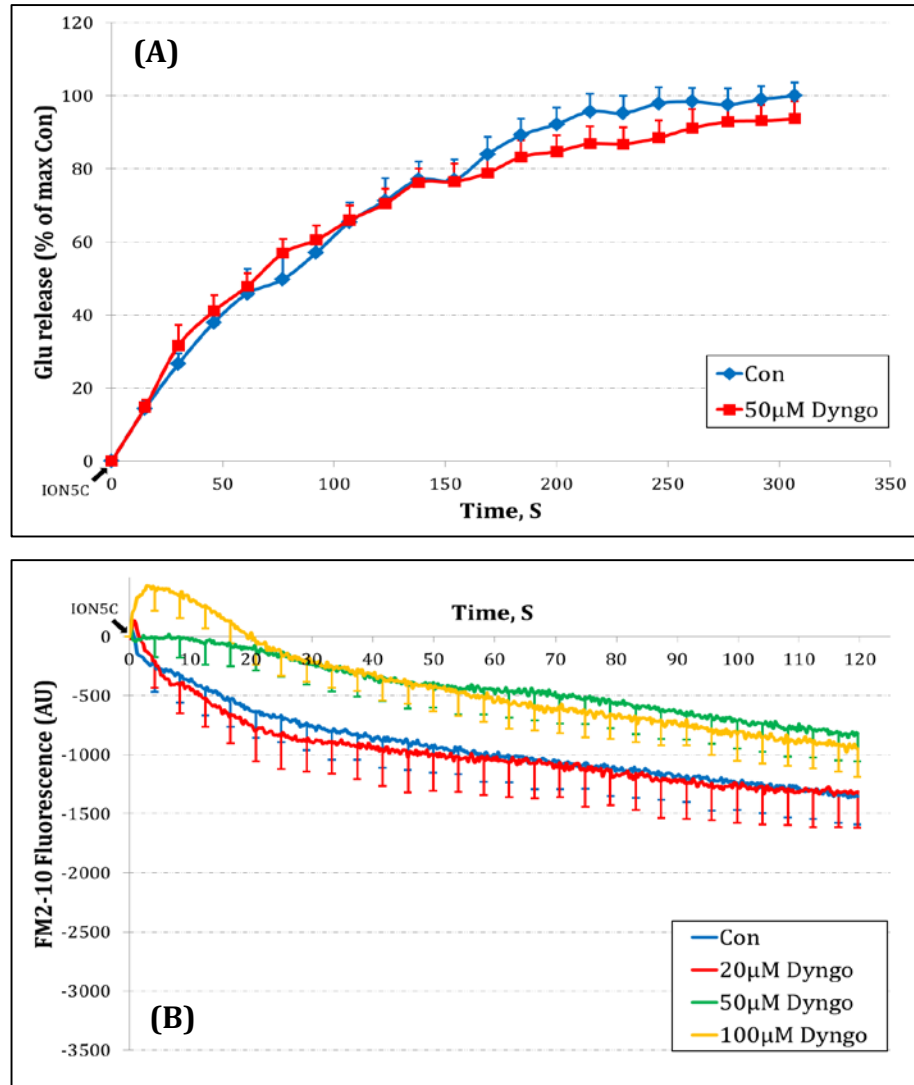


Figure 4.6: Dynamin-II isoforms may be required for FF of the RP. Inhibition of dynamin-II by 50 μM dyngo did not affect the (A) glutamate released (B) but it reduced the amount of FM2-10 dye released upon ION5C stimulation. It should also be noted that a higher dose of dyngo (100 μM) was not able to further decrease the FM2-10 dye released. The data is representative of more than 3 experiments with error bars representing SEM and $p > 0.05$ for all experiments.

4.2.3 Inhibition of Myosin-II

In section 4.2.1 it was established that dynamins may be implicated in the closure of the fusion pore during ION5C and 4AP5C stimulations as shown by the increase in FM2-10 dye release even when there was same number of SVs undergoing exocytosis. However, there was no increase in the FM2-10 dye release during HK5C stimulation when the DYN was used indicating that there must be a different protein involved in the closure of the fusion pore when HK5C was employed. Some of the previous research has indicated that Myosin-II may be able to regulate the fusion pore in other model systems (Chan *et al.*, 2010; Berberian *et al.*, 2009; Bhat & Thorn, 2009; Neco *et al.* 2008). Thus, In order to establish if Myosin-II may be involved in the closure of the fusion pore during HK5C stimulation conditions, myosin-II's action was blocked using blebbistatin (Blebb; 50 μ M). Blebb has a high affinity and selectivity for the non-muscle class-II myosin and inhibits them by inhibiting the actin-activated ATPase activity (Shu *et al.*, 2005; Kovacs *et al.*, 2004).

The results show that 50 μ M Blebb can produce exactly the opposite results for the FM2-10 dye release assay when compared to their DYN counterparts (Figure 4.8; 4.2) without affecting the Glu release (Figure 4.7). This finding indicates that myosin-II may be involved in the closure of the fusion pore during HK5C stimulation and dynamins may be required for this closure only during ION5C and 4AP5C stimulations. This raises an important question: why there would be two proteins performing the same function during different stimulation paradigms? One of the reasons could be explained by the fact that all the three stimuli discussed here produce different kinetics of $\Delta[\text{Ca}^{2+}]_i$ (Figure 3.3) which may then have implications on the regulation of activities of the two stated proteins, especially at the active zone release sites. Figure 4.9 shows the amount of

additional FM2-10 dye released upon the inhibition of these proteins versus the change in $[Ca^{2+}]_i$ measured after 2 sec, when all the RRP should be released. It is clear from the Figure that the inhibition of dynamins causes more FM2-10 dye release when the overall $\Delta[Ca^{2+}]_i$ is ≤ 140 nM at 2 sec of stimulation. In contrast the inhibition of myosin-II may contribute to the additional FM2-10 dye release only when the overall $\Delta[Ca^{2+}]_i$ is > 140 nM at 2 sec of stimulation.

It could be argued that 50 μ M blebbistatin may affect the overall change in $[Ca^{2+}]_i$ upon stimulation which could then possibly explain the differences in FM2-10 dye release as seen in this study. To rule out this, Fura-2-AM studies were conducted after treating the synaptosomes with 50 μ M blebbistatin to determine the $\Delta[Ca^{2+}]_i$ achieved during HK5C stimulation. However, it was found that blebbistatin somehow interfered with the Fura-2 fluorescence such that no apparent increase in the $[Ca^{2+}]_i$ was produced upon the application of a stimulus (HK5C in this case; data not shown). However, this cannot be a true reflection as the application of HK5C stimulation does produce an increase in the $[Ca^{2+}]_i$ and drives the SV exocytosis (Figure 3.3, 4.7A). Thus an attempt was made to determine the effect of blebbistatin indirectly by measuring Glu release at $[Ca^{2+}]_e$ of less than 5 mM. Figure 4.10 show that inhibition of myosin-II did not affect the amount of Glu released even when the external $[Ca^{2+}]_e$ was lowered to 1.2, 0.3 or 0.15 mM in the presence of 30mM K^+ . Thus, it can be concluded that use of 50 μ M Blebb does not affect the overall change in $[Ca^{2+}]_i$ upon stimulation otherwise a change in Glu release would be observed when the $[Ca^{2+}]_e$ was lowered than 5 mM due to its direct relation with the Glu release (Figure 3.2).

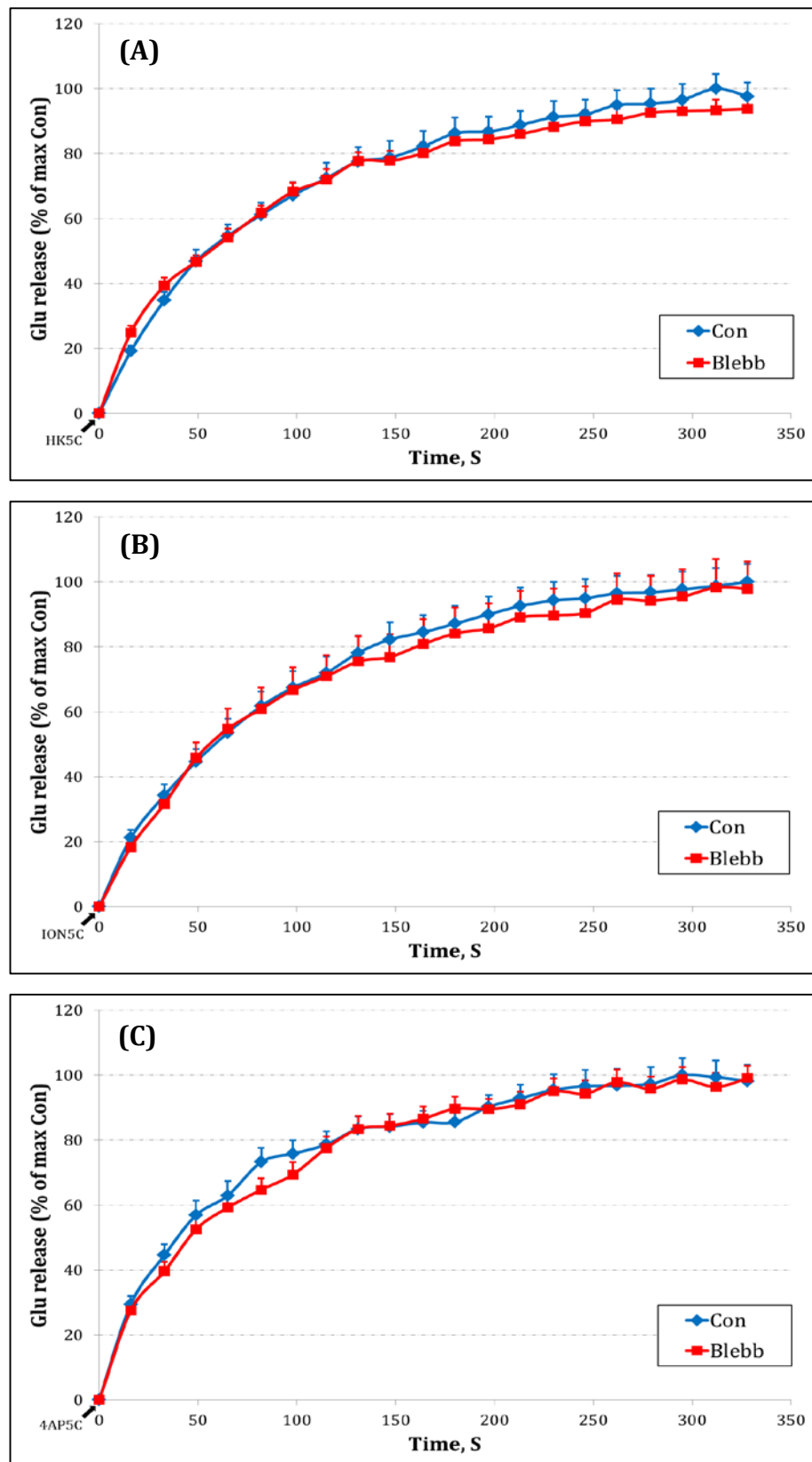


Figure 4.7: When non-muscle myosin-II was inhibited by 50 μ M blebbistatin, no differences in the Glu release was observed for all the three stimulation conditions employed in the study: (A) HK5C, (B) ION5C and (C) 4AP5C. The data is representative of more than 3 experiments with error bars representing SEM and $p > 0.05$ for all experiments.

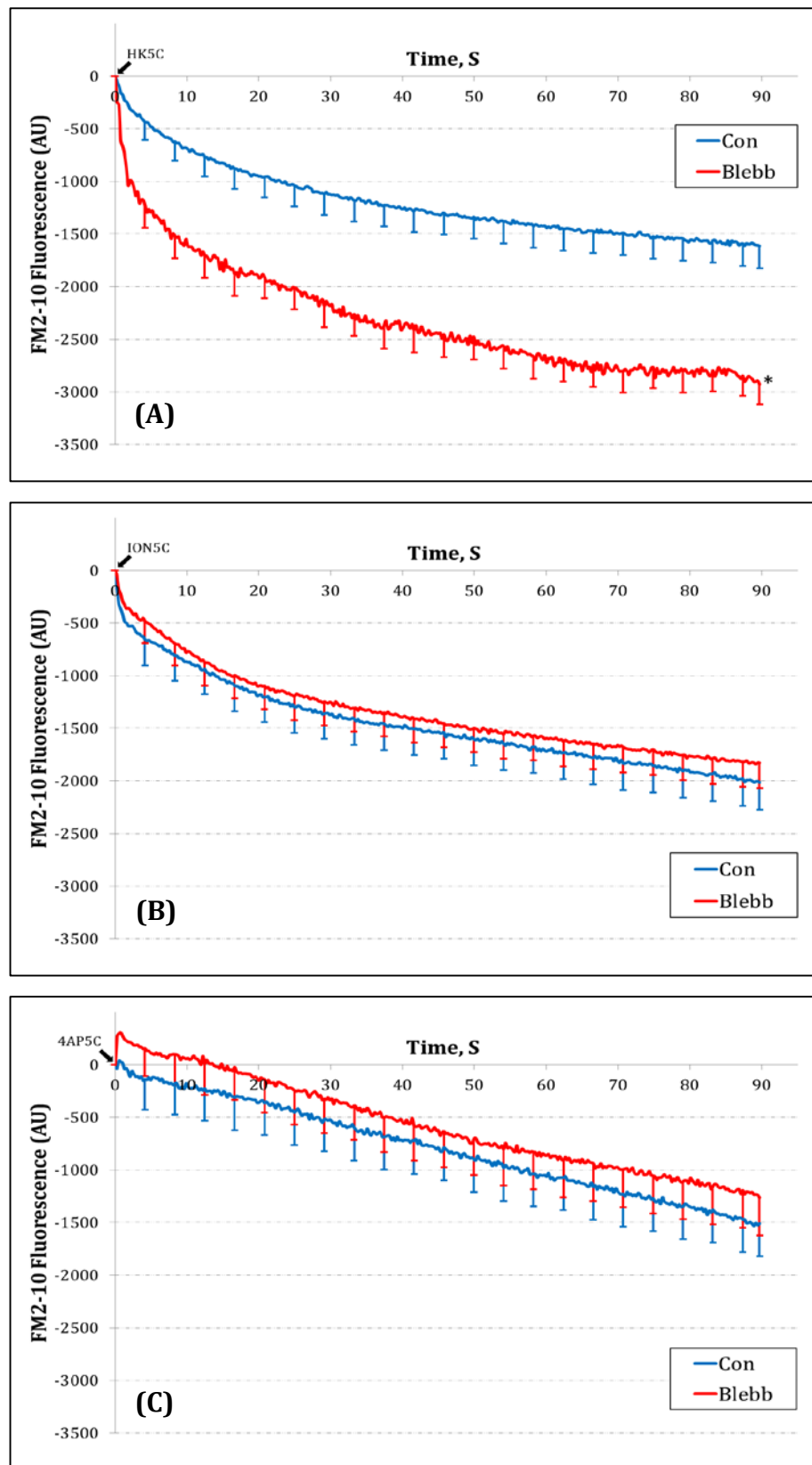


Figure 4.8: Myosin-II is required for KR of RRP when HK5C is employed as a stimulus. Inhibition of myosin-II by 50 μ M Blebb significantly increased the amount of FM2-10 dye released during (A) HK5C stimulation ($p < 0.0001$) but it had no effect during (B) ION5C ($p = 0.716$) and (C) 4AP5C ($p = 0.642$) stimulation conditions.

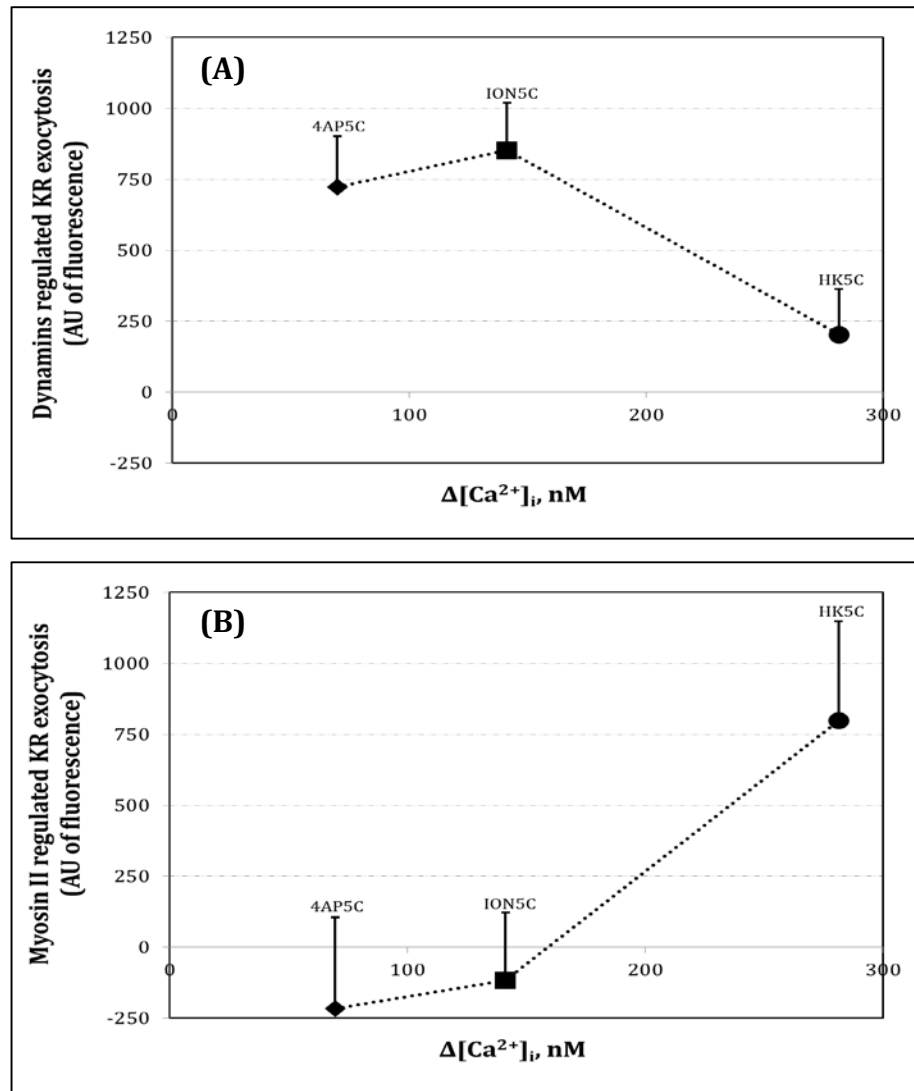


Figure 4.9: The activity of dynamin-I and myosin-II appears to be dependent on the $\Delta[\text{Ca}^{2+}]_i$ achieved upon stimulation. Contribution of (A) dynamin(s) and (B) myosin-II to the FM2-10 dye release from RRP of SVs is dependent on $\Delta[\text{Ca}^{2+}]_i$ achieved upon stimulation. These graphs were produced by plotting the $[\text{Ca}^{2+}]_i$ at two second of stimulation against the fluorescence of FM2-10 dye (AU) measured at two second of stimulation from the pre-treated synaptosomes. The data is representative of more than 3 experiments with error bars representing SEM.

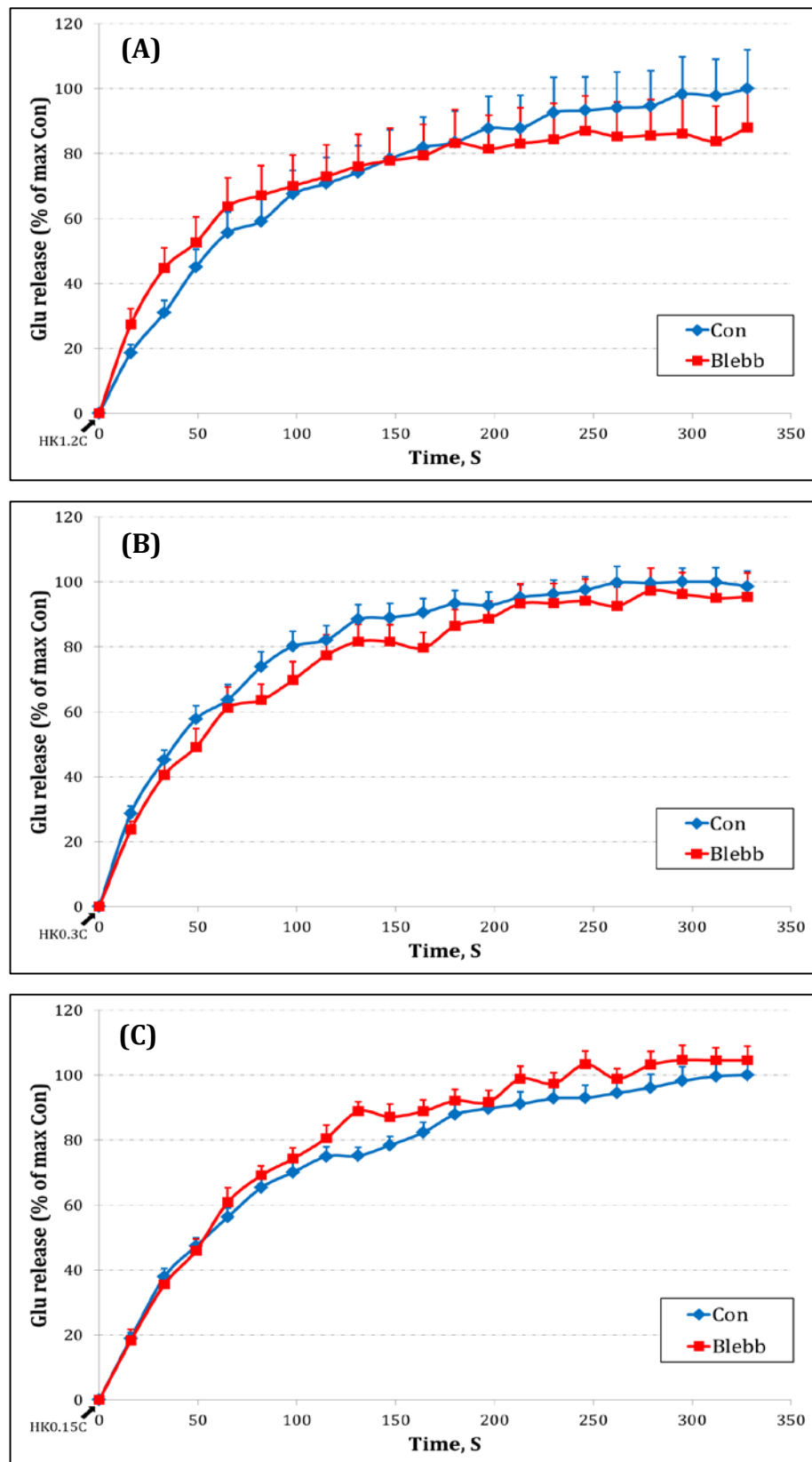


Figure 4.10: Pre-treatment with 50 μM blebbistatin does not affect the $[\text{Ca}^{2+}]_i$ achieved upon stimulation. In order to indirectly establish that the pre-treatment with 50 μM blebbistatin does not interfere with the changes in $[\text{Ca}^{2+}]_i$, the Glu release was measured in the presence of various $[\text{Ca}^{2+}]_e$ such as (A) 1.2 mM, (B) 0.3 mM or (C) 0.15 mM. It can be observed from the data that the Blebb

treatment does not affect the Glu release ($p>0.05$) irrespective of the $[Ca^{2+}]_e$. The data is representative of more than 3 experiments with error bars representing SEM.

4.3 Discussion

There is a lot of debate among the scientific community with regards to the existence of two distinct modes of neuronal SV exocytosis, viz. classical FF, and controversial KR (Saheki & De Camilli, 2012). There is a general consensus among the community for the existence of distinct modes of SV endocytosis (such as CME and bulk endocytosis) but the idea of multiple modes of SV exocytosis in central nervous system remains debatable (Südhof & Rizo, 2012). However, many of the recent studies have provided mounting evidence for the existence of KR in central nervous system (Ashton *et al.*, unpublished work; Zhang *et al.*, 2007) but nothing much is known with regards to its mechanism of regulation. Work done in Dr. A. Ashton's laboratory (unpublished work) clearly demonstrated the evidence of existence of two distinct modes of SV exocytosis in synaptosomes obtained from cerebral cortex of mature rats (see chapter 3). Building up on the previous work of Dr. A. Ashton and group, this study aims at identifying proteins that regulate the distinct modes of SV exocytosis, especially KR.

4.3.1 Inhibition of dynamins

In order to investigate the role of dynamins in this process, synaptosomes were pre-treated with 160 μM DYN and were then studied for its effect on the Glu and FM2-10 dye release (Figure 4.1; 4.2). Its effect on $\Delta[\text{Ca}^{2+}]_i$ was also determined as it has been previously shown to play a crucial role in SV exocytosis (Figure 4.3; Südhof & Rizo, 2012). The data in Figure 4.1 shows that pre-treatment with 160 μM DYN had no effect on the stimuli evoked Glu release. Considering quantal properties of SVs, this signifies that the inhibition of dynamins does not affect the total number of SVs exocytosing upon the application of a particular stimulus (Shupliakov & Brodin, 2010). These results indirectly support the argument

discussed in section 3.3 that all the three stimuli can induce only single round of SV release. This is because it has been confirmed by various studies that the dynamins are required for the CME and thus if the stimuli employed induced more than one round of release, then a decrease in the glutamate release would be observed upon the inhibition of dynamins (Royle & Lagnado, 2010; Hosoi et al., 2009). However, the results showed that all the three stimuli only induced a single round of release and that the inhibition of dynamins does not affect the total number of SVs undergoing exocytosis upon the application of a particular stimulus employed in this study.

On the other hand, inhibition of dynamins significantly increased the FM2-10 dye released upon ION5C ($p < 0.014$) and 4AP5C stimulations ($p < 0.034$; Figure 4.2). This observable fact can be explained by a hypothesis that the dynamins are generally required for the closure of the fusion pore – and the subsequent membrane fission action – during the application of these stimuli, and their inhibition would cause all the SVs undergoing KR to switch to a FF mode of exocytosis. It is also evident that the dynamin(s) are selective only to a sub-population of the SVs (the RRP) in their action of closing the fusion pore and thereby causing them to fuse by KR as opposed to the classical FF mode which the remaining RP population of the SVs would follow. It has been suggested previously that the SVs belonging to different pools – RRP and RP – might have different molecular characteristics making it one of the strong explanations for the specificity of dynamins observed in this study of FM2-10 dye release (Wu & Cooper, 2013; Vanden & Klingauf, 2006). However, the RRP may be released by a combination of KR and FF (as seen during 4AP5C, section 3.4) or released by FF entirely (as seen during spontaneous release at 37 °C) indicating that dynamin(s) may not be able to close the fusion pore at very low $[Ca^{2+}]_i$. Conversely, it also

appears that dynamin(s) may not play a role in the KR of RRP vesicles if the $\Delta[\text{Ca}^{2+}]_i$ achieved after stimulation is too large (as seen during HK5C; Figure 4.2 & 3.3). It is also important to note that the use of 160 μM DYN does not affect the overall $\Delta[\text{Ca}^{2+}]_i$ for any of the three stimuli used (Figure 4.3) as $\Delta[\text{Ca}^{2+}]_i$ has been linked to the activation and deactivation of various phosphatases and kinases which may control the mechanism of SV exocytosis and endocytosis (Saheki & De Camilli, 2012; Südhof & Rizo, 2011; Lilja *et al.*, 2004).

It has been well characterised that dynamins play an important role in the SV endocytosis, especially during clathrin mediated endocytosis (CME; Liu *et al.*, 2008; Lu *et al.*, 2008; Saheki & De Camilli, 2012). In order to determine if this role of dynamins is distinct from or independent of CME, 15 μM Pitstop 2 was used that selectively inhibits clathrin and thus CME (von Kleist *et al.*, 2011). It was found that inhibition of clathrin (and therefore CME) does not affect the Glu or FM2-10 dye release and that it does not prevent the action of DYN (Figure 4.4). Thus it can be suggested that the role of dynamins in the regulation of KR mode of SV exocytosis is independent of their role in CME. It should be noted that 15 μM PIT 2 is working to inhibit CME in these circumstances as it was shown that pre-treatment of synaptosomes with this drug prior to a pre-stimulation with HK5C produced a subsequent large reduction in HK5C evoked Glu release due to a failure for the pre-stimulated SVs to recycle via CDE (A. Ashton unpublished observation).

4.3.2 Inhibition of dynamin-I

It is clear from section 4.3.1 of this study that dynamin(s) play a crucial role in closure of the fusion pore during SV exocytosis of the RRP SVs thereby causing them to fuse by KR as opposed to the classical FF mode. In order to determine if this action of dynamins involves only one of the isoforms, specific dynamin

inhibitors were used that inhibit a specific isoform of dynamin in a dose dependent manner. The two drugs, dynole and dyngo, used for the inhibition of dynamin-I and II respectively were first tested for their effects on the FM2-10 dye release using various concentrations as no extensive literature was available for their *in vivo* IC₅₀ values due to their relatively recent discoveries. It has been claimed that Dynole specifically inhibits dynamin-I at lower concentrations (*in vitro* IC₅₀ 1.3 μM; Hill *et al.*, 2009) and thus one should see the effects of blockade of dynamin-I when lower concentrations of this drug is used.

The results presented in Figure 4.5 B indicates that while 10 μM dynole had no significant effect on the FM2-10 dye release, 20 μM dynole significantly increased the amount of dye released when ION5C was employed as a stimulus (p<0.0466). 20 μM dynole was then tested for its effect on the Glu release to rule out any discrepancies – such as an increase in release of the latter – which would then explain the increased FM2-10 dye release. However, it was found that it had no significant effect on the Glu release when compared to the control condition (Figure 4.5 A). This would indicate that during ION5C (and possibly 4AP5C) stimulation, dynamin-I may be involved in the closure of the fusion pore of the RRP vesicles causing them to release by KR. When the concentration of dynole was further increased to 50 μM, the amount of FM2-10 dye release was surprisingly reduced when compared to that of 20 μM dynole treatment but was comparable to that of control conditions. One could argue that at such a higher concentrations of dynole, dynamin-II may be inhibited (*in vitro* IC₅₀ 14.2 μM) which could then have implications on the FM2-10 dye release (explained further in 4.3.3).

Although there would be an obvious overlap of the SV exocytosis and endocytosis process, this new role of dynamin-I differ slightly from its role in SV endocytosis.

Under normal circumstances of SV exocytosis, dynamin-I may selectively restrict the fusion pore of certain vesicles (RRP), thus preventing their collapse into the plasma membrane through continuous expansion of the fusion pore. These narrow-neck fusion intermediates (“ Ω ” shape) will exist only for a short duration before their closure (and subsequent fission) by dynamin-I using its GTPase activity. The kinetics of this fission is very fast and closes the fusion pore before FM2-10 dye can depart from the vesicle membrane thus preventing latter’s release.

It has been previously shown by various studies that the GTPase activity of dynamin-I is not required for its early self-assembly or interaction with its PRD interacting partners (Heymann & Hinshaw, 2009). Since dynole affects the activity of dynamin-I simply by inhibiting its GTPase activity (as does DYN), it raises a question as to why there is an increased release of FM2-10 dye when dynamin-I was inhibited by this drug when compared to the control condition? One would expect to see no release of FM2-10 dye from RRP SVs as they would be arrested in the “ Ω ” shape due to its lack of GTPase activity (result of dynole treatment) which is required for the membrane fission. Thus dynamin-I lacking its GTPase activity could physically prevent the expansion of the fusion pore through its assembly into rings around the fusion pore neck (which does not require GTPase activity) thereby restricting the FM2-10 dye release in both the cases.

It has been recently shown that dynamins exhibit two distinct levels of GTPase activity in the presence of GTP nucleotides (Liu *et al.*, 2013). The assembly-assisted GTPase activity (AAGA) of dynamin-I has been reported to play an important role in the membrane fission during SV endocytosis whereas its basal GTPase activity (BGA) is thought to play additional roles in the early stages of vesicle endocytosis

but is yet poorly understood (Liu *et al.*, 2013). These distinct GTPase activity could help answer the question raised against the differences in FM2-10 dye release observed after inhibiting the GTPase activity of dynamin-I. Under control conditions, the BGA of dynamin-I would trigger its assembly around the neck of the exocytosing SVs which in turn could trigger AAGA of dynamin-I thereby causing membrane scission and closure of the fusion pore. On the other hand, dynole would block both, BGA and AAGA of dynamin-I but may not be able to prevent its assembly into rings around the fusion pore. These rings would thus be able to physically restrict the fusion pore for a prolonged period and the fusion pore size in this case may be larger when compared to the control conditions (due to absence of BGA activity) thereby facilitating the efflux of the FM2-10 dye out of the fusion pore. This model can be supported by the recent studies conducted by Liu *et al.*, (2013) where they used different dynamin-I mutants impaired with different GTPase activities. Their results suggests that the dynamin-I mutants lacking both the GTPase activities were able to arrest the endocytosis at an early stage and the mutants exhibiting only the BGA stabilised these intermediates at a later stage with many of them displaying long neck intermediates (Liu *at al.*, 2013). Thus, the lack of AAGA would delay the decision of fission and the assembled dynamin-I – along with other assembly partners – would restrict the fusion pore at the narrow-neck intermediate stage such that the fusion pore will remain open for a long duration (Liu *et al.*, 2011) so that the FM2-10 dye can now be released. The pore sizes and the structure of these intermediates would be dependent on the BGA where its lack may cause a wider pore size when compared to the long neck structures with relatively narrow pore size which would otherwise be observed in a much higher proportion.

The pore sizes of the releasing SVs were not measured as part of this study but many of the previous studies have reported the diameter of the fusion pore of SVs undergoing KR to be from 1 to 2.3 nm in various model systems (Wu *et al.* 2011; Jackson & Chapman, 2006). Recently, Wu *et al.* (2011) estimated the axial cross sectional area of FM2-10 dye to be around 1.03 nm and found that the efflux (from the fusion pore) time constant of the dye varied from 8.1 ± 0.4 sec to 20.5 ± 2.8 sec depending on the fusion pore diameter. Thus, during KR, the fusion pore diameter and the axial cross sectional area of the FM2-10 dye highly affects the efflux rate and thus associated decrease in its fluorescence kinetics. Along with the diameter of the fusion pore, the morphology of the fusion pore may also have possible implications on the efflux rate of the dye. Under control conditions, the BGA of dynamin-I would keep the fusion pore restricted with a relatively smaller fusion pore diameter and relatively long neck thereby decreasing the FM2-10 dye efflux rate and possibly restricting the FM2-10 dye release all together. It should be noted that the fusion pore at this stage will be closed quickly by the GTPase activity of dynamin resulting in “fast endocytosis” of the releasing vesicles which can still be termed as KR mode of exocytosis. However, when the dynole or dyansore is used, the lack of GTPase activity all together will restrict the fusion pore with a relatively large diameter and short neck there by increasing the FM2-10 dye efflux rate facilitating the early decrease in its fluorescence. The slower efflux rate of FM2-10 dye coupled with the long neck intermediates could also help explain why there is a continuous decrease in the FM2-10 dye fluorescence during 4AP5C even after 2 sec of stimulation even though the stimulus can only release RRP which should be exhausted in about 2 sec according to previous reports (Denker & Rizzoli, 2010; Richards *et al.*, 2003). The fact that 4AP5C stimulation involves release of Ca^{2+} from intracellular Ca^{2+} store by elevating inositol trisphosphate

levels could mean that the increase in $[Ca^{2+}]_i$ may be much slower when compared to rest of the two stimuli (Grimaldi *et al.*, 2001; Figure 3.3). This could add to the delay in FM2-10 dye release as the RPP SVs may take longer than 2 sec to release. This decrease in FM2-10 fluorescence after 2 sec of stimulation cannot be attributed to its de-partitioning or leakage from rest of the external plasma membrane as this would be compensated when subtracting the L_0 evoked FM2-10 dye fluorescence from the stimulation evoked fluorescence (section 2.2.3).

These discussions in which dynamin regulates the size of the pore during exocytosis (but not necessary scission) would mean that the RRP of SVs did not actually switch to FF as the SVs did not fully insert into the membrane. However, the results clearly indicate that KR does exist in nerve terminals and that it can be regulated by dynamins. FM2-10 dye release can occur if (i) the pore is sufficiently large to allow FM2-10 dye efflux (ii) the pore remains open for longer than 0.5 sec; (iii) the SV fully inserts into the membrane (FF). As dynamins are known to cause scission of the neck of clathrin coated vesicles then it is clear that dynamins could actually cause the closure of the fusion pore after their opening for less than 0.5 sec. In fact, the FM2-10 dye release measurements may actually be a combination of the three alternative ways that FM fluorescence can decrease. In very recent experiments, it would appear that a proportion of what has been described as FF of the RP, may actually represent the pore not closing (A. Ashton, unpublished observation: results due to differences in the biochemical properties, see section 5.3.1).

4.3.3 Inhibition of dynamin-II

It is clear from section 4.3.1 that dynamin-I play a significant role in determining the exocytosis fusion mode of certain RRP vesicles during the application of certain stimuli. In order to investigate the role of dynamin-II, dyngo was employed in this study whose *in vitro* IC₅₀ have been determined to be 380 μ M and 2.6 μ M for dynamin I and II respectively and it's *in vivo* IC₅₀ have been reported to be around 30 μ M for specific inhibition of dynamin-II (Howes *et al.*, 2010 & Harper *et al.*, 2011). Similar to dynole studies, different concentrations of dyngo were first tested for their effects on FM2-10 dye release and only a particular concentration was selected for assessing its effect on Glu release.

The data presented in Figure 4.6 B shows that 20 μ M dyngo had no significant effect on the amount of FM2-10 dye released when compared to that of control during ION5C stimulation. Surprisingly, however, 50 and 100 μ M dyngo reduced the amount of FM2-10 dye released during ION5C stimulation but these differences appeared not to be statistically significant, herein, ($p > 0.05$; $n = 22, 24$ & 19 for con, 50 & 100 μ M dyngo respectively; 3-4 independent experiments) but more experiments by A. Ashton and colleagues have indicated that this is a real statistically significant result. It is also important to note that 50 μ M dyngo does not affect the amount of Glu released when compared to that of control (Figure 4.6 A; $p > 0.05$, $n = 7$, 2 independent experiments).

This would suggest that when dynamin-II is inhibited by dynole, the RP vesicles undergo KR mode of exocytosis (instead of FF) thereby decreasing the amount of FM2-10 dye released. This switch in the mode can only be attributed to the RP as all the RRP vesicles already undergo KR during ION5C stimulation. It has been suggested in non-neuronal cells (especially chromaffin cells) that dynamin(s) can

regulate both, closure of the fusion pore as well as its expansion by poorly understood mechanisms (Gonzalez-Jamett *et al.*, 2013). The current knowledge suggests that in these non-neuronal cells, GTPase activity of dynamin-II coupled with actin polymerisation may drive the expansion of the fusion pore (Gonzalez-Jamett *et al.*, 2013). It has been suggested that this process also involves Synadapin (Samasilp *et al.*, 2012), GTPase Cdc42 (Gasman *et al.*, 2004) and N-WASp (a nucleation promoting factor; Shin *et al.*, 2008 & Hartig *et al.*, 2009). It is likely that in cerebral cortical neurons, dynamin-II may function in the same way in order to drive the expansion of the fusion pore. It can be suggested that dynamin-II may be required for the expansion of the fusion pore of RP vesicles causing them to release by FF and may not play any role during the release of the RRP vesicles as they usually undergo KR during HK or ION5C stimulations. However, it would be interesting to see the effects of 50 μ M dyngo on the HK5C and 4AP5C evoked release as it will ascertain if the action of dynamin-II is restricted to a specific pool of vesicles or is it indispensable for the expansion of the fusion pore. In fact, further experiments in A. Ashton's laboratory has shown that dyngo also reduces the amount of FM2-10 dye release evoked by HK5C, but that as expected dyngo does not perturb the release evoked by 4AP5C. This finding also suggests that 160 μ M DYN may only be able to inhibit the action of Dynamin-I in the model system employed in this study otherwise one would expect a switch in the exocytosis mode to KR for the RP vesicles during HK5C or ION5C stimulations (and therefore no dye release).

In this study, role of dynamin-III was not studied as a small population of dynamins constitute this particular isoform and is mainly believed to have similar functions to that of dynamin-I (Heymann & Hinshaw, 2009).

4.3.4 Inhibition of non-muscle myosin-II

From previous discussions it is clear that dynamin-I play a direct role in the involvement of KR mode of the RRP of SV exocytosis during ION5C and 4AP5C stimulations. However, the amount of FM2-10 dye released was not affected by the inhibition of dynamins by 160 μM DYN during HK5C stimulation. However, it is evident that some of the SVs (those belonging to RRP) undergoes KR mode of exocytosis during HK5C stimulation as the amount of FM2-10 and Glu released during HK5C stimulation is comparable to those during ION5C stimulation (see Figure 3.2, 3.5 and 3.6). Thus it is imperative that there would be at least one protein – but not dynamins – involved in the regulation of KR mode of exocytosis during HK5C stimulation. As discussed in introduction, non-muscle myosin-II was another strong contender for this role and their action was inhibited by using 50 μM blebbistatin (Blebb) in this study (Kovács *et al.*, 2004).

Data presented in Figure 4.7 clearly show that 50 μM blebbistatin does not affect the amount of Glu released during the application of any of the three stimuli indicating that the inhibition of myosin-II does not affect the total number of SVs exocytosing in these conditions. The FM2-10 dye release data, on the other hand, show exactly opposite trends to those seen during the inhibition of dynamins by dynasore (Figure 4.8 & 4.2). There was a significant decrease in the FM2-10 dye fluorescence when myosin-II was inhibited during HK5C stimulation ($p=0.001$) but it did not affect the fluorescence when ION5C or 4AP5C were employed. This indicates that myosin-II may be involved in the closure of the fusion pore of certain vesicles (RRP pool) causing them to release by KR during HK5C stimulation and when they are inhibited, all the releasable vesicles would undergo FF mode of exocytosis.

4.3.5 Why two proteins for the same process?

From the data presented so far it is clear that there are two distinct proteins involved in the regulation of KR during SV exocytosis. This involvement seems to be dependent on the $[Ca^{2+}]_i$ achieved at the active zone during the employment of a particular stimulation paradigm. As shown in Figure 3.3, all the three stimuli produce different changes in $[Ca^{2+}]_i$ with each having distinct kinetics associated with them. HK5C stimulation achieves the maximum $[Ca^{2+}]_i$ at an early stage (~6 sec) of the stimulation period after which it plateaus and maintains that high level of $[Ca^{2+}]_i$ throughout the stimulation period. Comparatively, ION5C produces an increase in the $[Ca^{2+}]_i$ with a much slower kinetic even though it eventually achieves the same magnitude of $[Ca^{2+}]_i$ as that achieved during HK5C stimulation. Finally, 4AP5C achieves relatively lower increase (~50%) in the $[Ca^{2+}]_i$ with a much slower kinetic when compared to that of HK5C and ION5C.

All the data obtained from Fura-2-AM measurement represents the change in total free $[Ca^{2+}]_i$ as opposed to the changes in $[Ca^{2+}]_i$ at the active zone alone. Since all the SV exocytosis occur at the active zone, the free $[Ca^{2+}]_i$ at or near the active zone would play an important role in regulating SV exocytosis. HK5C works by depolarising the nerve terminal which then activates various VGCCs there by facilitating the entry of free Ca^{2+} into the synaptosomes. Since all the VGCCs are located at or near the active zone, it could be argued that the initial increase in $[Ca^{2+}]_i$ would only be seen at or near the active zone before the Ca^{2+} finally diffuses away from the active zone due to the concentration gradient (Meiri et al., 1999). 4AP, on the other hand, increases free $[Ca^{2+}]_i$ partly by potentiating capacitative calcium entry and partly by elevating inositol trisphosphate levels and therefore causing Ca^{2+} release from intracellular calcium stores (Grimaldi *et al.*, 2001).

However, others have suggested that 4AP works by blocking delayed rectifier type K^+ channels (Choquet & Korn, 1992) but this may not be the case in non-depolarised synaptosomes. Thus the kinetic and magnitude of increase in $[Ca^{2+}]_i$ is very slow during 4AP5C stimulation especially at or near the active zone. Lastly, ION is a selective Ca^{2+} ionophore that inserts itself in the plasma membrane thereby allowing the entry of free Ca^{2+} into the cytosol independent of the VGCCs (Müller *at al.*, 2013). Since this Ca^{2+} influx is not restricted to the active zone, the free $[Ca^{2+}]_i$ at or near the active zone will be much lower than that induced by HK5C.

Thus it can be argued that all the three stimuli produces different levels of $\Delta[Ca^{2+}]_i$ at the active zone with HK5C producing the maximum increased, followed by ION5C and then by 4AP5C. These different levels of free $[Ca^{2+}]_i$ may then activate only a particular protein – either dynamin-I or myosin-II – which can then regulate the fusion pore of the RRP SVs. From Figure 4.9, it can be suggested that the dynamin-I would only be able to close the fusion pore of RRP SVs when the overall $\Delta[Ca^{2+}]_i$ is ≤ 140 : nM whereas myosin-II would be able to perform this function during high levels of $\Delta[Ca^{2+}]_i$ (> 140 : nM) during the release of RRP vesicles.

4.4 Conclusions

In summary, the data and arguments presented in this chapter of the thesis establish that dynamins and myosin-II are involved in the regulation of KR mode of exocytosis. This study also establishes for the first time that dynamin-I and myosin-II play a crucial role in the closure of the transiently open fusion pore during the SV exocytosis of RRP vesicles depending on the type of stimulus used. It should be noted that the action of dynamin-I is independent of clathrin and therefore it is different from its role in CME. The involvement of these proteins seems to be dependent on the amount of $[Ca^{2+}]_i$ achieved upon stimulation at the active zone. From the arguments provided it can also be assumed that this role of dynamin-I and myosin-II is independent of the role of each other. The data with 50 μ M dyngo also suggests that dynamin-II may be required for the expansion of the fusion pore during FF mode of exocytosis. However further studies are required to ascertain this part of the research.

Chapter 5

Role of Calcium

5.1 Introduction

Chapter 4 of this thesis extensively discussed about the involvement of two proteins – dynamin-I and myosin-II – in the regulation of KR mode of exocytosis in pre-synaptic neurons of mature rat cerebral cortex. Although both the proteins essentially perform the same function of closing the fusion pore during SV exocytosis, only one of them could be actively participating in this function depending on the $[Ca^{2+}]_i$ achieved at the active zone upon stimulation. It has also been shown by Dr. A. Ashton's previous work (unpublished work) that the inhibition of particular VGCCs – L-type for non-diabetic and N-type for diabetic – can switch the mode of SV exocytosis without affecting the amount of Glu being released. They have also previously shown that inhibition or activation of certain phosphatases and kinases can switch the mode of SV exocytosis in the given model system (Ashton *et al.*, unpublished work). Thus it seems reasonable to suggest that the two proteins – dynamin-I and myosin-II – may be targets of certain Ca^{2+} sensitive phosphatases and kinases which would then determine their role in the closure of the fusion pore during SV exocytosis. The role of two such enzymes, calcineurin and protein kinase C (PKC) was assessed in this study to determine if they played any role in the regulation of the activity of dynamin-I and myosin-II.

5.2 Results

5.2.1 Inhibition of calcineurin

Calcineurin is a well-studied Ca^{2+} sensitive phosphatase that has a wide range of target proteins that are involved in various processes (Cheung & Cousin, 2013; Kumashiro *et al.*, 2005). In this study, calcineurin was inhibited by using 1 μM cyclosporin A (Cys A) and its effect on Glu and FM2-10 dye release was assessed. It was found that 1 μM Cys A did not affect the amount of Glu released but it significantly decreased the amount of FM2-10 dye released during the employment of HK5C ($p < 0.025$) and ION5C stimulation ($p < 0.023$; Figure 5.1 & 5.2). When the effect of Cys A on the amount of $[\text{Ca}^{2+}]_i$ achieved during stimulation was assessed, it was found that the treatment significantly increased the $[\text{Ca}^{2+}]_i$ when compared to control for all the three stimuli (Figure 5.3). Together, these data would indicate that the inhibition of calcineurin causes more SVs to undergo KR mode of exocytosis and this could possibly be due to the increased $[\text{Ca}^{2+}]_i$ achieved during their inhibition. It should be noted that 1 μM Cys A does not affect the 4AP5C evoked Glu or FM2-10 dye release (Figure 5.1C, 5.2C) even when there is an increase in the $[\text{Ca}^{2+}]_i$ upon stimulation. This suggests that Cys A only acts on the RP of SVs and that since 4AP5C does not release the RP SVs, Cys A treatment has no effect on the mode of exocytosis.

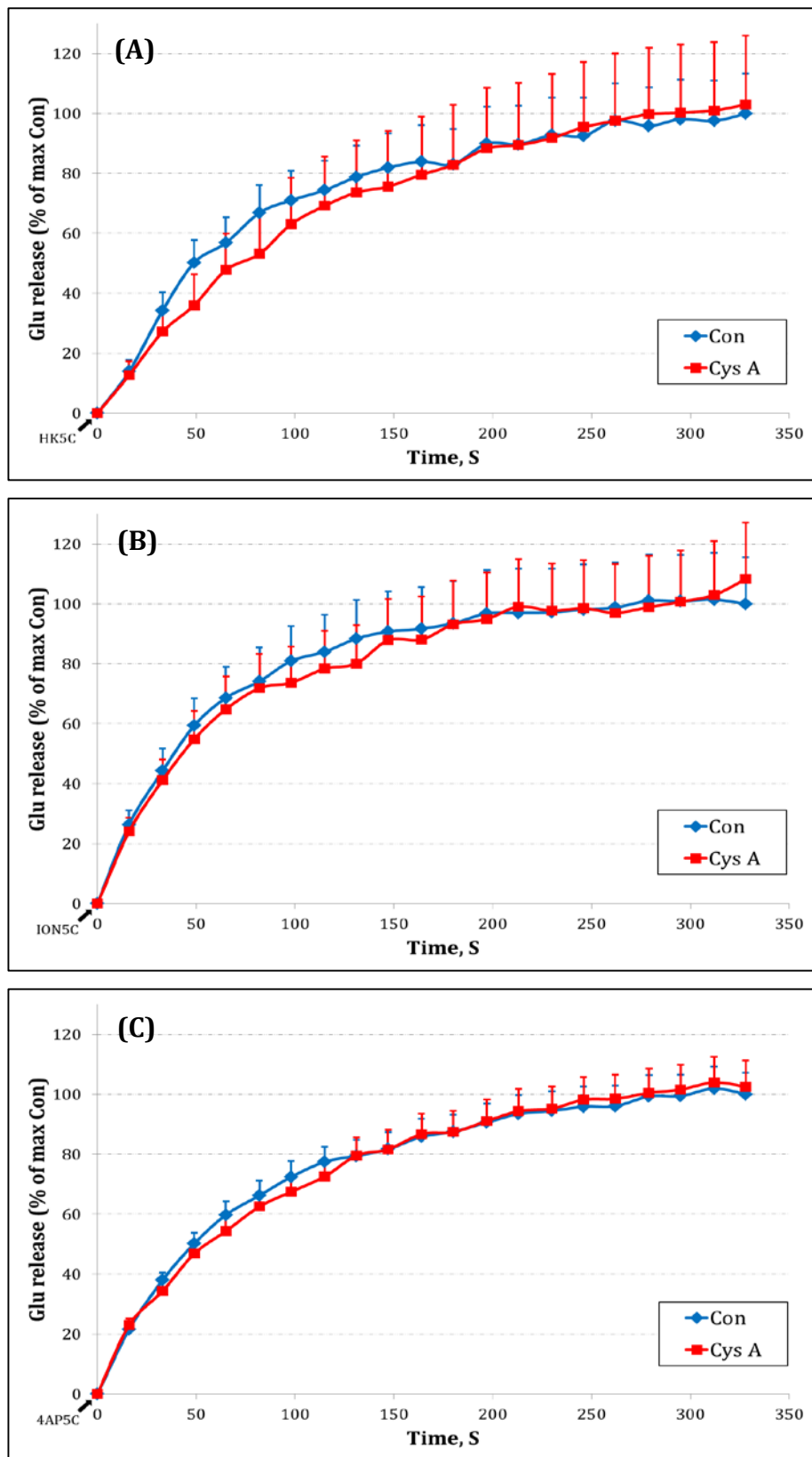


Figure 5.1: Blockade of calcineurin by 1 μ M Cyclosporin A does not affect the total amount of glutamate released upon the application of (A) HK5C, (B) ION5C and (C) 4AP5C stimulations. The data is representative of more than 3 experiments with error bars representing SEM and $p > 0.05$ for all experiments. The data points

represent amount Glu released, expressed as percentage, with error bars representing SEM. Student t test resulted in $p>0.05$ for all three experiments.

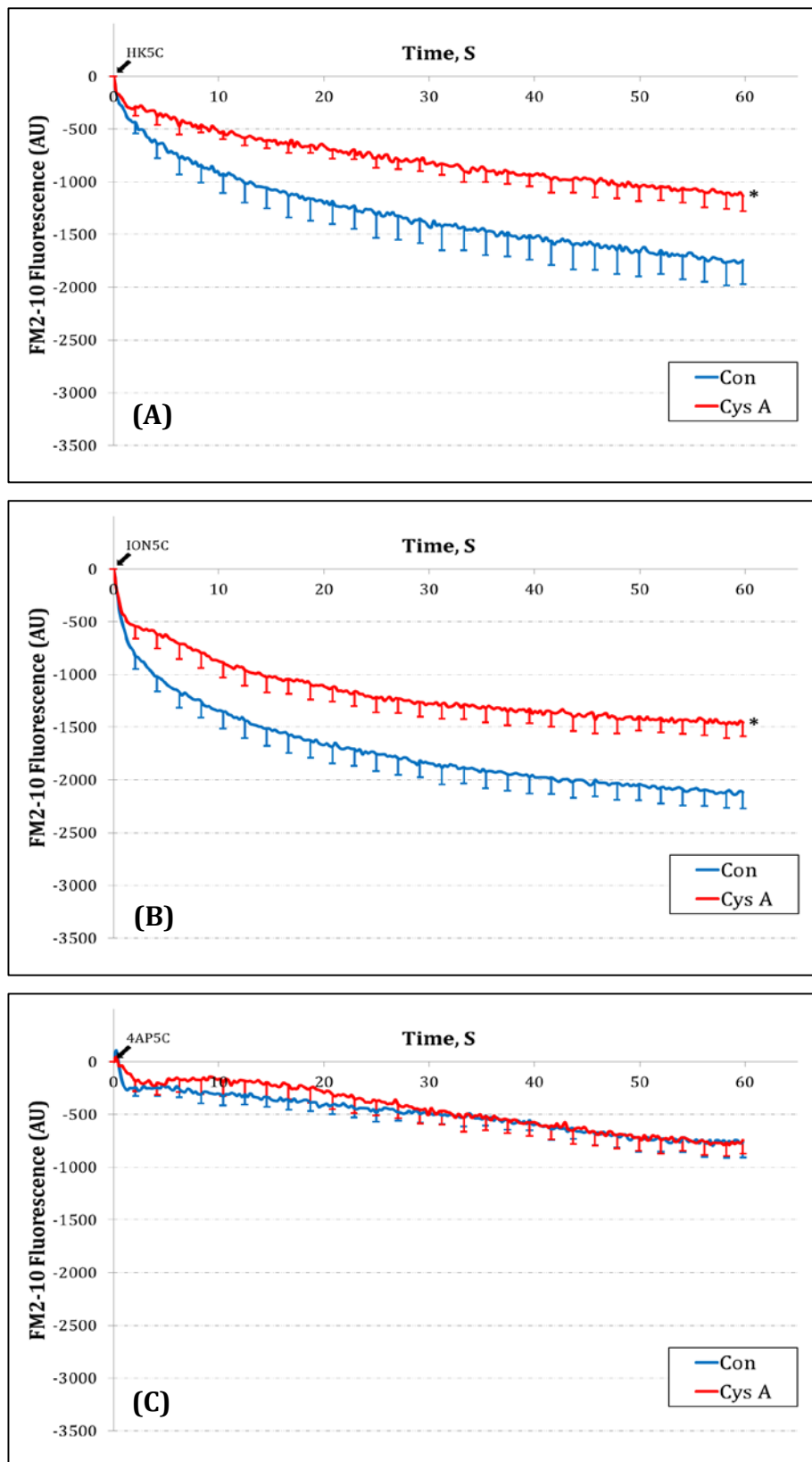


Figure 5.2: Inhibition of calcineurin causes some RP vesicles to undergo KR. When calcineurin was inhibited by pre-treatment with 1 μ M Cyclosporin A, it significantly decreased the amount of FM2-10 dye released during (A) HK5C ($p < 0.025$) and (B) ION5C ($p < 0.025$) stimulations but had no effect when the

synaptosomes were stimulated with (C) 4AP5C. The data is representative of more than 3 experiments with error bars representing SEM.

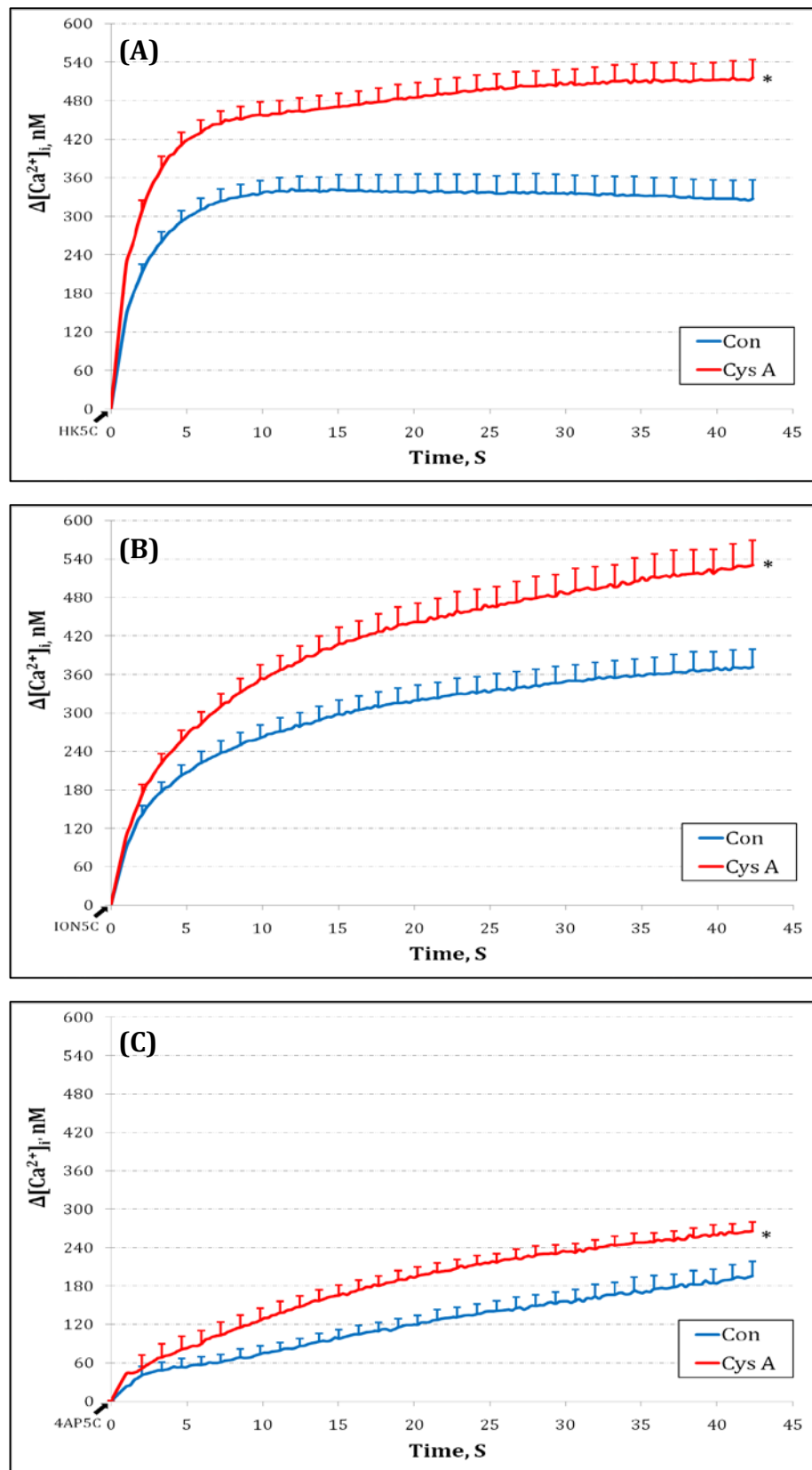


Figure 5.3: Cys A produces larger $\Delta[Ca^{2+}]_i$ for all three stimuli. Pre-treatment of synaptosomes with 1 μ M Cyclosporin A produced a higher change in $[Ca^{2+}]_i$ upon the application of various stimuli, (A) HK5C ($p < 0.001$) (B) ION5C ($p < 0.044$) and (C) 4AP5C ($p < 0.049$), when compared to their control counterparts. The data is representative of more than 3 experiments with error bars representing SEM.

In order to establish if Cys A treatment causes this increase in KR mode of exocytosis due to its action on any of the two proteins discussed earlier, Cys A was used in combination with either Blebb or DYN and their effects on FM2-10 and Glu release was studied. Data presented in Figure 5.4 suggests that the combination treatments do not affect the amount of Glu released during the employment of any of the three stimuli. On the other hand, the combination treatments evoked FM2-10 dye release with a distinct kinetics and amount during HK5C and ION5C stimulations (Figure 5.5A; 5.5B; section 5.3.1). However, during 4AP5C stimulation, the combination treatment increased the FM2-10 dye release similar to that observed during the use of DYN alone (Figure 5.5C). These data, along with the previous arguments, could suggest that the inhibition of calcineurin may inhibit the action of dynamin-II in the expansion of the fusion pore thereby causing the RP SVs to release by KR (see 5.3.1 for discussion).

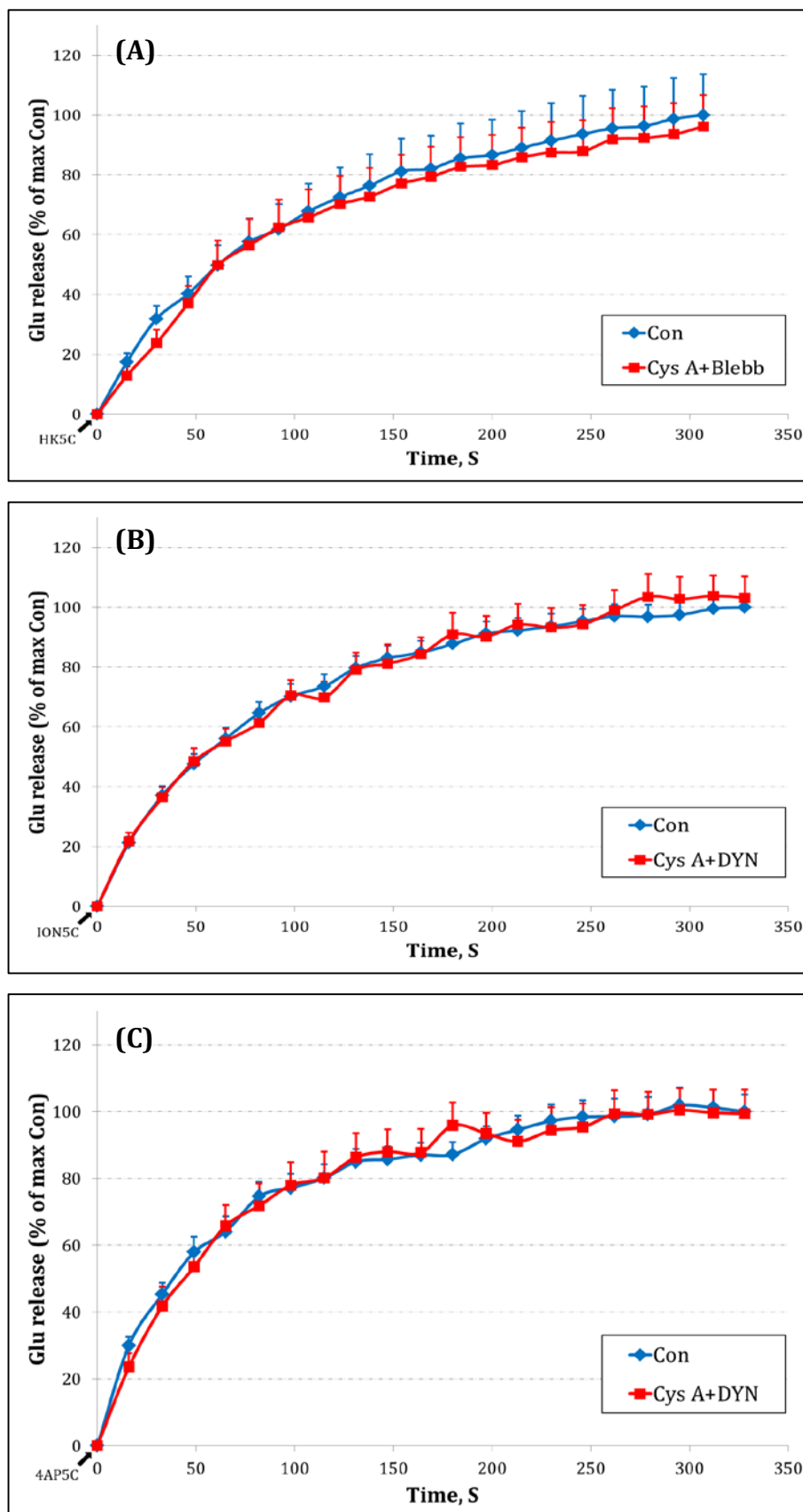


Figure 5.4: A combination treatment of CysA+Blebb or Cys A+DYN does not affect the Glu released during (A) HK5C, (B) ION5C or (C) 4AP5C stimulation conditions. The data is representative of more than 3 experiments with error bars representing SEM and $p > 0.05$ for all data sets.

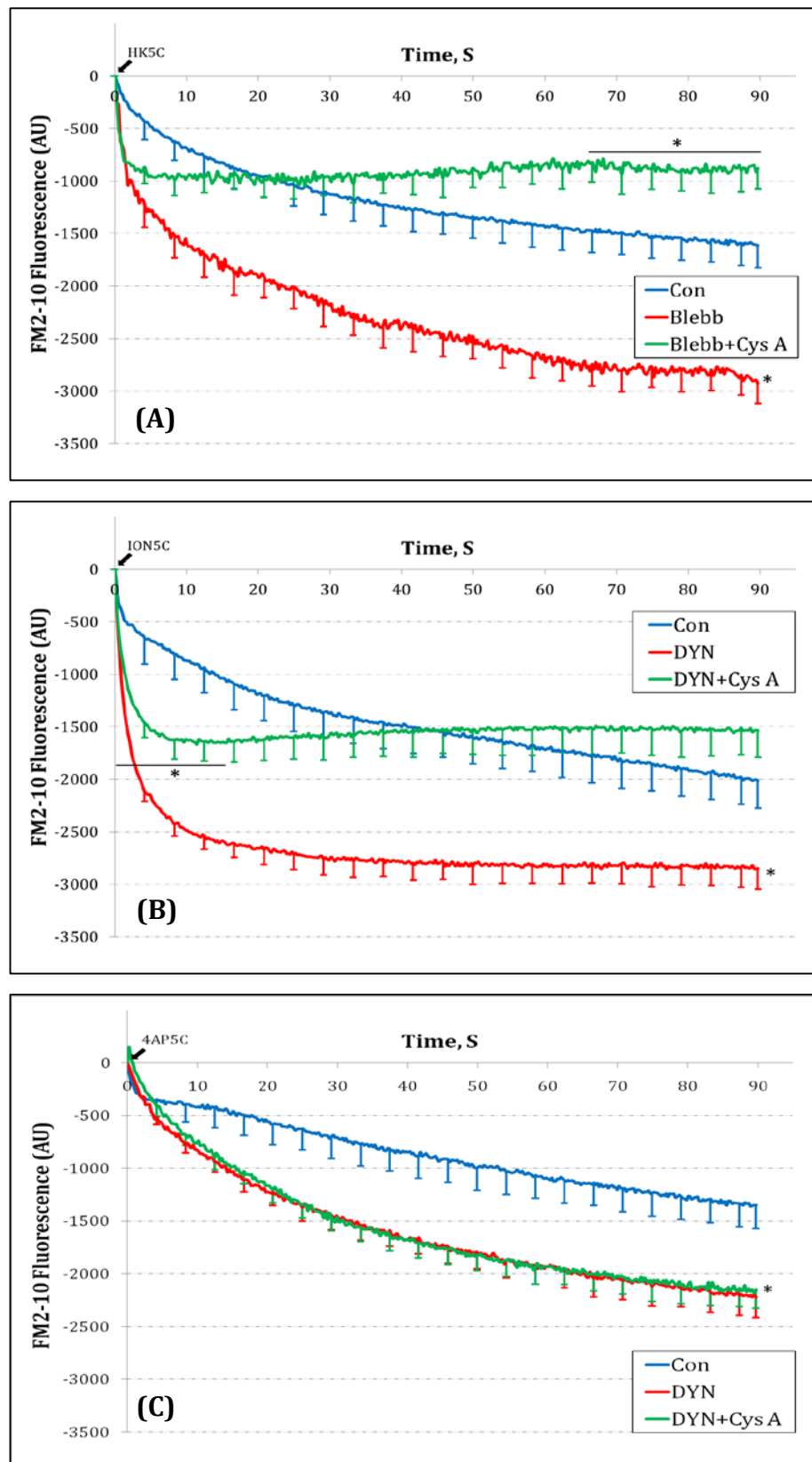


Figure 5.5: Distinct effects of DYN+Cys A and Blebb+Cys A treatment on FM2-10 dye release. Pre-treatment of synaptosomes with a combination of either (A) CysA+Blebb or (B) Cys A+DYN altered the kinetics of FM2-10 dye released during (A) HK5C and (B) ION5C stimulations when compared to that of control conditions. On the other hand, the combination treatment of Cys A+DYN released the same amount of dye as during DYN

treatment alone ($p>0.05$) when (C) 4AP5C stimulation condition was employed. (A) For Blebb+Cys A vs control $p\leq 0.029$ for data points from 60 to 90 sec, and (B) for DYN+Cys A vs control $p\leq 0.0259$ for data points from 0.26 to 12.4 sec, and (C) for DYN+Cys A vs control $p\leq 0.038$ from 16 to 90 sec

5.2.2 Inhibition of Protein Kinase C

It has been suggested by many research groups that dynamin-I and myosin-II are targets for phosphorylation by protein kinase C (PKC) – a Ca^{2+} sensitive kinase – for a variety of cellular functions (Chu *et al.*, 2012; Lipp & Reither, 2011). Thus, PKC was one of the strong kinase contenders for the regulation of dynamin-I and myosin-II and its potential role was assessed in this study by inhibiting it using 1 μM Go6983. Go6983 is a broad spectrum, cell permeable inhibitor of various PKC isoforms including PKC α , PKC β , PKC γ , PKC δ and PKC ζ but it does not inhibit PKC μ at the concentration used in this study (Gschwendt *et al.*, 1996).

Upon the inhibition of PKC by 1 μM Go6983 it was found that it did not affect the Glu or FM2-10 dye released upon stimulation with HK5C (Figure 5.6A & 5.7A). However, when Go6983 was used in combination with 160 μM DYN, it increased the amount of FM2-10 dye released during HK5C stimulation indicating that in the absence of active PKC, dynamin-I was playing a role in regulating the KR instead of myosin-II (Figure 5.7B). Interestingly, when 50 μM Blebb was used in combination with 1 μM Go6983, it did not affect the amount of FM2-10 dye released when compared to that of control condition indicating that myosin-II in this case may not be playing any role in the KR mode of exocytosis (Figure 5.7C). In both the cases, the various combinations of drugs did not affect the total number of SVs undergoing exocytosis during the application of a stimulus (Figure 5.6B & 5.6C). Thus, it could be concluded that dynamin-I and myosin-II are both targets of PKC and when PKC is activated by increased $[\text{Ca}^{2+}]_i$, it may phosphorylate dynamin-I and myosin-II rendering the former inactive and the latter in an active state.

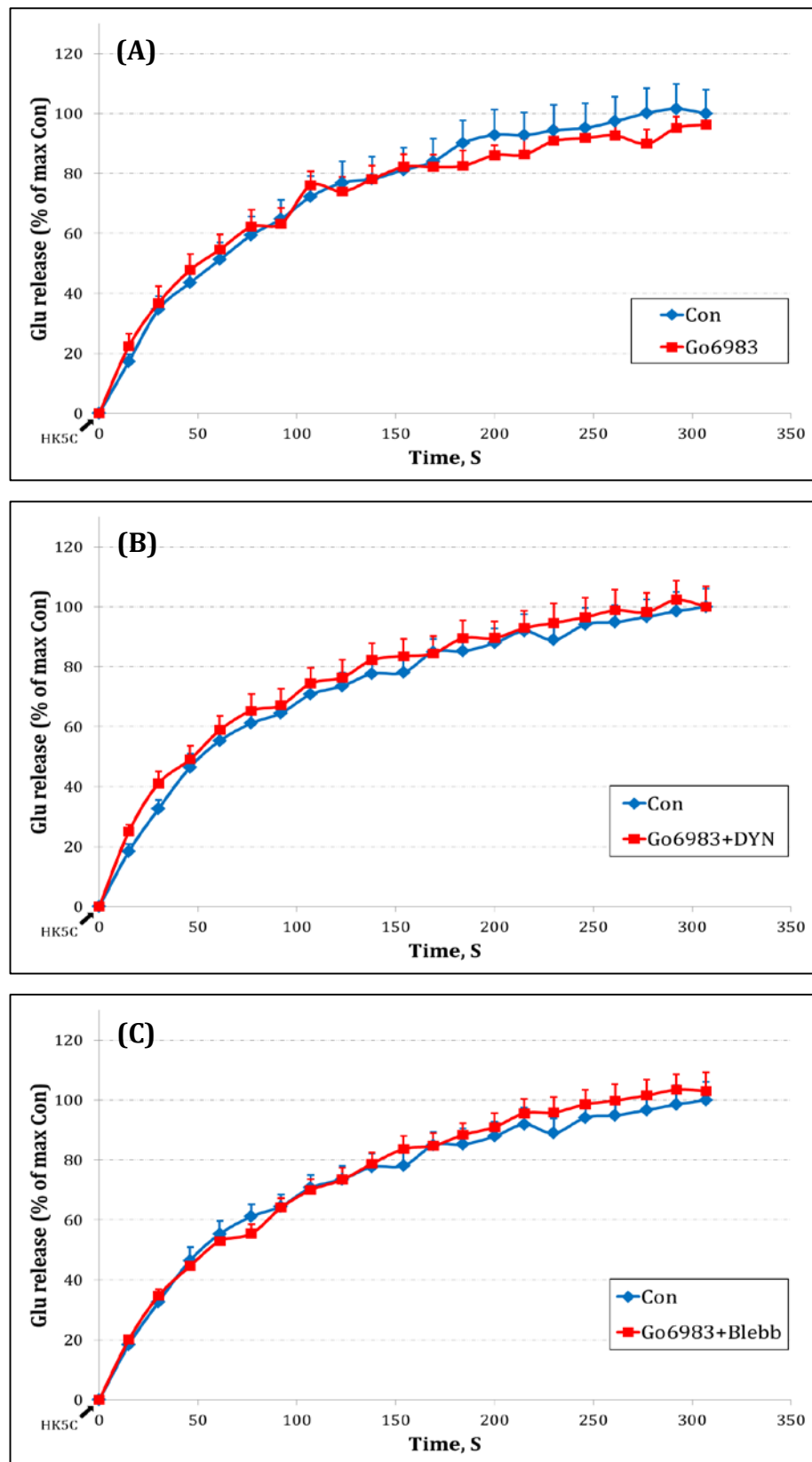


Figure 5.6: Inhibition of PKC, dynamins or myosin-II does not affect the total Glu released. Pre-treatment of synaptosomes with (A) 1 μM Go6983 alone or in combination with (B) 160 μM DYN or (C) 50 μM Blebb does not affect the amount of Glu released during HK5C stimulation. The data points represent amount Glu

released, expressed as percentage, with error bars representing SEM. Student t test resulted in $p>0.05$ for all three data sets.

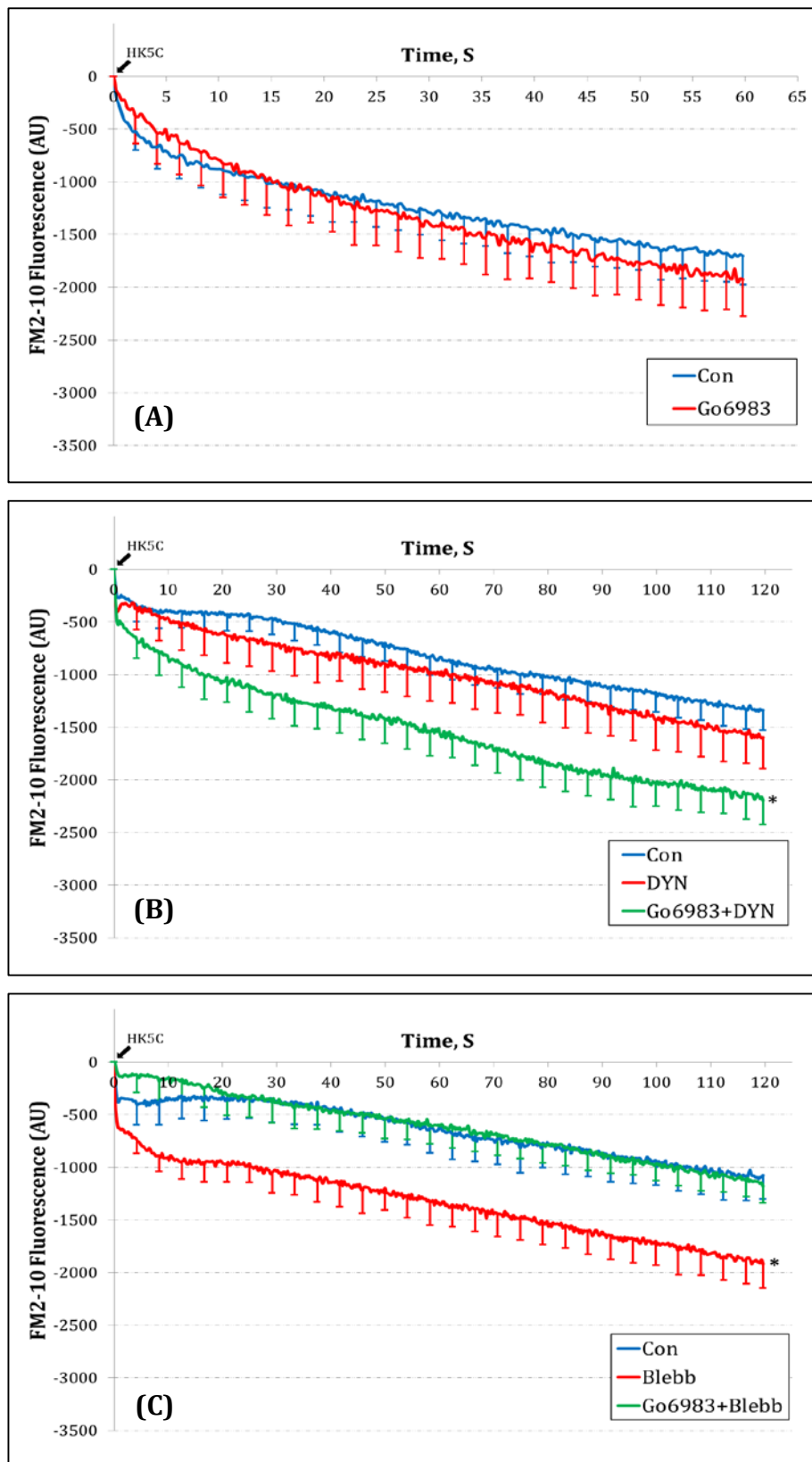


Figure 5.7: Inhibition of PKCs by 1 μ M Go6983 switched the protein dependence for KR during HK5C stimulation. (A) Inhibition of PKC by Go6983 did not affect the FM2-10 dye released but it increased the dye release when used in combination with (B) DYN ($p \leq 0.0387$) but did not cause any such increase (C)

with Blebb ($p=0.7008$). The data is representative of more than 3 experiments with error bars representing SEM.

5.2.3 Activation of Protein Kinase C

Data presented in section 5.2.2 suggested that inhibition of PKCs during HK5C stimulation changed the protein dependency for the KR – i.e., instead of myosin-II, dynamin-I played a role while PKCs were inhibited during HK5C stimulation. This indicates that – under control conditions – at a higher $[Ca^{2+}]_i$, PKC would be activated which would then inactivate dynamin-I and activate myosin-II by phosphorylating them. It would, thus, be interesting to see if this protein dependency could be switched at a relatively lower $[Ca^{2+}]_i$ (as achieved during ION5C stimulation) by activating PKCs.

One of the commonly used PKC activators is Phorbol 12-myristate 13-acetate (PMA) and similar to dynole and dyngo experiments (see 4.2.2), different concentrations of PMA was first tested for their effect on FM2-10 dye release and then – based on FM2-10 dye data – a particular concentration of interest was selected for its effect on Glu release. It can be noted from Figure 5.8 that use of 300, 200 & 100 nM of PMA caused an increase in the FM2-10 dye release in the presence or absence of 160 μ M DYN during ION5C stimulation. This indicates that these concentrations of PMA were unable to reduce the dependency on dynamin-I for closure of the fusion pore of the RRP SVs during ION5C stimulation. Indeed, 300 and 200 nM PMA were able to switch the RRP SVs to a FF like mode of release (Figure 5.8 A, B). This had been shown previously by A. Ashton (unpublished) when 1 μ M PMA was employed with HK5C stimulation. This result indicates that when

there is a large stimulation of possibly several PKCs using high PMA concentrations then RRP SVs release all their FM2-10 dye. The concentration of PMA was further reduced to 40 nM and this did not affect the FM2-10 dye released (Figure 5.9B & 5.9C). This concentration was then used in combination with 160 μ M DYN and such treatment resulted in FM2-10 dye release similar to that of control conditions (Figure 5.9B). On the other hand, when 40 nM PMA was used along with 50 μ M Blebb, it significantly increased the amount of FM2-10 dye released (Figure 5.9C; $p = 0.0072$). Use of 40 nM PMA alone or with combination of DYN or Blebb did not affect the overall Glu released when compared to control (Figure 5.9A). Together, these results indicate that activation of PKC by submaximal concentration of PMA (40 nM) was able to switch the protein dependency for regulating the fusion mode during ION5C stimulation. These, along with results in section 5.2.2, provide strong evidence that dynamin-I and myosin-II are targets of PKC phosphorylation during SV exocytosis at a high $[Ca^{2+}]_i$.

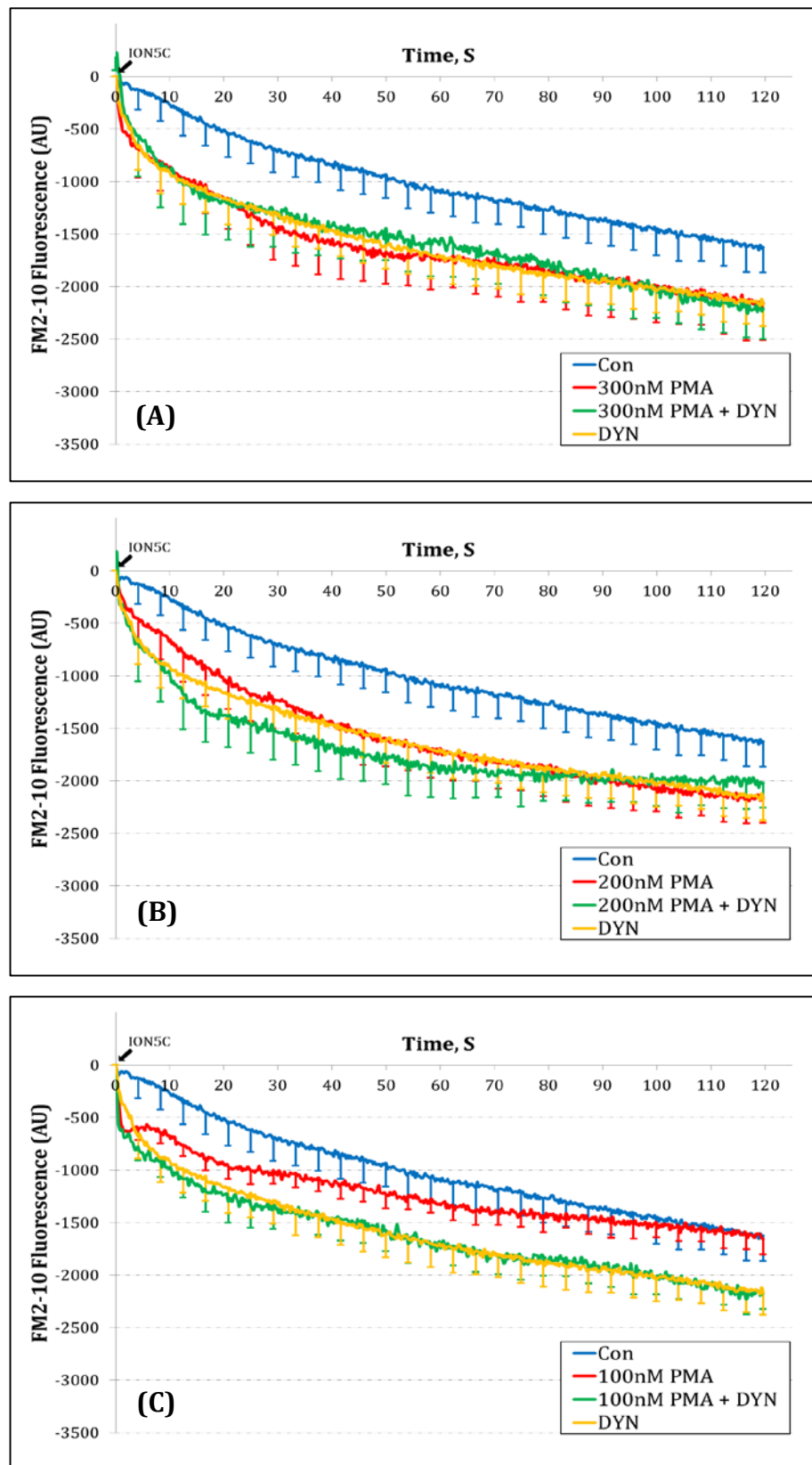


Figure 5.8: Various sub-maximal concentrations PMA failed to switch the protein dependency for KR mode of exocytosis. When PKCs were activated by various concentrations of PMA, such as (A) 300 nM, (B) 200 nM and (C) 100 nM, it failed to completely switch the protein dependency for KR during ION5C stimulation and this is demonstrated by an increase in the FM2-10 dye when the

synaptosomes were pre-treated with a combination of PMA and DYN. The data is representative of more than 3 experiments with error bars representing SEM and $p > 0.05$ for all data sets.

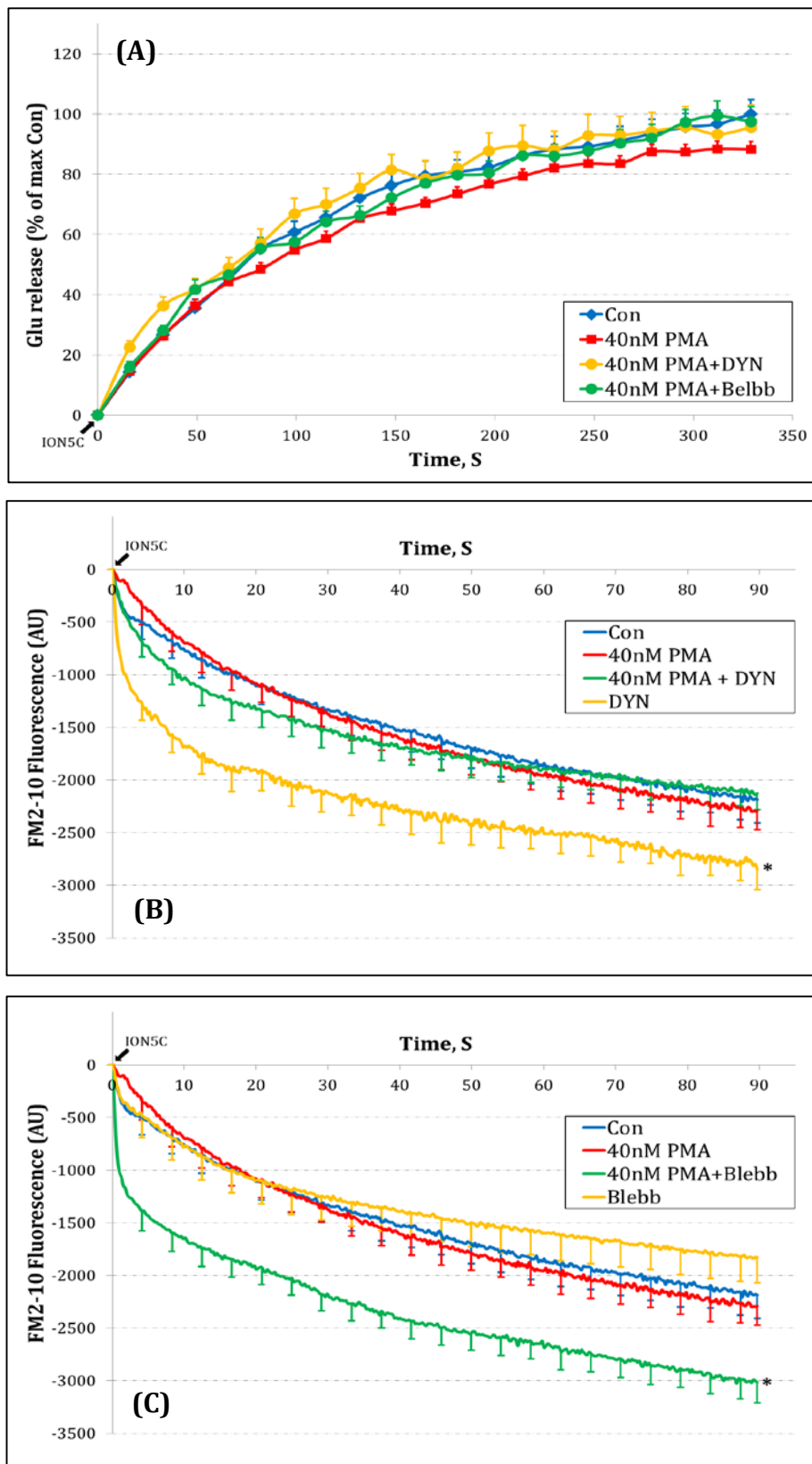


Figure 5.9: 40 nM PMA was able to switch the protein dependency for KR during ION5C stimulation. When the PMA concentration was further lowered to 40 nM, it completely switched the protein dependency during ION5C stimulation as demonstrated by (B) no change in the FM2-10 dye release following 40 nM PMA+DYN treatment ($p=0.7209$) and (C) increase in its release following 40 nM

PMA+Blebb treatment ($p \leq 0.0072$). (A) It should also be noted that none of the drug treatment significantly affected the total amount of Glu released ($p > 0.05$). The data is representative of more than 3 experiments with error bars representing SEM.

5.3 Discussions

This chapter of the study discusses potential kinase and phosphatase enzymes that may be involved in the regulation of the two proteins (dynamins and myosin-II) for their functions in regulating the fusion pore of the exocytosing vesicles. The study revealed two such enzymes, calcineurin and protein kinase C (PKC) that may phospho-regulate the two proteins being discussed.

5.3.1 Role of Calcineurin

Calcineurin is a Ca^{2+} sensitive phosphatase enzyme that has been shown to regulate many cellular processes when they are activated by elevated $[\text{Ca}^{2+}]_i$. When calcineurin was inhibited by using 1 μM Cys A, it had no effect on the amount of Glu released when compared to control conditions indicating that the same number of SVs were undergoing exocytosis upon stimulation (Figure 5.1). On the other hand, the Cys A treatment significantly reduced the amount of FM2-10 dye released during HK5C ($p < 0.025$) and ION5C stimulations ($p < 0.023$; Figure 5.2A; 5.2 B). This data suggests that when calcineurin is inhibited, there are more SVs undergoing KR when compared to that of control. Conversely, the inhibition of calcineurin did not switch the part of the RRP vesicles that undergo FF mode to KR during 4AP5C stimulation ($p = 0.985$; Figure 5.2C). Thus, the inhibition of calcineurin is able to switch the mode of exocytosis from FF to KR for the vesicles belonging exclusively to the RP. Section 4.3.3 of this thesis discussed possible requirement of dynamin-II in the expansion of the fusion pore of the RP vesicles thereby causing them to release by FF. Since, the inhibition of calcineurin switches these vesicles from FF to KR mode, it is possible that dynamin-II may require dephosphorylation by calcineurin in order for it to drive the expansion of the fusion pore of the RP vesicles.

As Cys A failed to prevent some FM dye being released from the RP SVs, this data might suggest that not all the RP SVs are switched to KR by this drug. However, this data does indicate that at least some of RP can switch to a KR mode. Alternatively, whilst there is a continuous decrease in the FM2-10 dye fluorescence from synaptosomes treated with Cys A during HK5C and ION5C stimulation (Figure 5.2A; 5.2B), all the exocytosing vesicles may be undergoing KR mode of exocytosis under these conditions but some SVs may remain open longer than 0.5 sec so that the dye will be released. Some supporting evidence for this comes from the previous research in Dr. A. Ashton's laboratory where they established that the treatment with Phenylarsine Oxide (PAO) prevents the exocytosis of all the vesicles that would normally undergoing FF mode but that the treatment does not prevent the release of vesicles exocytosing by KR (unpublished observation). Thus when the synaptosomes were treated with PAO, it significantly reduced the amount of Glu released during HK5C and ION5C stimulations due to blockade of the RP vesicle exocytosis. However, when PAO was used in combination with 1 μ M Cys A, no decrease in the Glu release was observed indicating that all the RRP and RP vesicles must be exocytosing by KR mode due to Cys A treatment (unpublished observation). Thus, it can be concluded that following Cys A treatment, the decrease in the FM2-10 dye fluorescence observed during HK5C and ION5C stimulation cannot be attributed to the FF mode of vesicular release and that all the SVs must be undergoing KR mode of exocytosis under these conditions.

Surprisingly, inhibition of calcineurin by Cys A produced a significant increase ($\sim 30.9 \pm 4.7\%$) in the $[Ca^{2+}]_i$ achieved upon stimulation by all the three stimuli, when compared to that of control conditions (Figure 5.3). However, this excess increase in $[Ca^{2+}]_i$ may not be responsible for the increase in the KR mode of exocytosis as the Cys A treatment failed to increase the proportion of the KR mode

of exocytosis even though it achieved a higher $[Ca^{2+}]_i$ upon stimulation by 4AP5C (Figure 5.2C; 5.3C). Moreover, Dr. A. Ashton's previous research has established that the L-type VGCCs exclusively play an important role in regulating the modes of exocytosis without affecting the overall Glu released from control synaptosomes (Ashton *et al.*, 2011). When they employed 1 μ M nifedipine (a L-type VGCC blocker) in combination with 1 μ M Cys A, they found that the treatment was unable to prevent the excess increase in the $[Ca^{2+}]_i$ caused by Cys A treatment (unpublished observation; data not shown). Thus, it can be concluded that the excess increase in $[Ca^{2+}]_i$ produced by Cys A treatment may be contributed by a VGCC sub-type different from L-type VGCC and this excess Ca^{2+} may not be responsible for the increase in the KR mode of exocytosis. It may be beneficial to inhibit the activity of calcineurin by a different inhibitor (e.g. FK506) as it may help to shed more light on the questions raised by the excess $[Ca^{2+}]_i$ achieved by Cys A treatment.

In order to further study the effects of Cys A treatment, it was used in combination with either 50 μ M Blebb or 160 μ M DYN during HK5C or ION5C and 4AP5C stimulations respectively. Neither of the combination treatments affected the amount of Glu released upon stimulation (Figure 5.4) but it changed the kinetics of decrease in the FM2-10 dye fluorescence during HK5C and ION5C stimulations (Figure 5.5A; 5.5B). During HK5C stimulation, the combination treatments of Cys A and Blebb produced a sharp decrease in the FM2-10 fluorescence during the initial measurement period which then plateaued after a very short period (\sim 3 sec) leaving a significantly higher fluorescence after \sim 66 sec when compared to that of control ($p = 0.029$ at 66.6 sec). This observation can be explained based on our previous results that the inhibition of myosin-II (by Blebb) would cause the RRP vesicles to fuse by FF mode of exocytosis there by producing a decrease in the

fluorescence during the initial stimulation period. After the RRP vesicles have been exhausted, the RP vesicles would undergo KR mode of exocytosis due to the inhibition of calcineurin by Cys A which would then prevent the action of dynamin-II in the expansion of the fusion pore. This KR mode of exocytosis of the RP vesicles would then prevent or reduce the amount of FM2-10 dye being released from these vesicles thereby preventing further decrease in the dye fluorescence. Similar to HK5C, the combination treatment of DYN and Cys A resulted in a sharp decrease in FM2-10 dye fluorescence during the initial stimulation period by ION5C which then plateaued after ~7 sec of stimulation (Figure 5.5B). In this case, the initial decrease in the dye fluorescence can be attributed to the inhibition of dynamin-I by DYN resulting in the FF mode of exocytosis of the RRP vesicles. Following the exhaustion of RRP, the RP would undergo KR mode of exocytosis due to the inhibition of calcineurin by Cys A. Interestingly, the combination treatment of DYN plus Cys A decreased the FM2-10 dye fluorescence comparable to that produced following the treatment with DYN alone during 4AP5C stimulation (Figure 5.5C). This would suggest that during 4AP5C stimulation, the RRP undergoes FF when dynamin-I is inhibited by DYN and that calcineurin (and therefore dynamin-II) may not play any role during the exocytosis of the RRP vesicles.

The kinetics of release for HK5C plus Blebb plus Cys A or ION5C plus DYN plus Cys A would seem to represent simply the FF of the RRP and under these circumstances no dye is being released by the RP due to Cys A dependent switch to KR. However, this seems to be in-consistent with the idea that some dye can still efflux out of some RP SVs that may be undergoing KR but whose pore opening is extended beyond 0.5 sec. Clearly, more studies need to be undertaken to ascertain this component of release but recent research (A. Ashton, unpublished observations) may suggest that the possibility that the RP SVs which release all

their dye may actually release most by the FF mode, but a small portion may actually represent extended pore opening time. This is important as there was always the possibility that all the supposed FF release could simply represent extended fusion pore opening times. This would verify that KR does exist but not indicate switching between the modes. The fact that there are some biochemical distinctions between the releases of dye in the RP does suggest that both FF and extended pore opening may co-exist.

5.3.2 Inhibition of Protein Kinase C (PKC)

Many studies have previously demonstrated that the activation or inhibition of PKC can regulate the phosphorylation on dynamin(s) and myosin-II (Carey *et al.*, 2005; Powell *et al.*, 2000). The results presented in this study indicate the involvement of two distinct proteins in the closure of the fusion pore depending on the $[Ca^{2+}]_i$ that the exocytosing vesicles are exposed to (see chapter 4). Thus a possible role of a Ca^{2+} sensitive kinase – PKC – was assessed in this study by either inhibiting them or activating them using Go6983 or PMA respectively.

Inhibition of PKCs by 1 μ M Go6983 did not affect the Glu or FM2-10 dye released upon stimulation by HK5C (Figure 5.6A, 5.7A). This would suggest that the inhibition of PKCs – by Go6983 – has no effect on the exocytosis mode of the releasable vesicles. However, when Go6983 was used in combination with 160 μ M DYN, it increased the amount of FM2-10 dye released upon stimulation with HK5C (Figure 5.7B; $p < 0.0387$) indicating that when the PKCs were inhibited, dynamin-I continues to play a role in the closure of the fusion pore even when a relatively higher $[Ca^{2+}]_i$ should be achieved during the application of this stimulus. Conversely, when Go6983 was used in combination with 50 μ M Blebb, it did not affect the amount of FM2-10 dye released during HK5C stimulation (Figure 5.7C)

indicating that Myosin-II may require active PKCs for their activation during high $[Ca^{2+}]_i$ as achieved during the application of this stimulus. Indeed, none of the drug treatments affect the total number of synaptic vesicle exocytosis (Figure 5.6) or the total FM2-10 dye loading (data not shown) thereby confirming that the changes in FM2-10 dye release is due to a switch in the mode of exocytosis.

Thus from these results it can be concluded that during a relatively higher $[Ca^{2+}]_i$ – as achieved by HK5C at the active zone – PKCs would be stimulated by increased Ca^{2+} which will then phosphorylate dynamin-I thereby preventing it from participating in the KR mode of exocytosis. However, at the same time, the activated PKCs would phosphorylate myosin-II rendering them active which would then be able to close the fusion pore causing the RRP to release by KR. Due to their action on both the proteins, the RRP vesicles would continue to undergo KR mode of exocytosis but this time under the regulation of a different protein (myosin-II instead of dynamin-I). This argument compliments the FM2-10 dye release data in the presence or absence of 1 μ M Go6983 alone where there was no change in this dye's release as the RRP would continue to exocytose by KR under the effect of dynamin-I when the activation of PKCs is prevented by this drug treatment (Figure 5.7A).

5.3.3 Activation of Protein Kinase C (PKC)

The data and arguments presented in section 5.3.2 suggests that at a relatively higher $[Ca^{2+}]_i$ at the active zone, PKCs would act as a “ Ca^{2+} sensor” which would then switch the protein dependency of the RRP pool for the KR mode of exocytosis. Thus, one could argue that if PKCs can be activated externally (by using a drug, such as PMA) during lower $[Ca^{2+}]_i$ – as achieved during ION5C stimulation – Myosin-II would regulate the KR mode of the RRP pool instead of dynamin-I. This hypothesis was tested here by using various concentrations of PMA during the employment of ION5C stimulation. Previous studies by Dr. A Ashton and group using 1 μ M PMA during HK5C stimulation raised possibilities of an off-target effects of PMA or an action on various PKC isoforms activated by this drug (unpublished observation). These activated PKCs isoforms may affect diverse cellular mechanisms due to their wide variety of substrates. One could argue that various isoforms of PKC may be localised at specific regions of a pre-synaptic neurons (Mackay *et al.*, 2001) and these different PKC isoforms may be activated by PMA with different IC_{50} values. Thus an attempt was made in this study to establish if lower concentrations of PMA (< 1 μ M) would be able to switch the protein dependency without affecting the overall amount of Glu or FM2-10 dye released during ION5C stimulation.

When the PMA concentration was lowered to 100 nM, it did not appear to change the protein dependencies as their combination with 160 μ M DYN was still able to increase the amount of FM2-10 dye released during ION5C stimulation indicating that dynamin-I is still required for the KR mode of exocytosis of the RRP SVs (Figure 5.8). Note that 300 or 200 nM PMA could switch the mode of exocytosis independent of dynasore (Figure 5.8 A, B; section 5.2.3). As the aim was to

establish a concentration of PMA that alone did not affect the FM2-10 dye release, the effects of 300, 200 or 100 nM PMA was only tested in a few experiments. Such that the error bars were relatively large and data was not really amenable to statistical testing. This was because these concentrations did exert an effect alone, and so a lower concentration of PMA was tested in a subsequent experiment. When the PMA concentration was reduced to 40 nM, such drug treatment was unable to produce any excess decrease in the FM2-10 dye fluorescence with ION5C – either alone ($p=0.7209$) or more intriguingly when in combination with DYN ($p=0.8271$) – when compared to the control conditions (Figure 5.9B). Furthermore, when 40 nM PMA was used in combination with 50 μ M Blebb, it produced a significant decrease in the FM2-10 dye fluorescence when compared to that of control ($p=0.0072$), Blebb or 40nM PMA alone (Figure 5.9C). Indeed, none of the drug treatments – in combination or alone – affect the amount of Glu released from the synaptosomes confirming that the increase in the FM2-10 dye released is due to a mode switch (Figure 5.9A). It can also be assumed that these drug treatments does not affect the $[Ca^{2+}]_i$ achieved upon stimulation as 1 μ M PMA did not affect this during previous studies undertaken by Dr. A Ashton and group (unpublished observations).

Thus, it can be concluded that when certain PKCs are activated by submaximal concentrations of PMA (40 nM) during mild stimulations (such as ION5C in this study), it can switch the protein dependency of the RRP vesicles for their KR mode of exocytosis. Hence it appears that dynamin-I and myosin-II both are regulated by certain classes of PKC for their role in the closure of the fusion pore of RRP vesicles causing them to release by KR mode of exocytosis. At relatively lower $[Ca^{2+}]_i$ (as achieved by ION5C and 4AP5C), these specific PKCs would remain inactive and thus dynamin-I would be able to regulate the fusion pore of the RRP vesicles.

However, when a relatively higher $[Ca^{2+}]_i$ is achieved upon stimulation, such as during the employment of HK5C, certain PKCs would be stimulated by these increased $[Ca^{2+}]_i$ which can then phosphorylate dynamin-I rendering it inactive such that it can no longer regulate the fusion pore of the RRP vesicles. However, at the same time, the stimulated PKCs would phosphorylate non-muscle myosin-II thereby activating this which would then be able regulate the fusion pore of the RRP vesicles. It is possible that the two proteins under discussion may be regulated by different PKC isoforms and this was not determined, herein. It would be interesting to identify the involvement of a specific PKC isoform(s) that may be involved in regulating these proteins for their role in the KR mode of exocytosis. The exact reason behind the involvement of two different proteins for the same function still remains to be determined and/or explained; however there are various known cellular functions where multiple proteins may be involved in performing similar functions.

5.4 Conclusions

This chapter of the thesis demonstrates, for the first time, that dynamin-II may require dephosphorylation by calcineurin for their role in the expansion of the fusion pore of the RP vesicles as the inhibition of the latter causes the RP vesicles to exocytose by KR mode. On the other hand, protein kinase C acts as a “Ca²⁺ sensor” for the RRP vesicles where elevated [Ca²⁺]_i can activate certain PKC isoforms. These stimulated PKCs can then inactivate dynamin-I and activate non-muscle myosin-II, probably by phosphorylating them, at the same time such that myosin-II can replace the function of dynamin-I in the closure of the fusion pore during the release of the RRP vesicles. The involvement of a particular PKC isoform still remains to be elucidated in this switch in the protein dependency of the RRP vesicles for closure of their fusion pore.

Chapter 6

Dynamin-I Phosphorylation Studies

6.1 Introduction

Chapter 4 of this thesis demonstrated the involvement of dynamin-I, II and non-muscle myosin-II in the regulation of fusion pore during SV exocytosis. The role that calcineurin and PKC play in regulation of these proteins was discussed in chapter 5. It is thus imperative that these proteins are under phosphoregulations for this particular role and it would be beneficial to identify the phosphorylation site(s) involved in this process. In this project, only dynamin-I was selected for the phosphorylation studies due to previous in-depth identification of its *in vivo* phosphorylation sites (Graham *et al.*, 2007) and commercial availability of antibodies against certain phosphorylation sites of dynamin-I. Three phosphorylation sites – viz. 774, 778 and 795 – of dynamin-I were assessed in this study.

6.2 Results

A substantial amount of time was invested behind optimising the western blot technique in order to study the phosphorylation sites of dynamin-I. As a result it was not possible to reproduce the western blot experiments in multiples of independent experiments – unless stated otherwise – due to lack of time for this aspect of the project. Thus, all the results presented in this chapter of the thesis should be treated as preliminary results and no statistical analysis could be performed for majority of the results presented herein. It should also be noted that much of the results obtained during and after optimisation process are not presented in order to keep this thesis as relevant and concise as possible. This aspect of the project is currently being further investigated by a different researcher in the group and so far all the results presented herein have been found to be reproducible.

Following the relevant drug treatment, the synaptosomes were stimulated with desired stimuli for various time periods and the samples were lysed using SDS sample buffer. The proteins from the whole synaptosomal lysate were then separated by SDS-PAGE using 4-12% gradient gel and probed with antibodies to phospho-Ser 774, phospho-Ser 778, phospho-Ser 795 or to pan-dynamin-I (see section 2.2.5 for more details). The western blot images thus obtained are presented in this chapter and are representative of all the independent experiments, wherever applicable, and are cropped to show only the band of interest for ease of presentation. For all full sized blot images, please see note given in appendix A.3. All the western blot images obtained from this study were subjected to densitometry analysis by using the volume analysis tool of the Image Lab™ software (BIO-RAD; version 3.0). The average of densitometry data are presented here as histograms showing S.E.M., wherever applicable, after compensating for total amount of dynamin-I measured on the same blots. All the statistical analyses in this chapter were performed using unpaired t-test and the “n” represents the number of independent experiments. If no “n” is mentioned then it should be assumed that the data is representative of only one independent experiment and thus no statistical test could be performed for such data sets.

6.2.1 Phosphorylation of dynamin-I on Ser-774

Representative blots obtained after immuno detection with p-774 are presented in Figure 6.1. The presence of prominent bands at 2 sec of stimulation period suggests the presence of a large pool of dynamin-I phosphorylated at this site and signify that dynamin-I must be constitutively phosphorylated at Ser 774. This observation is consistent with previous reports by Graham *et al*, 2007. The intensity of these bands decreases from 15 sec of depolarisation such that the band

obtained for 120 sec time period is either too faint (HK5C) or disappears completely (ION5C) when compared to that of L₀ samples. This observed decrease in the band intensities reflect actual decreases in phosphorylation at this site upon stimulation as re-probing of the same blot with anti-dynamin-I antibody revealed no such decrease in the protein band intensities (Figure 6.1 F; section 2.2.5). The blot presented in Figure 6.1 F is a representative blot obtained after such re-probing procedure and similar blots were obtained for all the phospho-antibody probed blots that are displayed in Figure 6.1 and thereafter. No difference in the amount of total dynamin-I, loaded or otherwise, was obtained irrespective of the stimulation, time period or drug treatment employed (only representative data shown).

Inhibition of PP1 and PP2A, by 0.8 μ M OA, also showed time dependent stimulation decrease in phosphorylation at this site similar to those observed during control conditions indicating that neither of the two phosphatases can be an *in vivo* phosphatase for phospho-Ser 795 (Figure 6.1 B). Inhibition of calcineurin by Cys A, on the other hand, showed no such decrease in the band intensities when the blot was probed with phosphoserine 774 antibodies (Figure F C). This implies that calcineurin is a phosphatase for phospho-Ser 774 of dyn-I and that its inhibition prevents time-dependent stimulation induced dephosphorylation of this site. Although it was expected that the inhibition of myosin-II by 50 μ M Blebb is unlikely to interfere with the phosphorylation of dynamin-I, it was included in this study to ensure this was the case. Indeed, 50 μ M Blebb treatment (and also inhibition of myosin-II) did not interfere with the post stimulation changes in the phosphorylation at Ser 774.

The optimal switch in the protein dependency was achieved with 40 nM PMA during ION5C stimulation (discussed in 5.3.3) and this concentration was used to investigate the phosphorylation state of dynamin-I in this study. Along with 40 nM, other concentrations like 80, 120 and 400 nM were used to examine their effects on phosphorylation of dynamin-I. It was found that 40, 80 and 120 nM PMA had essentially identical effects on all the phosphorylation sites tested in this study, thus an average of their densitometric values were taken to increase the sample size during statistical test. All the histograms and western blot images thus presented here are denoted by 80 nM PMA concentration (average of the three) but are also valid for samples pre-treated with 40 and 120 nM PMA. Blots presented in Figure 6.1 E reveal activation of PKCs does not interfere with the differences in the phosphorylation at this site seen at different stimulation time points for either HK5C or ION5C.

Histograms presented in Figures 6.2 complement the observations made in the earlier paragraphs and is consistent with the visual trends seen on the western blots presented in Figure 6.1. These histograms provide a mean to semi quantify the changes in phosphorylation seen on immuno blots. The decrease in the phosphorylated population of dynamin-I only becomes statistically significant when this population decreases by $40\pm 7\%$ at 15 sec of stimulation by ION5C (Figure 6.2). The decrease in HK5C stimulated samples become statistically significant only when they are stimulated for at least 30 sec (Figure 6.2). These observations suggest that the decrease in phosphorylation at Ser 774 only occurs when the synaptosomes are continuously stimulated for a substantial amount of time – at least 15 sec and may represent cellular processes preparing dynamin-I for endocytic processes, especially CME.

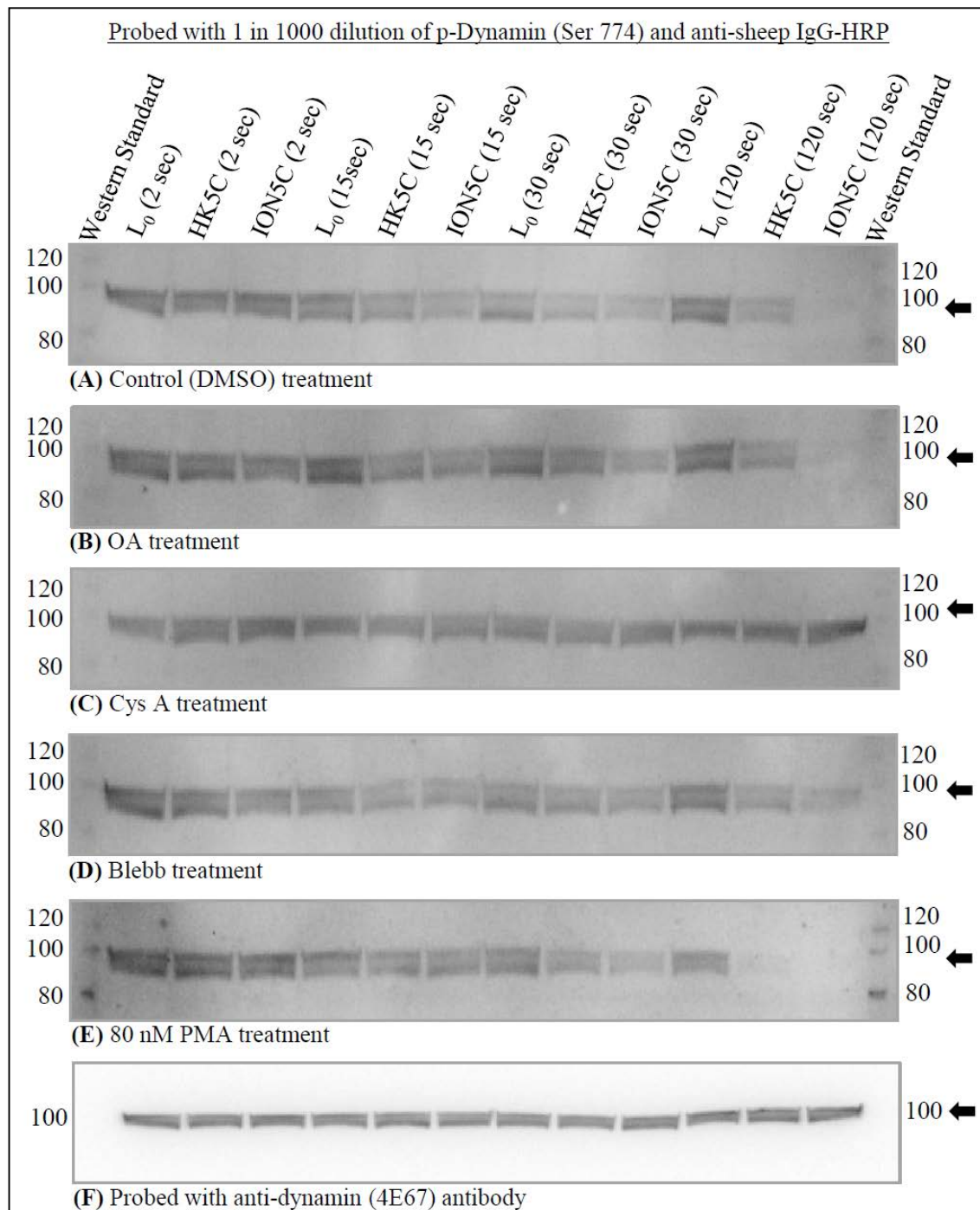
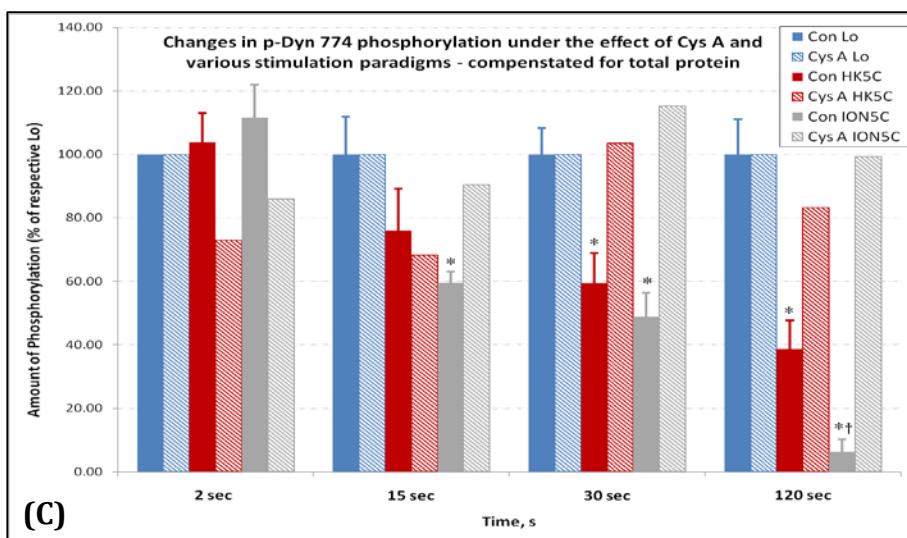
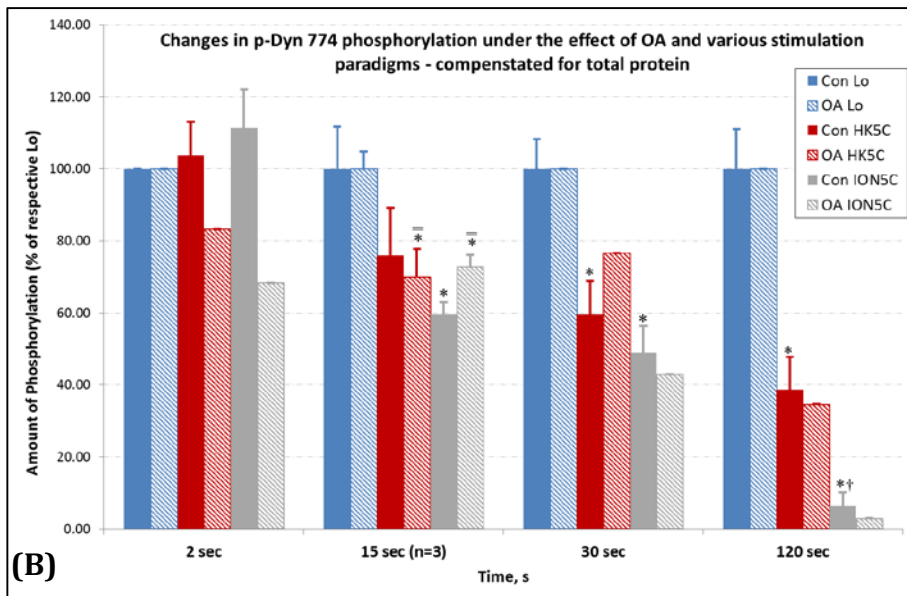
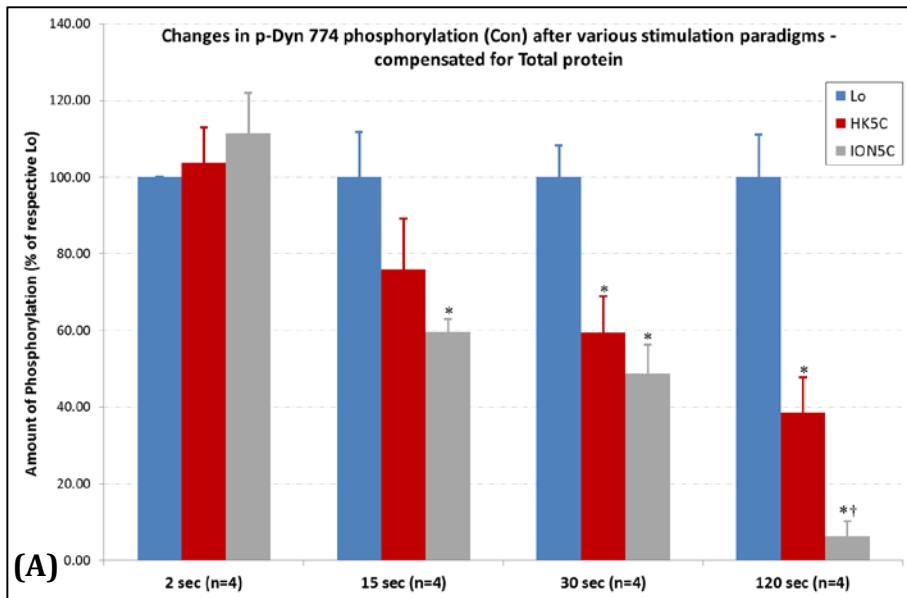


Figure 6.1: Western blot images showing dynamin-I phosphorylated at Ser 774 site.

(A) The amount of phosphorylation decreased with increasing stimulation times and that this decrease was greater for samples stimulated with ION5C when compared to that of HK5C. The drug treatments (B) OA, (D) Blebb & (E) 80 nM PMA failed to change any of these patterns of time dependent dephosphorylation whilst samples treated with (C) Cys A exhibited no dephosphorylation of Ser 774 irrespective of the stimulus and period used. (F) Re-probing of all the blots by anti-dynamin 4E67 revealed the same amount of dynamin-I protein in each lanes and this image is just a representative blot.



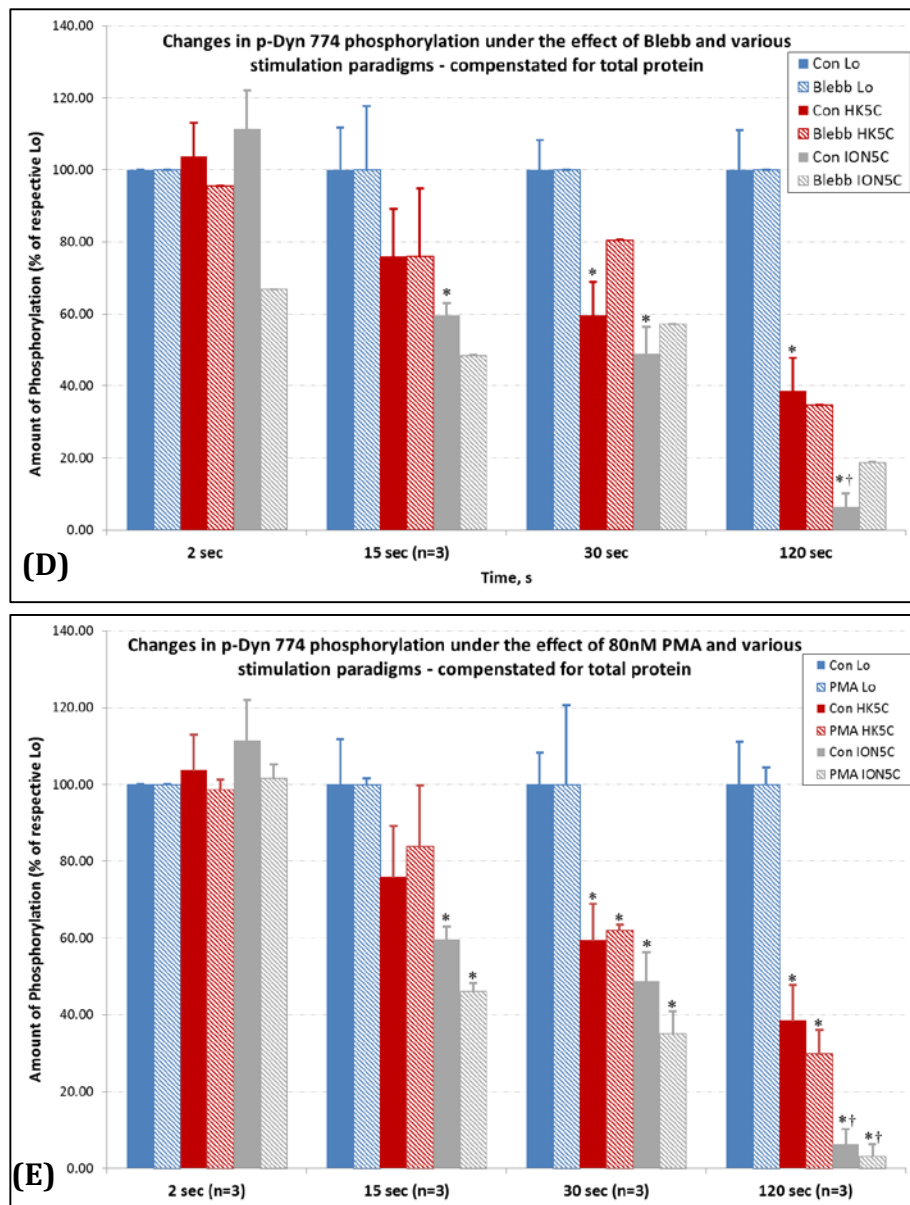


Figure 6.2: Inhibition of calcineurin prevents stimulation dependent dephosphorylation of dynamin-I at Ser 774 site. After image acquisition, the blots were subjected to semi-quantitative analysis using Densitometry technique. The arbitrary values obtained after densitometry were expressed as a percentage relative to their respective L_0 values for a given stimulation time period. These values were then compensated for the amount total dynamin-I, averaged ($n=4$) and presented as histograms with S.E.M. The histogram confirms the stimulation time period dependent decrease in the p-774 phosphorylation of dynamin-I for (A) Control condition, (B) OA treatment, (D) Blebb and (E) PMA treatment. (C) Cys A treatment, on the other hand, prevented this dephosphorylation of dynamin-I. 'n' value represents the number of independent experiments performed and an *

mark represents significance level less than 0.05 when compared to L₀. † indicates significant decrease ($p < 0.05$) in phosphorylation compared to HK5C counterparts.

6.2.2 Phosphorylation of dynamin-I on Ser-778

Another important phosphorylation site for dynamin-I is Ser 778 and this was investigated herein using the same approach as used for phospho-Ser 774. Similar to phospho-Ser 774, dynamin-I showed time dependent stimulation evoked dephosphorylation at phospho-Ser 778 for control, OA, Blebb and PMA (Figure 6.3 A, B, D, and E). However, there was blockade of dephosphorylation at phospho-Ser 778 when calcineurin was blocked by 1 μ M Cys A (Figure 6.3 C). These observations indicate that PP1, PP2A, and PKC do not regulate this phosphorylation site of dynamin-I but calcineurin can dephosphorylate Ser 778 in a Ca²⁺ dependent manner.

The histograms presented in Figure 6.4 complement the trends in dephosphorylation seen on the blots in Figure 6.3. Surprisingly, the decrease in phosphorylation only becomes statistically significant from 30 sec for ION5C (15 sec for phospho-Ser 774) and from 120 sec for HK5C (30 sec for phospho-Ser 774; Figure 6.4). This may suggest that the initiation of dephosphorylation process at phospho-Ser 778 may occur at a later stage than that of phospho-Ser 774 of dynamin-I.

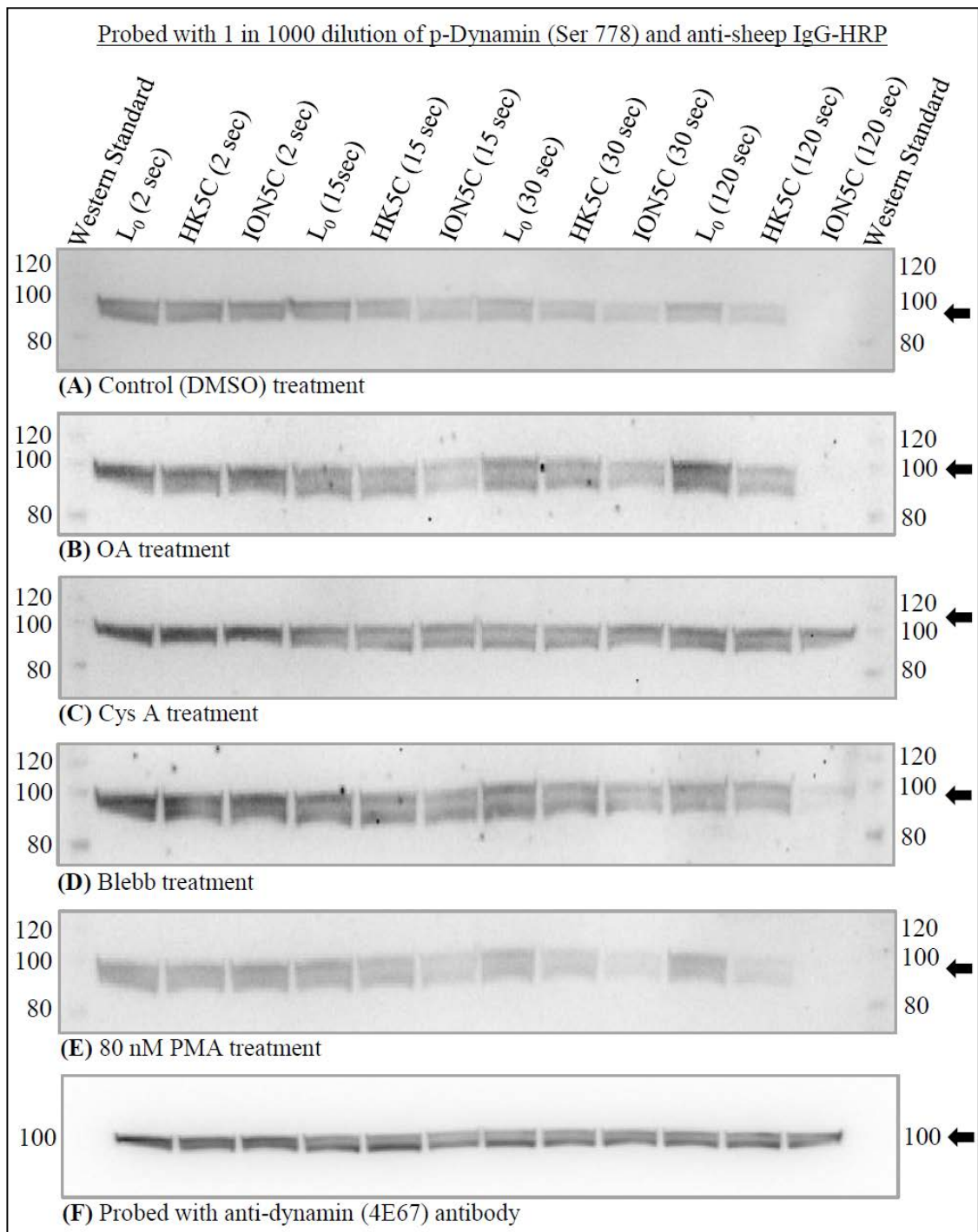
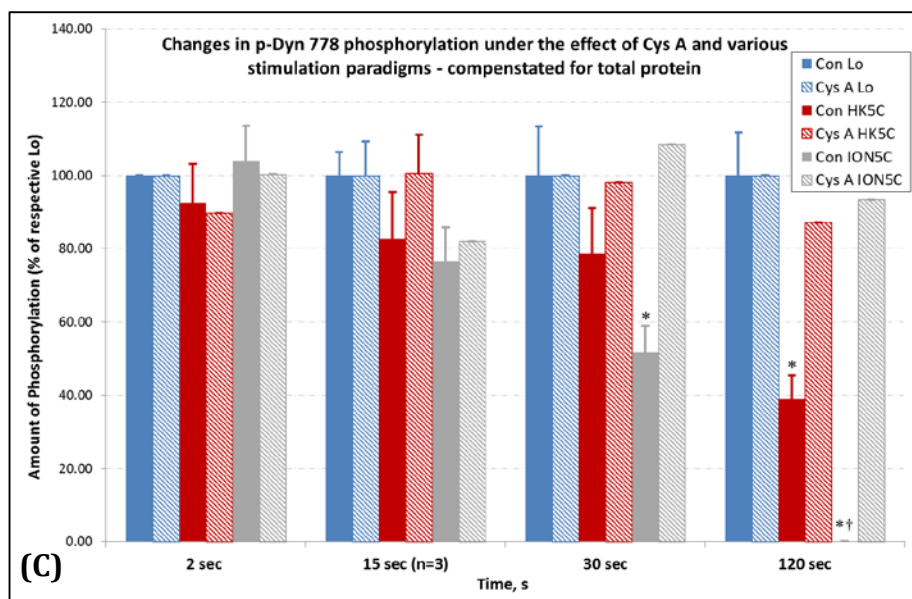
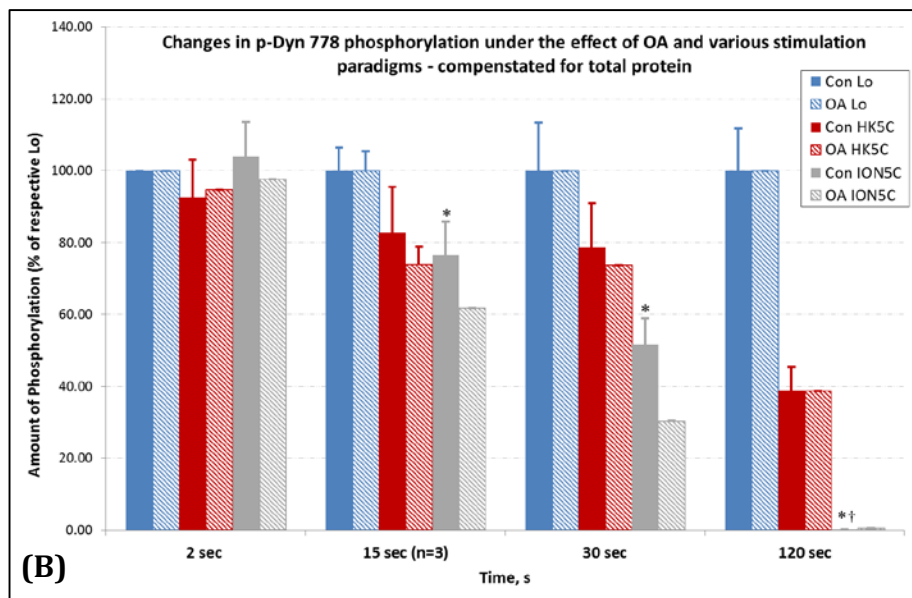
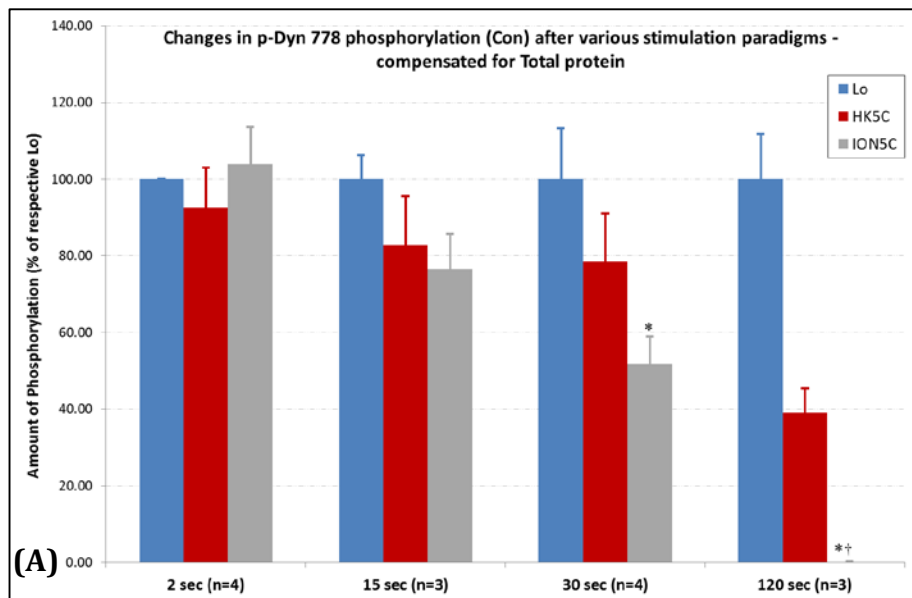


Figure 6.3: Western blot images showing dynamin-I phosphorylated at Ser 778 site following various treatments. (A) The amount of phosphorylation at Ser 778 decreased with increasing stimulation times and that this decrease was greater for samples stimulated with ION5C when compared to that of HK5C. The drug treatments (B) OA, (D) Blebb & (E) 80 nM PMA failed to change any of these patterns of time dependent dephosphorylation whilst samples treated with (C) Cys A exhibited no dephosphorylation of Ser 778 irrespective of the stimulus and period used. (F) Re-probing of all the blots by anti-dynamin 4E67 revealed the same amount of dynamin-I protein in each lanes and this image is just a representative blot.



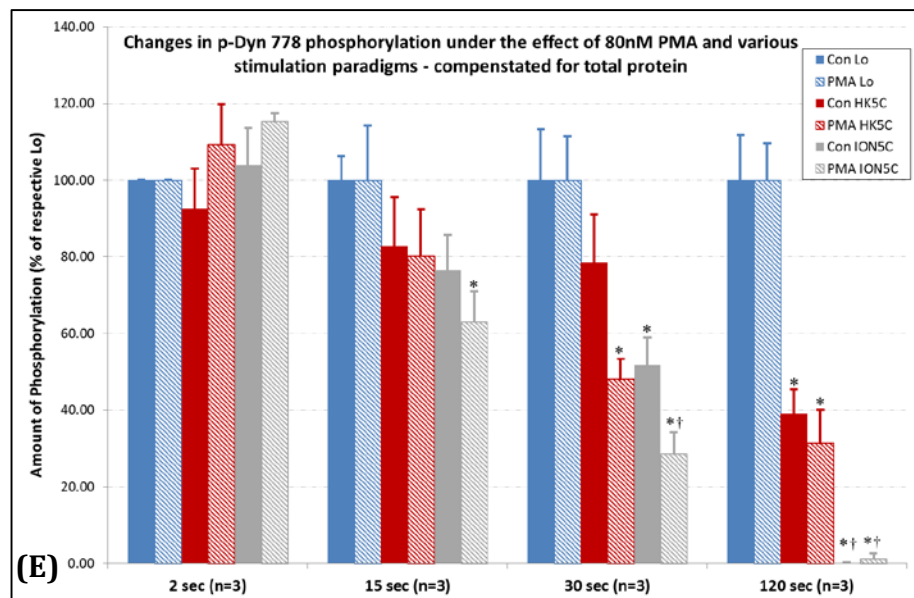
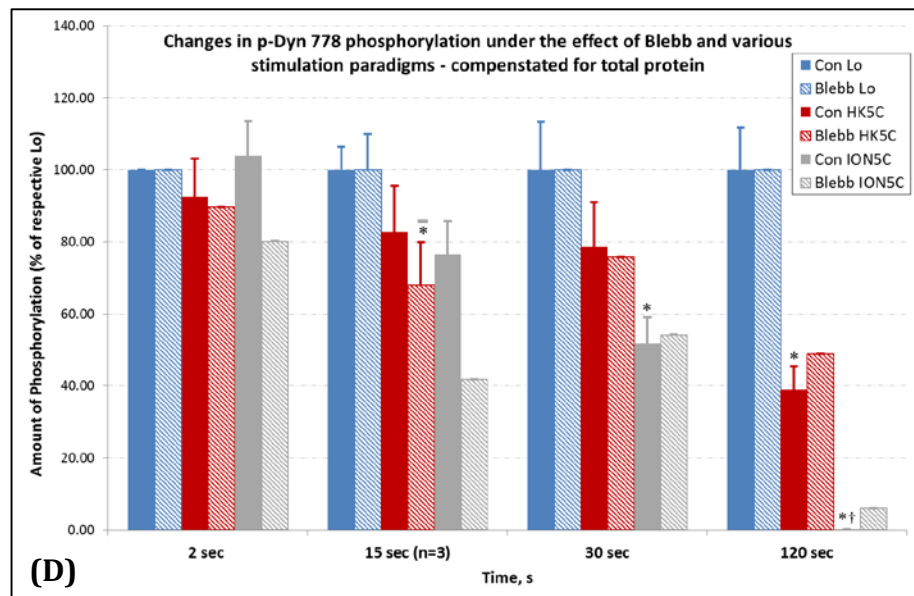


Figure 6.4: Densitometric analysis of blots presented in Figure 6.3 confirmed the stimulation time dependent decrease in the Ser 778 phosphorylation of dynamin-I. (A) Control condition, (B) OA treatment, (D) Blebb and (E) PMA treatment, all caused a stimulation dependent dephosphorylation at Ser 778 but (C) Cys A treatment prevented this dephosphorylation of dynamin-I. 'n' value represents the number of independent experiments performed. Nomenclature is as in Figure 6.2.

6.2.3 Phosphorylation of dynamin-I on Ser-795

Unlike phospho-Ser 778 and phospho-Ser 774 of dynamin-I, no phosphorylated Ser 795 of dynamin-I were observed in control or those treated with Cys A or Blebb indicating that dynamin-I may remain dephosphorylated at this site (Figure 6.5 A,C,D). The absence of phospho-Ser 795 is not related to the absence of protein or inability of the antibody to detect the phospho-Ser 795 as all the immuno blots obtained showed prominent presence of dynamin-I (Figure 6.5 F) and the antibody could recognise phospho-Ser 795 on the same blot (Figure 6.6 A and C). However, OA (Figure 6.5B) and PMA treatment (Figure 6.5 E), on the other hand, showed prominent phosphorylation of Ser 795 signifying that PP2A is a phosphatase and PKCs is a kinase of dynamin at the phospho-Ser 795 site. The presence of these bands proves, for the first time, the existence of *in vivo* phosphorylation at Ser 795 of dynamin-I.

OA treatment shows decrease in this phosphorylation only after 120 sec of stimulation indication that another phosphatase may be involved in the dephosphorylation of this site Figure 6.6A). However, this data is representative of only one independent experiment and more experimental evidence will be needed in order to ascertain such claims. The histogram in Figure 6.6B show that there also a decrease in phosphorylation at this site even when PKCs are activated suggesting that the concerned Ca^{2+} sensitive phosphatase may have faster kinetics when compared to that of phosphorylation by PKC. This phosphatase may be PP2A but this needs to be further examined by different experiments, such as a combination treatment with PMA and OA followed by phosphoserine 795 detection. The data presented in Figure 6.6 show that the phosphorylation at 795 increases with a corresponding increase in PMA concentration thus providing

further evidence that the phosphorylation at this site is a direct result of PKC activation.

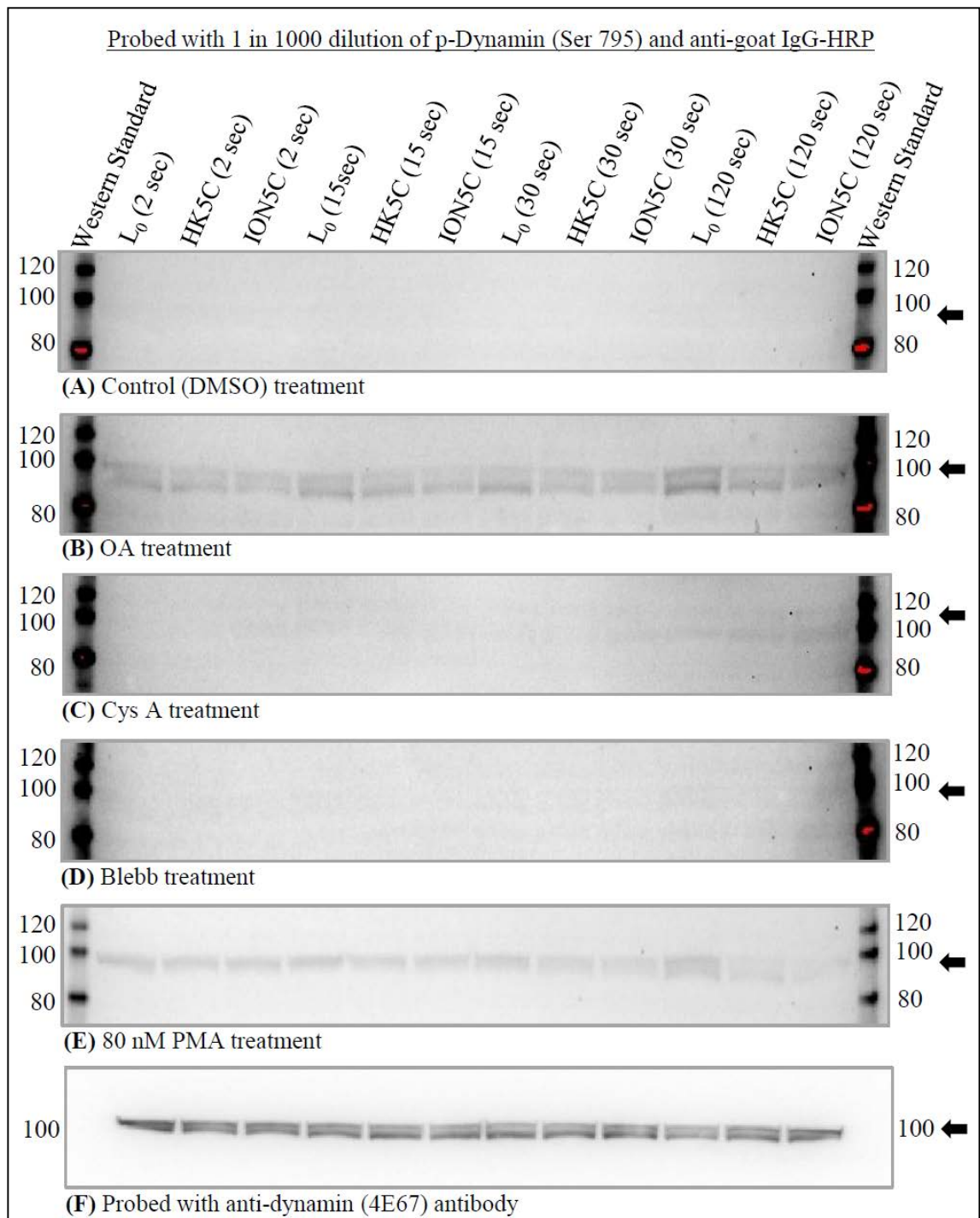


Figure 6.5: Phosphorylation at Ser 795 of dynamin-I seems to be under regulation of PP2A and PMA. Phosphorylation at Ser 795 was not detected in (A) control, (C) Cys A treated, or (D) Blebb treated terminals. However, (B) OA treatment revealed phospho-Ser 795 and this demonstrated some time dependent changes following the application of a stimulus. PMA treatment also showed some phospho-Ser 795 in dynamin-I and there were some changes upon the addition of the two stimuli. (F) is a representative blot for total dynamin-I content present in each track.

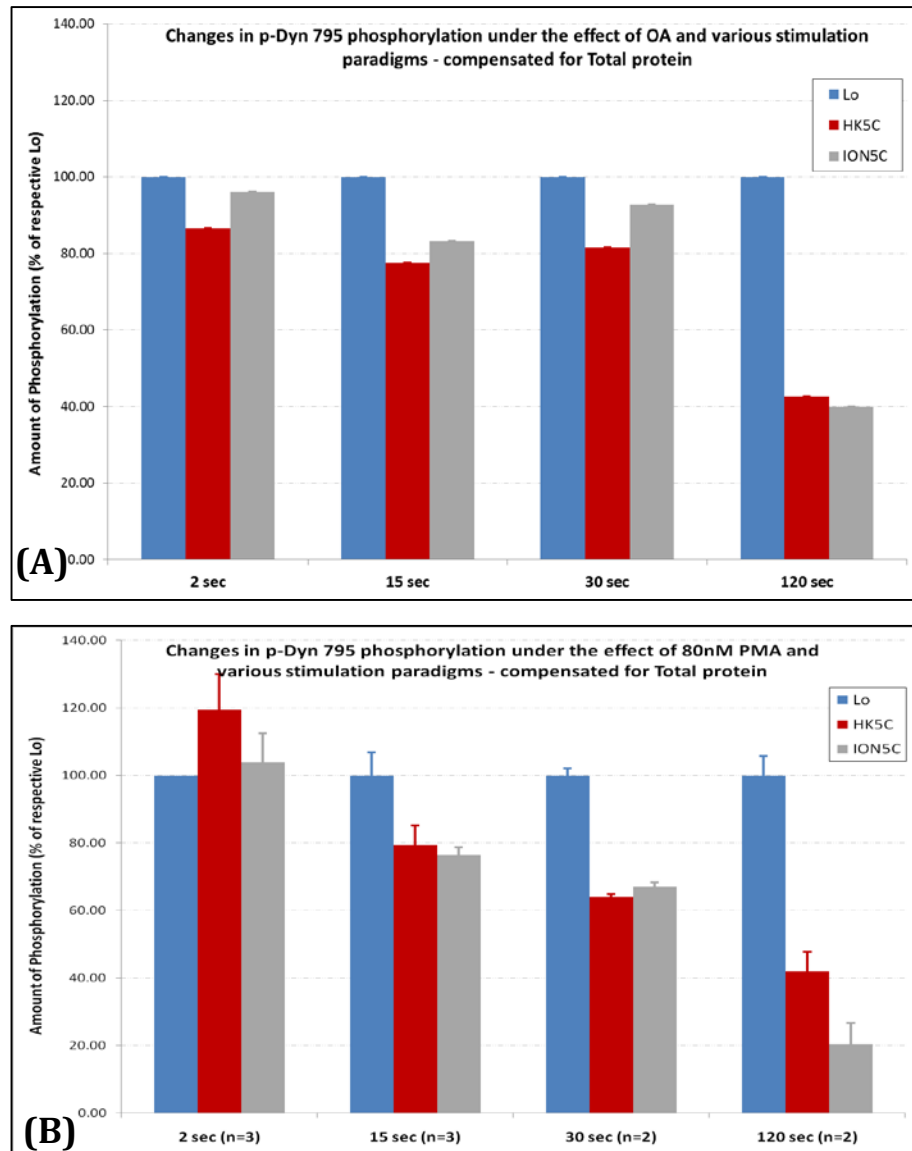


Figure 6.6: Densitometric analysis of blots presented in Figure 6.5 confirmed the stimulation time dependent decrease in the Ser 795 phosphorylation of dynamin-I. (A) OA, and (B) PMA pre-treatment revealed the presence of Ser 795 phosphorylation irrespective of the stimulation conditions but this phosphorylation decreased after 120 sec of stimulation with HK5C or ION5C stimulation. ‘n’ value represents the number of independent experiments performed and no statistical analysis could be performed for (A) due to lack of multiple independent experiments. Nomenclature is as in Figure 6.2.

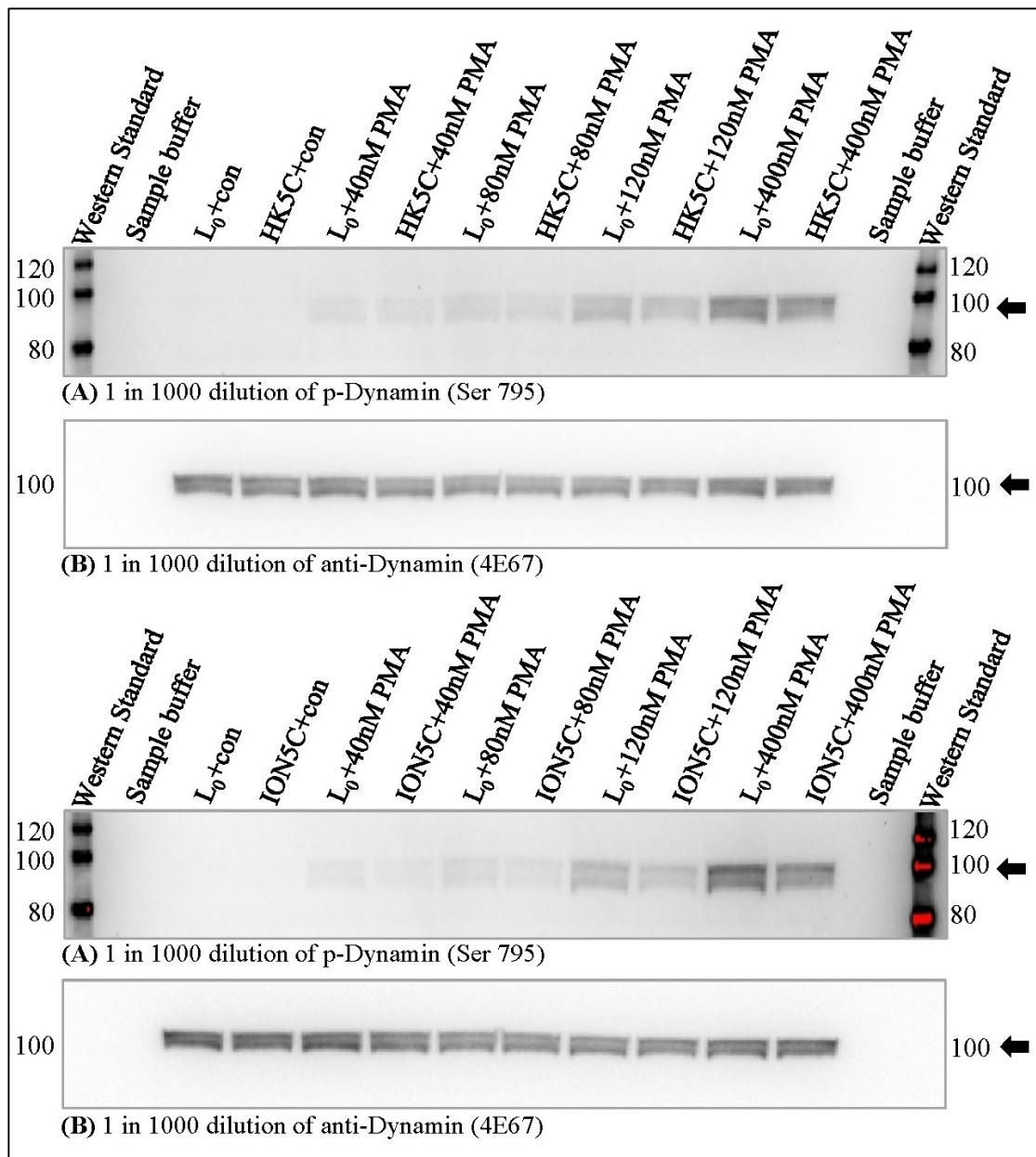


Figure 6.7: PMA exhibited a dose dependent phosphorylation of Ser 795 in intact synaptosomes and this was still apparent in samples stimulated for 15 sec with (A) HK5C or (C) ION5C although the total phospho-Ser 795 was less than in basal non-stimulated (L₀) terminals. (B) and (D) represent the reprobing of the blots with a pan-dynamin antibody indicating that each track had similar amounts of total dynamin-I protein.

6.3 Discussions

Three major phosphorylation sites of dynamin-I – viz., Ser 774, Ser 778 and Ser 795 – were investigated as part of this study in order to ascertain their role in the regulation of KR mode of exocytosis for RRP of SVs. Graham *et al.*, (2007) quantified the phosphorylation of dynamin-I from rat cerebrocortical synaptosomes and reported seven *in vivo* phosphorylation sites. All the sites reported were restricted to serine residues and no phosphorylated threonine or tyrosine residues were detected within their detection limits (>98% detection of total phosphorylated dynamin-I). Their study established that Dynamin-I is phosphorylated at Ser 774 ($\leq 47\%$), Ser 778 ($\leq 22\%$), Ser 822 (5%), Ser 851 & Ser 857 (12%, both combined; only present on dyn-I α), Ser 512 ($\leq 8\%$) and Ser 347 (1%). Among these seven sites, dynamin-I exhibited stimulation dependent dephosphorylation at Ser 774 (by 30%), Ser 778 (by 47%), Ser 851 & Ser 857 (by 34%, both combined) and Ser 822 (by 56%) (Graham *et al.*, 2007).

There are well established commercial phospho-specific antibodies against phospho-Ser 774, phospho-778 and phospho-795 and these were used for investigating the role of these phosphorylated sites in the KR mode of exocytosis. Intriguingly, phospho-Ser 795 was not reported as an *in vivo* phosphorylation site of dynamin-I by Graham *et al.*, (2007), but this site was investigated in this study. In studies by Graham *et al.*, (2007), 1.2 mM $[Ca^{2+}]_e$ was used for stimulating the synaptosomes prior to synaptosomal lysis. Data presented in section 3.3 clearly demonstrates that 1.2 mM $[Ca^{2+}]_e$ (in the presence of a secretagogue) induces sub maximal neurotransmitter release and that 5 mM $[Ca^{2+}]_e$ is required for maximal Glu release for all the three secretagogues studied, here in. Moreover, some of the evidence presented here strongly suggests a role of PKC in regulating the mode of

exocytosis (section 5.2.2; 5.2.3) and many previous reports have suggested that phospho-Ser 795 is a substrate site for this kinase (Zhang *et al.*, 2005; Tan *et al.*, 2003; Powell *et al.*, 2000). Thus it is possible that, due to methodology differences, Graham *et al.*, (2007) did not detect any *in vivo* phosphorylation at Ser 795, as they did not employ phosphatase inhibitors or kinase activators.

6.3.1 Phosphorylation of dynamin-I at Ser 774

Western blot images presented in Figure 6.1 represent detection of phospho-Ser 774 on dynamin-I and such blots reveal a time-dependent stimulation induced decrease in phosphorylation at this site. The blots show that the amount of phosphorylated Ser 774 of dynamin-I reduces with prolonged stimulation implicating a calcium dependent dephosphorylation process. Compared to HK5C, this decrease in phosphorylation appears to be greater in samples stimulated with ION5C and could be related to their distinct mechanism of action. Unlike HK5C, the Ca²⁺ influx induced by ION5C is not restricted to the active zone (section 4.3.5) and thus it could be argued that, compared to HK5C, a large amount of dynamin-I may be dephosphorylated at Ser 774 by ION5C because this can also act on dynamin-I localised away from the active zone. Note: an equal amount of Ca²⁺ influx will occur all over the nerve terminal with ION5C whilst HK5C causes a large Ca²⁺ influx at the active zone but no initial influx at other regions of the presynaptic terminal. If this possibility is true then the differences in dephosphorylation rates observed between HK5C and ION5C stimulation may not be that relevant as the excess decrease in phosphorylation of Ser 774 by ION5C may not have any implications on the regulation of the exocytosis mode. However, the data presented in Figure 6.2 show that the difference in dephosphorylation between the two stimuli becomes statistically significant only after 120 sec stimulation and so these

differences may not be relevant for the role of dynamin-I in KR mode of exocytosis of the RRP of SVs which occur by 2 sec stimulation. All the differences in Ser 774 phosphorylation seen in Figure 6.1 are true representative of changes in phosphorylation as the total amount of dynamin-I in each of the lanes was identical as demonstrated by Figure 6.1F. All the blots that were previously probed with a phosphoserine antibody were subsequently probed with anti-dynamin (4E67) and only a representative blot is presented in Figure 6.1F.

As mentioned, the RRP of SVs exocytose within two second of stimulation and thus any changes in phosphorylation of Ser 774 of dynmain-I related to the RRP must occur in this time period. It is important to note that the decrease in phosphorylation at Ser 774 only occurs at later time points (no change after 2 sec stimulation; Figure 6.2) and thus these later changes cannot be attributed to dynamin-I's role in regulating the KR mode of RRP SVs. However, the decrease in phosphorylation at later time points of stimulation can be attributed to its role in CME. In fact, the prolonged depolarisation (>30 sec) probably indicates dephosphorylation changes that lead to the biochemical interactions which are preparing dynamin-I to contribute to CME.

In order to determine if phospho-Ser 774 is dephosphorylated by PP1 or PP2A, the activity of these phosphatases was inhibited by pre-treatment of synaptosomes with 0.8 μ M OA prior to stimulation (section 2.2.5). Figure 6.1 B shows that there is time dependent stimulus induced decrease in the phosphorylation of dynamin-I at Ser 774 site similar to those observed during control conditions (Figure 6.1A) suggesting that this site is not under regulation by PP1 or PP2A. On the other hand, inhibition of Calcineurin (PP2B) by pre-treatment with 1 μ M Cys A prevented the decrease in amount of phospho-Ser 774 (Figure 6.1C; 6.4). This evidence suggests

that calcineurin is a phosphatase that dephosphorylates dynamin-I at phospho-Ser 774 during elevated Ca^{2+} levels as achieved upon stimulation and that when this phosphatase is inhibited, the stimulation dependent dephosphorylation does not occur. This is consistent with previous report where calcineurin was shown to dephosphorylate dynamin-I at Ser 774 and Ser 778 sites (Samasilp *et al.*, 2012; Graham *et al.*, 2007). However, dephosphorylation at Ser 774 of dynamin-I by calcineurin is probably not responsible for the increase in KR of the RP of SVs observed following pre-treatment with Cys A as dynamin-II, and not dynamin-I, is implicated in this process (section 5.3.1). Moreover, many studies have previously linked the stimulation dependent dephosphorylation of Ser 774 of dynamin-I by calcineurin to post-stimulation endocytosis, especially CME (Graham *et al.*, 2007).

The FM2-10 dye experiments demonstrated that 50 μM Blebb can switch the mode of SV exocytosis for RRP to FF during HK5C, but not during ION5C, stimulation (section 4.2.3; 4.3.4). It was, however, relevant to demonstrate that Blebb treatment itself does not regulate the phosphorylation of dynamin-I. Data presented in Figure 6.1D and 6.5 clearly demonstrate that pre-treatment with 50 μM Blebb does not interfere with the phosphorylation state of dynamin-I at Ser 774 site irrespective of the stimulation used.

Finally, it would be important to identify the phosphorylation site – under PKC regulation – that is responsible for inactivating dynamin-I during HK5C stimulations such that it can no longer play a role during the exocytosis of RRP SVs (section 5.3.3). The switch in the protein dependency was achieved with 40 nM PMA during ION5C stimulation (discussed in 5.3.3) and this concentration was used to investigate the phosphorylation state of dynamin-I in this study. It should be noted that all the results in this chapter denoted by 80 nM PMA are actually

representative or average of data obtained for 40, 80 and 120 nM PMA (section 6.2.1). The activation of PKCs sensitive to these concentrations of PMA did not affect the changes in phosphorylation of dynamin-I at Ser 774 irrespective of the stimulation used (Figure 6.1E; 6.6). These data also is an indication that such PKCs may not be a kinase that regulates dynamin-I phosphorylation at Ser 774 and support previous work by Clayton *et al* (2010) in which they demonstrated that GSK3 is the kinase responsible for phosphorylation of dynamin-I at Ser 774 site. However, in order to completely rule out PKC as a kinase for Ser 774 of dynamin-I, it needs to be demonstrated that their inhibition (such as by 1 μ M Go6983) prior to stimulation does not interfere with the phosphorylation levels. The preliminary data with Go6983 treated samples indeed support this hypothesis (data not shown). i.e. Go6983 treatment did not perturb Ser 774 phosphorylation and did not change any stimulus induced dephosphorylation of this site.

Thus, from all the arguments presented in this section, it can be concluded that Ser 774 is under Ca^{2+} dependent phosphoregulation. However, this phosphoregulation is not associated with the role of Dynamin-I in KR mode of exocytosis of the RRP of SVs and instead is probably associated with endocytosis, especially CME.

6.3.2 Phosphorylation of dynamin-I at Ser 778

The data presented in Figures 6.7 to 6.12 indicate that the changes in phosphorylation seen at Ser 778 is almost identical to those seen for phospho-Ser 774 for given treatment and stimulation conditions. Thus it can be said that phospho-Ser 778 is not dephosphorylated by PP1 and PP2A but that calcineurin can induce such stimulation evoked dephosphorylation (PP2B; Figure 6.7B, C). Similarly, it can also be said that PKC does not appear to be the kinase for the phosphorylation of Ser 778 of dynamin-I and Blebb treatment does not interfere

with the phosphorylation/dephosphorylation of this site (Figure 6.7 D, E). All these results are consistent with previous report that attributes calcineurin and Cdk5 as the phosphatase and kinase for Ser 778 site respectively (Xue *et al.*, 2011; Graham *et al.*, 2007). Close examination of histograms (Figure 6.2 and 6.8) reveal that the phospho-Ser 774 may be dephosphorylated earlier than phospho-Ser 778 as the decrease in phosphorylation becomes statistically significant at 15 sec for phospho-Ser 774 but only at 30 sec for phospho-Ser 778. However, more studies need to be performed in order to ascertain this hierarchy between the dephosphorylation of the two sites by calcineurin. It has been shown earlier that there may be a hierarchy in phosphorylation of these sites such that Ser 778 is phosphorylated by Cdk5 first, following which Ser 774 can be phosphorylated by GSK3 (Clayton *et al.*, 2010). From these arguments it can be concluded that, like Ser 774, Ser 778 may not play any role in regulating the activity of dynamin-I in the KR mode of exocytosis.

6.3.3 Phosphorylation of dynamin-I at Ser 795

It has been well established that PKC α can phosphorylate dynamin-I at Ser 795 during *in vitro* conditions (protein isolation; Powell *et al.*, 2000). However a functional role for this phosphorylation site still remains to be identified, subject to its *in vivo* existence. In the studies reported here in, it is demonstrated that activation or inhibition of certain PKCs can switch the protein requirement for closure of the fusion pore for KR exocytosis of the RRP SVs depending on the type of stimulation used (section 5.3.2 and 5.3.2). Thus it may be possible that the phosphoregulation of Ser 795 on dynamin-I may regulate this protein requirement and this could also regulate the mode of SV exocytosis under certain stimulation conditions and so this was consequently selected for study.

Some representative blots, probed for phosphoserine 795 are presented in Figure 6.13 and reveal that this site may not be phosphorylated under control conditions (Figure 6.13A). The absence of phosphoserine 795 band in Figure 6.13A, C and D is not due to inability of the antibody to recognise phosphorylated dynamin-I or related to the immunoblotting technique as p-795 bands were detected for PMA treated samples but were absent in control samples on the same immuno blot (Figure 6.16A, C). Thus it can be concluded that dynamin-I is either never phosphorylated at Ser 795 site or it can be phosphorylated but under normal circumstances phosphatases remove PO₄ (independent of Ca²⁺) from Ser 795 such that it remains dephosphorylated under control conditions (Figure 6.13A). There may be a small amount of dynamin-I that is phosphorylated at Ser 795 site during control conditions but this may be out of experimental detection range of the western blot technique employed here. Recent blotting experiments by other researchers in the group indicate that one can detect a very small amount of pospho-Ser 795 even in control conditions (A. Ashton *et al.*, unpublished observation).

When PP1 and PP2A were inhibited by pre-treatment with 0.8 μM OA, phosphorylation of Ser 795 was detected thereby indicating that either of these phosphatases may be responsible for dephosphorylation at Ser 795 site of dynamin-I (Figure 6.13, 6.14). Previous work by A. Ashton and group with Fostriecin (a more specific PP2A inhibitor) indicate that the action of OA is likely on PP2A rather than PP1 (data not shown). Thus it can be argued that Ser 795 of dynamin-I may be under constant dephosphorylation by PP2A and when this phosphatase is inhibited the amount of dynamin-I that is phosphorylated at Ser 795 increases significantly such that it can be detected in the system employed here. These results are exciting as it has been established by A. Ashton and

colleagues (Ashton *et al.*, 2011) that OA can switch the RRP of SVs to a FF mode of exocytosis (Figure 3.5). This applies for all three stimuli used in this study and although – as shown herein – under some conditions (HK5C) dynamin-I may not play a role, phosphorylation at Ser 795 will occur for all the three stimuli (as shown here for HK5C and ION5C). So for ION5C and 4AP5C it can be suggested that dynamin-I is unable to play its role in regulating the fusion pore if it is phosphorylated on Ser 795, in the presence of OA. Ser 795 of dynamin-I will also be phosphorylated even when HK5C is employed in the presence of OA. However, as OA pre-treatment also causes all the RRP of SVs to release by FF when stimulated with HK5C this must indicate that myosin-II activity must be regulated by phosphorylation and that this is also under phosphoregulation by PP2A (or PP1). It is clear that future experiments need to establish a correlation between OA induced phosphorylation of specific serines on the myosin-II and regulation of the fusion mode following HK5C stimulation (Figure 3.5; A. Ashton *et al.*, unpublished). This argument can also apply for the 40 nM PMA induced phosphorylation of dynamin-I on Ser 795 which needs to be compared to the PMA induced phosphorylation of non-muscle myosin-II. Such PKC phosphorylation sites on myosin-II are present on heavy chain, regulatory light chain and essential light chain of myosin-II and phosphorylation at these various sites can activate or inhibit this enzyme (Obara *et al.*, 2010; Ludowyke *et al.*, 2006; Somlyo & Somlyo, 2003).

Experiments involving inhibition of calcineurin (by Cyc A) indicate that it may not be the phosphatase responsible for dephosphorylating phospho-Ser 795 on dynamin-I site as blockade of this enzyme does not result in the appearance of phospho-Ser 795 on dynamin-I as detected by western blotting (Figure 6.13C). Similarly, Blebb treatment does not exert any action via regulation of phospho-Ser

795 on dynamin I as there was no detectable phosphorylation at this site (Figure 6.13D).

The fact that phosphorylation at Ser 795 can be dramatically increased by inhibiting a phosphatase (PP2A in this case) also suggests that there should be a kinase responsible for phosphorylating this site of dynamin-I under normal conditions. The data with various concentrations of PMA strongly suggests that this kinase may belong to the PKC family and may phosphorylate dynamin-I at 795 site only under very specific conditions including when these enzymes are activated externally, for e.g. by the action of PMA in this study (Figure 6.13E and 6.15). Figure 6.13E and 6.15 provide evidence that dynamin-I is phosphorylated *in vivo* following treatment with PMA. The term *in vivo* refers in this case to the use of synaptosomes which represent 'intact' preparation such that PMA would activate intra-terminal PKCs which would then work on their intracellular substrates. This mode does not represent a broken lysed preparation and there is not exogenous PKCs being added to the system. Similar to arguments presented for OA conditions, it can be argued that PMA treatment will induce phosphorylation at Ser 795 irrespective of the stimuli used such that this phosphorylation will render dynamin-I inactive and thus preventing it from participating in regulation of KR mode of exocytosis. However, as discussed earlier, PMA treatment will also phosphorylate myosin-II making it active under certain conditions even during mild stimulation (ION5C) and thus future experiments must investigate this correlation between dynamin-I and myosin-II phosphorylations in order to verify these conclusions.

Various concentrations of PMA were also employed in this study to examine if phosphorylation of Ser 795 showed any concentration dependent patterns. Figure

6.16 demonstrates that the amount of dynamin-I phosphorylated at Ser 795 increased with the use of increasing PMA concentrations. This suggests a direct correlation between the extent of PKC activation and the population of dynamin-I phosphorylated at Ser 795. This is consistent with previous arguments where it was suggested that the higher concentration of PMA ($>100 \mu\text{M}$) switched all the RRP vesicles to FF mode of exocytosis (section 5.3.3). But clearly with HK5C such high PMA concentrations can phosphorylate various substrates to override any contribution of myosin-II to closing the fusion pore and this could involve different phosphorylation sites on myosin-II itself. When a large population of dynamin-I is phosphorylated, it may then interact with other exocytosis regulatory pathways such that it can switch all the RRP to FF mode of exocytosis or at least keep the fusion pore open for longer than 0.5 sec such that maximal FM2-10 dye can be released from these vesicles. This also suggests that only a fraction of the total amount of dynamin-I (and probably only a single isoform/splice variant) may be responsible for the regulation of exocytosis mode for the RRP of SVs.

Thus, from arguments presented in this section, it can be suggested that dephosphorylation of Ser 795 residue is important for the role of dynamin-I in the KR of RRP of SVs and that dynamin-I cannot regulate this mode of exocytosis when this residue is phosphorylated. However, it should be noted that HK5C stimulated samples during control conditions (Figure 6.13A) do not appear to contain phospho-ser 795 and, yet, our data suggests that dynamin-I is rendered inactive by PKC activation during HK5C stimulation without the external application of PMA (chapter 4 and 5) and therefore, one would expect Ser 795 phosphorylation on dynamin-I during HK5C stimulation of control synaptosomes. It is possible that only a small population of dynamin-I may be phosphorylated at Ser 795 due to a specific localisation and partial activation of a particular PKCs by elevated $\Delta[\text{Ca}^{2+}]_i$

induced by HK5C and this may not be detected by the techniques employed. Conversely, when a phosphatase is inhibited by OA or a kinase is activated by PMA, this may affect a larger population of dynamin-I and therefore facilitating their easy detection using the techniques employed here. We have already

6.4 Conclusions

This chapter of the thesis provides further insight into the regulation of KR mode of exocytosis by dynamin-I. Phosphoregulation of Ser 774 and Ser 778 of dynamin-I is unlikely to be associated with this particular role of this protein and instead, as suggested by previous studies, this is probably associated with post stimulation endocytosis, especially CME. On the other hand, phosphoregulation of Ser 795 residue seems important for the role of dynamin-I in regulating the fusion mode of RRP of SVs such that dephosphorylation at this site causes KR and its phosphorylation prevents dynamin-I from closing the fusion pore eventually leading to FF of the RRP vesicles. This has never been reported previously and identifies a potential and important physiological role for phosphorylation of Ser 795 site of dynamin-I. The study also established that PP2A and PKC are the phosphatase and kinase responsible for the regulation of Ser 795 of dynmain-I. Similar studies with dynamin-II and myosin-II needs to be carried out in order to better understand the regulation of this process.

Chapter 7

General Discussion and Conclusion

7.1 General conclusions

Previous studies by A. Ashton and colleague had demonstrated the existence of KR mode of SV exocytosis in rat cerebral cortical synaptosomes. The aim of this study was to identify proteins involved in this regulation of exocytosis and their potential phosphorylation sites for the function under discussion. The results presented in this study strongly support the existence of KR mode of exocytosis in the central nervous system and also identified various proteins, enzymes and phosphorylation sites implicated in this physiological process.

It has been well established that the SV exocytosis is a Ca^{2+} dependent process and that an increase in $[\text{Ca}^{2+}]_i$ at the active zone is required in order to drive SV exocytosis. The work presented in this thesis strengthens the link between Ca^{2+} and SV exocytosis by demonstrating that $\Delta[\text{Ca}^{2+}]_i$ at the active zone is not only required for exocytosis but can also dictate the mode of exocytosis. If an action potential arriving at the nerve terminal produces a $\Delta[\text{Ca}^{2+}]_i$ – at the active zone – that is relatively low, the RRP vesicles are likely to undergo KR fusion under the regulation of dynamin-I (see Figure 7.1). Dynamin-I, in this case, is likely to assemble in to rings around the exocytosing vesicles and can then quickly close the fusion pore by utilising its GTPase activity. If this $\Delta[\text{Ca}^{2+}]_i$ is also sufficient to drive the exocytosis of the RP, the vesicles belonging to this pool is likely to be exocytosed by FF as the Ca^{2+} would have diffused away, due to concentration gradient, from the active zone by the time RP starts undergoing exocytosis. There is general consensus that in order for the RP to release, the RRP of SVs has to have exocytosed. Further, there is also consensus that the RP has distinct Ca^{2+} requirements for release and those levels will occur after the initial high $[\text{Ca}^{2+}]_i$ at the active zone. Therefore, the RP will release after the RRP has been exhausted.

More sophisticated techniques, than employed herein, would be needed to reveal if some RP SVs could start to exocytose before all the RRP SVs have fused.

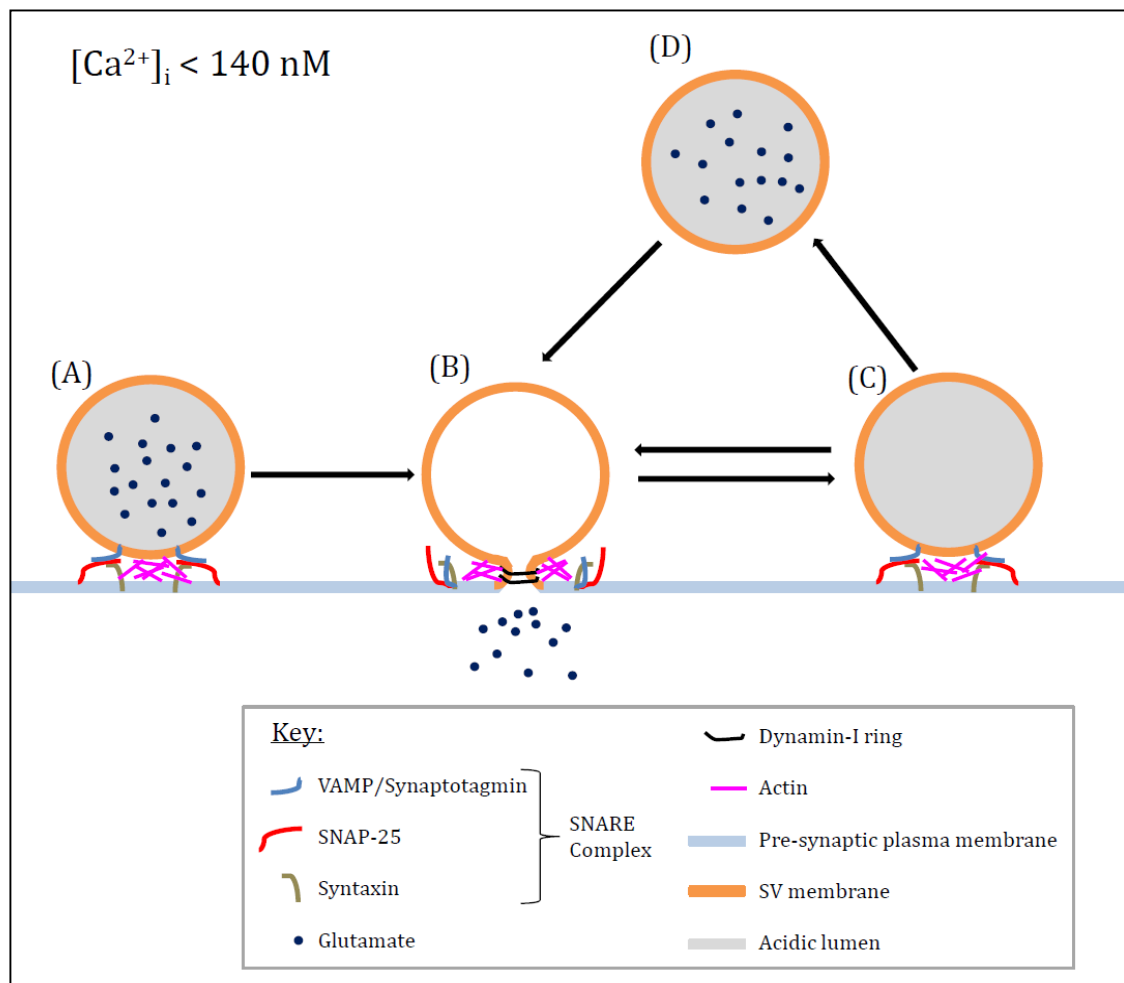


Figure 7.1: A schematic representation of exocytosis of a RRP vesicle during a mild stimulation ($\Delta[Ca^{2+}]_i$ less than 140 nM). (A) A RRP of SV is shown docked to the pre-synaptic membrane. If the changes in the average terminal $[Ca^{2+}]_i < 140$ nM then (B) the SV will release the neurotransmitter through a transiently open fusion pore which will be closed rapidly (< 0.5 sec) by dynamin-I rings assembled around the neck of the fusion pore. Once the pore is closed, (C) the vesicle may remain docked to the active zone where it can re-release following reuptake of the transmitter. (D) It can also move to the interior of the nerve terminal where it can be re-loaded, ready for next round of release. Please note that only one vesicle is shown for ease of presentation. The Representation is also over simplified, not true to scale and many other proteins involved in these processes are not shown/known.

In case where the arriving action potential produces a relatively higher $\Delta[\text{Ca}^{2+}]_i$, the RRP is likely to undergo KR under the regulation of non-muscle myosin-II (see Figure 7.2). This is because, the higher $\Delta[\text{Ca}^{2+}]_i$ is likely to activate PKC (by yet unknown mechanism) which will then phosphorylate dynamin-I at Ser 795 site making it inactive (see chapter 5 and 6). Thus phosphorylated dynamin-I will not be able to close the fusion pore of exocytosing vesicles. At the same time, however, PKC can also phosphorylate non-muscle myosin-II making it active such that myosin-II – instead of dynamin-I – can now close the fusion pore of RRP vesicles ensuring that they undergo KR. Once the RRP has been exhausted, the RP will be exocytosed by FF mode as the $[\text{Ca}^{2+}]_i$ levels at this time point will be less than the initial $[\text{Ca}^{2+}]_i$ but will be sufficient to drive exocytosis by FF. It should be noted that even though it is argued here that the RP will undergo FF irrespective of the magnitude of initial $\Delta[\text{Ca}^{2+}]_i$ at the active zone, nerve terminals obtained from a streptozotocin treated rat cerebral cortex showed that ~50% of the RP undergoes KR. This is because they naturally produced a larger $\Delta[\text{Ca}^{2+}]_i$ when compared to that of control samples even under identical stimulation/experimental conditions (A. Ashton *et al.*'s unpublished observations). This demonstrates that RP can indeed undergo KR but this is likely to be restricted to a diseased condition such as diabetes or other neurodegenerative disorders.

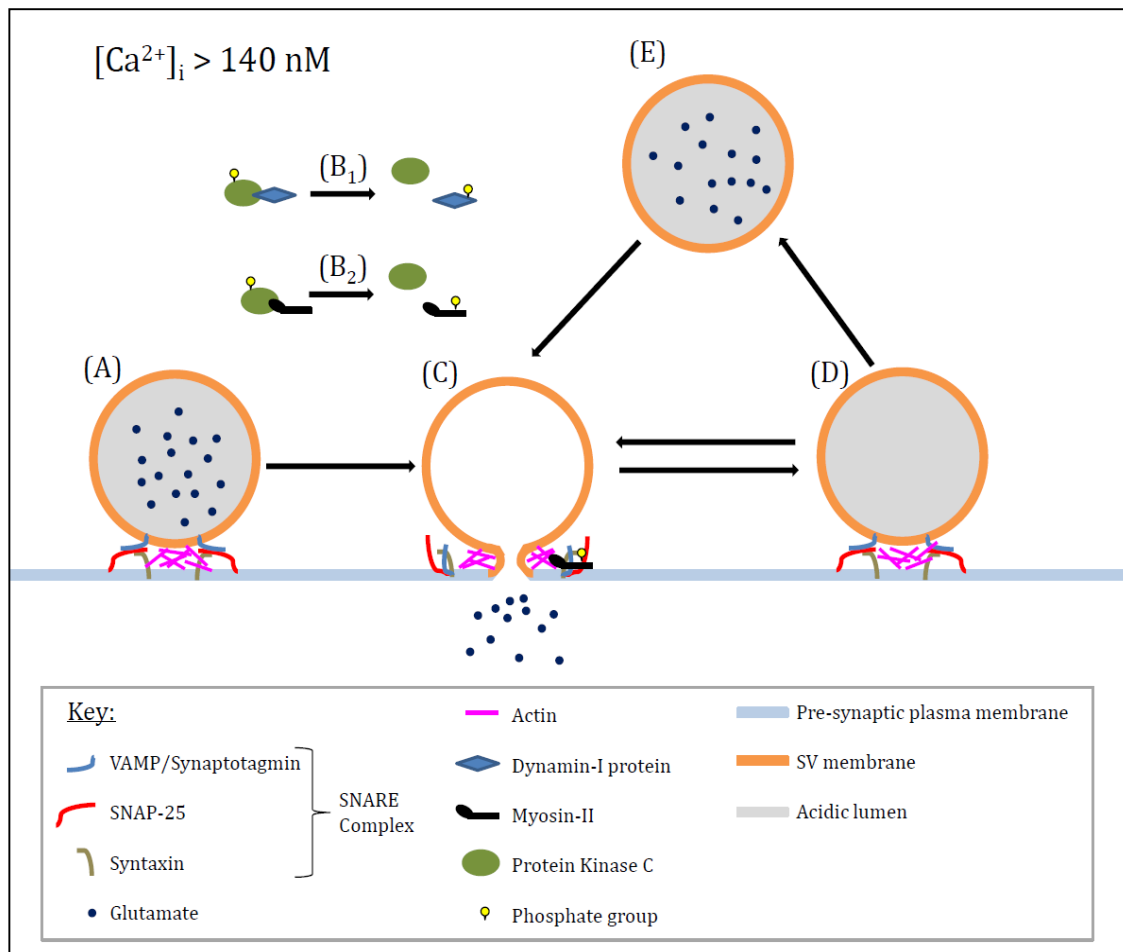


Figure 7.2: A schematic representation of exocytosis of a RRP vesicle during a strong stimulation ($[Ca^{2+}]_i$ more than 140 nM). (A) A RRP of SV is shown docked to the pre-synaptic membrane. If the depolarisation of the terminal achieves average $\Delta[Ca^{2+}]_i > 140 \text{ nM}$ then certain PKCs are activated which will then (B₁) phosphorylate dynamin-I at Ser 795 such that it becomes inactive and also (B₂) phosphorylate myosin-II – at a yet unknown site – such that it is activated and it can now close the fusion pore independent of dynamin-I thereby causing the RRP to release by KR. Following the closure of the fusion pore, the recycled vesicle can (C) remain docked to the plasma membrane or (D) internalised thus preparing it for next round of release. Please note that only one vesicle is shown for ease of presentation. The Representation is also over simplified, not true to scale and many other proteins involved in these processes are not shown/known

The exact threshold of changes in $[Ca^{2+}]_i$ at which the PKC will be activated is difficult to determine using the techniques used in this study. Ca^{2+} measurement studies suggest that if a particular stimulation event causes a change in overall $[Ca^{2+}]_i$ – as opposed at the active zone alone – that is less than ~ 140 nM, the relevant PKCs will not be activated thereby allowing dynamin-I to close the fusion pore and causing RRP vesicles to release by KR (Figure 7.3). On the other hand, if this overall change is more than ~ 140 nM, the relevant PKCs will be activated which will phosphorylate dynamin-I on Ser 795 making it inactive. At the same time, an activated PKC isoform will phosphorylate myosin-II, at a yet unknown site, making it active such that it can now cause the RRP to exocytose by KR. The RRP can also undergo FF in cases when the changes in $[Ca^{2+}]_i$ is very low as demonstrated by experiments with 4AP5C stimulation (see figure 3.6 and 3.7). The reported threshold value (140 nM) of $\Delta[Ca^{2+}]_i$ where the switch in protein dependency for KR would occur should be considered with caution as the value reported here represents the overall calcium concentration and the exact value can change depending on the working temperature and dissociation constant used during calculations.

Since dynamin-I belongs to the family of dephosphins, they must be dephosphorylated (at Ser 795) in order for it to regulate the KR mode of exocytosis. Results presented in chapter 6 of this study help conclude that protein phosphatase 2A (PP2A) is a phosphatase that keeps dynamin-I dephosphorylated at Ser 795 such that a pool of active dynamin-I is available for use during exocytosis thereby causing certain SVs to release by KR. At a higher $[Ca^{2+}]_i$ protein kinase C will be activated which can now phosphorylate dynamin-I at Ser 795 residue making it inactive and unable to participate in exocytosis. Thus this study, for the first time, identifies PP2A and PKC as phosphatase and kinase of dynamin-I

respectively that can phospho-regulate Ser 795 residue thereby regulating function of dynamin-I in KR mode of exocytosis.

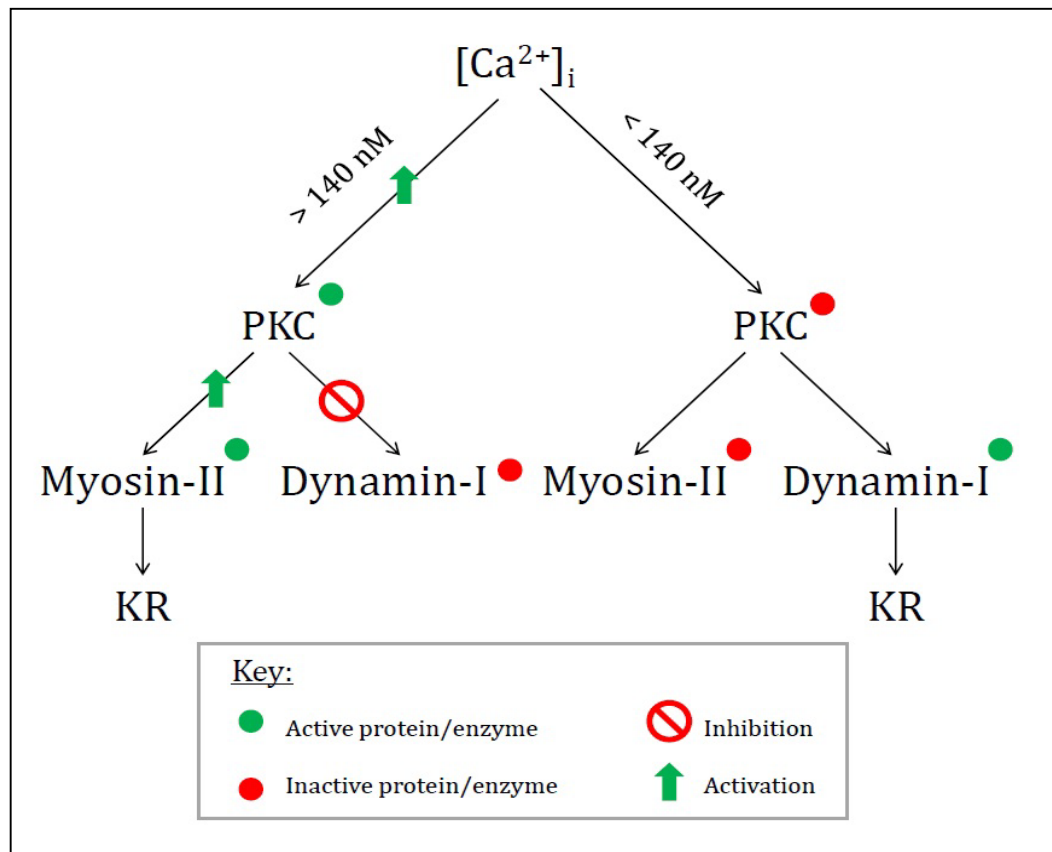


Figure 7.3: A schematic representation of mechanism responsible for switching the protein dependency for KR. If the depolarisation of the terminal achieves average $\Delta[Ca^{2+}]_i < 140$ nM then dynamin-I continues to be active and participates in causing the KR of the RRP vesicles. However, if the terminal achieves average $\Delta[Ca^{2+}]_i > 140$ nM then certain PKCs are activated which will then phosphorylate dynamin-I at Ser 795 thereby inhibiting it. The activated PKC will also cause phosphorylation of myosin-II making active which can now close the fusion pore of the exocytosing vesicles causing them to release by KR.

7.2 Future directions

The present study has contributed to our knowledge about SV exocytosis in the central nervous system. However, a substantial amount of work still needs to be undertaken in order to fully elucidate the regulation of SV exocytosis in nerve terminals. Some of the experiments/directions are suggested in this section that can be undertaken in order to add to the current knowledge and answer some of the questions raised by this study.

Chapter 4 of this study demonstrated that dynamin-II is required for the expansion of the fusion pore of the RP vesicles and therefore causing them to release by FF. However, these experiments (involving dyngo) were only performed using ION5C stimulation (Figure 4.6). In order to ascertain that this effect is exclusively on the RP vesicles, the experiment needs to be repeated with 4AP5C in which case one would expect to see no effect of dyngo treatment on the FM2-10 dye release as 4AP5C does not induce the release of RP vesicles. Moreover, it will also be important to replicate the same result, as with ION5C, with HK5C as both the stimuli induces the release of RP by FF mode. Moreover, experiments involving inhibition of calcineurin showed an increase KR of the RP (section 5.3.1). In order to determine if dynamin-II and calcineurin work via the same pathway it may be useful to perform the experiments where dyngo and Cys A are used in combination. It will also be helpful to determine if the inhibition of calcineurin (by Cys A) affects the phosphorylation of dynamin-II at a particular residue such that these effects can be linked to their role in FF of the RP vesicles.

The inhibition of calcineurin by 1 μ M Cys A induced a large $\Delta[\text{Ca}^{2+}]_i$ when compared to that of control conditions (Figure 5.3). It has been shown, herein, that the mode of exocytosis depends on the $[\text{Ca}^{2+}]_i$ achieved at the active zone and thus

one might argue that the increase in KR seen following Cys A treatment may be because of this excess $[Ca^{2+}]_i$ and not necessarily represent a switch in the mode of the RP vesicles due to a change in phosphorylation of a protein directly involved in the mode of exocytosis (chapter 5). Although, arguments and evidence has been provided to rule out the relation to excess $[Ca^{2+}]_i$, it may be beneficial to inhibit calcineurin using a different inhibitor (like FK506) that may not induce this excess increase in $[Ca^{2+}]_i$. It should be note that increasing the $[Ca^{2+}]_i$ by employing ION10C (i.e. 10 mM Ca^{2+} not 5 mM) does actually cause a switch of mode of the RP so that some undergoes KR (Ashton *et al.*, 2011). Clearly, more work needs to be done to investigate the role of high $[Ca^{2+}]_i$ on the RP mode of exocytosis and its relationship to changes in the properties of dynamin(s) (both I and II).

The two proteins, dynamin-I and myosin-II, are regulated by activation of PKCs during elevated $[Ca^{2+}]_i$. However, it is likely that these proteins are regulated by a specific PKC isoform and this may be same or different for the two proteins. Thus it will be of great advantage to identify the specific PKC isoform involved in this process. This can be achieved by employing various PKC isoform specific inhibitors available in the market. Lastly, similar to dynamin-I, phosphorylation studies needs to be undertaken to determine the phosphorylation sites of dynamin-II and myosin-II for their functions discussed in this thesis.

Majority of the experiments suggested here have been recently performed in A. Ashton's laboratory and the results obtained strongly support the conclusions and interpretations drawn in this thesis.

References

References

- Alabi ARA & Tsien RW (2013). Perspectives on Kiss-and-Run: Role in Exocytosis, Endocytosis, and Neurotransmission. *Annual Review of Physiology*, **75**, 393-422
- Andersson F, Jakobsson J, Low P, Shupliakov O, & Brodin L (2008). Perturbation of syndapin/PACSIN impairs synaptic vesicle recycling evoked by intense stimulation. *Journal of Neuroscience*, **28**, 3925–3933.
- Anggonno V, & Robinson PJ. *Dynamins*. (2009). *Elsevier Limited*, 725-735.
- Aoki R, Kitaguchi T, Oya M, Yanagihara Y, Sato M, Miyawaki A, & Tsuboi T (2010). Duration of fusion pore opening and the amount of hormone released are regulated by myosin II during kiss-and-run exocytosis. *Biochemical Journal*, **429**, 497-504.
- Aravanis AM, Pyle JL, & Tsien RW (2003). Single synaptic vesicles fusing transiently and successively without loss of identity. *Nature*, **423**, 643–647.
- Atlas D (2010). Signaling role of the voltage-gated calcium channel as the molecular on/off-switch of secretion. *Cell Signalling*, **22**, 1597-1603.
- Bähring R, & Covarrubias M (2011). Mechanisms of closed-state inactivation in voltage-gated ion channels. *Journal of Physiology*, **589(Pt 3)**, 461-79.
- Berberian K, Torres AJ, Fang Q, Kisler K, & Lindau M (2009). F-actin and myosin II accelerate catecholamine release from chromaffin granules. *Journal of Neuroscience*, **29(3)**, 863-70
- Bertolino M, & Llinas RR (1992). The central role of voltage-activated and receptor-operated calcium channels in neuronal cells. *Annual Review of Pharmacology and Toxicology*, **32**, 399-421.

- Bhat P, & Thorn P (2009). Myosin 2 Maintains an Open Exocytic Fusion Pore in Secretory Epithelial Cells. *Molecular Biology of the Cell*, **20**, 1795–1803.
- Bresnick AR (1999). Molecular mechanisms of nonmuscle myosin-II regulation. *Current Opinion in Cell Biology*, **11**, 26-33.
- Bresnick AR. (1999) Molecular mechanisms of nonmuscle myosin-II regulation. *Curr Opin Cell Biol.* **11(1)**, 26-33.
- Carey RM, Balcz BA, Lopez-Coviella I, & Slack BE (2005). Inhibition of dynamin-dependent endocytosis increases shedding of the amyloid precursor protein ectodomain and reduces generation of amyloid beta protein. *BMC Cell Biology*, **6**, 30
- Chan SA, Doreian B, & Smith C (2010). Dynamin and myosin regulate differential exocytosis from mouse adrenal chromaffin cells. *Cellular and Molecular Neurobiology*, **30(8)**, 1351-7.
- Cheung G, & Cousin MA (2011). Quantitative Analysis of Synaptic Vesicle Pool Replenishment in Cultured Cerebellar Granule Neurons using FM Dyes. *Journal of visualized experiments*, **57**, e3143.
- Cheung G, & Cousin MA (2013). Synaptic vesicle generation from activity-dependent bulk endosomes requires calcium and calcineurin. *Journal of Neuroscience*, **33(8)**, 3370-9. d
- Cheung G, Jupp OJ, & Cousin MA (2010). Activity-dependent bulk endocytosis and clathrin-dependent endocytosis replenish specific synaptic vesicle pools in central nerve terminals. *Journal of Neuroscience*, **30(24)**, 8151-8161.
- Chircop M, Sarcevic B, Larsen MR, Malladi CS, Chau N, Zavortink M, Smith CM, Quan A, Anggono V, Hains PG, Graham ME, & Robinson PJ (2011).

Phosphorylation of dynamin II at serine-764 is associated with cytokinesis.

Biochem Biophys Acta, **1813(10)**, 1689-1699.

- Choquet D, & Korn H (1992). Mechanism of 4-Aminopyridine Action on Voltage-gated Potassium Channels in Lymphocytes. *Journal of general physiology*, **99**, 217-240.
- Chu Y, Fioravante D, Thanawala M, Leitges M, & Regehr WG (2012). Calcium-dependent isoforms of protein kinase C mediate glycine-induced synaptic enhancement at the calyx of Held. *Journal of Neuroscience*, **32(40)**, 13796-804.
- Chung C, Barylko B, Leitz J, Liu X, & Kavalali ET (2010). Acute dynamin inhibition dissects synaptic vesicle recycling pathways that drive spontaneous and evoked neurotransmission. *Journal of Neuroscience*, **30**, 1363-1376.
- Clayton EL, & Cousin MA (2008 a). Differential labelling of bulk endocytosis in nerve terminals by FM dyes. *Neurochemistry International*, **53(3-4)**, 51-55.
- Clayton EL, Anggono V, Smillie KJ, Chau N, & Cousin MA (2009). The phospho-dependent dynamin-syndapin interaction triggers activity-dependent bulk endocytosis of synaptic vesicles. *Journal of Neuroscience*, **29**, 7706-7717.
- Clayton EL, Evans GJ, & Cousin MA (2008). Bulk synaptic vesicle endocytosis is rapidly triggered during strong stimulation. *Journal of Neuroscience*, **28**, 6627-6632.
- Clayton EL, Evans GJO, & Cousin MA (2008 b). Bulk synaptic vesicle endocytosis is rapidly triggered during strong stimulation. *Journal of Neuroscience*, **28**, 6627-6632.

- Clayton EL, Sue N, Smillie KJ, O'Leary T, Bache N, Cheung G, Cole AR, Wyllie DJ, Sutherland C, Robinson PJ, & Cousin MA (2010). Dynamin I phosphorylation by GSK3 controls activity-dependent bulk endocytosis of synaptic vesicles. *Nature Neuroscience*, **13(7)**, 845-851.
- Cousin MA, & Robinson PJ (2000). Two mechanisms of synaptic vesicle recycling in rat brain nerve terminals. *Journal of Neurochemistry*, **75**, 1645–1653.
- Denker A, & Rizzoli SO (2010). Synaptic vesicle pools: an update. *Frontiers in Synaptic Neuroscience*, **2**, 135.
- deVries KJ, Geijtenbeek A, Brian EC, de Graan PNE, Ghijsen WEJM, &Verhage M (2000). Dynamics of munc18-1 phosphorylation/dephosphorylation in rat brain nerve terminals. *European Journal of Neuroscience*, **12**, 385-390.
- Dolphin AC (2006). A short history of voltage-gated calcium channels. *British Journal of Pharmacology*, **147**, S56-S62.
- Ferguson SM, & De Camilli P (2012). Dynamin, a membraneremodelling GTPase. *Nature Review Molecular Cell Biology*, **13**, 75–88.
- Gasman S, Chasserot-Golaz S, Malacombe M, Way M, & Bader MF (2004). Regulated Exocytosis in Neuroendocrine Cells: A Role for Subplasmalemmal Cdc42/N-WASP-induced Actin Filaments. *Molecular Biology of the Cell*, **15**, 520–531.
- Graham ME, Anggono V, Bache N, Larsen MR, Craft GE, &Robinson PJ (2007). The in vivo phosphorylation sites of rat brain dynamin I. *The journal of Biological Chemistry*, **282(20)**, 14695-707.
- Grimaldi M, Atzori M, Ray P, & Alkon DL (2001). Mobilization of calcium from intracellular stores, potentiation of neurotransmitter-induced calcium

transients, and capacitative calcium entry by 4-aminopyridine. *The Journal of Neuroscience*, **21(9)**, 3135-43.

- Grynkiewicz G, Poenie M, & Tsien RY (1985). A new generation of Ca²⁺ indicators with greatly improved fluorescence properties. *Journal of Biological Chemistry*, **260**, 3440–3449.
- Gschwendt M, Dieterich S, Rennecke J, Kittstein W, Mueller HJ, & Johannes FJ (1996). Inhibition of protein kinase C mu by various inhibitors. Differentiation from protein kinase c isoenzymes. *Federation of European Biochemical Societies Letters*, **392(2)**, 77-80.
- Guan R, Dai H, Harrison SC, & Kirchhausen T (2010). Structure of the PTEN-like region of auxilin, a detector of clathrin-coated vesicle budding. *Structure*, **18**, 1191–1198.
- Harata NC, Aravanis AM, & Tsien RW (2006). Kiss-and-run and full-collapse fusion as modes of exo-endocytosis in neurosecretion. *Journal of Neurochemistry*, **97**, 1546–1570.
- Harata NC, Choi S, Pyle JL, Aravanis AM & Tsien RW (2006). Frequency dependent kinetics and prevalence of kiss-and-run and reuse at hippocampal synapses studied with novel quenching methods. *Neuron*, **49**, 243–256.
- Harper CB, Martin S, Nguyen TH, Daniels SJ, Lavidis NA, Popoff MR, Hadzic G, Mariana A, Chau N, McCluskey A, Robinson PJ, & Meunier FA (2011). Dynamin inhibition blocks botulinum neurotoxin type A endocytosis in neurons and delays botulism. *The Journal of Biological Chemistry*, **286(41)**, 35966-35976.
- Hartig S, Ishikura S, Hicklen R, Feng Y, Blanchard E, Voelker K, Pichot C, Grange R, Raphael R, Klip A, & Corey S (2009). The F-BAR protein CIP4

promotes GLUT4 endocytosis through bidirectional interactions with N-WASp and Dynamin-2. *Journal of Cell Science*, **122**, 2283–2291.

- Hayashi M, Raimondi A, O'Toole E, Paradise S, Collesi C, Cremona O, Ferguson SM, & De Camilli P (2008). Cell- and stimulus-dependent heterogeneity of synaptic vesicle endocytic recycling mechanisms revealed by studies of dynamin 1-null neurons. *Proceedings of the National Academy of Sciences*, **105**, 2175– 2180.
- He L, Wu XS, Mohan R, & Wu LG (2006). Two modes of fusion pore opening revealed by cell-attached recordings at a synapse. *Nature*, **444**, 102–105.
- Heymann JAW, & Hinshaw JE (2009). Dynamins at a glance. *Journal of Cell Science*, **122**, 3427-3431.
- Hilfiker S, Pieribone VA, Nordstedt C, Greengard P, & Czernik AJ (1999). Regulation of synaptotagmin I phosphorylation by multiple protein kinases. *Journal of Neurochemistry*, **73**, 921-932.
- Hill TA, Gordon CP, McGeachie AB, Venn-Brown B, Odell LR, Chau N, Quan A, Mariana A, Sakoff JA, Chircop M, Robinson PJ, & McCluskey A (2009). Inhibition of dynamin mediated endocytosis by the Dynoles-synthesis and functional activity of a family of Indoles. *Journal of Medicinal Chemistry*, **52**, 3762-3773.
- Hoopmann P, Rizzoli SO, & Betz WJ (2013). Imaging synaptic vesicle recycling by staining and destaining vesicles with FM dyes. *Cold Spring Harbor Protocols*, **10.1101**, pdb.prot067603.
- Howes MT, Kirkham M, Riches J, Cortese K, Walser PJ, Simpson F, Hill MM, Jones A, Lundmark R, Lindsay MR, Hernandez-Deviez DJ, Hadzic G, McCluskey A, Bashir R, Liu L, Pilch P, McMahon H, Robinson PJ, Hancock JF, Mayor S, & Parton RG (2010). Clathrin-independent carriers form a high

capacity endocytic sorting system at the leading edge of migrating cells. *The journal of cell biology*, **190(4)**, 675-691.

- Ikeda K, & Bekkers JM (2008). Counting the number of releasable synaptic vesicles in a presynaptic terminal. *Proceedings of the National Academy of Sciences of the United States of America*, **106 (8)**, 2945-2950.
- Jackson MB, & Chapman ER (2006). Fusion pores and fusion machines in Ca²⁺-triggered exocytosis. *Annual Review of Biophysics and Biomolecular Structure*, **35**, 135-60
- Kataoka M, Kuwahara R, Iwasaki S, Shoji-Kasai Y, & Takahashi M (2000). Nerve Growth Factor-Induced Phosphorylation of SNAP-25 in PC12 Cells: A Possible Involvement in the Regulation of SNAP-25 Localization. *Journal of Neurochemistry*, **74**, 2058–2066.
- Kovacs M, Toth J, Hetenyi C, Malnasi-Csizmadia A, & Sellers JR (2004). Mechanism of blebbistatin inhibition of myosin II. *Journal of Biological Chemistry*, **279**, 35557-35563.
- Kovács M, Tóth J, Hetényi C, Málnási-Csizmadia A, & Sellers JR (2004). Mechanism of blebbistatin inhibition of myosin II. *Journal of Biological Chemistry*, **279(34)**, 35557-63.
- Krupa B, & Liu G (2004). Does the fusion pore contribute to synaptic plasticity? *Trends in Neurosciences*, **27**, 62-66.
- Kumashiro S, Lu YF, Tomizawa K, Matsushita M, Wei FY, & Matsui H (2005). Regulation of synaptic vesicle recycling by calcineurin in different vesicle pools. *Neuroscience Research*, **51(4)**, 435-43
- Lang T, & Jahn R (2008). Core proteins of the secretory machinery, *Handbook of Experimental Pharmacology*, **184**, 107–127.

- Lilja L, Johansson JU, Gromada J, Mandic SA, Fried G, Berggren PO, & Bark C (2004). Cyclin-dependent kinase 5 associated with p39 promotes Munc18-1 phosphorylation and Ca²⁺-dependent exocytosis. *Journal of Biological Chemistry*, **279**, 29534-29541.
- Lipp P, & Reither G (2011). Protein kinase C: the "masters" of calcium and lipid. *Cold Spring Harbor Perspectives in Biology*, **3(7)**, a004556.
- Liu YW, Mattila JP, & Schmid SL (2013). Dynamin-catalyzed membrane fission requires coordinated GTP hydrolysis. *PLoS One*, **8(1)**, e55691
- Liu YW, Surka MC, Schroeter T, Lukiyanchuk V, & Schmid SL (2008). Isoform and splice-variant specific functions of dynamin-2 revealed by analysis of conditional knock-out cells. *Molecular Biology of the Cell*, **19(12)**, 5347-59
- Lu J, He Z, Fan J, Xu P, & Chen L (2008). Overlapping functions of different dynamin isoforms in clathrin-dependent and -independent endocytosis in pancreatic beta cells. *Biochemical and Biophysical Research Communications*, **371**, 315-319.
- Lu W, Ma H, Sheng ZH, & Mochida S (2009). Dynamin and activity regulate synaptic vesicle recycling in sympathetic neurons. *Journal of Biological Chemistry*, **284**, 1930-1937.
- Ludowyke RI, Elgundi Z, Kranenburg T, Stehn JR, Schmitz-Peiffer C, Hughes WE, & Biden TJ (2006). Phosphorylation of nonmuscle myosin heavy chain IIA on Ser1917 is mediated by protein kinase C beta II and coincides with the onset of stimulated degranulation of RBL-2H3 mast cells. *Journal of Immunology*, **177(3)**, 1492-9.

- Macia E, Ehrlich M, Massol R, Boucrot E, Brunner C, & Kirchhausen T (2006). Dynasore, a cell-permeable inhibitor of dynamin. *Developmental Cell*, **10**, 839-850.
- Mackay K, & Mochly-Rosen D (2001). Localization, anchoring, and functions of protein kinase C isozymes in the heart. *Journal of Molecular and Cellular Cardiology*, **33(7)**, 1301-7..
- Meir A, Ginsburg S, Butkevich A, Kachalsky SG, Kaiserman I, Ahdut R, Demircoren S, Rahamimoff R (1999). Ion channels in presynaptic nerve terminals and control of transmitter release. *Physiological Reviews*, **79(3)**, 1019-88
- Milosevic I, Giovedi S, Lou X, Raimondi A, Collesi C, Shen H, Paradise S, O'Toole E, Ferguson S, Cremona O, et al. (2011). Recruitment of endophilin to clathrin-coated pit necks is required for efficient vesicle uncoating after fission. *Neuron* **72**, 587–601.
- Montecucco C, Schiavo G, & Pantano, S. (2005). SNARE complexes and neuroexocytosis: how many, how close? *Trends in Biochemical Sciences*, **30**, 367–372.
- Müller MS, Obel LF, Waagepetersen HS, Schousboe A, & Bak LK (2013). Complex actions of ionomycin in cultured cerebellar astrocytes affecting both calcium-induced calcium release and store-operated calcium entry. *Neurochemical Research*, **38(6)**, 1260-5.
- Nagy G, Reim K, Matti U, Brose N, Binz T, Rettig J, Neher E, & Sorensen JB (2004). Regulation of releasable vesicle pool sizes by protein kinase A-dependent phosphorylation of SNAP-25. *Neuron*, **41**, 417-429.

- Neco P, Fernandez-Peruchena C, Navas S, Gutierrez LM, de Toledo GA, & Ales E (2008). Myosin II contributes to fusion pore expansion during exocytosis. *Journal of Biological Chemistry*, **283**, 10949-10957.
- Neco P, Fernández-Peruchena C, Navas S, Gutiérrez LM, de Toledo GA, Alés E (2008). Myosin II contributes to fusion pore expansion during exocytosis. *Journal of Biological Chemistry*, **283(16)**, 10949-57.
- Newton AJ, Kirchhausen T, & Murthy VN (2006). Inhibition of dynamin completely blocks compensatory synaptic vesicle endocytosis. *Proceedings of the National Academy of Sciences of the United States of America*, **103**, 17955-17960.
- Obara K, Mitate A, Nozawa K, Watanabe M, Ito Y, & Nakayama K (2010). Interactive role of protein phosphatase 2A and protein kinase Calpha in the stretch-induced triphosphorylation of myosin light chain in canine cerebral artery. *Journal of Vascular Research*, **47(2)**, 115-27.
- Omiatek DM, Cans AS, Heien ML, & Ewing AG (2010). Analytical approaches to investigate transmitter content and release from single secretory vesicles. *Analytical and Bioanalytical Chemistry*, **397**, 3269-3279.
- Powell KA, Valova VA, Malladi CS, Jensen ON, Larsen MR, & Robinson PJ (2000). Phosphorylation of dynamin I on Ser-795 by protein kinase C blocks its association with phospholipids. *Journal of Biological Chemistry*, **275(16)**, 11610-11617.
- Richards DA, Guatimosim C, Rizzoli SO, & Betz WJ (2003). Synaptic vesicle pools at the frog neuromuscular junction. *Neuron*, **39(3)**, 529-41
- Rizo J (2010). Synaptotagmin-SNARE coupling enlightened. *Nature Structural & Molecular Biology*, **17**, 260-

- Rizo J, & Rosenmund C (2008). Synaptic vesicle fusion. *Nature Structural & Molecular Biology*, **15**, 665-674.
- Rizzoli SO, & Betz WJ (2005). Synaptic vesicle pools. *Nature Reviews Neuroscience*, **6(1)**, 57-69.
- Rosenmund C, Sigler A, Augustin I, Reim K, Brose N, & Rhee JS (2002). Differential control of vesicle priming and short-term plasticity by Munc13 isoforms. *Neuron*, **33**, 411-424.
- Royle SJ, & Lagnado L (2010). Clathrin-mediated endocytosis at the synaptic terminal: bridging the gap between physiology and molecules. *Traffic*, **11(12)**, 1489-97.
- Ryan TA (1999). Inhibitors of Myosin Light Chain Kinase Block Synaptic Vesicle Pool Mobilization during Action Potential Firing. *Journal of Neuroscience*, **19**, 1317-1323.
- Saheki Y, & De Camilli P (2012). Synaptic vesicle endocytosis. *Cold Spring Harb Perspect Biol.*, **4(9)**, a005645.
- Saheki Y, & De Camilli P (2012). Synaptic Vesicle Endocytosis. *old Spring Harb Perspect Biol.*, **4(9)**, a005645.
- Samasilp P, Chan SA, & Smith C (2012). Activity-dependent fusion pore expansion regulated by a calcineurin-dependent dynamin-syndapin pathway in mouse adrenal chromaffin cells. *The Journal of Neuroscience*, **32**, 10438–10447.
- Samasilp P, Chan SA, & Smith C (2012). Activity-dependent fusion pore expansion regulated by a calcineurin-dependent dynamin-syndapin pathway in mouse adrenal chromaffin cells. *The Journal of Neuroscience*, **32(30)**, 10438-47.

- Shajahan AN, Timblin BK, Sandoval R, Tiruppathi C, Malik AB, & Minshall RD (2004). Role of Src-induced dynamin-2 phosphorylation in caveolae-mediated endocytosis in endothelial cells. *Journal of Biological Chemistry*, **279**, 20392-20400.
- Shin N, Ahn N, Chang-Ileto B, Park J, Takei K, Ahn SG, Kim SA, Di Paolo G, & Chang, S (2008). SNX9 regulates tubular invagination of the plasma membrane through interaction with actin cytoskeleton and dynamin 2. *Journal of Cell Science*, **121**, 1252–1263.
- Shu S, Liu X, & Korn ED (2005). Blebbistatin and blebbistatin-inactivated myosin II inhibit myosin II-independent processes in Dictyostelium. *Proceedings of the National Academy of Sciences of the United States of America*, **102**, 1472-1477.
- Shupliakov O, & Brodin L (2010). Recent insights into the building and cycling of synaptic vesicles. *Experimental Cell Research*, **316**, 1344-1350.
- Sihra T (1997). Protein Phosphorylation and Dephosphorylation in Isolated Nerve Terminals (Synaptosomes). From: *Neuromethods: regulatory protein modification: Techniques and Protocols*. H. C. Hemmings, Jr. *Humana Press Inc. Vol. 30*
- Smillie KJ, & Cousin MA (2005). Dynamin I Phosphorylation and the Control of Synaptic Vesicle Endocytosis. *Biochem Soc Symp.*, **72**, 87–97.
- Somlyo AP, & Somlyo AV (2003). Ca²⁺ sensitivity of smooth muscle and nonmuscle myosin II: modulated by G proteins, kinases, and myosin phosphatase. *Physiological Reviews*, **83(4)**, 1325-58.

- Südhof TC, & Rizo J (2011). Synaptic vesicle exocytosis. *Cold Spring Harb Perspect Biol.*, **3**(12).
- Takahashi M, Itakura M, & Kataoka M (2003). New aspects of neurotransmitter release and exocytosis: Regulation of neurotransmitter release by phosphorylation. *Journal of Pharmacological Sciences*, **93**, 41-45.
- Takamori S, Holt M, Stenius K, Lemke EA, Grønborg M, Riedel G, Urlaub H, Schenck S, Brügger B, Ringler P, Müller SP, Rammner B, Gräter F, Hub JS, De Groot BL, Mieskes G, Moriyama Y, Klingauf J, Grubmüller H, Heuser J, Wieland F, & Jahn R (2006). Molecular anatomy of a trafficking organelle. *Cell*, **127**, 831–846.
- Tan TC, Valova VA, Malladi CS, Graham ME, Berven LA, Jupp OJ, Hansra G, McClure SJ, Sarcevic B, Boadle RA, Larsen MR, Cousin MA, & Robinson PJ (2003). Cdk5 is essential for synaptic vesicle endocytosis. *Nature Cell Biology*, **5**(8), 701-710.
- Tian JH, Das S, & Sheng ZH (2003). Ca²⁺- dependent phosphorylation of syntaxin-1A by the death-associated protein (DAP) kinase regulates its interaction with Munc18. *Journal of Biological Chemistry*, **278**, 26265-26274.
- Tomizawa K, Sunada S, Lu YF, Oda Y, Kinuta M, Ohshima T, Saito T, Wei FY, Matsushita M, Li ST, Tsutsui K, Hisanaga S, Mikoshiba K, Takei K, & Matsui H (2003). Cophosphorylation of amphiphysin I and dynamin I by Cdk5 regulates clathrin-mediated endocytosis of synaptic vesicles. *Journal of Cell Biology*, **163**(4), 813-24.
- Vanden Berghe P, & Klingauf J (2006). Synaptic vesicles in rat hippocampal boutons recycle to different pools in a use-dependent fashion. *Journal of Physiology*, **572**(Pt 3), 707-20.

- Verma D, Gupta YK, Parashar A, & Ray SB (2009). Differential expression of L- and N-type voltage-sensitive calcium channels in the spinal cord of morphine+nimodipine treated rats. *Brain Research*, **1249**, 128-134.
- von Kleist L, Stahlschmidt W, Bulut H, Gromova K, Puchkov D, Robertson MJ, MacGregor KA, Tomilin N, Pechstein A, Chau N, Chircop M, Sakoff J, von Kries JP, Saenger W, Kräusslich HG, Shupliakov O, Robinson PJ, McCluskey A, & Haucke V (2011). Role of the clathrin terminal domain in regulating coated pit dynamics revealed by small molecule inhibition. *Cell*, **146(3)**, 471-484.
- Wright CE, & Angus JA (1996). Effects of N-, P- and Q-type neuronal calcium channel antagonists on mammalian peripheral neurotransmission. *British Journal of Pharmacology*, **119**, 49-56.
- Wu M, Huang B, Graham M, Raimondi A, Heuser JE, Zhuang X, & De Camilli P (2010). Coupling between clathrin- dependent endocytic budding and F-BAR-dependent tubulation in a cell-free system. *Nature Cell Biology*, **12**, 902–908.
- Wu WH, & Cooper RL (2013). Physiological separation of vesicle pools in low- and high-output nerve terminals. *Neuroscience Research*, **75(4)**, 275-82
- Wu Y1, Ma L, Cheley S, Bayley H, Cui Q, & Chapman ER (2011). Permeation of styryl dyes through nanometer-scale pores in membranes. *Biochemistry*, **50(35)**, 7493–7502
- Xu J, Pang ZPP, Shin OH, & Sudhof TC (2009). Synaptotagmin-1 functions as a Ca²⁺ sensor for spontaneous release. *Nature Neuroscience*, **12**, 759-U111.
- Xue J, Graham ME, Novelle AE, Sue N, Gray N, McNiven MA, Smillie KJ, Cousin MA, & Robinson PJ (2011). Calcineurin selectively docks with the

dynamamin Ixb splice variant to regulate activity-dependent bulk endocytosis. *J Biol Chem.*,**286(35)**, 30295-303.

- Zhang GR, Wang X, Kong L, Lu XG, Lee B, Liu M, Sun M, Franklin C, Cook RG, & Geller AI (2005). Genetic enhancement of visual learning by activation of protein kinase C pathways in small groups of rat cortical neurons. *Journal of Neuroscience*, **25(37)**, 8468-8481.
- Zhang Q, Cao YQ, & Tsien RW (2007). Quantum dots provide an optical signal specific to full collapse fusion of synaptic vesicles. *Proceedings of the National Academy of Sciences of the United States of America*, **104**, 17843-17848.
- Zhang Q, Li Y, & Tsien RW (2009). The dynamic control of kiss and run and vesicular reuse probed with single nanoparticles. *Science*,**323**, 1448-1453.
- Zhang Q, Li Y, & Tsien RW (2009). The dynamic control of kiss-and-run and vesicular reuse probed with single nanoparticles. *Science*, **323(5920)**, 1448-53.
- Zhu LQ, Liu D, Hu J, Cheng J, Wang SH, Wang Q, Wang F, Chen JG, & Wang JZ (2010). GSK-3 β inhibits presynaptic vesicle exocytosis by phosphorylating P/Q-type calcium channel and interrupting SNARE complex formation. *Journal of Neuroscience*, **30**, 3624-3633.

Appendix

A.1 List of Materials

Chemicals used in this study are listed below in the format: general name (short form used in this study, if any); chemical name/formula; name of the company; product/catalogue number.

- (S)-(-)-Blebbistatin (Blebb); $C_{18}H_{16}N_2O_2$; Tocris Bioscience, UK; 1852
- 4-Aminopyridine (4AP); $C_5H_6N_2$; Sigma-Aldrich, UK; A0152
- Advasep-7; $C_{42}H_{70-n}O_{35}(C_4H_6SO_3Na)_n$, avg. $n = 6.5$; Biotium Inc., USA; 70029 or Sigma-Aldrich, UK; A3723
- β -Nicotinamide adenine dinucleotide phosphate hydrate ($NADP^+$); $C_{21}H_{28}N_7O_{17}P_3 \cdot xH_2O$; Sigma-Aldrich, UK; N5755
- Bafilomycin A1 (BAF); $C_{35}H_{58}O_9$; Tocris Bioscience, UK; 1334
- Bromophenol Blue (BPB); Sigma-Aldrich, UK; B0126
- Cyclosporin A (Cys A); $C_{62}H_{111}N_{11}O_{12}$; Tocris Bioscience, UK; 1101
- Dynasore (DYN); $C_{18}H_{14}N_2O_4 \cdot xH_2O$; Sigma-Aldrich, UK; D7693
- Dyngo-4aTM; $C_{18}H_{14}N_2O_5$; AbcamBiochemicals, UK; Asc-689
- Dynole-34-2TM; $C_{25}H_{36}N_4O$; AbcamBiochemicals, UK; Asc-463
- FM2-10 dye; $C_{26}H_{41}Br_2N_3$; Life technologies, UK; T7508
- Fura-2, AM; C44H47N3O24; Life technologies, UK; F1221
- Go 6983; $C_{26}H_{26}N_4O_3$; Tocris Bioscience, UK; 2285
- Ionomycin (ION); $C_{41}H_{70}O_9 \cdot Ca$; Tocris Bioscience, UK; 1704
- L-Glutamic acid; $C_5H_9NO_4$; Sigma-Aldrich, UK; G1251
- L-Glutamic Dehydrogenase, Type II (GLDH2); EC number: 1.4.1.3; Sigma-Aldrich, UK; G2626
- Okadaic acid (OA); $C_{44}H_{68}O_{13}$; Tocris Bioscience, UK; 1136

- Phorbol 12-myristate 13-acetate (PMA); $C_{36}H_{56}O_8$; Tocris Bioscience, UK; 1201
- Pitstop 2™ (PIT 2); $C_{20}H_{13}BrN_2O_3S_2$; AbcamBiochemicals, UK; Asc-687

Important materials and chemicals used for the western blot technique were sourced from Life technologies, UK unless otherwise stated and are listed below in the format: name; name of the company (if different from life technologies); product/catalogue number.

- Bradford reagent; Sigma-Aldrich, UK; B6916
- iBlot® Transfer Stack, PVDF, regular size; IB4010-01
- MagicMark™ XP Western Protein Standard; LC5602
- Novex® Sharp Unstained Protein Standard; LC5801
- NuPAGE® antioxidant; NP0005
- NuPAGE® LDS Sample Buffer; NP0008
- NuPAGE® MES SDS Running Buffer (20X); NP0002
- NuPAGE®Novex® 4-12% Bis-Tris Midi Protein Gels, 12+2 well; WG1401BOX
- NuPAGE® sample reducing agent (dithiothreitol); NP0009
- Restore™ Plus Western Blot Stripping Buffer; Thermo scientific, USA; 46430
- SimplyBlue™ SafeStain; LC6060
- StartingBlock Blocking Buffer; Thermo scientific, USA; 37543
- SuperSignal™ West Dura Chemiluminescent Substrate; Thermo scientific, USA; 34076

Additionally, following antibodies were used and are presented in the format: name of the antibody; source and type; product/catalogue number. Please note that all the antibodies were sourced from Santa Cruz biotechnology, Inc., USA.

- Anti-goat IgG-HRP; donkey; sc-2020
- Anti-mouse IgG-HRP; goat; sc-2005
- Anti-sheep IgG-HRP; donkey; sc-2473
- Dynamin I Antibody (4E67); mouse monoclonal IgG; sc-58260
- p-Dynamin I Antibody (Ser 774); sheep polyclonal IgG; sc-135689
- p-Dynamin I Antibody (Ser 778); sheep polyclonal IgG; sc-135690
- p-Dynamin I Antibody (Ser 795); goat polyclonal IgG; sc-12937

Certain buffers and stimulation solutions were prepared in the laboratory using common reagents (sourced from Sigma-Aldrich, USA) and are listed below:

- Homogenization buffer: 320 mM Sucrose, 10 mM Hepes
- Physiological buffer (L₀): 125 mM NaCl, 5 mM KCl, 1 mM MgCl₂, 20 mM Hepes and 10 mM glucose; pH 7.4
- Stock HK5C: 130 mM KCl, 1 mM MgCl₂, 20 mM Hepes, 10 mM glucose and 25 mM CaCl₂; pH 7.4. This was diluted fivefold when added to synaptosomes so the final concentration of K⁺ was 30 mM and for [Ca²⁺]_e it was 5 mM.
- 4AP5C: L₀, 5 mM 4-Aminopyridine and 25 mM CaCl₂; pH 7.4. Final 4AP concentration that the synaptosomes were exposed to was 1 mM (plus 5 mM [Ca²⁺]_e).
- ION5C: L₀, 25 μM Ionomycin and 25 mM CaCl₂; pH 7.4. Please note that 25 μM Ionomycin is never added to the remaining buffer and is instead added to the samples simultaneously with the remaining buffer. This was necessary as it was found that Ionomycin lost its activity in the buffer solution (aqueous) after few minutes of buffer preparation. Final ION

concentration that the synaptosomes were exposed to was 5 μM (plus 5 mM $[\text{Ca}^{2+}]_e$).

- Wash buffer (TBST): 25 mM 2-Amino-2-(hydroxymethyl)-1,3-propanediol (Trizma[®] base), 0.15 M NaCl, pH 7.2. This buffer is called Tris-buffered saline (TBS). To this TBS, 0.05% of Tween-20 (final concentration) was freshly added to make it TBST and was used as a washing buffer for all the immuno blots.

A.2 Calculations for Biochemical Assays

All the data obtained from Glu, FM2-10 and Fura 2-am measurement assays required multiple calculation steps before it can be presented, as herein of chapters 3 to 5. The step by step guide for these calculations is outlined in appendix 6C (p121), appendix 6D (p129) and appendix 6E (p155) of MSc thesis authored by Pooja M Babar (2010). This information is very extensive and represents 46 pages of text. Thus it was deemed reasonable to omit this information and instead cite the work by Babar (2010).

Please note that this information can also be obtained by e-mailing the author (Bhuva, DA) on address: bhuvadilip@gmail.com

A.3 Sample size and p values

Table A.3.1: A table of information showing sample size and p values for data presented in chapter 4 of this thesis.

Figure Number	Condition- #1	vs	Condition- #2	p value	n (sample size)		Assay type	Stimulus used
					n (#1)	n (#2)		
4.1A	DYN	vs	Con	Not req	11	12	Glu release	HK5C
4.1B	DYN	vs	Con	p>0.05	10	12	Glu release	ION5C
4.1C	DYN	vs	Con	p>0.05	12	11	Glu release	4AP5C
4.2A	DYN	vs	Con	p=0.508	40	32	FM release	HK5C
4.2B	DYN	vs	Con	p=0.014	36	32	FM release	ION5C
4.2C	DYN	vs	Con	p=0.034	30	30	FM release	4AP5C
4.3A	DYN	vs	Con	p>0.05	11	9	[Ca ²⁺] _i achieved	HK5C
4.3B	DYN	vs	Con	p>0.05	6	9	[Ca ²⁺] _i achieved	ION5C
4.3C	DYN	vs	Con	p>0.05	12	12	[Ca ²⁺] _i achieved	4AP5C
4.4A	PIT 2	vs	Con	p>0.05	22	17	Glu release	ION5C

	DYN+PIT 2	vs	PIT 2	p>0.05	14	22	Glu release	ION5C
4.4B	PIT 2	vs	Con	p=0.6806	38	59	FM release	ION5C
	DYN+PIT 2	vs	Con	p=0.0254	40	59	FM release	ION5C
4.5A	20μM dynole	vs	Con	p>0.05	7	8	Glu release	ION5C
4.5B	10μM dynole	vs	Con	p<0.0466 (at 29 s)	13	20	FM release	ION5C
	20μM dynole	vs	Con	p>0.05	19	20	FM release	ION5C
	50μM dynole	vs	Con	p>0.05	15	20	FM release	ION5C
4.6A	50μM dyngo	vs	Con	p>0.05	7	7	Glu release	ION5C
4.6B	20μM dyngo	vs	Con	p>0.05	16	22	FM release	ION5C
	50μM dyngo	vs	Con	p=0.0798 (at 33.3 s); p=0.1183 (at 120 s)	24	22	FM release	ION5C
	100μM dyngo	vs	Con	p=0.0717(at 33.3 s); p=0.2364 (at 120 s)	19	22	FM release	ION5C
4.7A	Blebb	vs	Con	p>0.05	17	16	Glu release	HK5C
4.7B	Blebb	vs	Con	p>0.05	11	24	Glu release	ION5C

4.7C	Blebb	vs	Con	p>0.05	20	22	Glu release	4AP5C
4.8A	Blebb	vs	Con	p=0.0001	37	32	FM release	HK5C
4.8B	Blebb	vs	Con	p=0.716 (at 20 s)	32	32	FM release	ION5C
4.8C	Blebb	vs	Con	p=0.642 (at 40 s)	48	48	FM release	4AP5C
4.10A	Blebb	vs	Con	p>0.05	18	19	Glu release	HK1.2C
4.10B	Blebb	vs	Con	p>0.05	15	17	Glu release	HK0.3C
4.10C	Blebb	vs	Con	p>0.05	11	15	Glu release	HK0.15C

Table A.3.2: A table of information showing sample size and p values for data presented in chapter 5 of this thesis.

Figure #	Condition- #1	vs	Condition- #2	p value	n (total)		Assay	Stim
					n (#1)	n (#2)		
5.1A	Cys A	vs	Con	p>0.05	18	18	Glu release	HK5C
5.1B	Cys A	vs	Con	p>0.05	18	17	Glu release	ION5C
5.1C	Cys A	vs	Con	p>0.05	23	24	Glu release	4AP5C
5.2A	Cys A	vs	Con	p=0.025 (at 20s)	15	17	FM release	HK5C
5.2B	Cys A	vs	Con	p=0.023 (at 20s)	16	24	FM release	ION5C
5.2C	Cys A	vs	Con	p=0.985 (at 30s)	20	13	FM release	4AP5C
5.3A	Cys A	vs	Con	p<0.001	16	16	[Ca ²⁺] _i achieved	HK5C
5.3B	Cys A	vs	Con	p=0.044 (at 20s)	10	13	[Ca ²⁺] _i achieved	ION5C
5.3C	Cys A	vs	Con	p=0.0490	18	9	[Ca ²⁺] _i achieved	4AP5C
5.4A	CysA+Blebb	vs	Con	p>0.05	23	22	Glu release	HK5C

5.4B	Cys A+DYN	vs	Con	$p>0.05$	13	37	Glu release	ION5C
5.4C	Cys A+DYN	vs	Con	$p>0.05$	12	26	Glu release	4AP5C
5.5A	Blebb+Cys A	vs	Blebb	$p<0.05$	25	37	FM release	HK5C
	Blebb+Cys A	vs	Con	$p=0.029$ (at 66 s)	-	32	FM release	HK5C
5.5B	DYN+Cys A	vs	DYN	$p<0.05$	29	36	FM release	ION5C
	DYN+Cys A	vs	Con	$p=0.0259$ (at 12.4 s)	-	32	FM release	ION5C
5.5C	DYN+Cys A	vs	DYN	$p>0.05$	21	45	FM release	4AP5C
	DYN+Cys A	vs	Con	$p<0.038$ (at 16 s)	-	30	FM release	4AP5C
5.6A	Go6983	vs	Con	$p>0.05$	15	20	Glu release	HK5C
5.6B	Go6983+DYN	vs	Con	$p>0.05$	19	22	Glu release	HK5C
5.6C	Go6983+Blebb	vs	Con	$p>0.05$	24	22	Glu release	HK5C
5.7A	Go6983	vs	Con	$p=0.6263$	22	44	FM release	HK5C
5.7B	Go6983+DYN	vs	DYN	$p=0.1329$	13	16	FM release	HK5C

	Go6983+DYN	vs	Con	p<0.0387 (at 16 s)	13	31	FM release	HK5C
	DYN	vs	Con	p=0.4479	16	31	FM release	HK5C
5.7C	Go6983+Blebb	vs	Blebb	p=0.0090	22	17	FM release	HK5C
	Go6983+Blebb	vs	Con	p=0.7008	22	18	FM release	HK5C
	Blebb	vs	Con	p=0.0130	17	18	FM release	HK5C
5.8A	300 nM PMA+DYN	vs	DYN	p=0.2594	6	18	FM release	ION5C
	300 nM PMA	vs	Con	p=0.2182	12	24	FM release	ION5C
	DYN	vs	Con	p=0.1059	18	24	FM release	ION5C
5.8B	200 nM PMA	vs	Con	p=0.1684	12	24	FM release	ION5C
	200 nM PMA+DYN	vs	DYN	p= 0.4072	7	18	FM release	ION5C
	DYN	vs	Con	p=0.1059	18	24	FM release	ION5C
5.8C	100 nM PMA+DYN	vs	DYN	p=0.2738	6	18	FM release	ION5C
	100nM PMA	vs	Con	p=0.9292	12	24	FM release	ION5C

	DYN	vs	Con	p=0.1059	18	24	FM release	ION5C
5.9A	40nM PMA	vs	Con	p>0.05	11	13	Glu release	ION5C
	40nM PMA+Blebb	vs	Con	p>0.05	14	13	Glu release	ION5C
	40nM PMA+DYN	vs	Con	p>0.05	13	13	Glu release	ION5C
5.9B	40nM PMA	vs	Con	p=0.7209	24	26	FM release	ION5C
	40nM PMA+DYN	vs	DYN	p=0.8271	24	32	FM release	ION5C
	DYN	vs	Con	p=0.0263	32	26	FM release	ION5C
5.9C	40nM PMA+Blebb	vs	Blebb	p=0.0072	24	32	FM release	ION5C
	Con	vs	Blebb	p=0.2899	26	32	FM release	ION5C

A.4 Okadaic acid (OA) experiments

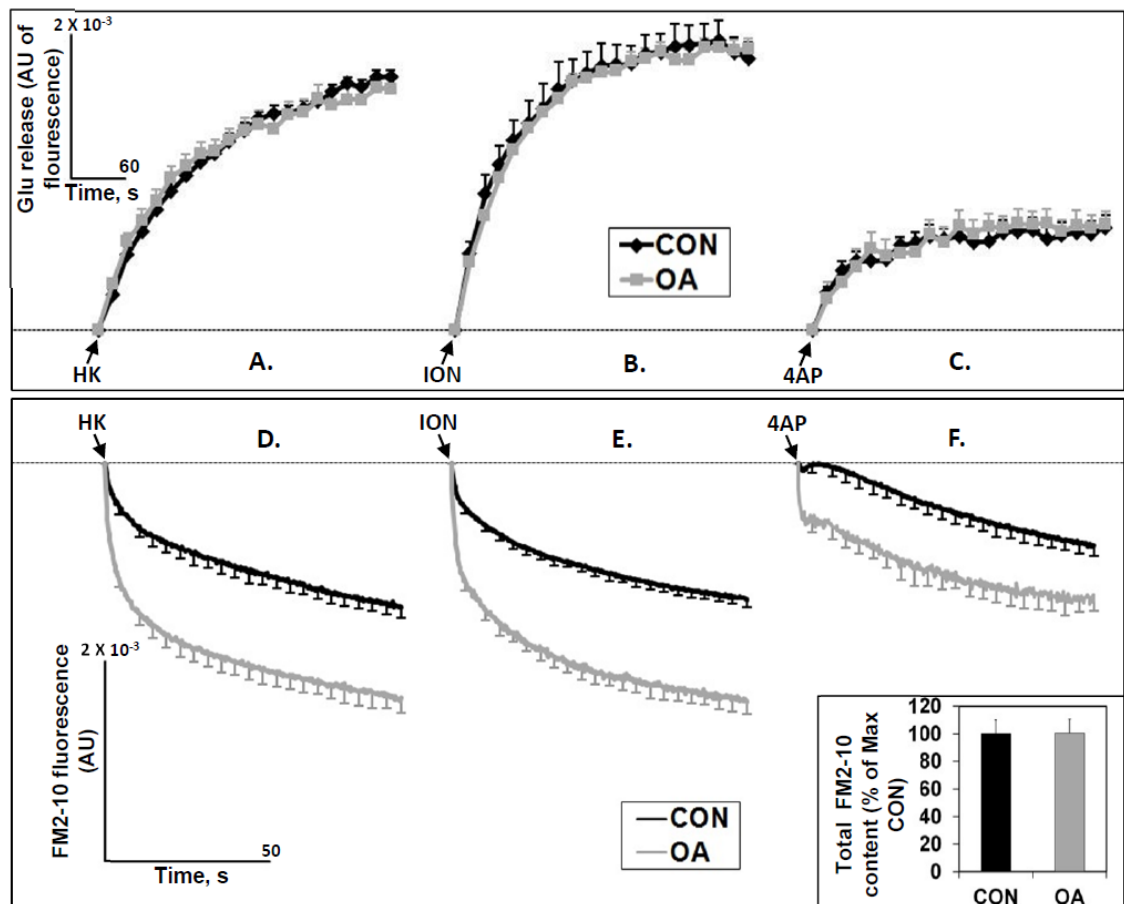
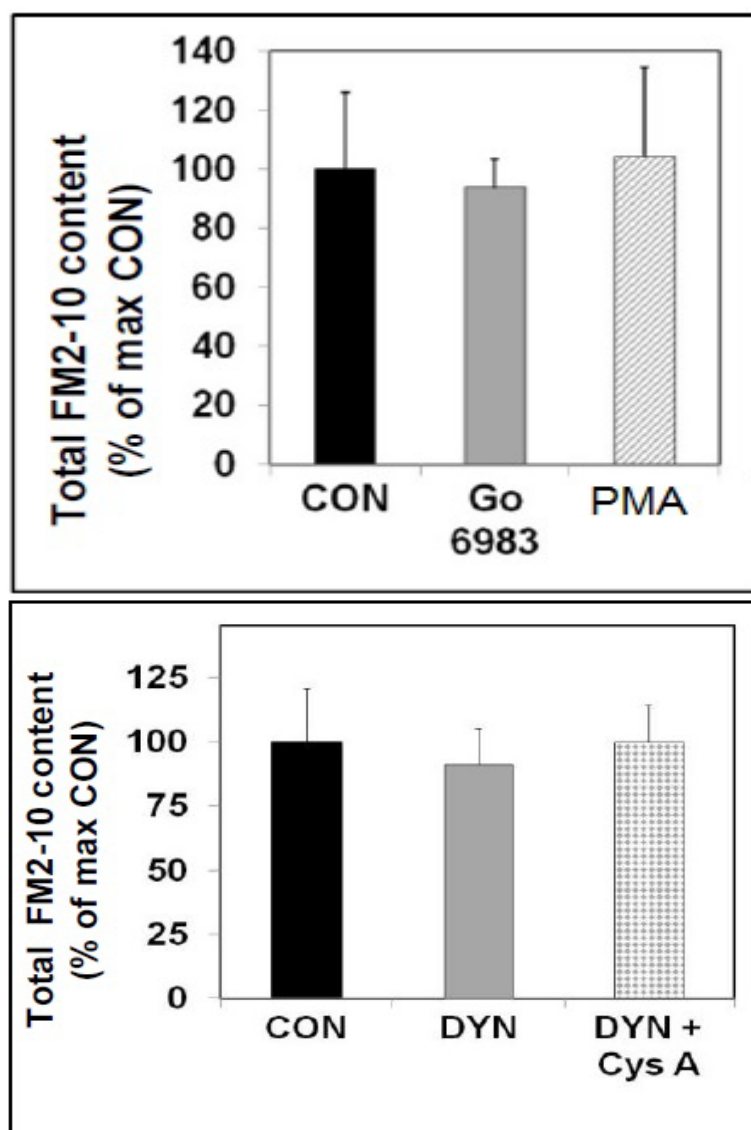
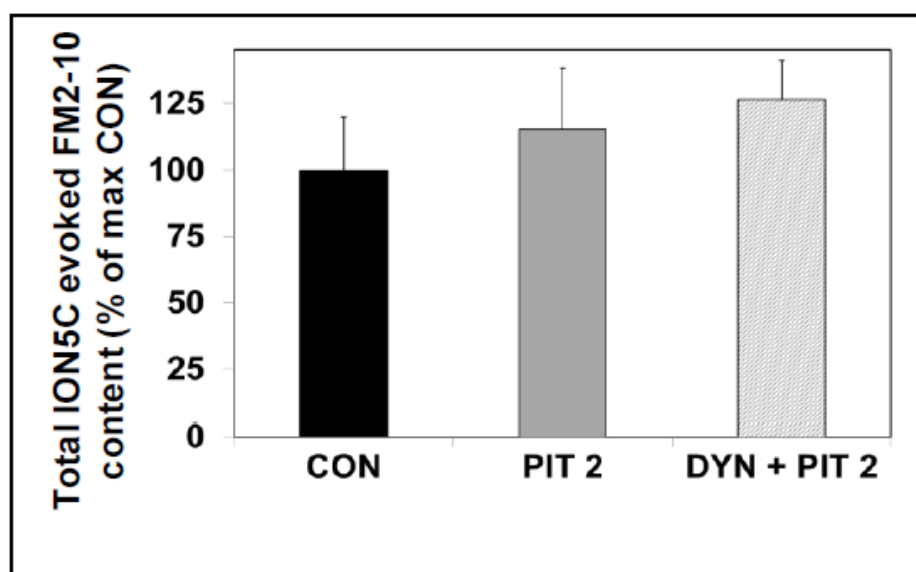
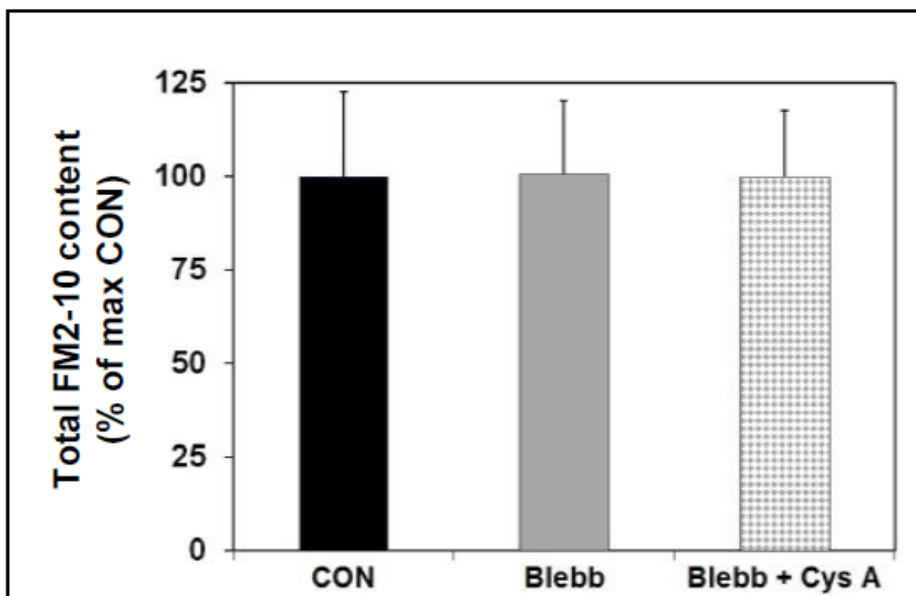
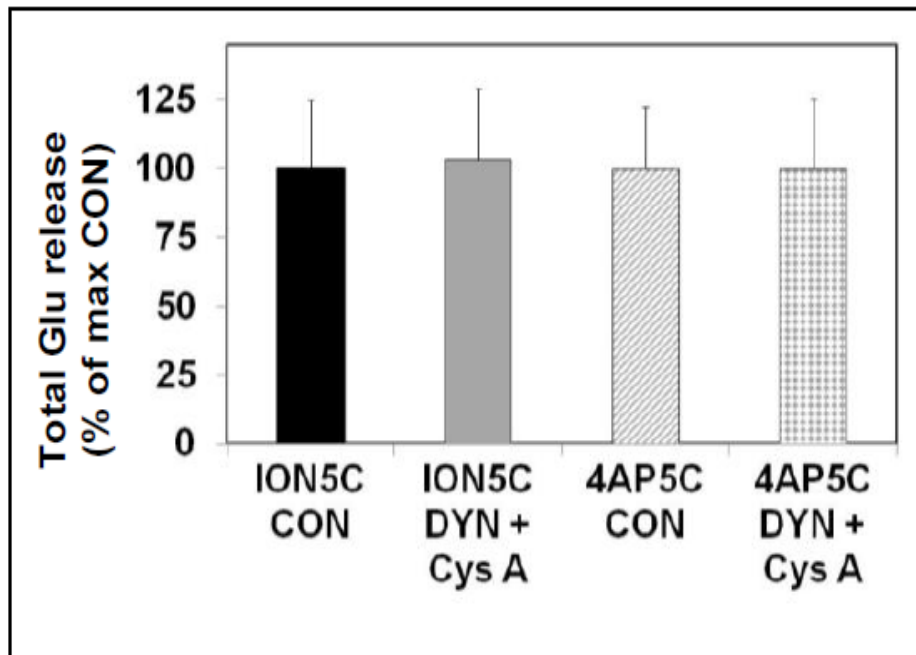


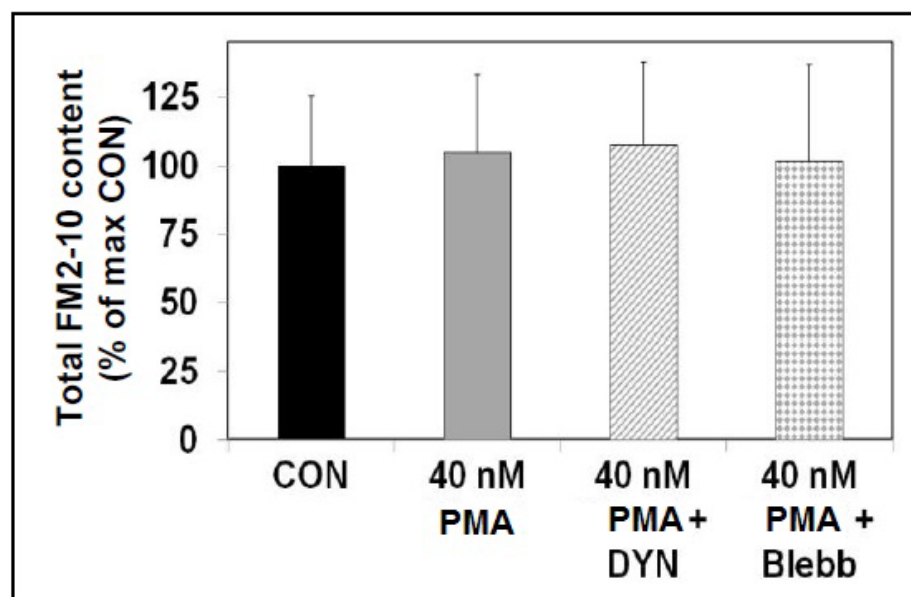
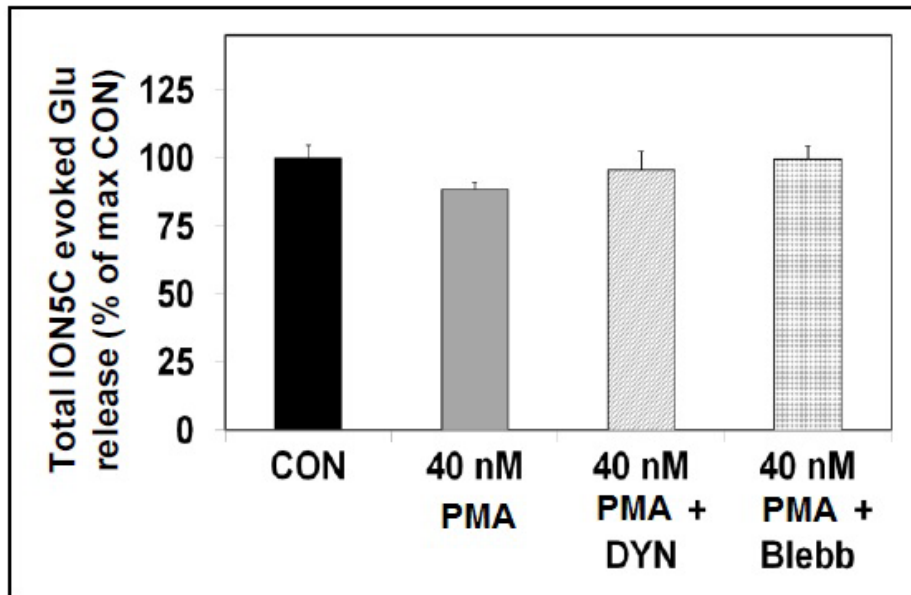
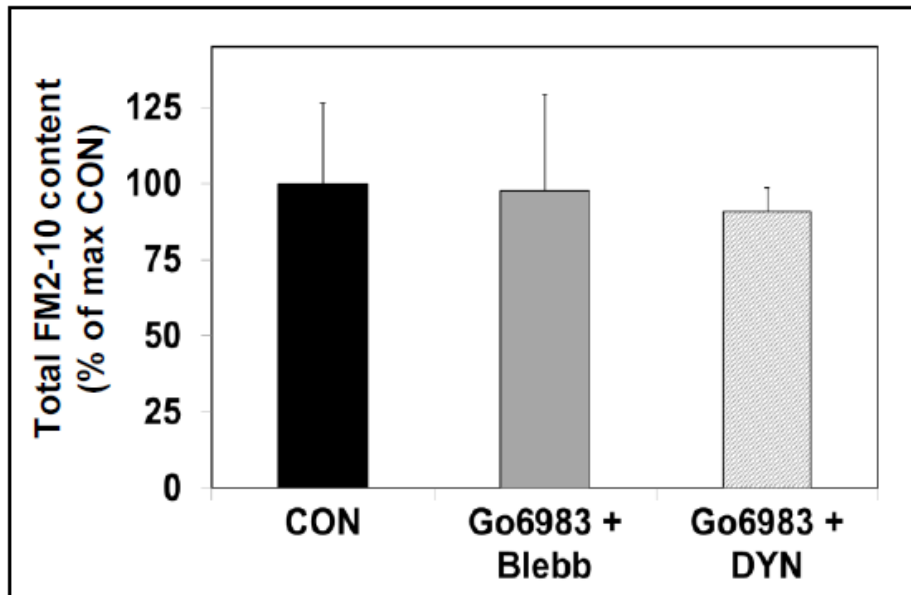
Figure A.4: OA treatment causes FF of all the releasable SVs. A, B and C represent glutamate data indicating the the OA treatment, inhibition of PP2A and PP1, does not interfere with the total amount of Glu released. However, it increases the FM2-10 dye released during (D) HK5C, (E), ION5C and (F) 4AP5C stimulations. The data in the inset represent the total FM2-10 dye content at the start of the experiment indicating that OA treatment does not interfere with the FM2-10 dye loading. For FM2-10 de data, when the control values are subtracted from the OA value, the difference represents the SVs that were previously undergoing KR but are now undergoing FF due to treatment with OA. When this was done for data points until 2 sec (Figure 3.7A and C), it reveals the RRP pool that was undergoing KR under control conditions. When the same procedure is repeated for data after 2 sec (once the values at 2 sec are normalised to zero), it reveals that no vesicles were undergoing KR during control condition (Figure 3.7B).

A.5 FM2-10 dye content at the start of measurement.

For the interpretations drawn in this thesis to be true, it is necessary to establish that any of the drug treatments themselves do not cause any discrepancies in the FM2-10 dye loading otherwise one cannot compare the FM and Glu release data. For this reason, the FM2-10 dye fluorescence value at time zero (just prior to stimulation) of a drug treated sample was compared to control. For all the drugs used in this study, none of the drugs interfered with the FM2-10 dye loading and few representative data are shown below. They were produced by averaging the fluorescence value at time zero before normalisation done during the subsequent calculations. The error bars represent standard error of means.







A.6 Full-sized immuno blots

For ease of presentation, Instead of full immuno blots, only the region of the blot that contained the band of interest (dynamin-I) is shown throughout this thesis. However, the full sized blots can be obtained by e-mailing the author on e-mail address: bhuvadilip@gmail.com

A.7 List of publications arising from this work

Conference proceedings

- Ashton AC, **Bhuva DA**, Singh DS, & Sihra TS (2013). The role of dynamin and myosin 2 in regulating the mode of synaptic vesicle exocytosis. *Annual society for neuroscience conference*, **424.14/G51**.
- Ashton AC, Patel MH, **Bhuva DA**, & Sihra TS (2011). Regulation of modes of synaptic vesicle release in control and diabetic nerve terminals. *Annual society for neuroscience conference*, **445.17/D42**.
- **Bhuva DA**, & Ashton AC (2012). Dynamins and myosin II may regulate the switching between the distinct modes of exocytosis in control and diabetic nerve terminals in a Ca^{2+} dependent manner. Proceedings of the physiological society. 27, PC64

Peer reviewed journal articles

- Ashton AC, Sihra TS, Babar P, Patel MH, **Bhuva DA**, Singh DS, & Green J (2013). Switching between distinct modes of synaptic vesicle exocytosis depends upon changes in protein phosphorylation and calcium: the contribution of dynamins and myosin 2. In preparation for submission to *Neuron*.